NATIELLE GOMES CORDEIRO

CARACTERIZAÇÃO DA DINÂMICA E BIOMASSA DE *HOTSPOTS* MUNDIAIS PARA CONSERVAÇÃO

LAVRAS – MG
2023

NATIELLE GOMES CORDEIRO

CARACTERIZAÇÃO DA DINÂMICA E BIOMASSA DE *HOTSPOTS* MUNDIAIS PARA CONSERVAÇÃO

Tese apresentada à Universidade Federal de Lavras, como parte das exigências do Programa de Pós-Graduação em Engenharia Florestal, área de concentração em Ciências Florestais, para obtenção do título de Doutor.

Prof. Dr. José Márcio de Mello

Orientador

Prof. Dra. Marcela de Castro Nunes Santos Terra

Co-orientadora

LAVRAS – MG
2023

Ficha catalográfica elaborada pelo Sistema de Geração de Ficha Catalográfica da Biblioteca Universitária da UFLA, com dados informados pelo(a) próprio(a) autor(a).

Cordeiro, Natielle Gomes.
Caracterização da dinâmica e biomassa de *hotspots* mundiais para conservação / Natielle Gomes Cordeiro. - 2023.
232 p. : il.

Orientador(a): José Márcio de Mello.
Coorientador(a): Marcela Castro Nunes Santos Terra.
Tese (doutorado) - Universidade Federal de Lavras, 2023.
Bibliografia.

1. Biomassa Acima do Solo. 2. Sensoriamento Remoto. 3. Dinâmica da Comunidade Arbórea. I. Mello, José Márcio de. II. Terra, Marcela Castro Nunes Santos. III. Título.

NATIELLE GOMES CORDEIRO

CARACTERIZAÇÃO DA DINÂMICA E BIOMASSA DE *HOTSPOTS* MUNDIAIS PARA CONSERVAÇÃO

DYNAMICS AND BIOMASS CHARACTERIZATION OF GLOBAL HOTSPOTS FOR CONSERVATION

Tese apresentada à Universidade Federal de Lavras, como parte das exigências do Programa de Pós-Graduação em Engenharia Florestal, área de concentração em Ciências Florestais, para obtenção do título de Doutor.

Aprovada em 26 de junho de 2023

Dr. José Márcio de Mello	UFLA
Dr. Fausto Weimar Acerbi Junior	UFLA
Dr. Samuel José Silva Soares da Rocha	UFLA
Dr. André Ferreira Rodrigues	UFMG
Dra. Marcela de Castro Nunes Santos Terra	UFSJ

Prof. Dr. José Márcio de Mello

Orientador

Prof. Dra. Marcela de Castro Nunes Santos Terra

Co-orientadora

LAVRAS – MG
2023

Aos meus pais e irmão, pelo apoio, dedicação e incentivo durante esta jornada.

Dedico

AGRADECIMENTOS

Mais um ciclo está se finalizando e, com ele, a gratidão por todo aprendizado.

Primeiramente, agradeço a Deus por me abençoar a cada dia. A Ele, meu melhor amigo, por fazer com que tudo cooperasse para o meu bem e, por sempre me conceder forças para lutar. Gratidão pela oportunidade de viver tantas maravilhas, alcançar tantas vitórias e contemplar a misericórdia Divina.

Aos meus pais, Antonio Cordeiro e Karlla Gomes, por me apoiar, incentivar e entender a minha ausência em muitos momentos. Pelos conselhos, ensinamentos de cada dia e, muito mais, pelo amor a mim dedicado. Mesmo com a distância, sempre foram minha base e força diária. Essa vitória é nossa!

Ao meu irmão, Carlos Antônio, pelo companheirismo e amizade. Gratidão pelo incentivo e por sempre acreditar que eu conseguiria. Este momento é ainda mais especial quando penso em você e nos nossos pais.

À minha amiga de profissão e da vida, Kelly, que me acompanhou em todos os momentos. Obrigada por compartilhar comigo os bons e maus momentos. Gratidão pela pessoa que você é. Esta caminhada não seria possível sem a sua parceria e incentivo.

Ao meu orientador, José Márcio, pela maestria, exemplo profissional, disponibilidade e incentivo. Obrigada por todos os ensinamentos.

À minha coorientadora, Marcela Terra, por todo suporte, incentivo, consideração e orientação. Você fez a diferença nesta jornada.

A todos os professores da UFLA pelos ensinamentos e convivência.

À Universidade Federal de Lavras (UFLA), pela estrutura disponibilizada.

"O presente trabalho foi realizado com apoio da Coordenação de Aperfeiçoamento de Pessoal de Nível Superior – Brasil (CAPES) – Código de Financiamento 001".

"A menos que modifiquemos a nossa maneira de pensar, não seremos capazes de resolver os problemas causados pela forma como nos acostumamos a ver o mundo". (Albert Einstein)

RESUMO GERAL

As formações naturais abrigam uma grande diversidade de espécies animais e vegetais, e por isso, são de importância significativa no âmbito social, ambiental e econômico. Contudo, nas últimas décadas, com a crescente urbanização e industrialização, as pressões antrópicas, desmatamentos e uso desenfreado dos recursos naturais tem ocasionado uma fragmentação dos ecossistemas. A transformação destes ambientes em pequenas manchas florestais tem resultado em perda de biodiversidade, extinção de espécies raras e endêmicas. Além das pressões antrópicas, eventos climáticos extremos têm sido apontados como um risco potencial no estabelecimento e crescimento das formações florestais. Assim, a partir da importância que os *hotspots* mundiais, como a Mata Atlântica e Cerrado, apresentam na prestação de serviços ecossistêmicos e conservação ambiental, este estudo visa avaliar a dinâmica, biomassa e seus respectivos direcionadores em áreas destes domínios no sudeste do Brasil. Para tanto, realizamos a caracterização de um fragmento de Mata Atlântica durante um intervalo de 30 anos de mensuração. Assim, procedemos com estimativas da biomassa, área basal, bem como analisamos a estrutura e composição da floresta. Em um segundo momento, empregamos os produtos advindos de sensores ópticos e de radar, associados a medidas de textura, para a determinação da biomassa acima do solo em um remanescente de Mata Atlântica. Também, utilizamos variáveis de terreno, solo e climáticas na predição do comportamento da dinâmica em áreas de Cerrado. Nossos resultados mostraram que dados de sensoriamento remoto auxiliam na predição de biomassa acima do solo em áreas de Mata Atlântica. Além disso, as medidas de textura, associadas aos dados ópticos e de radar, considerando a sazonalidade climática da região, permitem inferir sobre o status da vegetação. Ademais, nossas análises mostram que a dinâmica da comunidade arbórea pode ser predita, principalmente, por variáveis de terreno nas áreas de Cerrado. Estas áreas tendem a apresentar um maior ganho em número de indivíduos e área basal mediante a disponibilidade de água. Em suma, os *hotspots* mundiais possuem grande relevância na conservação da biodiversidade e prestação de serviços ecossistêmicos. Assim, entender o comportamento, estrutura e biomassa destas áreas garantem a proposição de estratégias de conservação e manutenção destes ambientes.

Palavras-Chave: Biomassa acima do solo. Sensoriamento Remoto. Dinâmica da comunidade arbórea.

GENERAL ABSTRACT

The natural forests provide habitat to a great diversity of animal and plant species, and for that, are of importance in social, environmental, and economic aspects. Over the last decades, ecosystems fragmentation has increased due to urbanization, industrialization, human pressures, deforestation, and unsustainable use of natural resources. The environments' fragmentation into small forest patches has led to a loss of biodiversity and extinction of rare and endemic species. In addition to anthropic pressures, extreme climate events have also been identified as potential risk in forest growth and structure. Overall, global hotspots such as the Atlantic Forest and Cerrado play vital roles in providing ecosystem services and conserving the environment. Therefore, our study aims to evaluate tree dynamics, biomass, and their respective drivers in areas of the Atlantic Forest and Cerrado in southeastern Brazil. First, we carried out a characterization of an Atlantic Forest remnant over a 30-year measurement interval. We calculated the aboveground biomass, basal area, and analyzed the forest structure and composition. Then, we used optical and radar sensors' products, including texture parameters, to predict the aboveground biomass in an Atlantic Forest remnant. Finally, we used terrain, soil and climate variables to model the pattern of vegetation dynamics rates in Cerrado areas. Our results showed remote sensing data as good predictors of aboveground biomass in the Atlantic Forest area. Furthermore, texture parameters derived from optical and radar data, while considering the region climatic seasonality, allow inferring as the vegetation status. Also, our findings indicate that tree community dynamics in Cerrado areas are mainly driven by terrain variables. These areas tend to show a greater gain in number of individuals and basal area depending on water availability. The world's hotspots have great relevance in the conservation of biodiversity and providing ecosystem services. Thus, understanding the pattern, structures and biomass of these areas provides insights to the elaboration of conservation and maintenance strategies for these environments.

Keywords: Aboveground biomass. Remote sensing. Tree community dynamics.

SUMÁRIO

PRIMEIRA PARTE

1. INTRODUÇÃO GERAL

O crescimento acelerado dos grandes centros urbanos aumentou a demanda por produtos, bens e serviços, o que tem ocasionado em fragmentação dos ambientes naturais, com consequente perda da biodiversidade (SCARANO; CEOTTO, 2015). Em concomitância, as mudanças climáticas têm gerado uma série de alterações na dinâmica das formações naturais, principalmente para as plantas, que possuem uma maior sensibilidade às alterações do clima, bem como uma menor capacidade adaptativa em consequência da necessidade de um maior tempo para adequação a situações estressantes (LINDNER et al., 2010; SCARANO; CEOTTO, 2015; THOMAS et al., 2004). Dessa forma, os centros globais prioritários para a conservação da biodiversidade, que se encontram sob grandes pressões antrópicas, isto é, os *hotspots* mundiais, estão entre os ecossistemas mais ameaçados pelas alterações climáticas (SCARANO; CEOTTO, 2015). Assim, entender o comportamento dos fragmentos em resposta a eventos extremos ainda é uma lacuna na literatura.

No Brasil, o Cerrado e a Mata Atlântica são áreas com elevada riqueza natural, ou seja, se destacam por apresentar uma grande diversidade ecológica, contudo, com diversas espécies ameaçadas de extinção (LIMA et al., 2020; MYERS et al., 2000; PEREIRA et al., 2020). Os *hotspots* brasileiros estão situados em regiões populosas do país e as modificações sofridas pelos domínios são decorrentes, principalmente, da expansão urbana e construção de cidades, além do direcionamento das áreas de vegetação natural para o desenvolvimento de atividades agropecuárias (COLOMBO; JOLY, 2010; SANO et al., 2019). Em decorrência destas atividades, o desmatamento e degradação dos ambientes naturais nestas regiões tem se tornado cada dia mais evidente. Além disso, estes ambientes têm se tornado mais susceptíveis às mudanças climáticas, alterando a composição florística local com a extinção de diversas espécies endêmicas (COLOMBO; JOLY, 2010; SCARANO; CEOTTO, 2015).

O mosaico de fisionomias no Cerrado e Mata Atlântica são oriundos de mudanças temporais e locais dos ambientes (CUNHA; SILVA JÚNIOR, 2014; LEHMANN et al., 2014; PAUSAS; DANTAS, 2017). No entanto, apesar da alteração na função destes ecossistemas, diminuição na riqueza de espécies, bem como a redução das áreas vegetadas, estes desempenham um papel de grande importância. Estas áreas prestam diversos serviços ecossistêmicos, como controle biológico, ciclagem de nutrientes, sequestro de carbono, atuam na regulação hídrica e servem como abrigo para espécies de plantas e animais (CORDEIRO et

al., 2018; HERTZOG et al., 2019; MITCHELL; BENNETT; GONZALEZ, 2014; PEREIRA et al., 2020).

Neste contexto, considerando que a composição florestal de uma determinada área está diretamente relacionada com as condições ambientais (FIGUEIREDO FILHO et al., 2010; ZHANG; HUANG; HE, 2015), compreender e prever as consequências das alterações climáticas sobre as formações naturais têm se tornado um desafio crescente. Para tanto, a avaliação da estrutura florestal, por meio do estudo da dinâmica, permite entender a riqueza presente, complexidade local, bem como as flutuações, em número de indivíduos e área basal, ao longo do tempo (MAGALHÃES et al., 2017). Além disso, a quantificação da biomassa presente na comunidade arbórea propicia inferir quanto ao potencial que a formação vegetal possui em atuar na mitigação climática. Diante da problemática, nosso estudo tem como objetivo avaliar a dinâmica e biomassa dos *hotspots* mundiais para conservação em Minas Gerais. Para isso, avaliamos a influência dos filtros ambientais e eventos climáticos extremos na composição e biomassa de áreas do Cerrado e Mata Atlântica, respectivamente.

2. REFERENCIAL TEÓRICO

2.1. Hotspots mundiais para conservação

O território brasileiro é marcado por uma biodiversidade representativa, abrangendo áreas correspondentes aos domínios da Amazônia, Caatinga, Cerrado, Mata Atlântica, Pampas e Pantanal (SCOLFORO et al., 2017). Destes, o Cerrado e a Mata Atlântica, devido à diversidade que possuem, tanto em fauna quanto flora, bem como pelas fortes pressões antrópicas sofridas, são classificados como *hotspots* mundiais para conservação (FERREIRA; ALVES; SHIMABUKURO, 2014; MYERS et al., 2000; SANO et al., 2019).

O Cerrado, considerado como a maior savana neotropical do mundo, apresenta um mosaico de formações que vão desde campos, savanas a florestas (BARBOSA; LAKSHMI KUMAR; SILVA, 2015; EITEN, 1972; RIBEIRO; WALTER, 2008). Tais diferenciações são provenientes de características como sazonalidade climática, solo, bem como em função do regime de fogo (LEHMANN et al., 2014; PAUSAS; DANTAS, 2017; SCHWIEDER et al., 2016). Com uma extensão original de aproximadamente 2 milhões de km^2, o equivalente a 23% do território brasileiro (SANO et al., 2019; SCHWIEDER et al., 2016; SILVA; AZEVEDO; SILVEIRA, 2011), o Cerrado se faz presente principalmente nos estados de Goiás, Tocantins, Mato Grosso do Sul, Mato Grosso, Minas Gerais, Distrito Federal, Bahia, Maranhão, Piauí e São Paulo (EITEN, 1972; SANO et al., 2019).

A diversidade florística do Cerrado é evidente, uma vez que este domínio fitogeográfico é extremamente rico em espécies endêmicas e com características intrínsecas (CORDEIRO et al., 2018; PEREIRA et al., 2018; SANO et al., 2019). A vegetação, classificada como xeromórfica, apresenta uma gama de particularidades (EITEN, 1972; SCHWIEDER et al., 2016). A saber, as principais idiossincrasias da vegetação são árvores e arbustos com cascas grossas, troncos e galhos tortuosos, folhas grandes e rígidas (EITEN, 1972). Além da importância fitossociológica, o domínio desempenha um papel vital no tocante dos recursos hídricos, sendo considerado como a "caixa d'água do Brasil" (NASCIMENTO; NAVARRO; DUTRA, 2023). Em outras palavras, o Cerrado é berço de importantes bacias hidrográficas, como a Amazônica, do Rio São Francisco e a Prata (NASCIMENTO; NAVARRO; DUTRA, 2023). Em suma, o Cerrado, assim como a Mata Atlântica, desempenha importante papel na provisão de bens e serviços ecossistêmicos (LIRA; PORTELA; TAMBOSI, 2021; PEREIRA et al., 2020).

A Mata Atlântica também se destaca por abrigar uma rica biodiversidade, em que muitas espécies são endêmicas (LIMA et al., 2020). Do total de espécies animais e vegetais ameaçadas de extinção no Brasil, cerca de 60% são de origem desta formação vegetal (REZENDE et al., 2018). O domínio é marcado por fisionomias que compreendem florestas ombrófilas e estacionais, pântanos, restingas e manguezais (LIMA et al., 2020; MARQUES et al., 2021). As florestas ombrófilas podem ainda ser classificadas em densa, aberta e mista (LIMA et al., 2020; MARQUES et al., 2021). Por outro lado, as florestas estacionais se distinguem em decíduas e semidecíduas (BERTONCELLO et al., 2011; LIMA et al., 2020). Tais diferenciações são decorrentes de características edafoclimáticas locais, bem como de fatores históricos que têm interferência direta no gradiente florístico (CUNHA; SILVA JÚNIOR, 2014).

No Brasil, as áreas da Mata Atlântica se fazem presentes nos estados de Alagoas, Bahia, Ceará, Espírito Santo, Goiás, Mato Grosso do Sul, Minas Gerais, Paraíba, Paraná, Pernambuco, Piauí, Rio de Janeiro, Rio Grande do Norte, Rio Grande do Sul, Santa Catarina, São Paulo e Sergipe (COLOMBO; JOLY, 2010; JOLY; METZGER; TABARELLI, 2014). Além disso, as áreas ainda consideradas como preservadas, estão situadas principalmente nas regiões costeiras no Sul e Sudeste, regiões com altitudes elevadas, que dificultam as ações antrópicas no ambiente (BERTONCELLO et al., 2011).

Em função da localização do Cerrado e Mata Atlântica é notável um aumento das atividades antrópicas, como a industrialização, exploração de minérios e urbanização. Além disso, as áreas naturais destes domínios têm apresentado altos índices de desmatamento nas últimas décadas, sendo suas áreas direcionadas para o cultivo de espécies agrícolas e florestais

exóticas, como cana-de-açúcar, café, cacau, eucalipto e pinus, além do uso para pecuária (COLOMBO; JOLY, 2010; JOLY; METZGER; TABARELLI, 2014; PEREIRA et al., 2020; SILVA; AZEVEDO; SILVEIRA, 2011). A transformação dos habitats originais em pequenas manchas tem acarretado perda na riqueza e diversidade de espécies, bem como redução das áreas vegetadas, dada a interferência, tamanho e formatos das áreas remanescentes (HADDAD et al., 2015). Ainda assim, esses fragmentos desempenham um papel preponderante, pois servem como abrigo para espécies de plantas e animais, sendo que muitas delas são raras e ameaçadas de extinção, além dos serviços ecossistêmicos prestados (CORDEIRO et al., 2018; JOLY; METZGER; TABARELLI, 2014; PEREIRA et al., 2020; RIBEIRO et al., 2011).

A partir da contribuição que estes domínios fitogeográficos apresentam na provisão de funções e serviços como a mitigação climática, fornecimento de produtos madeireiros e não madeireiros, dentre outros (CORDEIRO et al., 2018; PEREIRA et al., 2020), faz-se necessário o estudo aprofundado para que se proponha estratégias de conservação e manutenção destas áreas. Em síntese, conhecer a dinâmica e composição da formação vegetal, bem como o potencial em acumular biomassa, subsidia a obtenção de informações que podem ser utilizadas em tomadas de decisão que visem a proteção destas áreas.

2.2 Dinâmica da comunidade vegetal

A dinâmica da comunidade vegetal, expressa pela mortalidade, crescimento e recrutamento de indivíduos, está intrinsecamente relacionada com a resiliência das plantas em função dos gradientes ambientais (FIGUEIREDO FILHO et al., 2010; ZHANG; HUANG; HE, 2015). Sabe-se que as características edáficas e climáticas de uma região influenciam diretamente nas taxas demográficas, favorecendo ou não o estabelecimento dos indivíduos.

A interação dos fatores que ocorrem dentro da formação vegetal, principalmente no que diz respeito aos distúrbios, interferem diretamente nos processos e dinâmica da comunidade arbórea (MAGALHÃES et al., 2017). Assim, mediante o conhecimento dos processos ecológicos ocorrentes em uma fisionomia vegetal, que influem diretamente na composição florestal, faz-se possível a elaboração de estratégias conservacionistas, bem como o uso sustentável dos recursos, mitigação climática e diminuição dos impactos negativos oriundos da ação humana (MEWS et al., 2011; NGUYEN et al., 2018).

A avaliação da estrutura da comunidade arbórea, por meio da dinâmica, subsidia o entendimento das mudanças no ecossistema, riqueza presente, bem como a complexidade local, visto que a composição florestal de uma determinada área está diretamente relacionada com as condições ambientais (MAGALHÃES et al., 2017). Ademais, as alterações que acontecem

dentro de uma comunidade arbórea, nos níveis temporais e espaciais, são consideradas de suma importância na análise da dinâmica, bem como da composição e estrutura do ecossistema (MEYER et al., 2015).

A dinâmica da formação vegetal é obtida a partir da realização do inventário florestal contínuo, isto é, considerando a alocação de parcelas permanentes que serão medidas e remedidas periodicamente (FIGUEIREDO FILHO et al., 2010). Assim, por meio do levantamento, obtém-se informações quanto à estrutura horizontal, vertical, composição florística, bem como para com as mudanças em número de indivíduos, seja ligada à mortalidade, recrutamento ou sobrevivência. A mortalidade é determinada principalmente por fatores naturais, assim como pela presença de pragas, doenças, mudanças brutas no quesito climático e supressão dos indivíduos (DAS; STEPHENSON; DAVIS, 2016; STURROCK et al., 2011). Em relação ao recrutamento, essa taxa pode ser favorecida pelas condições ambientais, abertura de dossel, dentre outros fatores (CLARK et al., 1999).

Os estudos de dinâmica da comunidade vegetal desenvolvidos em área de Cerrado e Mata Atlântica são normalmente realizados com o intuito de apresentar a diferença em número de indivíduos e área basal da comunidade ao longo do tempo (CORDEIRO et al., 2020; RUSCHEL et al., 2009; SILVA NETO et al., 2017). Contudo, entender como as espécies se comportam em relação a variáveis de solo, clima e terreno, por exemplo, é de grande relevância. Tais parâmetros permitem inferir a respeito do impacto que estes apresentam nos atributos da vegetação local. Nesse sentido, a realização de análises que abordem a relação da riqueza de espécies com as variáveis edafoclimáticas são de suma importância para a determinação da resiliência e crescimento dos indivíduos a depender do ambiente.

2.3 Os hotspots e a biomassa acima do solo

A crescente na emissão de gases do efeito estufa (GEE) e, consequente, aquecimento global, tem provocado a aceleração das mudanças climáticas em todo o mundo (ALLEN et al., 2010; BERNINGER et al., 2018). Este comportamento se faz cada dia mais evidente em função das fortes pressões impostas aos ecossistemas (ALLEN et al., 2010). A saber, o uso desordenado, degradação e desmatamento das comunidades arbóreas são apontados como os principais impulsionadores do aumento dos GEE na atmosfera, dentre eles o dióxido de carbono (BERNINGER et al., 2018). Além disso, a exploração predatória dos ecossistemas vegetais são as principais causas da fragmentação, evento este que tem impacto direto no papel que as comunidades vegetais exercem no combate às mudanças climáticas (SCARANO; CEOTTO, 2015).

As formações naturais, que originalmente correspondem a aproximadamente 30% da superfície terrestre, são extremamente relevantes na provisão de serviços ecossistêmicos, dentre eles, a mitigação climática (JINSHENG, 2012; STRASSBURG et al., 2016). A exemplo, os *hotspots* mundiais, como o Cerrado e a Mata Atlântica, possuem importante papel no ciclo global do carbono, atuando como sumidouros (CORDEIRO et al., 2020; PEREIRA et al., 2020; SILVEIRA et al., 2019a; ZANINI et al., 2021). Em síntese, estes ambientes sequestram o dióxido de carbono (CO_2), ou gás carbônico, por meio dos estômatos para o processo da fotossíntese (YUSUF et al., 2019). O CO_2 é então convertido em biomassa, possibilitando o crescimento e evolução das espécies vegetais (NUNES et al., 2020).

Em função da importância que a biomassa possui na regulação do clima, a sua quantificação de forma precisa tem influência direta na elaboração de estratégias e políticas públicas para a conservação e manutenção das áreas naturais. Usualmente, a quantificação da biomassa pode ser realizada a partir de métodos diretos ou indiretos (FAN et al., 2020; TORRE-TOJAL et al., 2022). Basicamente, estas metodologias consistem nos levantamentos de dados em campo, seja de forma destrutiva ou não destrutiva (SAFARI; SOHRABI, 2020; TORRE-TOJAL et al., 2022; WAI; SU; LI, 2022). Contudo, ainda que os resultados advindos da amostragem em campo sejam mais precisos, a realização do inventário é onerosa, demorada, bem como depende de mão de obra especializada (LU et al., 2016; SEIDEL et al., 2011). Assim, buscando otimizar estes processos, novas metodologias vêm sendo aplicadas na estimativa de biomassa acima do solo, a exemplo, o sensoriamento remoto (LI; ZHOU; XU, 2021; NANDY et al., 2017; NANDY; SRINET; PADALIA, 2021; WAI; SU; LI, 2022).

Os dados de sensoriamento remoto têm mostrado boa relação com a estimativa de variáveis florestais, principalmente a biomassa acima do solo (LI et al., 2020; MORADI et al., 2022; NAIK; DALPONTE; BRUZZONE, 2021; SILVEIRA et al., 2019b, 2019c). A partir de uma gama de possibilidades, as imagens de sensoriamento podem ser obtidas por meio de sensores radar ou ópticos. Geralmente, os dados ópticos são os mais difundidos na predição de variáveis biofísicas, como o índice de área foliar e a fração de cobertura vegetal (BALIDOY BALOLOY et al., 2018; CAMPOS-TABERNER et al., 2018; VERRELST et al., 2019). No entanto, estes sensores são mais suscetíveis à interferência de fatores climáticos como chuva e intensidade de nuvens (SHAO; ZHANG, 2016; SINHA et al., 2015). Assim, visando atenuar tais influências, os sensores do tipo radar vêm ganhando atenção nos últimos anos, uma vez que estes não possuem dependência do clima (DEBASTIANI et al., 2019; FORKUOR et al., 2020; HUANG et al., 2018).

Os produtos advindos de ambos os sensores, ópticos e de radar, possuem boa capacidade para caracterização da estrutura, composição e fenologia da vegetação, por exemplo, determinação da área foliar, bem como biomassa acima do solo (DAVID; ROSSER; DONOGHUE, 2022; SAFARI; SOHRABI, 2020; SILVEIRA et al., 2019b). Contudo, ao utilizar os dados de sensoriamento remoto, o usuário está propício a enfrentar problemas como a saturação dos dados, principalmente em áreas com maiores valores de biomassa (DAVID; ROSSER; DONOGHUE, 2022; FARARODA et al., 2021; WAI; SU; LI, 2022). Assim, não obstante, buscando solucionar esta questão, novas abordagens têm sido exploradas, como o uso de índices de vegetação oriundos de dados do Sentinel-2, bem como medidas de texturas (LU et al., 2012; WAI; SU; LI, 2022). Dentre as diversas técnicas para obtenção das texturas, tem-se a matriz de co-ocorrência de nível de cinza (do inglês, *grey-level co-ocurrance matrix* / GLCM) (HARALICK; SHANMUGAM; DINSTEIN, 1973; SINGH; SRIVASTAVA; AGARWAL, 2017). Em outras palavras, a GLCM é um método estatístico que permite a descrição de medidas de textura (LIAO; HE; QUAN, 2020; SINGH; SRIVASTAVA; AGARWAL, 2017). Tais metodologias têm mostrado ótima capacidade preditiva da biomassa, aumentando a precisão dos modelos (DEBASTIANI et al., 2019; LU et al., 2012; NANDY et al., 2017).

A matriz de co-ocorrência de níveis de cinza considera a relação entre dois pixels por vez, sendo eles o pixel de referência e o pixel vizinho (GHOSAL; DAS BHATTACHARYA; PAUL, 2022; KELSEY; NEFF, 2014; SINGH; SRIVASTAVA; AGARWAL, 2017). Assim, a GLCM pode ser definida como uma matriz que inclui a combinação variada do nível de cinza presente em uma imagem (GHOSAL; DAS BHATTACHARYA; PAUL, 2022; KELSEY; NEFF, 2014; SINGH; SRIVASTAVA; AGARWAL, 2017). Ademais, as medidas de texturas são capazes de discriminar o conteúdo da imagem, visto que possui relação direta com a distribuição dos pixels (KELSEY; NEFF, 2014; SINGH; SRIVASTAVA; AGARWAL, 2017). Em síntese, as texturas capturam a variação em escala de cinza dos pixels em relação aos seus vizinhos espaciais (HALL-BEYER, 2017; SINGH; SRIVASTAVA; AGARWAL, 2017). De forma geral, uma vez que as medidas de textura estão relacionadas com a resolução espacial e ao tamanho dos objetos, estas podem aumentar a segregação da informação espacial de forma independente do tom (LIAO; HE; QUAN, 2020). Por fim, a partir da crescente demanda por entender o comportamento das comunidades vegetais como potenciais sumidouros de carbono, a utilização de novas técnicas, como o sensoriamento remoto e a matriz de co-ocorrência de níveis de cinza, se apresentam como promissoras e necessárias.

2.4 Variáveis preditoras da dinâmica e biomassa nos hotspots

Os eventos climáticos extremos, como a seca, vêm sendo apontados como direcionadores da composição, estrutura e dinâmica da biomassa nas formações vegetais (ALLEN et al., 2010; MEIRA JUNIOR et al., 2020; SULLIVAN et al., 2020). Estes eventos são tidos como as principais manifestações das mudanças climáticas, estas apontadas como uma das ameaças à conservação e manutenção dos ambientes naturais (HISANO; SEARLE; CHEN, 2017; LIMA et al., 2019; MAXWELL et al., 2019; MENEZES-SILVA et al., 2019). Tais alterações nos padrões climáticos promovem mudanças nos processos ecológicos e fisiológicos dos ecossistemas, influenciando o estabelecimento e distribuição, ou até mesmo induzindo a extinção de determinadas espécies (COLOMBO; JOLY, 2010; SCARANO; CEOTTO, 2015; THOM et al., 2017). Contudo, características de terreno, solo e clima também podem influenciar na distribuição, dinâmica e biomassa da vegetação (SILVEIRA et al., 2019a, 2019b).

As variáveis de terreno permitem inferir quanto a dinâmica dos recursos hídricos, bem como propriedades do solo, em escala local e global (FORKUOR et al., 2017; PELEGRINO et al., 2016; SILVEIRA et al., 2019a). Assim, estas variáveis apresentam relação direta com as características que moldam os padrões da vegetação: sombreamento, acúmulo de água, relevo, dentre outros (SILVEIRA et al., 2019b). O uso destes atributos como preditores da biomassa em áreas de Cerrado e Mata Atlântica tem se mostrado eficiente (SILVEIRA et al., 2019a). De forma geral, as variáveis de terreno incluem aspectos que impactam diretamente o crescimento e produtividade de uma vegetação, isto é, direcionam o comportamento da estrutura, biomassa e dinâmica da comunidade arbórea (FORKUOR et al., 2017; SILVEIRA et al., 2019b; SUN; SHAO; LIU, 2013).

As variáveis meteorológicas, como a temperatura e precipitação, também afetam a estrutura da formação vegetal. Mais especificamente, situações de déficit hídrico podem ser apontadas como responsáveis pelo aumento de temperatura e, este padrão interfere na sobrevivência das árvores (ALLEN et al., 2010). Em casos de déficit hídrico acontece uma maior perda de água por meio da transpiração. Assim, pode-se inferir que, a variabilidade da precipitação influi na disponibilidade de água no solo e, consequentemente, na dinâmica da vegetação (ALLEN et al., 2010). Dentro deste panorama, geralmente, regiões com baixas temperaturas e maior precipitação tendem a apresentar uma maior capacidade em acumular biomassa (OGAYA et al., 2015; SILVEIRA et al., 2019b, 2019c).

Não menos importante, as variáveis de solo também são necessárias para uma melhor compreensão do comportamento da formação vegetal (BATALHA et al., 2011). As

características do solo como textura, pH, nutrientes, saturação de base e capacidade de troca catiônica, por exemplo, estão conectados com a capacidade de retenção de água, bem como a probabilidade de ocorrência de eventos como erosão, tendo como base a proporção relativa das partículas sólidas na massa do solo (BATALHA et al., 2011). A saber, a erosão do solo e cobertura vegetal possuem uma relação negativa, isto é, quanto maior a incidência de erosão, menor a capacidade de fixação das árvores na área (ALTIERI et al., 2018). Em outras palavras, a erosão do solo implica em perda na diversidade, composição, estrutura e biomassa da comunidade arbórea. Por fim, as características de solo, clima e terreno atuam como filtros ambientais nas formações naturais, estas que possuem papel fundamental na manutenção da biodiversidade global, assim como na provisão de serviços ecossistêmicos (STRASSBURG et al., 2016). Portanto, compreender os direcionadores da dinâmica e biomassa da formação vegetal fornece *insights* para as tomadas de decisão no tocante à proteção destas áreas.

3. CONSIDERAÇÕES FINAIS

As mudanças climáticas e suas consequências são cada dia mais evidentes. Dentre tais, cita-se as alterações nos padrões de temperatura e precipitação, modificação na composição e estrutura das formações naturais, perda de funções e serviços ecossistêmicos. Estes são alguns exemplos dos impactos negativos que a degradação, desmatamento e uso não sustentável dos recursos naturais estão promovendo. Diante deste cenário, estudos que busquem compreender os direcionadores da dinâmica da comunidade, bem como biomassa, se fazem necessários.

No Brasil, os domínios fitogeográficos do Cerrado e Mata Atlântica são tidos como *hotspots* mundiais para conservação. Estas formações apresentam papel fundamental na provisão de bens e serviços. Contudo, os domínios se encontram nos principais centros urbanos do país, sendo assim, alvo de constante exploração e processos de fragmentação. Por meio deste estudo, para as áreas de Cerrado foram propostas novas interpretações sobre o comportamento da dinâmica da comunidade arbórea em função de variáveis climáticas, de solo e terreno. Além disso, uma análise da influência da sazonalidade na predição de biomassa acima do solo foi realizada para a Mata Atlântica. Para tanto, o uso de dados de sensor radar e óptico foram essenciais, provando o potencial preditivo da biomassa por meio de seus produtos.

A aplicação de novas ferramentas e metodologias são necessárias, trazendo confiabilidade, precisão nos resultados, assim como otimização de tempo e custo na obtenção de informações. A partir do trabalho desenvolvido, é possível compreender quanto a interferência de fatores como clima, terreno e solo, tanto na dinâmica quanto na biomassa da

vegetação. Assim, os resultados fornecem *insights* para a elaboração de estratégias de conservação e manutenção dos ecossistemas naturais, bem como auxilia na replicação dos métodos em estudos que envolvam escala local, regional ou global.

REFERÊNCIAS

ALLEN, C. D. et al. A global overview of drought and heat-induced tree mortality reveals emerging climate change risks for forests. **Forest Ecology and Management**, v. 259, n. 4, p. 660–684, 2010.

ALTIERI, V. et al. The role of silvicultural systems and forest types in preventing soil erosion processes in mountain forests: a methodological approach using cesium-137 measurements. **Journal of Soil Sediments**, v. 18, p. 3378-3387, 2018.

BALIDOY BALOLOY, A. et al. Estimation of Mangrove Forest aboveground biomass using multispectral bands, vegetation indices and biophysical variables derived from optical satellite imageries: Rapideye, planetscope and Sentinel-2. **ISPRS Annals of the Photogrammetry, Remote Sensing and Spatial Information Sciences**, v. 4, n. 3, p. 29–36, 2018.

BARBOSA, H. A.; LAKSHMI KUMAR, T. V.; SILVA, L. R. M. Recent trends in vegetation dynamics in the South America and their relationship to rainfall. **Natural Hazards**, v. 77, p. 883–899, 2015.

BATALHA, M. A. et al. Phylogeny, traits, environment, and space in cerrado plant communities at Emas National Park (Brazil). **Flora: Morphology, Distribution, Functional Ecology of Plants**, v. 206, n. 11, p. 949–956, 2011.

BERNINGER, A. et al. SAR-based estimation of above-ground biomass and its changes in tropical forests of Kalimantan using L- and C-band. **Remote Sensing**, v. 10, n. 6, 2018.

BERTONCELLO, R. et al. A phytogeographic analysis of cloud forests and other forest subtypes amidst the Atlantic forests in south and southeast Brazil. **Biodiversity and Conservation**, v. 20, p. 3413–3433, 2011.

CAMPOS-TABERNER, M. et al. Global estimation of biophysical variables from Google Earth Engine platform. **Remote Sensing**, v. 10, n. 8, p. 1–17, 2018.

CLARK, J. S. et al. Interpreting Recruitment Limitation in Forests. **American Journal of Botany**, v. 86, n. 1, p. 1–16, 1999.

COLOMBO, A.; JOLY, C. Brazilian Atlantic Forest lato sensu: the most ancient Brazilian

forest, and a biodiversity hotspot, is highly threatened by climate change. **Brazilian Journal of Biology**, v. 70, n. 3 suppl, p. 697–708, 2010.

CORDEIRO, N. G. et al. Variação temporal do estoque de carbono e volume de madeira em um fragmento de Cerrado sensu stricto. **Enciclopédia Biosfera**, v. 15, n. 28, p. 931–941, 2018.

CORDEIRO, N. G. et al. Structural and compositional shifts in Cerrado fragments in up to 11 years monitoring. **Acta Scientiarum. Biological Sciences**, v. 42, n. 1, p. e48357, 2020.

CUNHA, M. C. L.; SILVA JÚNIOR, M. C. Flora e Estrutura de Floresta Estacional Semidecidual Montana nos Estados da Paraíba e Pernambuco. **Nativa**, v. 2, n. 2, p. 95–102, 2014.

DAS, A. J.; STEPHENSON, N. L.; DAVIS, K. P. Why do trees diefl Characterizing the drivers of background tree mortality. **Ecology**, v. 97, n. 10, p. 2616–2627, 2016.

DAVID, R. M.; ROSSER, N. J.; DONOGHUE, D. N. M. Improving above ground biomass estimates of Southern Africa dryland forests by combining Sentinel-1 SAR and Sentinel-2 multispectral imagery. **Remote Sensing of Environment**, v. 282, n. July 2021, p. 113232, 2022.

DEBASTIANI, A. B. et al. Evaluating SAR-optical sensor fusion for aboveground biomass estimation in a Brazilian tropical forest. **Annals of Forest Research**, v. 62, n. 1, p. 109–122, 2019.

EITEN, G. The Cerrado Vegetation of Brazil. **Botanical Review**, v. 38, n. 2, p. 201–341, 1972.

FAN, G. et al. AdQSM: A new method for estimating above-ground biomass from TLS point clouds. **Remote Sensing**, v. 12, n. 18, 2020.

FARARODA, R. et al. Improving forest above ground biomass estimates over Indian forests using multi source data sets with machine learning algorithm. **Ecological Informatics**, v. 65, p. 101392, 2021.

FERREIRA, M. P.; ALVES, D. S.; SHIMABUKURO, Y. E. Forest dynamics and land-use transitions in the Brazilian Atlantic Forest: the case of sugarcane expansion. **Regional**

Environmental Change, v. 15, p. 365–377, 2014.

FIGUEIREDO FILHO, A. et al. Crescimento, Mortalidade, Ingresso E Distribuição Diamétrica Em Floresta Ombrófila Mista. **Floresta**, v. 40, n. 4, p. 763–776, 2010.

FORKUOR, G. et al. High resolution mapping of soil properties using Remote Sensing variables in south-western Burkina Faso: A comparison of machine learning and multiple linear regression models. **PLoS ONE**, v. 12, n. 1, p. 1–21, 2017.

FORKUOR, G. et al. Above-ground biomass mapping in West African dryland forest using Sentinel-1 and 2 datasets - A case study. **Remote Sensing of Environment**, v. 236, n. November 2019, p. 111496, 2020.

GHOSAL, K.; DAS BHATTACHARYA, S.; PAUL, P. K. Estimation of aboveground forest biomass in Himalayan region of West Bengal, India using IRS P6 LISS-IV data. **Arabian Journal of Geosciences**, v. 15, n. 7, 2022.

HADDAD, N. M. et al. Habitat fragmentation and its lasting impact on Earth'secosystem. **Science Advances**, v. 1, 2015.

HALL-BEYER, M. GLCM Texture: A Tutorial. **17th International Symposium on Ballistics**, v. 3, 2017.

HARALICK, R. M.; SHANMUGAM, K.; DINSTEIN, I. Textural Features for Image Classification. p. 610–621, 1973.

HERTZOG, L. R. et al. Forest fragmentation modulates effects of tree species richness and composition on ecosystem multifunctionality. **Ecology**, v. 100, n. 4, p. 1–9, 2019.

HISANO, M.; SEARLE, E. B.; CHEN, H. Y. H. Biodiversity as a solution to mitigate climate change impacts on the functioning of forest ecosystems. **Biological Reviews**, v. 93, n. 1, p. 439–456, 2017.

HUANG, X. et al. Assessment of forest above ground biomass estimation using multi-temporal C-band Sentinel-1 and Polarimetric L-band PALSAR-2 data. **Remote Sensing**, v. 10, n. 9, 2018.

JINSHENG, H. E. Carbon cycling of Chinese forests : From carbon storage, dynamics to

models. **Science China - Life Sciences**, v. 55, n. 2, p. 188–190, 2012.

JOLY, C. A.; METZGER, J. P.; TABARELLI, M. Experiences from the Brazilian Atlantic Forest: Ecological findings and conservation initiatives. **New Phytologist**, v. 204, p. 459–473, 2014.

KELSEY, K. C.; NEFF, J. C. Estimates of aboveground biomass from texture analysis of landsat imagery. **Remote Sensing**, v. 6, n. 7, p. 6407–6422, 2014.

LEHMANN, C. E. R. et al. Savanna vegetation-fire-climate relationships differ among continents. In: **Science**. [s.l: s.n.]. v. 343p. 548–552.

LI, C.; ZHOU, L.; XU, W. Estimating aboveground biomass using sentinel-2 msi data and ensemble algorithms for grassland in the shengjin lake wetland, China. **Remote Sensing**, v. 13, n. 8, 2021.

LI, Y. et al. Forest aboveground biomass estimation using Landsat 8 and Sentinel-1A data with machine learning algorithms. **Scientific Reports**, v. 10, n. 1, p. 1–12, 2020.

LIAO, Z.; HE, B.; QUAN, X. Potential of texture from SAR tomographic images for forest aboveground biomass estimation. **International Journal of Applied Earth Observation and Geoinformation**, v. 88, n. January, p. 102049, 2020.

LIMA, A. A. DE et al. Impacts of climate changes on spatio-temporal diversity patterns of Atlantic Forest primates. **Perspectives in Ecology and Conservation**, v. 17, n. 2, p. 50–56, 2019.

LIMA, R. A. F. DE et al. Defining endemism levels for biodiversity conservation: Tree species in the Atlantic Forest hotspot. **Biological Conservation**, v. 252, n. October, p. 108825, 2020.

LINDNER, M. et al. Climate change impacts, adaptive capacity, and vulnerability of European forest ecosystems. **Forest Ecology and Management**, v. 259, n. 4, p. 698–709, 2010.

LIRA, P. K.; PORTELA, R. DE C. Q.; TAMBOSI, L. R. Land-Cover Changes and an Uncertain Future: Will the Brazilian Atlantic Forest Lose the Chance to Become a Hopespot? In: MARQUES, M. C. M.; GRELLE, C. E. V. (Eds.). . **The Atlantic Forest: History,**

Biodiversity, Threats and Opportunities of the Mega-diverse Forest. [s.l: s.n.]. p. 233–251.

LU, D. et al. Aboveground Forest Biomass Estimation with Landsat and LiDAR Data and Uncertainty Analysis of the Estimates. **International Journal of Forestry Research**, v. 2012, n. 1, p. 1–16, 2012.

LU, D. et al. A survey of remote sensing-based aboveground biomass estimation methods in forest ecosystems. **International Journal of Digital Earth**, v. 9, n. 1, p. 63–105, 2016.

MAGALHÃES, J. H. R. et al. Dinâmica do estrato arbóreo em uma fl oresta estacional semidecidual em Uberlândia, Minas Gerais, Brasil. **Iheringia - Serie Botanica**, v. 72, n. 3, p. 394–402, 2017.

MARQUES, M. C. M. et al. The Atlantic Forest: An Introduction to the Megadiverse Forest of South America. In: **The Atlantic Forest: History, Biodiversity, Threats and Opportunities of the Mega-diverse Forest**. [s.l: s.n.]. p. 03–23.

MAXWELL, S. L. et al. Conservation implications of ecological responses to extreme weather and climate events. **Diversity and Distributions**, v. 25, p. 613-625, 2019.

MEIRA JUNIOR, M. S. DE et al. The impact of long dry periods on the aboveground biomass in a tropical forests: 20 years of monitoring. **Carbon Balance and Management**, v. 15, n. 1, p. 1–15, 2020.

MENEZES-SILVA, P. E. et al. Different ways to die in a changing world: Consequences of climate change for tree species performance and survival through an ecophysiological perspective. **Ecology and Evolution**, v . 9, p. 11979-11999, 2019.

MEWS, H. A. et al. Dinâmica da comunidade lenhosa de um Cerrado Típico na região Nordeste do Estado de Mato Grosso, Brasil. **Biota Neotropica**, v. 11, n. 1, p. 73–82, 2011.

MEYER, P. B. et al. Dinâmica estrutural em um fragmento de floresta estacional semideciduifólia em Lavras, MG, Brasil. **Cerne**, v. 21, n. 2, p. 259–265, 2015.

MITCHELL, M. G. E.; BENNETT, E. M.; GONZALEZ, A. Forest fragments modulate the provision of multiple ecosystem services. **Journal of Applied Ecology**, v. 51, n. 4, p. 909–918, 2014.

MORADI, F. et al. Estimating Aboveground Biomass in Dense Hyrcanian Forests by the Use of Sentinel-2 Data. **Forests**, v. 13, n. 1, 2022.

MYERS, N. et al. Biodiversity hotspots for conservation priorities. **Nature**, v. 403, p. 853–858, 2000.

NAIK, P.; DALPONTE, M.; BRUZZONE, L. Prediction of forest aboveground biomass using multitemporal multispectral remote sensing data. **Remote Sensing**, v. 13, n. 7, 2021.

NANDY, S. et al. Neural network-based modelling for forest biomass assessment. **Carbon Management**, v. 8, n. 4, p. 305–317, 2017.

NANDY, S.; SRINET, R.; PADALIA, H. Mapping Forest Height and Aboveground Biomass by Integrating ICESat-2, Sentinel-1 and Sentinel-2 Data Using Random Forest Algorithm in Northwest Himalayan Foothills of India. **Geophysical Research Letters**, v. 48, n. 14, p. 1–10, 2021.

NASCIMENTO, P. H. DOS S.; NAVARRO, F. K. S. P.; DUTRA, R. M. S. A percepção do bioma cerrado por estudantes do Instituto Federal de Educação, Ciência e Tecnologia de Goiás (IFG), Brasil. **Brazilian Journal of Development**, v. 9, n. 1, p. 2407–2423, 2023.

NGUYEN, T. H. et al. A spatial and temporal analysis of forest dynamics using Landsat time-series. **Remote Sensing of Environment**, v. 217, p. 461–475, 2018.

NUNES, L. J. R. et al. Forest contribution to climate change mitigation: Management oriented to carbon capture and storage. **Climate**, v. 8, n. 2, 2020.

OGAYA, R.; BARBETA, A.; BASNOU, C.; PEÑUELAS, J. Satellite data as indicators of tree biomass growth and forest dieback in a Mediterranean holm oak forest. **Annals of Forest Science**, v. 72, p. 135-144, 2015.

PAUSAS, J. G.; DANTAS, V. DE L. Scale matters: fire–vegetation feedbacks are needed to explain tropical tree cover at the local scale. **Global Ecology and Biogeography**, v. 26, n. 4, p. 395–399, 2017.

PELEGRINO, M. H. P. et al. Mapeamento de solos em duas sub-bacias hidrográficas usando dados legados e sua extrapolação para áreas similares do entorno. **Ciencia e Agrotecnologia**, v. 40, n. 5, p. 534–546, 2016.

PEREIRA, K. M. G. et al. Relações estruturais e de diversidade de uma floresta ripária em unidade de conservação e sua zona de amortecimento. **Revista Verde de Agroecologia e Desenvolvimento Sustentável**, v. 13, n. 4, p. 508, 2018.

PEREIRA, K. M. G. et al. Protection status as determinant of carbon stock drivers in Cerrado sensu stricto. **Journal of Plant Ecology**, v. 13, n. 3, p. 361–368, 2020.

REZENDE, C. L. et al. From hotspot to hopespot: An opportunity for the Brazilian Atlantic Forest. **Perspectives in Ecology and Conservation**, v. 16, p. 208–214, 2018.

RIBEIRO, J. F.; WALTER, B. M. T. Fitofisionomias do bioma Cerrado. In: SANO, S. M.; ALMEIDA, S. P. DE (Ed.). **Cerrado: ambiente e flora**. Planaltina: EMBRAPA-CPAC, 2008. p. 89–166.

RIBEIRO, M. C. et al. The Brazilian Atlantic Forest: A Shrinking Biodiversity Hotspot. In: ZACHOS, F. E.; HABEL, J. C. (Eds.). **Biodiversity hotspots**. [s.l.] Springer Verlag Berlin Heidelberg, 2011. p. 405–434.

RUSCHEL, A. R. et al. Caracterização e dinâmica de duas fases sucessionais em floresta secundária da Mata Atlântica. **Revista Árvore**, v. 33, n. 01, p. 101–115, 2009.

SAFARI, A.; SOHRABI, H. Integration of synthetic aperture radar and multispectral data for aboveground biomass retrieval in Zagros oak forests, Iran: an attempt on Sentinel imagery. **International Journal of Remote Sensing**, v. 41, n. 20, p. 8069–8095, 2020.

SANO, E. E. et al. Cerrado ecoregions: A spatial framework to assess and prioritize Brazilian savanna environmental diversity for conservation. **Journal of Environmental Management**, v. 232, n. July 2018, p. 818–828, 2019.

SCARANO, F. R.; CEOTTO, P. Brazilian Atlantic forest: impact, vulnerability, and adaptation to climate change. **Biodiversity and Conservation**, v. 24, p. 2319–2331, 2015.

SCHWIEDER, M. et al. Mapping Brazilian savanna vegetation gradients with Landsat time series. **International Journal of Applied Earth Observation and Geoinformation**, v. 52, p. 361–370, 2016.

SCOLFORO, H. F. et al. A new model of tropical tree diameter growth rate and its application to identify fast-growing native tree species. **Forest Ecology and Management**, v.

400, p. 578–586, 2017.

SEIDEL, D. et al. Review of ground-based methods to measure the distribution of biomass in forest canopies. **Annals of Forest Science**, v. 68, n. 2, p. 225–244, 2011.

SHAO, Z.; ZHANG, L. Estimating forest aboveground biomass by combining optical and SAR data: A case study in genhe, inner Mongolia, China. **Sensors (Switzerland)**, v. 16, n. 6, 2016.

SILVA NETO, A. J. DA et al. Dinâmica da comunidade arbórea em um fragmento de cerrado Sensu Stricto em Minas Gerais, Brasil. **Scientia Forestalis**, v. 45, n. 113, p. 21–29, 2017.

SILVA, S. DE S.; AZEVEDO, G. G.; SILVEIRA, O. T. Social wasps of two Cerrado localities in the northeast of Maranhão state, Brazil (Hymenoptera, Vespidae, Polistinae). **Revista Brasileira de Entomologia**, v. 55, n. 4, p. 597–602, 2011.

SILVEIRA, E. M. DE O. et al. Carbon-diversity hotspots and their owners in Brazilian southeastern Savanna, Atlantic Forest and Semi-Arid Woodland domains. **Forest Ecology and Management**, v. 452, p. 117575, 2019a.

SILVEIRA, E. M. DE O. et al. Object-based random forest modelling of aboveground forest biomass outperforms a pixel-based approach in a heterogeneous and mountain tropical environment. **International Journal of Applied Earth Observation and Geoinformation**, v. 78, p. 175–188, 2019b.

SILVEIRA, E. M. DE O. et al. Modelling aboveground biomass in forest remnants of the Brazilian Atlantic Forest using remote sensing, environmental and terrain-related data. **Geocarto International**, 2019c.

SINGH, S.; SRIVASTAVA, D.; AGARWAL, S. GLCM and its application in pattern recognition. **5th International Symposium on Computational and Business Intelligence, ISCBI 2017**, p. 20–25, 2017.

SINHA, S. et al. A review of radar remote sensing for biomass estimation. **International Journal of Environmental Science and Technology**, v. 12, n. 5, p. 1779–1792, 2015.

STRASSBURG, B. B. N. et al. The role of natural regeneration to ecosystem services provision and habitat availability: a case study in the Brazilian Atlantic Forest. **Biotropica**, v.

48, n. 6, p. 890–899, 2016.

STURROCK, R. N. et al. Climate change and forest diseases. **Plant Pathology**, v. 60, n. 1, p. 133–149, 2011.

SULLIVAN, M. J. P. et al. Long-term thermal sensitivity of Earth's tropical forests. **Science (New York, N.Y.)**, v. 368, n. 6493, p. 869–874, 2020.

SUN, W.; SHAO, Q.; LIU, J. Soil erosion and its response to the changes of precipitation and vegetation cover on the Loess Plateau. **Journal of Geographical Sciences**, v. 23, n. 6, p. 1091–1106, 2013.

THOM, D. et al. The impacts of climate change and disturbance on spatio-temporal trajectories of biodiversity in a temperate forest landscape. **Journal of Applied Ecology**, v. 54, n. 1, p. 28–38, 2017.

THOMAS, C. D. et al. Extinction risk from climate change. **Nature**, v. 427, p. 145–148, 2004.

TORRE-TOJAL, L. et al. Above-ground biomass estimation from LiDAR data using random forest algorithms. **Journal of Computational Science**, v. 58, 2022.

VERRELST, J. et al. Quantifying Vegetation Biophysical Variables from Imaging Spectroscopy Data: A Review on Retrieval Methods. **Surveys in Geophysics**, v. 40, n. 3, p. 589–629, 2019.

WAI, P.; SU, H.; LI, M. Estimating Aboveground Biomass of Two Different Forest Types in Myanmar from Sentinel-2 Data with Machine Learning and Geostatistical Algorithms. **Remote Sensing**, v. 14, n. 9, 2022.

YUSUF, H. A. et al. Carbon Stocks in Aboveground and Belowground Biomass of Sub-Humid Tropical Forest in Southwestern Nigeria. **OALib**, v. 06, n. 08, p. 1–12, 2019.

ZANINI, A. M. et al. The effect of ecological restoration methods on carbon stocks in the Brazilian Atlantic Forest. **Forest Ecology and Management**, v. 481, n. October 2020, p. 118734, 2021.

ZHANG, J.; HUANG, S.; HE, F. Half-century evidence from western Canada shows forest

dynamics are primarily driven by competition followed by climate. **PNAS**, v. 112, n. 13, p. 4009–4014, 2015.

SEGUNDA PARTE - ARTIGOS

CAPÍTULO DE LIVRO

Caracterização de um fragmento de Floresta Estacional Semidecidual Montana ao longo de 30 anos de monitoramento

Natielle Gomes Cordeiro, Marcela de Castro Nunes Santos Terra, André Ferreira Rodrigues, Vanessa Alves Mantovani, Carlos Rogério de Mello, José Márcio de Mello

Capítulo de livro a ser publicado em um livro descritivo sobre os aspectos hidrológicos e florestal da Matinha da UFLA.

Caracterização de um fragmento de Floresta Estacional Semidecidual Montana ao longo de 30 anos de monitoramento

RESUMO

As florestas nativas, em função da rica biodiversidade que abrigam, possuem importância significativa na provisão de serviços ecossistêmicos. Dessa forma, conhecer a dinâmica, estrutura e composição destes ambientes é de suma relevância. Neste capítulo, nosso objetivo foi avaliar o comportamento da vegetação de um fragmento de Mata Atlântica ao longo de 30 anos de mensuração. A área de estudo é conhecida como Matinha da UFLA (Universidade Federal de Lavras). No passado, a área era explorada e hoje é tida como área de preservação permanente da instituição. O remanescente florestal é considerado como um laboratório natural, sendo fonte para o desenvolvimento de diversos trabalhos científicos. Primeiramente, realizamos a descrição sobre o isolamento do fragmento como área de preservação permanente e, posteriormente, procedemos com a caracterização da vegetação. Nossas análises incluem a caracterização da florística e estrutura da floresta, estimativa da área basal e biomassa acima do solo. A área basal ao longo dos 30 anos de mensuração variou entre 19,35 m^2/ha a 24,63 m^2/ha. A biomassa acima do solo variou entre 131,47 Mg/ha e 184,41 Mg/ha. A área apresenta uma diversidade de espécies importantes, sendo muitas destas pertencentes à família Fabaceae e Annonaceae. Em suma, podemos inferir que, apesar da pequena dimensão, o remanescente possui papel fundamental para a conservação das características de um dos principais domínios brasileiros, a Mata Atlântica.

Palavras-chave: Mata Atlântica; Florística; Estrutura florestal; Biomassa acima do solo.

Characterization of a Montana Semideciduous Seasonal Forest remnant over 30-year measurement

ABSTRACT

Native forests harbor a great biodiversity and play a vital role by providing ecosystem services. Therefore, understanding the tree community dynamics, forest structure, and the composition of these environments is truly important. Our study aims to evaluate the vegetation pattern of an Atlantic Forest fragment over 30 years of measurement. The remnant is known as "Matinha da UFLA" (Federal University of Lavras). In previous years, the fragment was a target of anthropic pressure, however, in 1992 the fragment was classified as a permanent preservation area of the University. Also known as a natural laboratory, plenty of studies are carried out in the remnant. In this chapter, we first described the area status until the moment of the effective protection. Then, we proceed with the vegetation characterization. We analyzed the forest floristics and structure, calculated the basal area and aboveground biomass. The basal area over the 30 years of measurement ranged from 19.35 m^2/ha to 24.63 m^2/ha. The aboveground biomass varied between 131.47 Mg/ha and 184.41 Mg/ha. The area has an important diversity of species, many of which belong to the Fabaceae and Annonaceae family. Overall, despite the fragment size, it plays a fundamental role in the conservation of the characteristics of one of the main Brazilian domains, the Atlantic Forest.

Keywords: Atlantic Forest; Floristic; Forest structure; Aboveground biomass.

1. Introdução

As florestas nativas, em função da rica biodiversidade que abrigam, possuem importância significativa na provisão de serviços ecossistêmicos e, por isso, estão intimamente relacionadas com aspectos sociais, ambientais e econômicos (HERTZOG et al., 2019; MITCHELL; BENNETT; GONZALEZ, 2014; PEREIRA et al., 2020). Contudo, nas últimas décadas, devido à rápida expansão dos grandes centros urbanos, observa-se um aumento das pressões antrópicas nos ambientes naturais (FENGLER et al., 2020; SILVA; SANTOS; ROCHA, 2022). Tal desenvolvimento implica no aumento das demandas por produtos madeiros e não madeireiros, industrialização, agricultura, conversão do uso do solo, dentre outros (CUNHA et al., 2021; MARCILIO-SILVA; MARQUES; CAVENDER-BARES, 2018). Consequentemente, perdas expressivas têm sido detectadas nos ecossistemas naturais.

A alta taxa de desmatamento e degradação das florestas implicam na diminuição das funções ecológicas, diversidade de espécies vegetais e animais, bem como afetam os processos ecológicos (FERREIRA et al., 2018; JOLY; METZGER; TABARELLI, 2014a; LIMA et al., 2020). Ademais, em decorrência destes fatores, pode-se inferir que os habitats naturais estão sendo alterados, o que inclui a intensificação da fragmentação ambiental (FERREIRA et al., 2018; JOLY; METZGER; TABARELLI, 2014a; LIRA; PORTELA; TAMBOSI, 2021). A fragmentação é definida como o processo em que ocorre modificações no habitat natural, sejam estas relacionadas com atividades como agricultura, pecuária, queimadas, urbanização ou exploração madeireira (FERREIRA et al., 2018; JOLY; METZGER; TABARELLI, 2014b). Em suma, a fragmentação representa a quebra do habitat natural, isto é, a divisão de grandes áreas em pequenas manchas de vegetação (FERREIRA et al., 2018).

A partir da fragmentação do habitat, os ecossistemas inicialmente grandes e contínuos, transformam-se em pequenos fragmentos (FERREIRA et al., 2018). Apesar de serem negligenciados, esses fragmentos ainda assim possuem importância na conservação dos ambientes naturais, uma vez que abrigam uma biodiversidade fundamental para a conservação das formações vegetais. Contudo, cabe ressaltar que, a fragmentação impõe alterações na estrutura da floresta, composição florística, assim como na dinâmica da vegetação (JOLY; METZGER; TABARELLI, 2014a).

Os efeitos da fragmentação podem ser identificados tanto na flora quanto na fauna local (FERREIRA et al., 2018). Além dos impactos negativos advindos das atividades antrópicas, as mudanças climáticas também vêm sendo apontadas como direcionadoras dessas mudanças na estrutura florestal (SINGH; HUANG, 2022). Assim, cabe destacar a importância de se

compreender a composição e estrutura destes ambientes para então propor estratégias eficazes na gestão, conservação e manutenção dos remanescentes florestais (FIGUEIREDO et al., 2022).

No Brasil, os *hotspots* mundiais estão situados nos grandes centros urbanos e estão suscetíveis à fragmentação (SANO et al., 2019; SINGH; HUANG, 2022). A exemplo, a Mata Atlântica nas últimas décadas vem apresentando perdas expressivas na vegetação nativa em decorrência das alterações climáticas, bem como de fatores antrópicos (SINGH; HUANG, 2022). Atualmente, o domínio pode ser identificado em aproximadamente 245.173 fragmentos florestais, estes apresentando tamanhos diversos (SINGH; HUANG, 2022). Em suma, a Mata Atlântica é um domínio fitogeográfico altamente modificado, em que cerca de 83% dos fragmentos possuem menos de 50 hectares de área (SINGH; HUANG, 2022).

As manchas de vegetação da Mata Atlântica podem ser encontradas em diversas regiões do país. Na região sudeste, mais especificamente em Minas Gerais, tem-se a "Matinha da UFLA" como exemplo de um remanescente florestal da Mata Atlântica. O fragmento florestal será objeto deste estudo, que tem por objetivo conhecer a estrutura e composição da vegetação, bem como a capacidade do fragmento em atuar na provisão de serviços ecossistêmicos.

2. Histórico do fragmento florestal

A "Matinha da UFLA" é um laboratório natural situado no domínio da Mata Atlântica sob as coordenadas 21º13'40''S e 44º57'50''W no campus da Universidade Federal de Lavras (UFLA), município de Lavras em Minas Gerais, sudeste do Brasil (Figura 1). O remanescente florestal, considerado como área de preservação permanente (APP) da instituição, possui vegetação predominante de Floresta Estacional Semidecidual Montana (BOTREL; CARVALHO, 2004; VELOSO; RANGEL FILHO; LIMA, 1991). A área foi tombada pela Portaria N° 212 de 01 de junho de 1992 (*ver anexo A*). Este documento declara como preservação permanente as áreas recobertas com vegetação nativa que estejam situadas no campus da universidade. De acordo com o Código Florestal, Lei Nº 12.651, que dispõe sobre a proteção da vegetação nativa, as áreas de preservação permanente são estabelecidas com o intuito de se preservar os recursos hídricos, a biodiversidade e paisagem, assim como facilitar o fluxo gênico das espécies vegetais e animais e propiciar a proteção do solo (BRASIL, 2012). Estas áreas, que são protegidas, têm o intuito de atingir um ambiente ecologicamente equilibrado, sem a intervenção do homem.

Figura 1 - Fragmento de Mata Atlântica, com vegetação predominante de Floresta Estacional Semidecidual Montana, situado em Minas Gerais, região sudeste do Brasil.

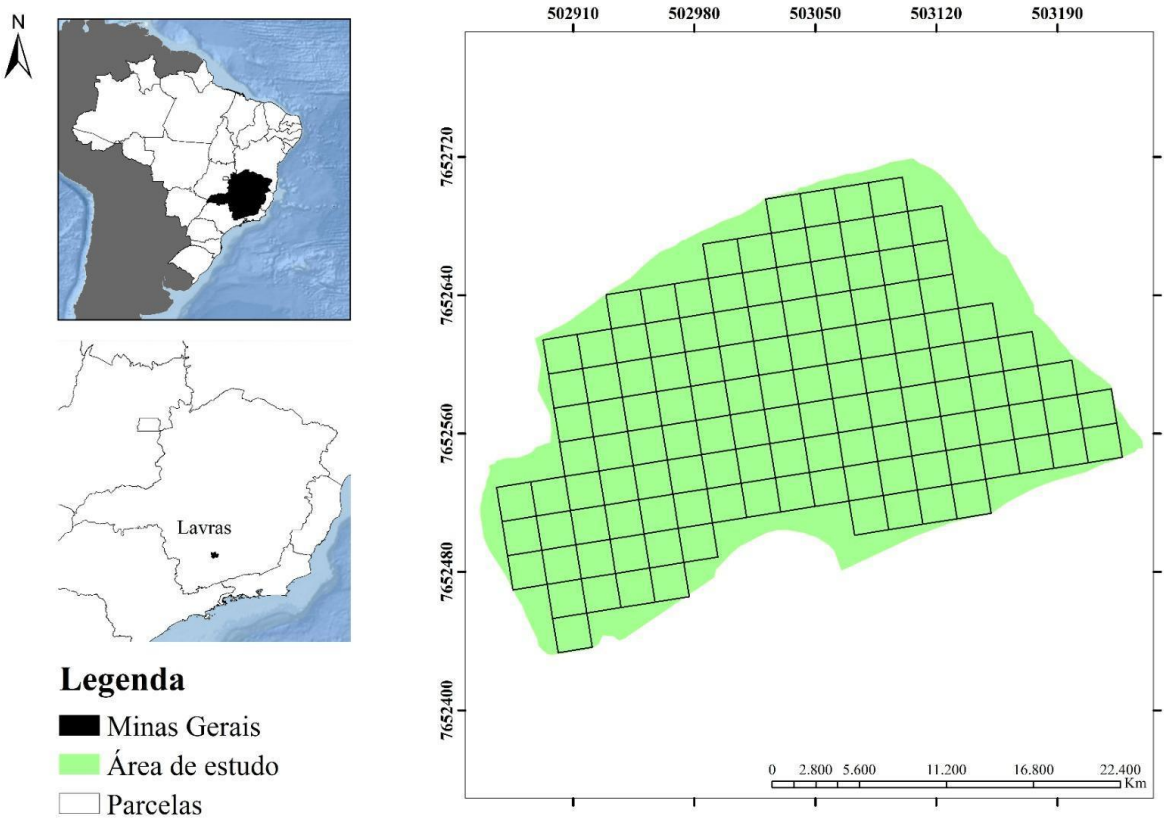

A Matinha da UFLA possui área de 6,35 hectares, com relevo variando entre 5 e 15% e altitude média de 925 metros (JUNQUEIRA JUNIOR et al., 2017). O clima da região, de acordo com a classificação de Köppen, é do tipo Cwa, com verões chuvosos e invernos secos (ALVARES et al., 2014). Ressalta-se que a estação chuvosa acontece entre os meses de outubro e março, e a estação seca entre abril e setembro. Considerando as Normais Climatológicas (1991-2020), a precipitação média anual é de 1383,4 mm e a temperatura média anual de 20,6 °C (INMET, 2023). O solo é classificado como Latossolo Vermelho Distroférrico típico, bem drenado e com textura muito argilosa a argilosa (JUNQUEIRA JUNIOR et al., 2017).

O fragmento florestal se encontra próximo ao Departamento de Zootecnia, a um plantio de eucalipto, ao setor de transporte da UFLA, ao setor de cafeicultura, bem como a um viveiro de mudas do Departamento de Ciências Florestais (DCF). O posicionamento geográfico da mata mostra que o cercamento foi fundamental para impedir sua degradação por agentes externos. A Matinha da UFLA tem sido fonte de dados para diversos estudos ao longo dos anos (BOTREL; CARVALHO, 2004; GUAUQUE-MELLADO et al., 2022; OLIVEIRA-FILHO; MELLO; SCOLFORO, 1997; RODRIGUES et al., 2021; SOUZA et al., 2021). Contudo,

ressalvas devem ser feitas em relação ao fragmento. A delimitação da área se mantém praticamente a mesma desde a década de 1920, uma vez que a partir do referido ano não ocorre corte raso no remanescente. A única ocasião foi em 1970, em que houve interferência na área, pois se procedeu com corte na borda leste do fragmento. Durante o intervalo entre 1920 e 1986, ainda que não ocorresse o corte raso na área, outros estudos e atividades envolvendo corte da vegetação eram desenvolvidos. Um exemplo de corte seletivo muito comum que ocorreu até o final de década de 80, foi o corte de indivíduos jovens da *Xylopia brasiliensis* (pindaíba) com a finalidade de confeccionar cabos de enxada para o viveiro florestal e para o setor de cafeicultura da antiga Escola Superior de Agricultura de Lavras – ESAL, hoje UFLA. Esses cortes foram relatados por antigos funcionários do viveiro e do setor de café. Segundo estes colaboradores, o tronco da pindaíba é um excelente cabo de enxada. A saber, a prática do corte de indivíduos arbóreos desta espécie resultou em clareiras na área e, consequentemente, possibilitou a abertura de trincheiras, subsidiando estudos de perfil do solo. Nessa premissa, a área foi cercada em 1985 no intuito de aumentar a proteção e conservação dos recursos naturais ali existentes.

3. Levantamento e inventário florestal

O inventário florestal consiste no levantamento de informações qualitativas e quantitativas de uma formação vegetal, sendo este procedimento o principal método para gerar informações que subsidiem as tomadas de decisão (BATISTA et al., 2016; MOREIRA et al., 2020; SCOTT; GOVE, 2002; VIBRANS et al., 2020). A partir do inventário florestal é possível conhecer a dinâmica ecológica das espécies, estoque volumétrico, estoque de carbono e potencial de utilização da área (BATISTA et al., 2016; SAFARI; SOHRABI, 2020; TORRE-TOJAL et al., 2022; VILLANOVA et al., 2019).

No ano de 1985, o Departamento de Ciências Florestais (DCF) idealizou, por meio do Professor Dr. José Roberto Soares Scolforo, o projeto para monitoramento da comunidade arbórea do fragmento florestal. Assim, nesse mesmo ano, definiu-se sobre a necessidade de realizar o cercamento do fragmento. Esta ação foi fundamental para coibir ações antrópicas dentro do fragmento. Inicialmente a área foi cercada com arame farpado e, posteriormente, foi colocado um alambrado (tela). Além disso, nessa mesma época foram demarcadas e alocadas 126 parcelas de 20 x 20 m (400 m^2), totalizando 5,04 hectares de área a ser monitorada, sendo assim, um inventário 100% (censo). Estas parcelas foram alocadas uma ao lado da outra, de forma a cobrir toda a extensão do fragmento (Figura 1). A saber, a diferença de aproximadamente um hectare, em relação ao mapa do fragmento, forma as bordas, onde não

foi possível encaixar uma parcela com as dimensões supracitadas. Por fim, o tamanho da parcela foi definido em 400 m^2 com o intuito de se proceder estudos com diferentes tamanhos de unidade amostral para realização do inventário florestal e estudos ecológicos.

O primeiro levantamento foi realizado no ano de 1987, pelo então estudante de engenharia florestal da UFLA, Sebastião Venâncio, hoje professor da Universidade Federal de Viçosa. Na ocasião, foram mensurados todos os indivíduos arbóreos com diâmetro à 1,30 metros do solo (comumente conhecido como diâmetro à altura do peito - DAP) maior ou igual a 5 cm.

Para todas as plantas que atenderam o critério de inclusão (DAP maior ou igual a 5 cm), realizou-se a identificação botânica. A identificação das árvores, seja em nível de gênero ou espécies, foi realizada mediante o auxílio de especialistas, consultas a herbários e literaturas específicas. Além disso, todos os indivíduos arbóreos mensurados foram demarcados com plaquetas de alumínio, contendo a identificação do número da árvore e da parcela. O plaqueamento é fundamental para que se possa efetuar a dinâmica de crescimento das árvores dentro de uma comunidade arbórea de vegetação nativa. Esta ação garante que haja a mensuração dos mesmos indivíduos entre os levantamentos de campo.

As mensurações posteriores foram realizadas nos anos de 1992, 1996, 2001, 2006, 2010, 2015 e 2017. Observa-se que os profissionais do DCF, envolvidos nos trabalhos de medição, sempre procuraram respeitar um período de aproximadamente 5 anos entre as medições. Nestas ocasiões foram quantificadas e identificadas as árvores sobreviventes, recrutas, assim como identificados os indivíduos mortos. Entende-se por árvores recrutas, ou recrutamento, a mensuração das árvores que no inventário anterior não foram incluídas, mas que no inventário atual atendem ao critério de inclusão.

Em 1992, realizou-se a mensuração da altura do fuste comercial. Para isso, foi utilizado um bambu graduado. Além disso, o fuste foi classificado quanto a sua estrutura em: fuste retilíneo (1), fuste ligeiramente tortuoso (2) e fuste defeituoso ou morto. Ademais, procedeu-se com uma avaliação da sanidade da árvore, usando os seguintes critérios: árvore sadia (1), árvore doente ou atacada por inseto (2), árvore morta e/ou seca (3). Para o ano de 1996, além das características supracitadas, foi mensurada também a altura total das árvores com o auxílio de uma vara telescópica. No ano de 2017, o inventário florestal foi realizado objetivando principalmente a conferência da demarcação dos indivíduos arbóreos, parcelas e conferência da identificação botânica. Em 2018/2019, todos os indivíduos identificados com uma plaqueta foram georreferenciados. Este procedimento tem como intuito subsidiar a realização de

diversos trabalhos, principalmente no âmbito de estudos espaciais das espécies presentes na mata.

4. Análise estrutural da floresta

O conhecimento quanto à florística e estrutura de uma formação vegetal possui fundamental importância no fornecimento de informações que subsidiem planos de conservação e preservação das florestas (FIGUEIREDO et al., 2022; MOREIRA et al., 2020). Tais estudos permitem compreender a estrutura, composição e dinâmica da comunidade vegetal (FIGUEIREDO et al., 2022).

Ao longo dos anos de mensuração, o número de indivíduos amostrados na área de interesse sofreu variação (Figura 2A). No intervalo entre 1987 e 2001 foi possível observar uma estabilidade no número de indivíduos. Contudo, nas medições de 2006 e 2010, houve um decréscimo no número de plantas por hectare. Esta diminuição está fortemente relacionada com a maior taxa de mortalidade nessas duas medições. A mortalidade dos indivíduos arbóreos, além de fatores ecológicos, também pode ser resultante de outros agentes. A exemplo, no ano hidrológico de 2009/2010, observou-se no município de Lavras uma elevada precipitação. Considerando que antigamente o entorno do fragmento não era pavimentado, a água da chuva adentrava na Matinha e derrubava as árvores em diversas parcelas. Por fim, estas quedas das árvores foram registradas durante o levantamento florestal em 2010. A saber, as espécies que apresentaram maiores perdas, ao longo dos 30 anos de mensuração, foram: *Casearia arborea* (Rich) Urb., *Miconia chartacea* Triana, *Miconia pepericarpa* DC., *Miconia trianae* Cogn., *Myrcia splendens (Sw.)* DC., *Ocotea odorifera (Vell.)* Rohwer, *Siparuna guianensis* Aubl., *Tachigali rugosa* (Mart. ex Benth.) Zarucchi & Pipoly e *Tapirira obtusa* (Benth.) J.D. Mitch. (Figura 2B).

As formações naturais respondem fortemente às pressões antrópicas, bem como a preservação dos ambientes antes explorados (MAGNAGO et al., 2015). Assim, a fragmentação dos ambientes naturais pode ocasionar mudanças rápidas na estrutura e composição de espécies (LAURANCE et al., 2006; MAGNAGO et al., 2015). No que diz respeito à Matinha da UFLA, o histórico permite inferir que a vegetação passou de um ambiente perturbado para uma área preservada. Contudo, essa transição pode influenciar nas respostas adaptativas das espécies no interior da floresta (LAURANCE et al., 2006; MAGNAGO et al., 2015).

Figura 2 - Estrutura da vegetação do fragmento de Floresta Estacional Semidecidual Montana ao longo de 30 anos de mensuração. A) Número de indivíduos amostrados por

hectare em cada ano. B) Número de indivíduos amostrados ao longo dos anos de mensuração para as espécies: *Casearia arborea* (Rich) Urb., *Miconia chartacea* Triana, *Miconia pepericarpa* DC., *Miconia trianae* Cogn., *Myrcia splendens (Sw.)* DC., *Ocotea odorifera (Vell.)* Rohwer, *Siparuna guianensis* Aubl., *Tachigali rugosa* (Mart. ex Benth.) Zarucchi & Pipoly e *Tapirira obtusa* (Benth.) J.D. Mitch. Em que: N é o número de indivíduos.

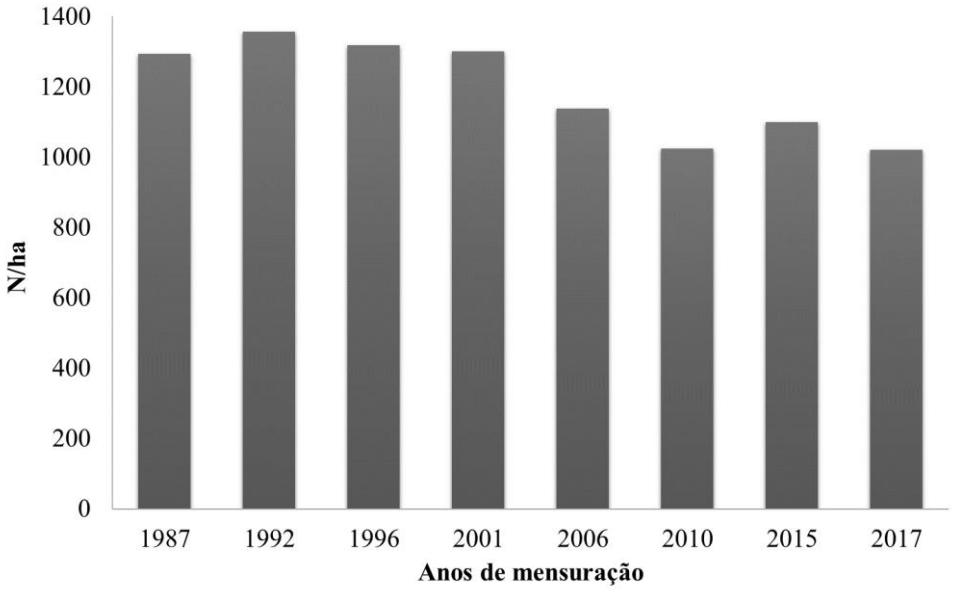

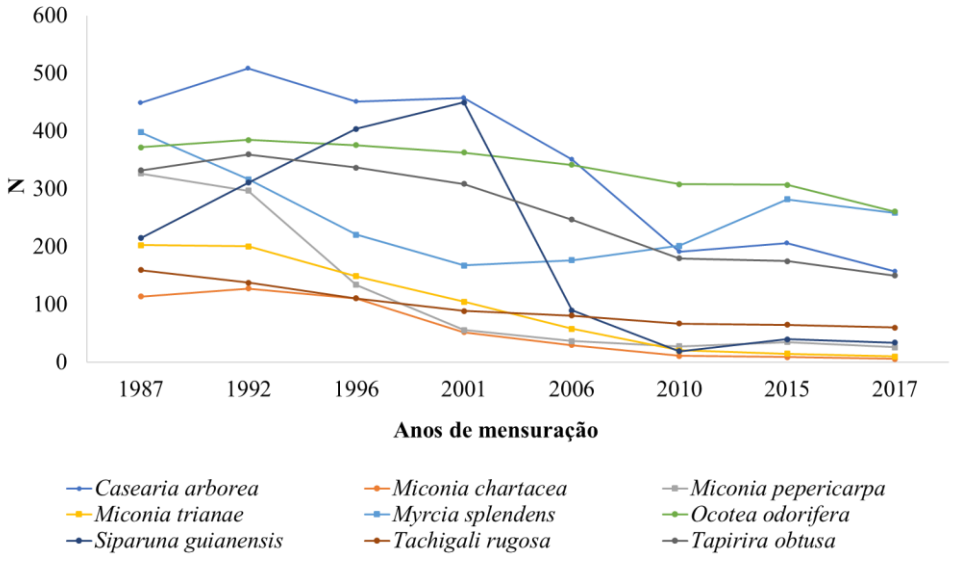

5. Composição florística do fragmento florestal

A composição florística de uma formação vegetal é comumente expressa pela diversidade, isto é, em função do número de espécies diferentes que ocorrem em uma comunidade, bem como pelo grau de dominância destas espécies (FIGUEIREDO et al., 2022; MOREIRA et al., 2020; POORTER et al., 2017; RODRIGUES; VILLA; NERI, 2019). Tal diferenciação na composição florística de uma formação vegetal se dá em função de diversos fatores, por exemplo, aspectos climáticos e edáficos, que possuem forte influência na heterogeneidade de uma floresta (LIMA et al., 2019; POORTER et al., 2017; RODRIGUES; VILLA; NERI, 2019).

O estudo da composição florística é dado em função do conhecimento das espécies presentes em uma área. Para tanto, a análise é realizada por meio da coleta de material botânico e, consequente identificação do mesmo. A partir deste procedimento, obtém-se a lista de espécies ocorrentes na área de interesse e, portanto, a possibilidade de inferir quanto a diversidade e riqueza.

Ao longo de 30 anos de mensuração foram identificadas 220 espécies na Matinha da UFLA, sendo estas distribuídas em 120 gêneros e 54 famílias (Tabela 1). Para o ano de 2017, um indivíduo foi classificado somente a nível de gênero (*Casearia* sp.). Ressalta-se também a não identificação de espécies para os anos de 2010, 2015 e 2017 (“indeterminadas”). Assim, cabe destacar que, ainda que o fragmento apresente uma pequena extensão em área, a sua composição florística é diversa. Comumente, em áreas de Mata Atlântica ocorre uma grande diversidade de espécies e, consequentemente significativa heterogeneidade nos padrões dos indivíduos arbóreos quanto à altura, DAP, idade, densidade da madeira, dentre outros (MANTOVANI et al., 2022; MYERS et al., 2000).

De maneira geral, as famílias com maior abundância para os anos de 1987 a 2001 foram: Melastomataceae, Fabaceae, Lauraceae, Myrtaceae e Rubiaceae. Com o passar dos anos durante este intervalo, a família Fabaceae se tornou mais abundante. Em relação ao intervalo de 2006 a 2017, as famílias com maior número de indivíduos foram: Fabaceae, Lauraceae, Annonaceae, Rubiaceae e Myrtaceae. Assim, é possível inferir que ao longo dos anos, a família Annonaceae se tornou mais abundante, substituindo a família Melastomataceae.

Áreas de Mata Atlântica tendem a apresentar uma maior representatividade, em número de indivíduos e espécies, das famílias Annonaceae e Fabaceae (FIGUEIREDO et al., 2022; GOMES et al., 2018; MOREIRA et al., 2020; SAFAR; MAGNAGO; SCHAEFER, 2020). A família Fabaceae se destaca por ser uma das famílias mais diversas em todo o mundo, em que suas espécies apresentam papel importante no âmbito ecológico e econômico (FIGUEIREDO

et al., 2022; GOMES et al., 2018). Dentre as principais funções, as espécies da família Fabaceae possuem capacidade de fixação de nitrogênio, bem como apresentam usos medicinais, (CALIMAN et al., 2020; FIGUEIREDO et al., 2022; SILVA OLIVEIRA et al., 2021).

Apesar da importância e diversidade de espécies que o fragmento apresenta, de acordo com o Flora do Brasil, 72,51% das espécies amostradas na Matinha da UFLA não possuem classificação quanto a ameaça de extinção. Este dado demonstra que poucos estudos são realizados a nível de espécie, buscando compreender o comportamento e adaptação aos diferentes fatores bióticos e abióticos. Do total de espécies amostradas, um percentual de 4,22% está em situação de perigo (Figura 3). Informações quanto ao status de conservação das espécies são necessárias para a manutenção destas nos ecossistemas, uma vez que cada uma apresenta uma função intrínseca à composição florestal.

Figura 3 - Classificação quanto ao status de conservação das espécies amostradas no fragmento de Floresta Estacional Semidecidual Montana ao longo de 30 anos. Ameaça das espécies de acordo com o "Flora do Brasil" (BFG, 2021).

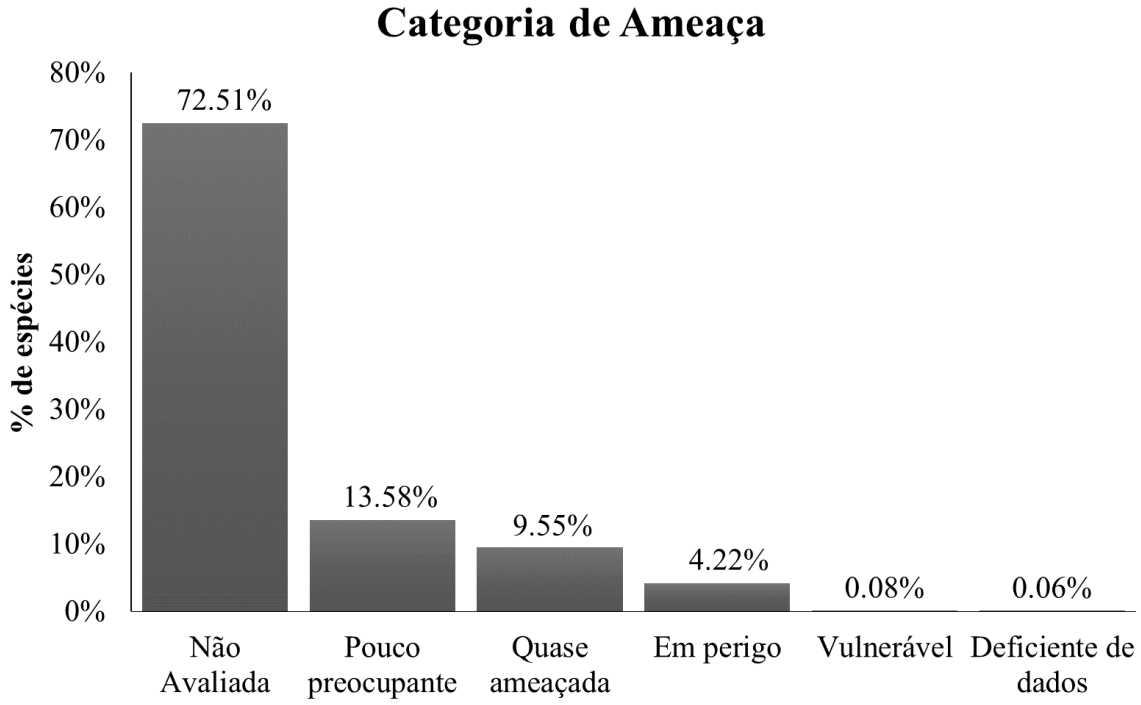

Tabela 1 – Lista de espécies presentes no fragmento de Mata Atlântica, em uma vegetação predominante de Floresta Estacional Semidecidual Montana, ao longo de 30 anos de mensuração (1987-2017). As espécies estão ordenadas de acordo com a família a qual pertencem. Em que x indica a presença da espécie no ano de mensuração.

Família	Espécies	Anos de mensuração							
		1987	1992	1996	2001	2006	2010	2015	2017
Anacardiaceae	*Astronium fraxinifolium* Schott	x	x	x	x	x	x	x	x
	Astronium graveolens Jacq.	x	x	x	x	x	x	x	x
	Schinus lentiscifolia Marchand	x	x	x	x	x	x	x	x
	Schinus terebinthifolia Raddi			x					
	Tapirira guianensis Aubl.	x	x	x	x	x	x	x	x
	Tapirira obtusa (Benth.) J.D.Mitch.	x	x	x	x	x	x	x	x
Annonaceae	*Annona cacans* Warm.	x	x	x	x	x	x	x	x
	Annona dolabripetala Raddi	x	x	x	x	x	x	x	x
	Annona sylvatica A.St.-Hil.	x				x			
	Duguetia lanceolata A.St.-Hil.	x	x	x	x	x	x	x	x
	Guatteria australis A.St.-Hil.	x	x	x	x	x	x	x	x
	Xylopia aromatica (Lam.) Mart.								x
	Xylopia brasiliensis Spreng.	x	x	x	x	x	x	x	x
Apocynaceae	*Aspidosperma parvifolium* A.DC.	x	x	x	x	x	x	x	x
	Aspidosperma polyneuron Müll.Arg.	x	x	x	x	x	x	x	x
	Aspidosperma spruceanum Benth. ex Müll.Arg.	x	x	x	x	x	x	x	x
	Tabernaemontana hystrix Steud.	x	x	x	x	x	x	x	x
Aquifoliaceae	*Ilex cerasifolia* Reissek	x	x	x	x	x	x	x	x
Araliaceae	*Dendropanax cuneatus* (DC.) Decne. & Planch.	x	x	x	x	x			
	Schefflera calva (Cham.) Frodin & Fiaschi	x	x	x	x	x	x	x	x
Arecaceae	*Geonoma schottiana* Mart.	x	x	x	x	x	x	x	x
	Syagrus flexuosa (Mart.) Becc.				x	x			

	Syagrus romanzoffiana (Cham.) Glassman				x				
Asteraceae	*Piptocarpha macropoda* (DC.) Baker	x	x	x	x	x	x	x	x
	Vernonanthura divaricata (Spreng.) H.Rob	x	x	x					
Bignoniaceae	*Cybistax antisyphilitica* (Mart.) Mart.	x	x	x	x	x	x	x	x
	Handroanthus serratifolius (Vahl) S.Grose	x	x	x	x	x	x	x	x
	Jacaranda macrantha Cham.	x	x	x	x	x	x	x	x
	Jacaranda puberula Cham.	x	x	x	x	x	x	x	x
	Zeyheria tuberculosa (Vell.) Bureau ex Verl.	x	x	x	x	x	x	x	x
Boraginaceae	*Cordia sellowiana* Cham.	x	x	x	x	x	x	x	x
	Cordia trichotoma (Vell.) Arráb. ex Steud.	x	x	x					
Burseraceae	*Protium heptaphyllum* (Aubl.) Marchand	x	x	x	x	x	x	x	x
	Protium spruceanum (Benth.) Engl.	x	x	x	x	x	x	x	x
	Protium widgrenii Engl.	x	x	x	x	x	x	x	x
	Trattinnickia ferruginea Kuhlm.						x	x	x
Canellaceae	*Cinnamodendron dinisii* Schwacke	x	x	x	x	x			
Cannabaceae	*Trema micrantha* (L.) Blume	x	x	x					
Celastraceae	*Monteverdia gonoclada* (Mart.) Biral	x	x	x	x	x	x	x	x
	Salacia elliptica (Mart.) G. Don	x	x	x	x	x	x	x	x
Chrysobalanaceae	*Hirtella glandulosa* Spreng.	x	x	x	x	x	x	x	x
	Hirtella hebeclada Moric. ex DC.	x	x	x	x	x	x	x	x
Clethraceae	*Clethra scabra* Pers.	x	x	x	x	x	x	x	x
Clusiaceae	*Garcinia brasiliensis* Mart.	x	x	x	x	x	x	x	x
	Garcinia gardneriana (Planch. & Triana) Zappi	x	x	x	x	x	x	x	x
Combretaceae	*Terminalia glabrescens* Mart.	x							
Connaraceae	*Connarus regnellii* G.Schellenb.	x	x	x	x	x	x	x	x
Cunoniaceae	*Lamanonia ternata* Vell.	x	x	x	x	x	x	x	x
Elaeocarpaceae	*Sloanea hirsuta* (Schott) Planch. ex Benth.	x	x	x	x				

Erythroxylaceae	*Erythroxylum citrifolium* A.St.-Hil.	x							
	Erythroxylum pelleterianum A.St.-Hil.	x	x	x	x	x	x	x	x
Euphorbiaceae	*Alchornea glandulosa* Poepp. & Endl.	x	x	x	x	x	x	x	x
	Croton erythroxyloides Baill.							x	x
	Croton floribundus Spreng.	x	x	x	x	x	x	x	x
	Gymnanthes klotzschiana Müll.Arg.	x	x	x	x	x	x	x	x
	Maprounea guianensis Aubl.	x	x	x	x	x	x	x	x
Fabaceae	*Albizia polycephala* (Benth.) Killip ex Record	x	x	x	x	x	x	x	x
	Anadenanthera colubrina (Vell.) Brenan	x	x	x	x	x	x	x	x
	Anadenanthera peregrina (L.) Speg.							x	x
	Bowdichia virgilioides Kunth	x	x	x	x	x	x	x	x
	Cassia ferruginea (Schrad.) Schrad. ex DC.	x	x	x	x				
	Copaifera langsdorffii Desf.	x	x	x	x	x	x	x	x
	Dalbergia nigra (Vell.) Allemão ex Benth.	x	x	x	x	x	x	x	x
	Dalbergia villosa (Benth.) Benth.	x	x	x	x	x	x	x	x
	Hymenaea courbaril L.	x	x	x	x	x	x	x	x
	Inga striata Benth.				x	x			
	Inga vera Willd.						x	x	x
	Leucochloron incuriale (Vell.) Barneby & J.W.Grimes	x	x	x	x	x	x	x	x
	Machaerium amplum Benth.	x	x	x	x	x			
	Machaerium brasiliense Vogel	x	x	x	x	x			
	Machaerium debile (Vell.) Stellfeld	x	x	x	x	x	x	x	x
	Machaerium hirtum (Vell.) Stellfeld	x	x	x	x	x	x	x	x
	Machaerium nyctitans (Vell.) Benth.	x	x	x	x	x	x	x	x
	Machaerium stipitatum Vogel				x	x			
	Machaerium villosum Vogel	x	x	x	x	x	x	x	x
	Ormosia arborea (Vell.) Harms				x	x	x	x	x

	Ormosia fastigiata Tul.							x	x
	Piptadenia gonoacantha (Mart.) J.F.Macbr.	x	x	x	x	x	x	x	x
	Platycyamus regnellii Benth.	x	x	x	x	x	x	x	x
	Platypodium elegans Vogel	x	x	x	x	x	x	x	x
	Pseudopiptadenia leptostachya (Benth.) Rauschert	x	x	x	x	x	x	x	
	Senna macranthera (DC. ex Collad.) H.S.Irwin & Barneby	x	x	x	x	x		x	x
	Senna multijuga (Rich.) H.S.Irwin & Barneby	x	x	x					
	Senna velutina (Vogel) H.S.Irwin & Barneby								x
	Tachigali rugosa (Mart. ex Benth.) Zarucchi & Pipoly	x	x	x	x	x	x	x	x
Hypericaceae	*Vismia brasiliensis* Choisy	x	x	x	x	x	x	x	x
	Vismia guianensis (Aubl.) Choisy							x	x
Lacistemataceae	*Lacistema hasslerianum* Chodat	x							
Lamiaceae	*Vitex agnus-castus* L.	x	x	x	x	x	x	x	x
	Vitex megapotamica (Spreng.) Moldenke	x	x	x	x	x	x	x	x
	Vitex polygama Cham.	x	x	x	x	x	x	x	x
Lauraceae	*Cryptocarya aschersoniana* Mez	x	x	x	x	x	x	x	x
	Nectandra cissiflora Nees						x	x	x
	Nectandra grandiflora Nees	x	x	x	x	x	x	x	x
	Nectandra oppositifolia Nees	x	x	x	x	x	x	x	x
	Ocotea aciphylla (Nees & Mart.) Mez							x	x
	Ocotea brachybotrya (Meisn.) Mez								x
	Ocotea corymbosa (Meisn.) Mez	x	x	x	x	x	x	x	x
	Ocotea diospyrifolia (Meisn.) Mez	x	x	x	x	x	x	x	x
	Ocotea laxa (Nees) Mez	x	x	x	x	x	x	x	x
	Ocotea odorifera (Vell.) Rohwer	x	x	x	x	x	x	x	x
	Ocotea pulchella (Nees & Mart.) Mez	x	x	x	x	x	x	x	x
	Persea major (Meisn.) L.E.Kopp	x	x	x	x	x	x	x	x

Malpighiaceae	*Byrsonima laxiflora* Griseb.	x	x	x	x	x	x	x	x
	Heteropterys byrsonimifolia A.Juss.	x	x	x	x	x	x	x	x
Malvaceae	*Guazuma ulmifolia* Lam.	x	x	x	x	x	x	x	x
	Luehea grandiflora Mart. & Zucc.	x	x	x	x	x	x	x	x
Melastomataceae	*Leandra melastomoides* Raddi	x							
	Miconia albicans (Sw.) Triana	x		x	x		x	x	
	Miconia argyrophylla DC.	x	x	x	x	x	x	x	x
	Miconia chartacea Triana	x	x	x	x	x	x	x	x
	Miconia cinnamomifolia (DC.) Naudin	x	x	x	x	x	x	x	x
	Miconia minutiflora (Bonpl.) DC.	x							
	Miconia pepericarpa DC.	x	x	x	x	x	x	x	x
	Miconia sellowiana Naudin						x	x	x
	Miconia trianae Cogn.	x	x	x	x	x	x	x	x
	Miconia tristis Spring		x	x	x	x	x	x	x
	Miconia urophylla DC.						x	x	x
	Miconia willdenowii Klotzsch ex Naudin	x	x	x	x	x	x	x	x
	Mouriri glazioviana Cogn.	x	x	x	x	x	x	x	x
	Pleroma stenocarpum (Schrank et Mart. ex DC.) Triana	x	x	x	x				
Meliaceae	*Cabralea canjerana* (Vell.) Mart.	x	x	x	x	x	x	x	x
	Cedrela fissilis Vell.	x	x	x	x	x	x	x	
	Guarea macrophylla Vahl	x	x	x	x	x	x	x	x
	Trichilia casaretti C.DC.				x	x	x	x	x
	Trichilia catigua A.Juss.	x	x	x	x	x	x	x	x
	Trichilia emarginata (Turcz.) C.DC.	x	x	x	x	x	x	x	x
	Trichilia pallens C.DC.						x	x	x
	Trichilia pallida Sw.	x	x	x	x	x	x	x	x
Monimiaceae	*Mollinedia argyrogyna* Perkins	x	x	x	x	x	x	x	x

	Mollinedia lanceolata Ruiz & Pav.						x	x	x
	Mollinedia widgrenii A.DC.	x	x	x	x	x	x	x	x
Moraceae	*Ficus gomelleira* Kunth	x	x						
	Ficus pertusa L.f.	x	x	x	x	x	x	x	x
	Sorocea bonplandii (Baill.) W.C.Burger et al.	x	x	x	x	x	x	x	x
Myrtaceae	*Blepharocalyx salicifolius* (Kunth) O.Berg	x	x	x	x	x	x	x	x
	Calyptranthes widgreniana O.Berg		x	x	x	x	x	x	x
	Eugenia acutata Miq.	x	x	x	x	x	x	x	x
	Eugenia cerasiflora Miq.	x	x	x	x	x	x	x	x
	Eugenia dodonaeifolia Cambess.	x	x	x	x				
	Eugenia florida DC.	x	x	x	x	x	x	x	x
	Eugenia francavilleana O.Berg				x	x			
	Eugenia handroana D.Legrand							x	x
	Eugenia hiemalis Cambess.	x	x	x	x	x	x	x	x
	Eugenia involucrata DC.				x	x			
	Eugenia sonderiana O.Berg	x	x	x	x	x	x	x	x
	Myrcia cruciflora A.R.Lourenço & E.Lucas	x	x	x	x	x	x	x	x
	Myrcia eriocalyx DC.	x	x	x	x	x	x	x	
	Myrcia hebepetala DC.	x	x	x	x	x		x	x
	Myrcia neoclusiifolia A.R.Lourenço & E.Lucas	x	x	x	x	x	x	x	x
	Myrcia racemosa (O.Berg) Kiaersk.	x	x	x	x	x	x	x	x
	Myrcia splendens (Sw.) DC.	x	x	x	x	x	x	x	x
	Myrcia subcordata DC.	x	x	x	x	x	x	x	x
	Myrcia tomentosa (Aubl.) DC.	x	x	x	x				
	Myrcia vellozoi Mazine	x	x	x	x	x	x	x	x
	Myrcia venulosa DC.	x	x	x	x	x	x	x	x
	Myrciaria floribunda (H.West ex Willd.) O.Berg				x	x	x		x

	Pimenta pseudocaryophyllus (Gomes) Landrum	x	x	x	x	x	x	x	
	Psidium rufum Mart. ex DC.	x	x	x	x	x	x	x	x
	Siphoneugena crassifolia (DC.) Proença & Sobral	x	x	x	x	x	x	x	x
	Siphoneugena densiflora O.Berg	x	x	x	x	x	x	x	x
	Siphoneugena reitzii D.Legrand				x	x	x	x	x
Nyctaginaceae	*Guapira graciliflora* (Mart. ex Schmidt) Lundell	x	x	x	x	x	x	x	x
	Guapira opposita (Vell.) Reitz	x	x	x	x	x	x	x	x
Ochnaceae	*Ouratea semiserrata* (Mart. & Nees) Engl.			x	x	x	x	x	x
Olacaceae	*Heisteria silvianii* Schwacke	x	x	x	x	x	x	x	x
Opiliaceae	*Agonandra excelsa* Griseb.	x	x	x	x	x	x	x	x
Pentaphylacaceae	*Ternstroemia brasiliensis* Cambess				x				
Peraceae	*Pera glabrata* (Schott) Baill.	x	x	x	x	x	x	x	x
Polygonaceae	*Coccoloba warmingii* Meisn.	x	x	x	x	x	x	x	x
Primulaceae	*Myrsine coriacea* (Sw.) R.Br. ex Roem. & Schult.	x	x				x	x	x
	Myrsine gardneriana A.DC.	x	x	x	x	x	x	x	x
	Myrsine lineata (Mez) Imkhan.	x	x	x	x	x	x	x	x
	Myrsine umbellata Mart.	x	x	x	x	x	x	x	x
Proteaceae	*Roupala montana* Aubl.	x	x						
Rhamnaceae	*Colubrina glandulosa* Perkins	x	x	x	x	x	x	x	x
Rubiaceae	*Alseis floribunda* Schott							x	x
	Amaioua guianensis Aubl.	x	x	x	x	x	x	x	x
	Amaioua intermedia Mart. ex Schult. & Schult.f.	x	x	x	x	x	x	x	x
	Cordiera concolor (Cham.) Kuntze	x	x	x	x	x	x	x	x
	Cordiera sessilis (Vell.) Kuntze	x	x	x	x	x	x	x	x
	Coutarea hexandra (Jacq.) K.Schum.						x	x	x
	Faramea hyacinthina Mart.						x	x	x
	Faramea latifolia (Cham. & Schltdl.) DC.	x	x	x	x	x	x	x	x

	Faramea marginata Cham.	x	x	x	x	x	x	x	x
	Ixora brevifolia Benth.	x	x	x	x	x	x	x	x
	Psychotria vellosiana Benth.		x	x	x	x	x	x	x
	Rudgea viburnoides (Cham.) Benth.	x	x	x	x	x	x	x	x
Rutaceae	*Esenbeckia febrifuga* (A.St.-Hil.) A. Juss. ex Mart.						x	x	x
	Galipea jasminiflora (A.St.-Hil.) Engl.	x	x	x	x	x	x	x	x
	Metrodorea stipularis Mart.	x	x	x	x	x	x	x	x
	Zanthoxylum caribaeum Lam.	x	x	x	x	x	x	x	x
	Zanthoxylum fagara (L.) Sarg.					x			
	Zanthoxylum monogynum A.St.-Hil.		x	x					
	Zanthoxylum rhoifolium Lam.	x	x	x	x	x	x	x	x
Salicaceae	*Casearia arborea* (Rich.) Urb.	x	x	x	x	x	x	x	x
	Casearia decandra Jacq.	x	x	x	x	x	x	x	x
	Casearia lasiophylla Eichler	x	x	x	x	x	x	x	x
	Casearia obliqua Spreng.	x	x	x	x	x	x	x	x
	Casearia sp.								x
	Casearia sylvestris Sw.	x	x	x	x	x	x	x	x
	Xylosma ciliatifolia (Clos) Eichler	x	x						
Sapindaceae	*Allophylus edulis* (A.St.-Hil. et al.) Hieron. ex Niederl.					x			
	Cupania vernalis Cambess.	x	x						
	Cupania zanthoxyloides Radlk.			x	x	x	x	x	x
	Diatenopteryx sorbifolia Radlk.	x	x	x	x	x	x	x	x
Siparunaceae	*Siparuna brasiliensis* (Spreng.) A.DC.								x
	Siparuna guianensis Aubl.	x	x	x	x	x	x	x	x
Solanaceae	*Solanum leucodendron* Sendtn.	x	x	x	x	x	x	x	x
	Solanum pseudoquina A.St.-Hil.	x	x	x	x				
Styracaceae	*Styrax camporum* Pohl		x	x	x	x	x	x	x

	Styrax latifolius Pohl	x	x	x	x	x	x	x	x
	Styrax pohlii A.DC.	x	x	x	x	x	x	x	x
Thymelaeaceae	*Daphnopsis fasciculata* (Meisn.) Nevling	x	x	x	x	x	x	x	x
	Daphnopsis utilis Warm.	x	x	x	x	x	x	x	x
Urticaceae	*Cecropia glaziovii* Snethl.		x	x					
	Cecropia pachystachya Trécul	x	x	x	x	x	x	x	x
Vochysiaceae	*Qualea cryptantha* (Spreng.) Warm.								x
	Qualea grandiflora Mart.	x	x	x	x	x	x	x	x
	Qualea multiflora Mart.	x	x	x	x	x	x	x	x
	Vochysia tucanorum Mart.	x	x	x	x	x	x	x	x

Os levantamentos florísticos, principalmente os monitoramentos ecológicos de longa duração, estão sujeitos a equívocos e ajustes nomenclaturais. Assim, podemos inferir que, por exemplo, a ocorrência de algumas espécies em apenas um inventário pode estar atrelada a estes fatores. Contudo, é importante ressaltar que, durante o inventário florestal é de suma importância que o profissional se atente à coleta de materiais botânicos que auxiliem a identificação de forma eficaz.

6. Estrutura diamétrica

A caracterização da estrutura diamétrica abrange a definição do número de indivíduos arbóreos, isto é, de árvores, por classe de diâmetro (ARAÚJO et al., 2018; BATISTA et al., 2016). Além de estrutura vertical e distribuição diamétrica, essa caracterização também pode ser denominada como distribuição dos diâmetros.

A distribuição diamétrica também se caracteriza como um importante procedimento subsidiando o conhecimento quanto à sucessão ecológica na floresta de interesse, tipo de vegetação, status de conservação e regimes de manejo (IMAÑA-ENCINAS et al., 2013). Nesse sentido, é possível inferir quanto ao crescimento e desenvolvimento da formação florestal, bem como em relação à dinâmica (BATISTA et al., 2016; IMAÑA-ENCINAS et al., 2013; VILLANOVA et al., 2018).

A distribuição dos diâmetros é usualmente verificada por meio de histogramas de frequência. Para tanto, estabelece-se o número e amplitude de classes de diâmetro. A definição deste procedimento pode ser realizada de forma empírica ou estatística. Para a análise da estrutura diamétrica na Matinha da UFLA, procedeu-se com a determinação empírica. Este procedimento foi definido para se estabelecer um mesmo número de classes para todos os anos, possibilitando assim uma melhor comparação ao longo dos intervalos mensurados. Assim, foram definidas 10 classes com amplitude de 10 cm de diâmetro a 1,30 metros do solo.

De forma geral, para a distribuição diamétrica de florestas inequiâneas, espera-se encontrar uma curva de distribuição exponencial negativa. Em outras palavras, essa curva apresenta-se em forma de j-invertido ou j-inverso (ARAÚJO et al., 2018; PONTES; ENGEL; PARROTTA, 2019; VILLANOVA et al., 2018). Esse comportamento implica em uma maior concentração dos indivíduos arbóreos nas menores classes de diâmetro (BATISTA et al., 2016; VILLANOVA et al., 2018). A saber, a denominação de florestas inequiâneas está intrinsecamente relacionada com as formações naturais, em que há uma variação na idade das árvores que compõem a comunidade vegetal.

Para o fragmento da Matinha da UFLA, a distribuição diamétrica apresentou o comportamento esperado para uma floresta nativa, isto é, j-inverso. Ao longo dos anos de mensuração é possível visualizar uma maior concentração das árvores na primeira classe diamétrica. A partir do ano de 2006, a migração dos indivíduos arbóreos menores para as classes posteriores fica mais nítida, principalmente para as classes de 35 e 45 cm (Figura 4).

A análise da distribuição dos indivíduos arbóreos em classes diamétricas também está diretamente atrelada à interpretação da dinâmica da comunidade (ARAÚJO et al., 2018; VILLANOVA et al., 2018). Em outras palavras, a partir desta avaliação é possível compreender quanto aos padrões de recrutamento e mortalidade dentro do remanescente florestal (ARAÚJO et al., 2018; VILLANOVA et al., 2018). Uma vez que a "Matinha da UFLA" é uma área de preservação permanente, uma menor perturbação é identificada no fragmento. Assim, a estabilidade do número de árvores entre as classes de diâmetro pode estar atrelado ao status de conservação da área.

Figura 4 - Distribuição diamétrica dos indivíduos arbóreos amostrados ao longo dos 30 anos de mensuração na Matinha da UFLA. Em que o eixo x representa o centro de classe do diâmetro à 1,30 metros do solo; eixo y é a frequência, isto é, quantos indivíduos ocorrem na classe de interesse no ano.

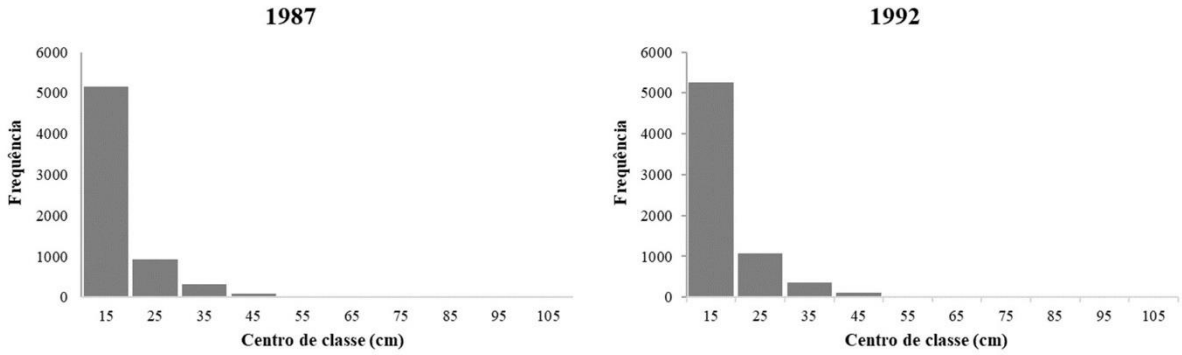

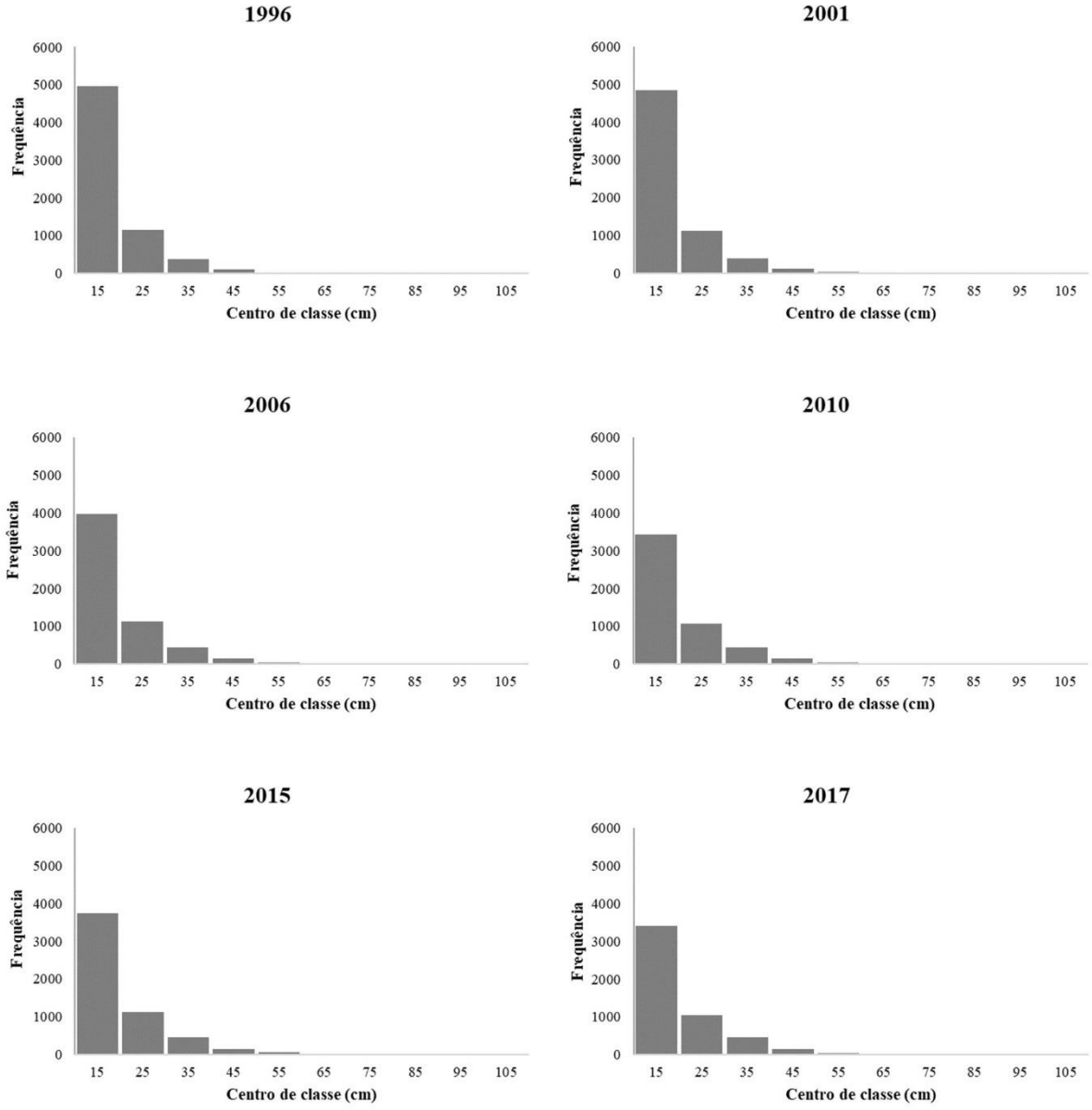

A composição florística, assim como a distribuição dos indivíduos arbóreos permitem afirmar que, após a proteção integral da área, o fragmento está avançando no aspecto da sucessão. Em outras palavras, as espécies tardias, com estratégias conservacionistas estão tomando lugar no remanescente quando comparado com as espécies pioneiras (POORTER et al., 2019). Este comportamento permite inferir que ocorre um auto desbaste na floresta e, consequentemente, uma diminuição do número de árvores. Contudo, os indivíduos remanescentes são as plantas com maiores diâmetros, o que representa uma maior contribuição para a biomassa (ARCANJO; TOREZAN, 2023). Em suma, as espécies conservativas possuem a capacidade de sobreviver em áreas com limitação nos recursos disponíveis (WIGLEY et al., 2016).

7. Grau de ocupação e estimativa da biomassa acima do solo

A área basal é uma importante variável florestal. Esta característica indica o grau de ocupação que os indivíduos arbóreos representam em uma formação vegetal e é usualmente expressa em metros quadrados por hectare (m^2/ha).

Durante o período de avaliação na Matinha da UFLA, observou-se uma tendência de diminuição no número de indivíduos por hectare. Contudo, a área basal apresentou um comportamento contrário. Em outras palavras, a área basal apresentou um crescimento ao longo dos 30 anos de mensuração (variando de 19,35 m^2/ha em 1987 a 24,63 m^2/ha em 2015. Apenas no ano de 2017 houve um pequeno decréscimo na média da área basal (Figura 5A).

O aumento em área basal para o fragmento pode estar atrelado com o crescimento dos indivíduos arbóreos sobreviventes. Este comportamento é esperado em formações em recuperação pós-distúrbio. Como destacado, o fragmento antes explorado, passou a ter a sua área totalmente protegida. Além disso, é importante ressaltar que a região na qual a formação florestal está situada passou por um crítico período de seca entre os anos de 2014 e 2017, o que possivelmente afetou a dinâmica da floresta. Nesse sentido, as consequências na estrutura e composição da floresta são observadas nos anos posteriores de mensuração.

Figura 5 - Distribuição da média em área basal por hectare (A) e biomassa acima do solo (AGB) (B) para o fragmento de Floresta Estacional Semidecidual Montana, Matinha da UFLA, situado na região sudeste do Brasil.

A)

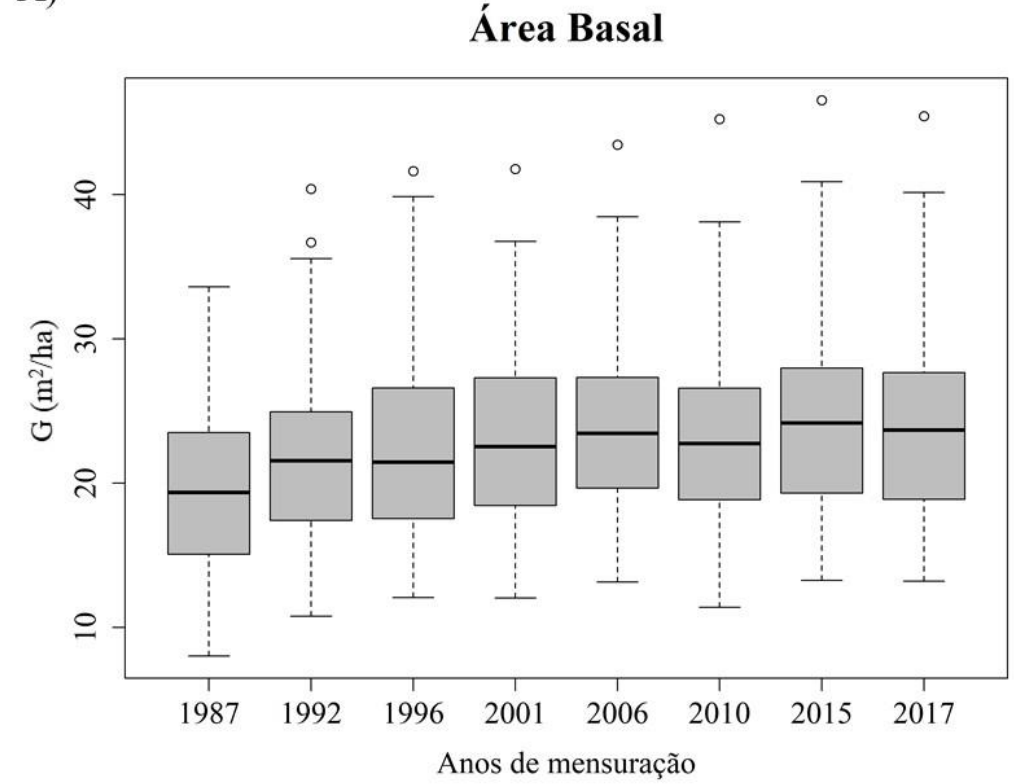

B)

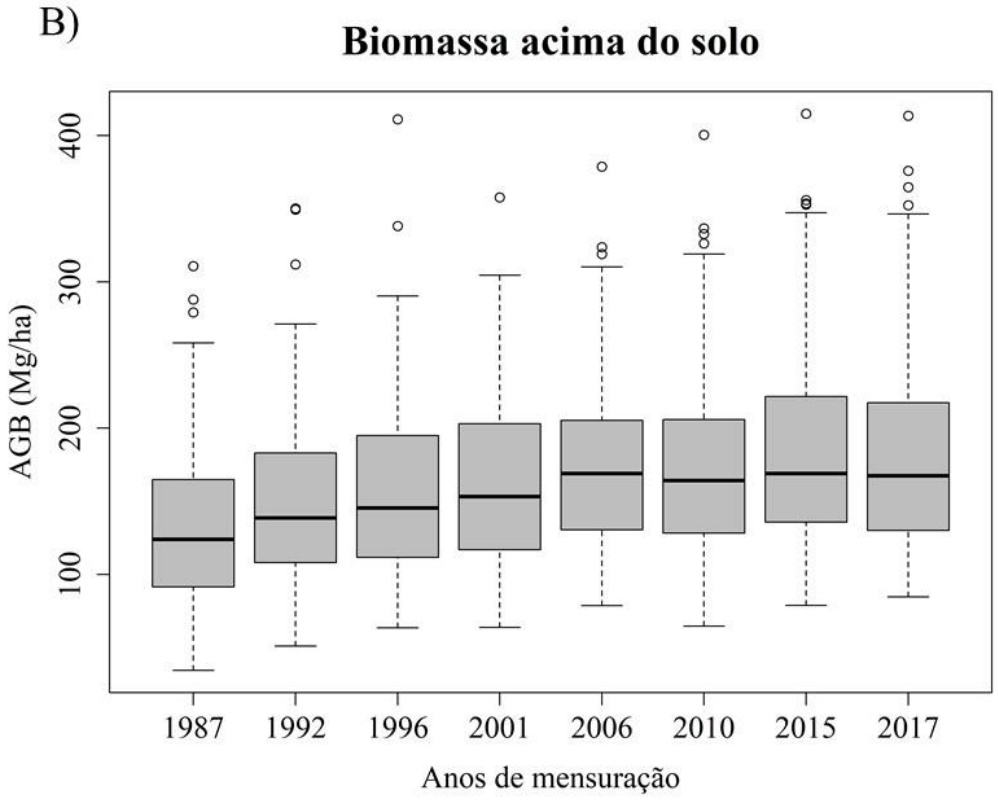

Em adição a área basal, a biomassa acima do solo se caracteriza como uma importante variável da floresta. A saber, ambas são altamente correlacionadas, isto é, quanto maior a área

basal, maior a biomassa (CLARK; CLARK, 2000; TEIXEIRA et al., 2020). Conhecida também como AGB, da abreviação de *Aboveground Biomass*, essa variável é usualmente empregada para a determinação do estoque de carbono em uma determinada área. Além disso, a quantificação da biomassa acima do solo e, consequentemente, do carbono estocado, é de suma relevância na definição de estratégias públicas e políticas ambientais. O intuito dessas medidas está diretamente relacionado com a definição de planos que visem frear o desmatamento e a degradação ambiental. Tais atividades são consideradas as principais fontes no aumento da emissão de dióxido de carbono (CO_2), um dos gases responsáveis pelo efeito estufa.

A biomassa acima do solo pode ser quantificada de forma direta ou indireta (FAN et al., 2020; TORRE-TOJAL et al., 2022). No método direto realiza-se o abate das árvores, isto é, os indivíduos arbóreos são cortados (SAFARI; SOHRABI, 2020; TORRE-TOJAL et al., 2022; WAI; SU; LI, 2022). Posteriormente, emprega-se a mensuração dos compartimentos da árvore (SAFARI; SOHRABI, 2020; TORRE-TOJAL et al., 2022; WAI; SU; LI, 2022). Já o método indireto é baseado no uso de equações alométricas que são ajustadas por meio de medidas diretas. Nesse sentido, a aplicação deste procedimento requer dados de densidade da madeira, diâmetro a 1,30 metros do solo e, em alguns casos, altura total da árvore.

Para a análise da biomassa acima do solo na "Matinha da UFLA", empregou-se a equação proposta por Chave et al. (2014) e modificada por Réjou-Méchain et al. (2017) (Equação 1). Esta equação é recomendada quando não há disponibilidade de dados de altura dos indivíduos arbóreos. Assim, a equação possui como variáveis independentes o diâmetro à 1,30 metros do solo (DAP), a densidade da madeira e uma medida de estresse ambiental (E), esta obtida por meio das coordenadas geográficas. A densidade da madeira é determinada por espécie e obtida por meio do banco de dados *The Global Wood Density* (GWD) (ZANNE et al., 2009). Contudo, caso não tenha a informação por espécie, a densidade é definida pela média do gênero, família ou do conjunto de dados. O processamento da biomassa acima do solo ocorreu por meio do pacote *Biomass* (RÉJOU-MÉCHAIN et al., 2017), a partir do uso do software R (R CORE TEAM, 2020).

$$AGB = exp\ (-2.024 - 0.896*E + 0.920*log(WD) + 2.795*log(D) - 0.0461*(log(D)^2))$$

Equação 1

Em que:

AGB: Above ground biomass (biomassa acima do solo);

exp: Exponencial;

E: Variável de estresse ambiental;

WD: Wood density (densidade da madeira) (g.cm^3);
log: logaritmo;
D: Diâmetro à 1,30 metros do solo (DAP).

De forma geral, a biomassa acima do solo apresentou um comportamento semelhante à área basal para o fragmento. Em outras palavras, a biomassa acima do solo apresentou médias crescentes ao longo dos anos de mensuração (variando entre 131,48 Mg/ha em 1987 e 184,41 Mg/ha em 2015). No intervalo entre os anos de 2015 e 2017, houve uma diminuição de 2,52 Mg/ha (Figura 5B). Esta redução está relacionada com a redução da área basal de 2015 para 2017 (Figura 5A). O aumento da biomassa acima do solo encontrada é resultado do crescimento das árvores já existentes na área. No último intervalo de mensuração (2015-2017), a diminuição da biomassa observada pode estar associada com a perda expressiva de indivíduos com menor diâmetro. Além disso, esta redução também pode estar atrelada com o evento de seca que ocorreu na região nos anos que antecedem o intervalo.

8. Considerações finais

O conhecimento da estrutura e composição florestal de uma determinada formação vegetal é de suma relevância. A partir das informações obtidas é possível compreender quanto a riqueza de espécies, crescimento e dinâmica florestal da comunidade. O levantamento de tais informações possibilita propor estratégias que viabilizem a conservação das áreas naturais. Além disso, estes estudos podem ser fontes para planos de recuperação e restauração de áreas com as mesmas características.

As formações florestais, principalmente no que diz respeito às florestas tropicais, possuem grande importância na conservação da biodiversidade e na manutenção de estoque e sequestro de carbono. Contudo, devido às fortes pressões antrópicas sofridas, estes ambientes estão passando de atuantes na absorção para fontes de emissão do dióxido de carbono. Além de fatores como o desmatamento e degradação ambiental, as condições climáticas também possuem forte influência sobre a biomassa. Nesse sentido, conhecer a dinâmica da floresta e entender como esses ecossistemas respondem a eventos extremos, como a seca, subsidiam a elaboração de medidas preventivas.

Referências

ALVARES, C. A. et al. Köppen's climate classification map for Brazil. **Meteorologische Zeitschrift**, v. 22, n. 6, p. 711–728, 2014.

ARAÚJO, L. H. B. DE et al. Spatial Distribution and Diametric Structure of Tree Species in a Dense Ombrophilous Forest in Rio Grande do Norte, Brazil. **Journal of Experimental Agriculture International**, v. 28, n. 2, p. 1–10, 2018.

ARCANJO, F. A.; TOREZAN, J. M. D. Aboveground biomass accumulation and tree size distribution in seasonal Atlantic Forest restoration sites. **Restoration Ecology**, v. 31, n. 1, p. 1–7, 2023.

BATISTA, A. P. B. et al. Dynamics and Prediction of Diametric Structure in Two Atlantic Forest Fragments in Northeastern Brazil. **Revista Árvore**, v. 40, n. 2, p. 307–317, 2016.

BOTREL, M. C. G.; CARVALHO, D. DE. Variabilidade isoenzimática em populações naturais de jacarandá paulista (Machaerium villosum Vog.). **Revista Brasileira de Botânica**, v. 27, n. 4, p. 621–627, 2004.

BRASIL. **Lei no 12.727 de 17 de outubro de 2012 do Código Florestal.**, 2012. Disponível em: <www.planalto.gov.br/ccivil_03/_ato2011-2014/2012/lei/l12651.htm?fbclid=IwAR2qP30j%0AZN_N4bL86v9rddVqSN-PNdypSi3HJzhB8kJz5nQR91ekBgLs30U%0A>

CALIMAN, J. P. et al. Seasonal pattern of nutrient cycling in the Atlantic Forest across a topographic gradient. **Scientia Forestalis/Forest Sciences**, v. 48, n. 125, p. 1–16, 2020.

CHAVE, J. et al. Improved allometric models to estimate the aboveground biomass of tropical trees. **Global Change Biology**, v. 20, n. 10, p. 3177–3190, 2014.

CLARK, D. B.; CLARK, D. A. Landscape-scale variation in forest structure and biomass in a tropical rain forest. **Forest Ecology and Management**, v. 137, n. 1–3, p. 185–198, 2000.

CUNHA, E. R. DA et al. Future scenarios based on a CA-Markov land use and land cover simulation model for a tropical humid basin in the Cerrado/Atlantic forest ecotone of Brazil. **Land Use Policy**, v. 101, n. September 2020, 2021.

FAN, G. et al. AdQSM: A new method for estimating above-ground biomass from TLS point clouds. **Remote Sensing**, v. 12, n. 18, 2020.

FENGLER, F. H. et al. Fengler, F. H., Moraes, J. F. L. de, Ribeiro, A. I., Carvalho, M. M., Filho, A. P., Medeiros, G. A. de, … Faria, L. de A. (2020). A framework to evaluate the environmental quality and simulate future scenarios of urban forests: atlantic forest case study. **IEEE International Smart Cities Conference**, p. 1–8, 2020.

FERREIRA, I. J. M. et al. Spatial dimension landscape metrics of atlantic forest remnants in paraná state, Brazil. **Acta Scientiarum - Technology**, v. 40, p. 1–8, 2018.

FIGUEIREDO, J. C. G. et al. Relationship of woody species composition with edaphic characteristics in threatened riparian Atlantic Forest remnants in the upper Rio Doce basin, Brazil. **Nordic Journal of Botany**, v. 2022, n. 11, p. 1–10, 2022.

GOMES, G. et al. Botanical Composition of Fabaceae Family in the Brazilian Northeast, Maranhão, Brazil. **Asian Journal of Environment & Ecology**, v. 6, n. 4, p. 1–10, 2018.

GUAUQUE-MELLADO, D. et al. Evapotranspiration under Drought Conditions: The Case Study of a Seasonally Dry Atlantic Forest. **Atmosphere**, v. 13, n. 6, 2022.

HERTZOG, L. R. et al. Forest fragmentation modulates effects of tree species richness and composition on ecosystem multifunctionality. **Ecology**, v. 100, n. 4, p. 1–9, 2019.

IMAÑA-ENCINAS, J. et al. Dendrometrical characteristics of an atlantic forest fragment at santa maria de jnetbá county, state of espirito Santo, Brazil. **Floresta**, v. 43, n. 2, p. 255–260, 2013.

INMET. **NORMAIS CLIMATOLÓGICAS DO BRASIL 1991-2020**. Disponível em: <https://portal.inmet.gov.br/normais#>.

JOLY, C. A.; METZGER, J. P.; TABARELLI, M. Experiences from the Brazilian Atlantic Forest: Ecological findings and conservation initiatives. **New Phytologist**, v. 204, p. 459–473, 2014a.

JOLY, C. A.; METZGER, J. P.; TABARELLI, M. Experiences from the Brazilian Atlantic Forest: Ecological findings and conservation initiatives. **New Phytologist**, v. 204, n. 3, p. 459–473, 2014b.

JUNQUEIRA JUNIOR, J. A. et al. Time-stability of soil water content (SWC) in an Atlantic Forest - Latosol site. **Geoderma**, v. 288, p. 64–78, 2017.

LAURANCE, W. F. et al. Rapid decay of tree-community composition in Amazonian forest fragments. **Proceedings of the National Academy of Sciences of the United States of America**, v. 103, n. 50, p. 19010–19014, 2006.

LIMA, A. A. DE et al. Impacts of climate changes on spatio-temporal diversity patterns of Atlantic Forest primates. **Perspectives in Ecology and Conservation**, v. 17, n. 2, p. 50–56, 2019.

LIMA, R. A. F. DE et al. The erosion of biodiversity and biomass in the Atlantic Forest biodiversity hotspot. **Nature Communications**, v. 11, n. 1, p. 1–16, 2020.

LIRA, P. K.; PORTELA, R. DE C. Q.; TAMBOSI, L. R. Land-Cover Changes and an Uncertain Future: Will the Brazilian Atlantic Forest Lose the Chance to Become a Hopespot? In: MARQUES, M. C. M.; GRELLE, C. E. V. (Eds.). . **The Atlantic Forest: History, Biodiversity, Threats and Opportunities of the Mega-diverse Forest**. [s.l: s.n.]. p. 233–251.

MAGNAGO, L. F. S. et al. Would protecting tropical forest fragments provide carbon and biodiversity cobenefits under REDD+? **Global Change Biology**, v. 21, n. 9, p. 3455–3468, 2015.

MANTOVANI, V. A. et al. Spatial and Temporal Patterns in Carbon and Nitrogen Inputs by Net Precipitation in Atlantic Forest, Brazil. **Forest Science**, v. 68, n. 1, p. 113–124, 2022.

MARCILIO-SILVA, V.; MARQUES, M. C. M.; CAVENDER-BARES, J. Land-use trade-offs between tree biodiversity and crop production in the Atlantic Forest. **Conservation Biology**, v. 32, n. 5, p. 1074–1084, 2018.

MITCHELL, M. G. E.; BENNETT, E. M.; GONZALEZ, A. Forest fragments modulate the provision of multiple ecosystem services. **Journal of Applied Ecology**, v. 51, n. 4, p. 909–918, 2014.

MOREIRA, D. M. et al. Floristic survey in an Atlantic Forest remnant in the Recôncavo da Bahia, Bahia State, Brazil. **Hoehnea**, v. 47, 2020.

MYERS, N. et al. Biodiversity hotspots for conservation priorities. **Nature**, v. 403, p. 853–858, 2000.

OLIVEIRA-FILHO, A. T. DE; MELLO, J. M. DE; SCOLFORO, J. R. S. Effects of past disturbance and edges on tree community structure and dynamics within a fragment of tropical semideciduos forest in south-eastern Brazil over a five-year period (1987-1882). **Plant EcologyPlant Ecology**, v. 131, p. 45–66, 1997.

PEREIRA, K. M. G. et al. Protection status as determinant of carbon stock drivers in Cerrado sensu stricto. **Journal of Plant Ecology**, v. 13, n. 3, p. 361–368, 2020.

PONTES, D. M. F.; ENGEL, V. L.; PARROTTA, J. A. Forest structure,wood standing stock, and tree biomass in different restoration systems in the Brazilian Atlantic forest. **Forests**, v. 10, n. 7, p. 1–18, 2019.

POORTER, L. et al. Biodiversity and climate determine the functioning of Neotropical forests. **Global Ecology and Biogeography**, v. 26, n. 12, p. 1423–1434, 2017.

POORTER, L. et al. Wet and dry tropical forests show opposite successional pathways in wood density but converge over time. **Nature Ecology and Evolution**, v. 3, n. 6, p. 928–934, 2019.

R CORE TEAM. **R: A language and environment for statistical computing.R Foundation for Statistical Computing,**Vienna, Austria, 2020. Disponível em: <https://www.r-project.org/.>

RÉJOU-MÉCHAIN, M. et al. Biomass: an R package for estimating above-ground biomass and its uncertainty in tropical forests. **Methods in Ecology and Evolution**, v. 8, p. 1163–1167, 2017.

RODRIGUES, A. C.; VILLA, P. M.; NERI, A. V. Fine-scale topography shape richness, community composition, stem and biomass hyperdominant species in Brazilian Atlantic forest. **Ecological Indicators**, v. 102, n. May 2018, p. 208–217, 2019.

RODRIGUES, A. F. et al. Modeling canopy interception under drought conditions: The relevance of evaporation and extra sources of energy. **Journal of Environmental Management**, v. 292, n. January, 2021.

SAFAR, N. V. H.; MAGNAGO, L. F. S.; SCHAEFER, C. E. G. R. Resilience of lowland Atlantic forests in a highly fragmented landscape: Insights on the temporal scale of landscape restoration. **Forest Ecology and Management**, v. 470–471, n. September 2019, p. 118183, 2020.

SAFARI, A.; SOHRABI, H. Integration of synthetic aperture radar and multispectral data for aboveground biomass retrieval in Zagros oak forests, Iran: an attempt on Sentinel imagery. **International Journal of Remote Sensing**, v. 41, n. 20, p. 8069–8095, 2020.

SANO, E. E. et al. Cerrado ecoregions: A spatial framework to assess and prioritize Brazilian savanna environmental diversity for conservation. **Journal of Environmental Management**, v. 232, n. July 2018, p. 818–828, 2019.

SCOTT, C. T.; GOVE, J. H. Forest inventory. In: EL-SHAARAWI, A. H.; PIEGORSH, W. W. (Eds.). . **Encyclopedia of Environmetrics**. Chichester: John Wiley & Sons, 2002. v. 2p. 814–820.

SILVA, J. C. DA; SANTOS, D. S. DOS; ROCHA, T. B. DA. Identifying geomorphological diversity hotspots for conservation purposes: Application to a coastal protected area in Rio de Janeiro State, Brazil. **Applied Geography**, v. 142, n. March, p. 102689, 2022.

SILVA OLIVEIRA, F. G. DA et al. Medicinal Plants with Acetylcholinesterase Inhibitory Activity: Therapeutic Potential of Brazilian Plants for the Treatment of Alzheimer's Disease. **Pharmacognosy Reviews**, v. 13, n. 26, p. 45–49, 2021.

SINGH, M.; HUANG, Z. Analysis of Forest Fire Dynamics, Distribution and Main Drivers in the Atlantic Forest. **Sustainability (Switzerland)**, v. 14, n. 2, 2022.

SOUZA, C. R. et al. Long-term ecological trends of small secondary forests of the atlantic forest hotspot: A 30-year study case. **Forest Ecology and Management**, v. 489, n. February, 2021.

TEIXEIRA, H. M. et al. Linking vegetation and soil functions during secondary forest succession in the Atlantic forest. **Forest Ecology and Management**, v. 457, n. July 2019, p. 117696, 2020.

TORRE-TOJAL, L. et al. Above-ground biomass estimation from LiDAR data using random

forest algorithms. **Journal of Computational Science**, v. 58, 2022.

VELOSO, H. P.; RANGEL FILHO, A. L. R.; LIMA, J. C. A. **Classificação da Vegetação Brasileira Adaptada a um Sistema Universal**. [s.l: s.n.].

VIBRANS, A. C. et al. Insights from a large-scale inventory in the southern Brazilian Atlantic Forest. **Scientia Agricola**, v. 77, n. 1, p. 1–12, 2020.

VILLANOVA, P. H. et al. Prognosis of the Diameter Distribution and Carbon Stock in a Secondary Atlantic Forest By Markov Chain. **Revista Árvore**, v. 42, n. 2, 2018.

VILLANOVA, P. H. et al. Carbon stock growth in a secondary atlantic forest. **Revista Arvore**, v. 43, n. 4, p. 1–9, 2019.

WAI, P.; SU, H.; LI, M. Estimating Aboveground Biomass of Two Different Forest Types in Myanmar from Sentinel-2 Data with Machine Learning and Geostatistical Algorithms. **Remote Sensing**, v. 14, n. 9, 2022.

WIGLEY, B. J. et al. Leaf traits of African woody savanna species across climate and soil fertility gradients: evidence for conservative versus acquisitive resource-use strategies. **Journal of Ecology**, v. 104, n. 5, p. 1357–1369, 2016.

ZANNE, A. E. et al. **Data from: Towards a Worldwide Wood Economics Spectrum.** Disponível em: <https://doi.org/10.5061/dryad.234>.

ANEXO A – Portaria N° 212

Portaria N° 212 que declara a Matinha da UFLA como uma área de preservação permanente.

SERVIÇO PÚBLICO FEDERAL

Portaria n.º 212 de 01 de junho de 19 92

O Diretor da Escola Superior de Agricultura de Lavras, no uso de suas atribuições regimentais, e "Ad Referendum" da Congregação,

RESOLVE:

Declarar de preservação permanente, as áreas localizadas no Campus da ESAL, recobertas com vegetação nativa.

SILAS COSTA PEREIRA
Diretor da ESAL

ARTIGO I

The effect of seasonal droughts on remotely sensed-based predictive variables of forest aboveground biomass

Natielle Gomes Cordeiro, Kelly Marianne Guimarães Pereira, Inácio Thomaz Bueno, André Ferreira Rodrigues, Marcela de Castro Santos Nunes Terra, José Márcio de Mello

Artigo a ser publicado

The effect of seasonal droughts on remotely sensed-based predictive variables of forest aboveground biomass

ABSTRACT

Forests are related to the global carbon cycle by playing a vital role in climate mitigation. However, carbon storage may shift as a function of intense global climate changes, especially considering the forest aboveground biomass (AGB). Actually, droughts have been pointed out as one of the main drivers of AGB decrease. Thus, accurate biomass estimates are needed for public policy elaboration of forest conservation. Our study aimed to evaluate the predictive capacity of radar and optical sensors products to estimate AGB during the years of 2015 and 2017 in an Atlantic Forest remnant. We have modeled the AGB using Sentinel-1 and Sentinel-2 images, as well as Gray Level Co-occurrence Matrix (GLCM) textures, considering the weather seasonality (dry and wet season). The AGB estimates were 184.41 Mg/ha and 181.90 Mg/ha in 2015 and 2017, respectively. SAR signal was directly proportional to AGB in 2015, which means that higher backscatter in leaves were related to a higher biomass accumulation. On the other hand, only optical variables were selected for the AGB estimates in 2017. Overall, our findings pointed out that the synergy of optical and radar satellite' images with the GLCM texture is a great and accurate method to estimate AGB.

Keywords: Tropical Forest; Atlantic Forest; Gray level co-occurrence matrix; Radar imagery; Optical imagery.

1. Introduction

Droughts are natural hazards that affect the different phases of the hydrological cycle (i.e., soil, streams, and groundwater), ecosystems, and society. Although drought behavior and drivers are most investigated from the hydrological point-of-view (VAN LOON, 2015; VAN LOON et al., 2019), its impacts on biomes and the likely feedback still demand a deep investigation. Droughts have been pointed out as one of the main drivers of aboveground biomass (AGB) decrease, mainly during extreme events (XU et al., 2019). Therefore, a more significant impact on vegetation is expected in the near future as the frequency and severity of such events have risen over the past years (VICENTE-SERRANO et al., 2022). Forests are related to the global carbon cycle, playing a vital role in climate mitigation. However, carbon storage may shift as a function of intense global climate changes, especially considering the forest AGB.

The forest AGB estimates usually rely on tree species characteristics such as diameter, tree height, wood density, canopy, among others. Nevertheless, extreme climate events may affect tree morphology and plant community diversity. In terms of dry conditions, some species decrease transpiration (by closing their stomata) and lose their leaves in response to limited soil water (PIRASTEH-ANOSHEH et al., 2016). Overall, dry conditions influence the tree-specific traits, and, thus, affect the AGB estimates. As a potential indicator of carbon stocks, an accurate biomass estimation based on field campaigns is necessary (DAVID; ROSSER; DONOGHUE, 2022). However, field surveys are impractical due to their time-consuming and labor-intensive methodologies (SU et al., 2021). Thus, remote sensing has obtained an increasing interest in AGB estimation in the past years. Remotely sensed data shows great capacity in predicting forest variables once the satellites have good consistency in capturing land surface features. For instance, radar and optical data are commonly used to predict forest AGB (NUTHAMMACHOT et al., 2022; SAFARI; SOHRABI, 2020; SILVEIRA et al., 2019).

Synthetic aperture radar (SAR) can penetrate the forest canopy until a certain depth. Besides, SAR is not weather dependent and shows a sensitivity to the vegetation water content (BERNINGER et al., 2018; DAVID; ROSSER; DONOGHUE, 2022; SAFARI; SOHRABI, 2020). SAR satellites may have different wavelengths (e.g., X, C, L, P) and polarization (e.g., HH, VV, HV, VH). The X and C-band are classified as short-wavelength and show a better interaction with canopy elements (BERNINGER et al., 2018). On the other hand, the L and P-band are defined as long-wavelength and show greater relation to forest vertical structure (e.g., branch, trunk) (BERNINGER et al., 2018).

Optical satellites provide sensor data of different spatial, spectral, and temporal resolutions. The optical data processed using mathematical operations result in vegetation indices (e.g., normalized difference vegetation index - NDVI, enhanced vegetation index - EVI) crucial to understanding the spatio-temporal dynamics of vegetation systems (SILVEIRA et al., 2019). Due to the capacity of contrasting canopy reflectance, those indices are effective in analyzing forest dynamics and, consequently, used for AGB estimates (XUE; SU, 2017). Despite the broad use of optical data, some forest intrinsic characteristics (e.g., phenology and species diversity) may represent hindrances to the use of optical products for AGB prediction purposes. Thus, regardless of the remarkable potential of optical data for forest variable evaluation, it still faces limitations such as weather dependency, especially cloud cover (CHABALALA; ADAM; ALI, 2022; MERANER et al., 2020).

Overall, remote sensing data is efficient in estimating forest AGB (SAFARI; SOHRABI, 2020; SILVEIRA et al., 2019). However, data saturation problem may emerge in some vegetation types, especially areas with high biomass values (DAVID; ROSSER; DONOGHUE, 2022). In this context, new approaches have been explored to solve the saturation problem. Lately, texture related to remote data has become an important alternative to improve land cover or vegetation classification (MISHRA et al., 2019; XIE et al., 2019) and,

for that, it may be assumed that the texture may be helpful to AGB estimates. The most common texture measure is the grey-level co-occurrence matrix (GLCM) (GRÜNER; WACHENDORF; ASTOR, 2020; LIANG et al., 2022).

In summary, remote sensing data and grey-level co-occurrence matrix (GLCM) have the potential to predict the AGB in different vegetation types and densities (LI; ZHOU; XU, 2021; WAI; SU; LI, 2022). However, there is still a lack of information on how image collection over a seasonality may influence AGB estimates. Our study aimed to evaluate the predictive capacity of radar and optical sensors products in the estimates of AGB during the years 2015 and 2017 in an Atlantic Forest remnant. Specifically, we have modeled the AGB using Sentinel-1 and Sentinel-2 images, as well as GLCM textures, considering the weather seasonality (dry and wet season).

Tropical regions have experienced anomalously dry years in the last decades, and our study site went through a prolonged drought period between 2013 and 2019 (RODRIGUES et al., 2022). Forests show a late response to drought events (RODRIGUES et al., 2022), which expand their effects over multiple years (ANDEREGG et al., 2020). Thus, we hypothesize that radar images will stand out as better predictors to estimate AGB in 2015 since the forest structure was under a moderate drought to normal condition (GUAUQUE-MELLADO et al., 2022; RODRIGUES et al., 2021), given the sensitivity of radar to the vegetation water content. Meanwhile, we expect the optical images to better describe the AGB in 2017, when drought effects were more apparent in the forest, thus detectable by optical products.

2. Material and Methods

2.1. Study area

The study area comprises a seasonal Atlantic Forest remnant of 6.35 hectares in the Minas Gerais state, Southeast Brazil (Figure 1). The forest remnant is classified as semi-

deciduous at an advanced successional stage after full protection in 1986 (SOUZA et al., 2021). Semi-deciduousness is an adaptation of seasonally dry forests to couple with water-limited periods, which are characterized by trees that lose their leaves in such a way as to restrict the loss of water (OLIVEIRA-FILHO; FONTES, 2000). The forest canopy is heterogeneous and can be distributed into three compartments (TERRA et al., 2018): (i) the main body has trees ranging from 10 m to 15 m in height; (ii) higher trees (up to 20 m in height) scatter across the main body and forms the upper layer; and (iii) small trees, seedlings, and bushes compose the understory. Gaps arise due to fallen trees and complement the heterogeneity of the canopy formation (RODRIGUES et al., 2021).

The climate of the study area is Cwa (Köppen classification), which is characterized by rainy summers and dry winters (ALVARES et al., 2014). The region shows well-defined seasons (dry and wet), in which the dry season lasts from April to September and the wet season extends from October to March, i.e., the hydrological year starts in October of the previous year and ends in September. The mean annual temperature in the region ranges between 15.7°C and 27.5°C, whereas the mean annual precipitation is 1383.4 mm (INMET, 2023). The soil is classified as Dystrophic Red Latosol, and the relief is slightly undulated, ranging from 5 to 15%, with a mean altitude of 925 m a.s.l. (JUNQUEIRA JUNIOR et al., 2017).

There is a meteorological station placed in a clearing near the remnant, monitoring the rainfall, wind speed and direction, air temperature, solar radiation, and air humidity at a daily step spanning the period of 1960 to 2019. The prolonged drought was observed at the end of the monitoring period (hydrological years of 2013-2014, 2014-2015, 2015-2016, 2016-2017, 2017-2018, and 2018-2019), changing the hydrology and forest dynamics of the remnant (GUAUQUE-MELLADO et al., 2022; RODRIGUES et al., 2022). The hydrological years were classified as severely dry, moderately dry, near normal, moderately dry, severely dry, and near normal, respectively (GUAUQUE-MELLADO et al., 2022; RODRIGUES et al., 2022).

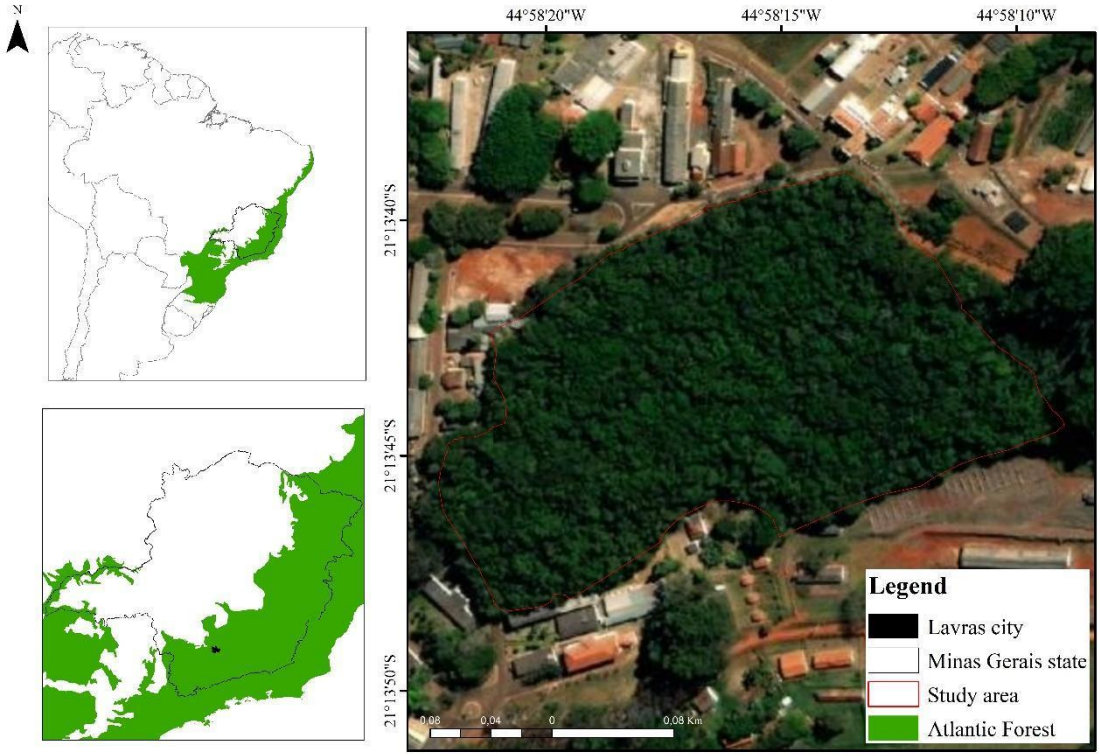

Figure 1. The geographical location of an Atlantic Forest remnant, Southeast Brazil.

2.2. Data collection

2.2.1. Forest Inventory

We used a permanent plot network sampled at the study area. A total of 126 plots of 20 x 20 m (400 m^2) were systematically allocated in the area for the first time in 1987. These plots were remeasured in 1992, 1996, 2001, 2006, 2010, 2015, and 2017. In each forest inventory, all trees with a diameter at breast height (DBH) ≥ 5 cm were identified and measured.

All surviving trees, recruits, and dead trees have been counted during the field surveys. Botanical materials were collected for species identification and herbarium visits. According to the APG IV classification system, the taxonomy was standardized using the dataset “Flora do Brasil” (APG IV, 2016; BFG, 2021). Tree individuals with multiple stems had their diameter

transformed into one value by applying the following equation (MACDICKEN; WOLF; BRISCOE, 1991) (Equation 1):

$$D = \sqrt{d_{n1}^2 + d_{n2}^2 + \cdots + d_n^2} \qquad \text{(Equation 1)}$$

Where:

D is the transformed diameter;

d_n is the tillered tree diameter.

2.3. Data Processing

2.3.1. Above Ground Biomass Estimates

We calculated the AGB for the 2015 and 2017 years, which were our main interval of analysis. We used the pantropical equation proposed by Chave et al. (2014) that considers the tree DBH and species mean wood density obtained from The Global Wood Density Database (ZANNE et al., 2009) (Equation 2). In those cases where information was unavailable to species, the wood density was estimated considering genus or family. Height data is not required in this equation, however, a measure of environmental stress (E) calculated based on the site coordinates (latitude and longitude) were used to replace the tree height absence. We processed the AGB through the Biomass package (RÉJOU-MÉCHAIN et al., 2017) in the R language (R CORE TEAM, 2020).

$$AGB = exp\,(-2.024 - 0.896 * E + 0.920 * \log(WD) + 2.795 * log\,(D) - 0.0461 * (\log(D)^2)) \qquad \text{Equation 2}$$

Where:

AGB: Above ground biomass (Mg);

E: measure of environmental stress estimated from the geographical coordinates;

WD: Wood density;

D: Diameter at breast height (cm).

2.4. Predictive variables

2.4.1. Optical and Radar data acquisition

We used Sentinel-1 and Sentinel-2 products to predict the aboveground biomass in the Atlantic Forest remnant in 2015 and 2017. The image collection is provided by the European Space Agency (ESA) within the Copernicus Programme. We relied on a sensing period based on the study area hydrological year (Wet: October/March; Dry: April/September) to account for weather seasonality when modelling the AGB (see table S1 in supplementary material). We calculated the median pixel value to extract information of each predictive variable in both seasons (dry and wet). Google Earth Engine (GEE) platform was used to obtain and process the images. GEE is a cloud-based platform of satellite imagery and geospatial application, which is widely used to assess changes on Earth's surface (GORELICK et al., 2017).

The Sentinel-1 mission provides data from a C-band SAR instrument with a central frequency of 5.405 GHz. In our study, we used Level-1 Ground Range Detected (GRD) scenes with backscatter coefficient (σ°) in decibels (dB). The images were obtained by Interferometric Wide Swath instrument which provides dual-band cross-polarization (VV and VH: vertical transmit-horizontal receive) of 10 meters resolution. GEE provides Sentinel-1 preprocessed scenes, that includes applying orbit file, GRD border noise removal, thermal noise removal, application of radiometric calibration values, and terrain correction.

Sentinel-2 provides high-resolution multispectral data. From all 13 spectral bands available, we used only the B2 (blue), B3 (green), B4 (red), and B8 (near-infrared) bands. The

QA60 bitmask band was applied to detect and mask out clouds and cirrus. A cloud percentage of less than 5% was applied as a criterion to the image selection. As additional variables, we computed the following vegetation indices: enhanced vegetation index (EVI), normalized difference vegetation index (NDVI), green normalized difference vegetation index (GNDVI), soil-adjusted vegetation index (SAVI), modified soil-adjusted vegetation index (MSAVI). Optical sensor's spectral products, such as vegetation indices, have been demonstrated as good predictors of AGB (NUTHAMMACHOT et al., 2022; WAI; SU; LI, 2022).

2.4.2. Gray Level Co-occurrence Matrix (GLCM) textures

GLCM defines the different combinations of gray levels (pixel brightness values) present in an image (HALL-BEYER, 2017). This matrix considers two pixels' relation and represents the main technique to evaluate image textures through a set of statistics. We computed 17 textures (Table 1) for each period (wet and dry) in both years (2015 and 2017) (CONNERS; TRIVEDI; HARLOW, 1984; HARALICK; SHANMUGAM; DINSTEIN, 1973). These textures were processed into the GEE platform using the image (Sentinel-1 and Sentinel-2) and a kernel (or window size) of 3x3 pixels (LI et al., 2022).

Table 1 - The list of textures calculated for each predictive variable from the Sentinel-1 and Sentinel-2 data.

GLCM Metrics	Description
ASM	Angular Second Moment; measures the number of repeated pairs
Contrast	Contrast; measures the local contrast of an image
Corr	Correlation; measures the correlation between pairs of pixels
Var	Variance; measures how spread out the distribution of gray-levels is
Idm	Inverse Difference Moment; measures the homogeneity

Savg	Sum Average
Svar	Sum Variance
Sent	Sum Entropy
Ent	Entropy. Measures the randomness of a gray-level distribution
Dvar	Difference variance
Dent	Difference entropy
Imcorr1	Information Measure of Corr. 1
Imcorr2	Information Measure of Corr. 2
Diss	Dissimilarity
Inertia	Inertia
Shade	Cluster Shade
Prom	Cluster prominence

2.4.3. Acquisition of variables values

Our dataset is composed of 126 plots in which the aboveground biomass was estimated. Thus, we extracted the corresponding values of all predictors for each plot. From the center point of the plot, we created a buffer of five meters to compute the variables values. Finally, the mean value of each predictor was extracted and associated with the respective plot.

2.4.4. Selection of the predictive variables

A total of 234 and 396 predictors were extracted in 2015 and 2017, respectively. Highly correlated predictors may increase model complexity; thus, we applied a filter method to eliminate unnecessary variables. We used Spearman's correlation coefficient to identify any relationship between the predictors (SPEARMAN, 1904). Then, we used the "findCorrelation" function in R (R CORE TEAM, 2020) to remove highly correlated variables ($\rho \geq 0.7$) (COHEN,

1988). From the remaining predictors, 31 and 29 variables were used to model the aboveground biomass in 2015 and 2017, respectively (see Table S2 in supplementary information).

2.5. Random Forest model

We used the Random Forest algorithm (RF) (BREIMAN, 2001) to predict the aboveground biomass as a function of optical, radar data, and GLCM textures described above. RF is an ensemble learning type that uses multiple decision trees to avoid overfitting and generalizes (OSHIRO; PEREZ; BARANAUSKAS, 2012). RF shows great capacity in both selecting and ranking the most important variables, and is less sensitive to noise in the training data (OSHIRO; PEREZ; BARANAUSKAS, 2012; SILVEIRA et al., 2019).

We processed the data using the *randomforest* package (LIAW; WIENER, 2002) available in the R software (R CORE TEAM, 2020). We grouped the AGB data of all 126 plots into six classes to ensure that training and validation processes have values from all dataset intervals. We evaluated the dataset composition using a frequency histogram, and classes were defined following the data range, that is, we observed the minimum and maximum value of the AGB.

Sentinel-2 data was not available to the study area during the wet season (October 2015 to March 2016). Thus, we fitted the aboveground biomass of 2015 as a function of Sentinel-1 data and Sentinel-2 data at dry season. We randomly selected 70% of the data to use as a training sample to fit the model, and the remaining 30% were applied to validation. The decision tree number (ntr*ee*) was fixed at 1,000; *mtry* parameter was obtained by the "*tuneRF*" function, once it provides the best value of *mtry* to achieve the lowest out-of-bag error (DAVID; ROSSER; DONOGHUE, 2022). We applied the recursive feature elimination (RFE) to select the most optimum variables. The RFE is a backward feature elimination method, which eliminates the

least important variables (%IncMSE) from the model in each interaction (DAVID; ROSSER; DONOGHUE, 2022; GUYON et al., 2002).

The coefficient of determination (R2), root mean square error (RMSE), and mean absolute error (MAE) was calculated for each one of the fitted models (DAVID; ROSSER; DONOGHUE, 2022). These parameters allow us to measure the effect of fitting between the predicted and observed values as well as calculate the estimation error of the models.

3. Results

3.1. Above ground biomass

The estimates aboveground biomass was 184.41 Mg/ha and 181.90 Mg/ha in 2015 and 2017, respectively. The most potential species in accumulating biomass to both intervals were *Copaifera langsdorffii* Desf., *Xylopia brasiliensis* Spreng. and *Cryptocarya aschersoniana* Mez. Also, the AGB concentration was greater in arboreal individuals with diameter between 10 and 35 cm (Figure 2; see also the violin plot in Figure S1 and Figure S2, supplementary material). The AGB decreased by 2.51 Mg/ha between 2015 and 2017. However, there was no statistical difference (Figure 3).

Figure 2. Aboveground biomass accumulation per diameter class for each interval in the Forest Atlantic remnant, southeast Brazil. The tree individuals were classified into three categories: Small (5 < DBH < 10 cm), Medium (10 < DBH < 35 cm), and Larger (greater than 35 cm).

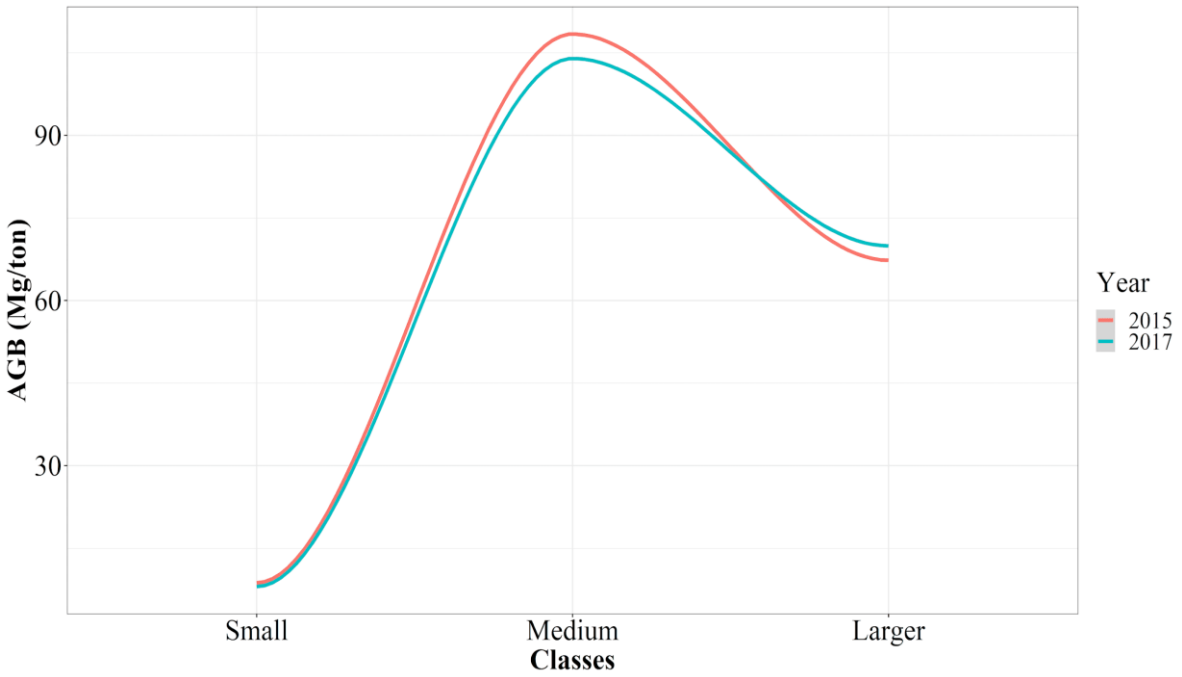

Figure 3 - Estimates of the aboveground biomass for each interval in the Forest Atlantic remnant, southeast Brazil. Same letter for the variable represents that there are no statistically different values (t.test - α = 5%).

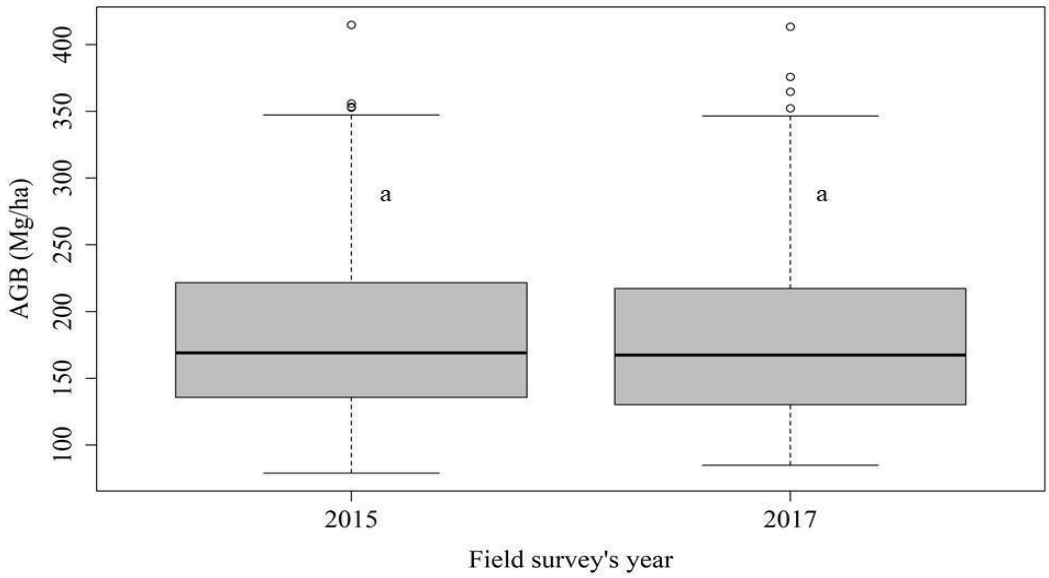

3.2. Random forest products

The random forest model had a coefficient of determination (R^2) of 0.56 and 0.58 to 2015 and 2017, respectively. The RMSE and MAE did not show large differences between the models (Table 2).

Table 2 - Model accuracy to the estimates aboveground biomass for each interval in the study remnant, southeast Brazil.

Year	AGB (Mg/ha)	CV (%)	R^2	RMSE (%)	MAE (Mg/ha)
2015	184.41	34.50	0.56	154.47%	0.90
2017	181.9	35.09	0.58	140.53%	0.69

In which: CV is the coefficient of variance; R^2 is the coefficient of determination; RMSE is the root mean square error; MAE is the mean absolute error.

Overall, the predictors of aboveground biomass were mainly represented by the GLCM textures associated with the Sentinel-1 polarizations and Sentinel-2 bands. The AGB estimates in 2015 was predicted by variables related to the wet and dry season (*VH_wet_dent*, *VH_dry_imcorr1*, *VV_wet_shade*, *B2_dry_corr* and *B8_dry_shade*). In 2017, GLCM textures from band 8 during the dry season were the main predictors to AGB (*B8_dry*, *B8_dry_corr*, *B8_dry_savg* and *B8_dry_shade*). All variables showed similar importance values to the AGB prediction (Figure 4; see also Table S3 in supplementary information).

Figure 4. Selected variables by the random forest model to estimate the aboveground biomass for each interval in the Forest Atlantic remnant, southeast Brazil.

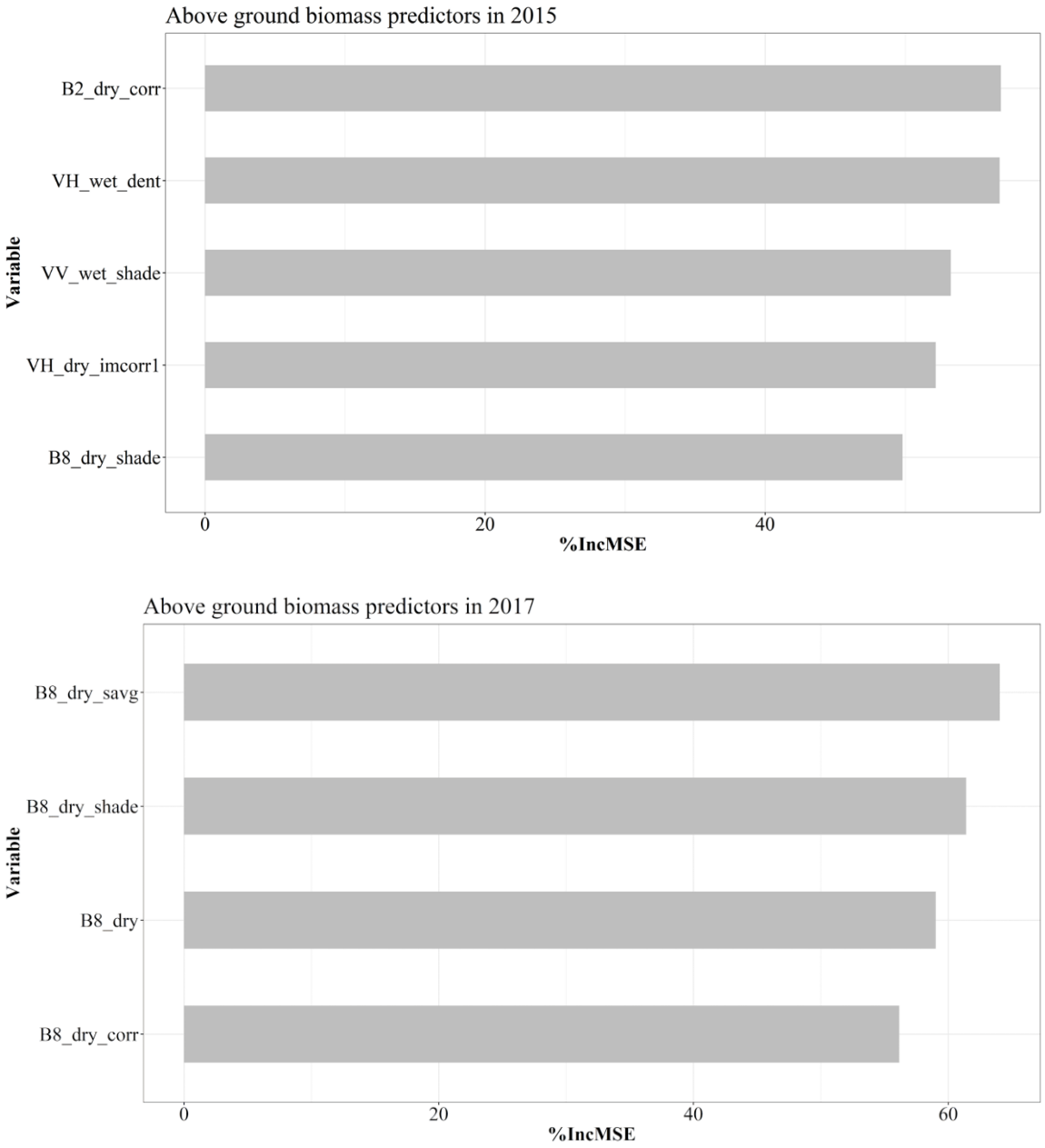

4. Discussion

We assessed to what extent radar and optical images may predict the aboveground biomass during a prolonged drought period. Our hypothesis that the AGB predictors may be different between the years was confirmed. SAR signal is directly proportional to AGB, that is, the higher the AGB, the higher backscatter in leaves. This pattern was observed in the AGB estimates in 2015 but not in 2017. We identified that only optical variables were selected for the AGB prediction in 2017. The absence of radar images as predictors may be related to the

accumulation effect of dry conditions at the second interval. Droughts imply vegetation with fewer leaves to avoid water loss and, consequently, a lower backscatter and radar signal is observed. Leaf loss is a mechanism of seasonally dry forests to couple with drought conditions, as well as stomata closure and water uptake from deeper layers (OLIVEIRA-FILHO; FONTES, 2000; PIRASTEH-ANOSHEH et al., 2016). In this sense, the observed drought changed the canopy structure as it extended. Forest responses are latent and may take months to years to manifest after drought onset (RODRIGUES et al., 2022). Therefore, the greater importance of optical images in 2017 was likely due to the cumulative effect of water-limitation conditions on the remnant's canopy.

4.1. Above ground biomass

There was a slight decrease in the AGB between 2015 and 2017 in the forest remnant. Although AGB has not shown a significant difference, the lower amount in 2017 may have been due to species composition and changes in the number of individuals compared to 2015. Overall, tree mortality overcame recruitment in our study area, implying lower AGB. This is likely due to a prolonged drought observed in the study period (RODRIGUES et al., 2022), which led to substantial changes across vegetation, causing tree mortality and decreasing forest structure and composition (ALLEN et al., 2010; WILLIAMS et al., 2013).

The remnant has experienced anomalous drought events in the past years, mainly between 2013 and 2018 (GUAUQUE-MELLADO et al., 2022; RODRIGUES et al., 2022). The vegetation response to drought depends on several aspects, but the region's climate (e.g., arid, semi-arid, and humid) directly affects it (GUAUQUE-MELLADO et al., 2022). Semideciduous vegetation is used to dry conditions because it has developed mechanisms to overcome water-limited periods, such as leaf loss (known as leaf senescence) and stomatal control (OLIVEIRA-FILHO; FONTES, 2000; PIRASTEH-ANOSHEH et al., 2016). However, prolonged drought

may be stressful enough to decrease tree growth and cause mortality (ANDEREGG; KANE; ANDEREGG, 2013). The prolonged drought (2013-2018) observed in the study remnant has caused an increased individual loss and a negative trend in the basal area between 2015 and 2017 (RODRIGUES et al., 2022). Loss of individuals, smaller trees, and leaf senescence directly impact the AGB, justifying its observed reduction. These changes in forest structure and composition have also impacted the spectral variables accounting for AGB (see topic 4.2) and highlight how droughts affect forest monitoring and management by means of remote sensing.

4.2. Predictors of above ground biomass

We observed an increasing trend of dry-season spectral variables as potential predictors of the AGB in 2017. The AGB was predicted by optical bands as well as by both polarizations from radar data (VV and VH), encompassing the dry and wet seasons, in 2015. In the same direction of seasonality, the greater amount of aboveground biomass in 2015 and decrease in 2017 is related to radar and optical data, respectively.

SAR products have a good relation to AGB estimates through the C-band (COUGO et al., 2015). SAR is an active sensor that operates in the microwave specter and shows a great capacity to penetrate the vegetation canopy and components (HUANG et al., 2018; THAPA et al., 2015). Biomass accumulation until a specific value implies a greater backscatter, which justify the importance of SAR signal (BERNINGER et al., 2018). Usually, the vegetation accumulates a greater amount of AGB during wetter conditions (JUMP et al., 2017). This pattern explains the SAR-based variables selection as the main predictors to near normal meteorological conditions in 2015 (GUAUQUE-MELLADO et al., 2022; RODRIGUES et al., 2022). In addition, SAR data overcomes the optical sensor under intense cloud cover and rain

since the satellite has no climate dependence (HUANG et al., 2018; KUPLICH; CURRAN; ATKINSON, 2005; THAPA et al., 2015).

Optical data were more helpful in the dry than in the wet season in predicting the AGB in a year of severe drought conditions (2017) in the study remnant (GUAUQUE-MELLADO et al., 2022; RODRIGUES et al., 2022). Due to a long-term drought condition, the remnant has experienced a loss of tree individuals and, consequently, a decrease in its total AGB. In addition to climate dependence, optical data have less capacity to capture the vertical structure of trees (OLESK et al., 2016).

Texture parameters are not exclusive to one type of satellite. In fact, incorporating the GLCM textures into radar and optical sensor data may improve the model capacity in predicting forest biophysical parameters and AGB (KUPLICH; CURRAN; ATKINSON, 2005; LU et al., 2012; THAPA et al., 2015). Textures are related to characteristics such as regularity, smoothness, and tonal variation of the object (THAPA et al., 2015). Those aspects may be influenced by climate and vegetation (LU et al., 2012). Also, texture characteristics provide better AGB estimates compared to radar and optical original bands individually (THAPA et al., 2015). Such improvement is possible since textures are able to decrease the forest structure complexity (THAPA et al., 2015). Also, textures play an important role in saturation data problem solutions with optical and radar images (OLESK et al., 2016). Forest structure, radar polarization, and climate conditions are one of the drivers of the saturation problem (OLESK et al., 2016).

Using the sentinel-1 and sentinel-2 according to seasonality produce better accurate results to AGB estimates. Vegetation biophysical features such as biomass and leaf area are a tree response to dry or wet season adaptation. Forest moisture may differ between a dry and wet season. The AGB sensitivity to radar and optical data shows a dependence on the image seasonality conditions.

5. Conclusion

From the modeling of aboveground biomass as a function of remote sensor data, our findings pointed out that the synergy of optical and radar satellite' images with the Gray Level Co-occurrence Matrix (GLCM) is a great and accurate method to estimate aboveground biomass. Using texture images is an alternative to solve saturation data problems and improve the AGB estimates. Overall, the combination of remote sensor images to texture potentially increases the AGB estimates in dry and wet seasons, highlighting the role and relation of each satellite to the vegetation structure.

References

ALLEN, C. D. et al. A global overview of drought and heat-induced tree mortality reveals emerging climate change risks for forests. **Forest Ecology and Management**, v. 259, n. 4, p. 660–684, 2010.

ALVARES, C. A. et al. Köppen's climate classification map for Brazil. **Meteorologische Zeitschrift**, v. 22, n. 6, p. 711–728, 2014.

ANDEREGG, W. R. L. et al. Climate-driven risks to the climate mitigation potential of forests. **Science**, v. 368, n. 6497, 2020.

ANDEREGG, W. R. L.; KANE, J. M.; ANDEREGG, L. D. L. Consequences of widespread tree mortality triggered by drought and temperature stress. **Nature Climate Change**, v. 3, n. 1, p. 30–36, 2013.

APG IV. An update of the Angiosperm Phylogeny Group classification for the orders and families of flowering plants: APG IV. **Botanical Journal of the Linnean Society**, v. 181, n. 1, p. 1–20, 2016.

BERNINGER, A. et al. SAR-based estimation of above-ground biomass and its changes in tropical forests of Kalimantan using L- and C-band. **Remote Sensing**, v. 10, n. 6, 2018.

BFG. **Jardim Botânico do Rio de Janeiro.** Disponível em: <https//floradobrasil.jbrj.gov.br/.>.

BREIMAN, L. Random forests. **Random Forests**, v. 45, p. 5–32, 2001.

CHABALALA, Y.; ADAM, E.; ALI, K. A. Machine Learning Classification of Fused Sentinel-1 and Sentinel-2 Image Data towards Mapping Fruit Plantations in Highly Heterogenous Landscapes. **Remote Sensing**, v. 14, n. 11, p. 1–26, 2022.

CHAVE, J. et al. Improved allometric models to estimate the aboveground biomass of tropical trees. **Global Change Biology**, v. 20, n. 10, p. 3177–3190, 2014.

COHEN, J. Differences between Correlation Coefficients. In: **Statistical Power Analysis for the Behavioral Sciences**. 2. ed. [s.l.] Routledge, 1988. p. 35.

CONNERS, R. W.; TRIVEDI, M. M.; HARLOW, C. A. Segmentation of a high-resolution urban scene using texture operators (Sunnyvale, California). **Computer Vision, Graphics, & Image Processing**, v. 25, n. 3, p. 273–310, 1984.

COUGO, M. F. et al. Radarsat-2 backscattering for the modeling of biophysical parameters of regenerating mangrove forests. **Remote Sensing**, v. 7, n. 12, p. 17097–17112, 2015.

DAVID, R. M.; ROSSER, N. J.; DONOGHUE, D. N. M. Improving above ground biomass estimates of Southern Africa dryland forests by combining Sentinel-1 SAR and Sentinel-2 multispectral imagery. **Remote Sensing of Environment**, v. 282, n. July 2021, p. 113232, 2022.

GORELICK, N. et al. Google Earth Engine: Planetary-scale geospatial analysis for everyone. **Remote Sensing of Environment**, v. 202, p. 18–27, 2017.

GRÜNER, E.; WACHENDORF, M.; ASTOR, T. The potential of UAV-borne spectral and textural information for predicting aboveground biomass and N fixation in legume-grass mixtures. **PLoS ONE**, v. 15, n. 6, p. 1–21, 2020.

GUAUQUE-MELLADO, D. et al. Evapotranspiration under Drought Conditions: The Case Study of a Seasonally Dry Atlantic Forest. **Atmosphere**, v. 13, n. 6, 2022.

GUYON, I. et al. Gene selection for cancer classification using DCA. **Machine Learning**, v. 46, p. 389–422, 2002.

HALL-BEYER, M. GLCM Texture: A Tutorial. **17th International Symposium on Ballistics**, v. 2, n. March, p. 18–19, 2017.

HARALICK, R. M.; SHANMUGAM, K.; DINSTEIN, I. Textural Features for Image

Classification. p. 610–621, 1973.

HUANG, X. et al. Assessment of forest above ground biomass estimation using multi-temporal C-band Sentinel-1 and Polarimetric L-band PALSAR-2 data. **Remote Sensing**, v. 10, n. 9, 2018.

INMET. **NORMAIS CLIMATOLÓGICAS DO BRASIL 1991-2020**. Disponível em: <https://portal.inmet.gov.br/normais#>. Acesso em: 1 mar. 2023.

JUMP, A. S. et al. Structural overshoot of tree growth with climate variability and the global spectrum of drought-induced forest dieback. **Global Change Biology**, v. 23, n. 9, p. 3742–3757, 2017.

JUNQUEIRA JUNIOR, J. A. et al. Time-stability of soil water content (SWC) in an Atlantic Forest - Latosol site. **Geoderma**, v. 288, p. 64–78, 2017.

KUPLICH, T. M.; CURRAN, P. J.; ATKINSON, P. M. Relating SAR image texture to the biomass of regenerating tropical forests. **International Journal of Remote Sensing**, v. 26, n. 21, p. 4829–4854, 2005.

LI, C.; ZHOU, L.; XU, W. Estimating aboveground biomass using sentinel-2 msi data and ensemble algorithms for grassland in the shengjin lake wetland, China. **Remote Sensing**, v. 13, n. 8, 2021.

LI, H. et al. Estimation of Forest Aboveground Biomass of Two Major Conifers in Ibaraki Prefecture, Japan, from PALSAR-2 and Sentinel-2 Data. **Remote Sensing**, v. 14, n. 3, p. 468, 2022.

LIANG, Y. et al. Improved estimation of aboveground biomass in rubber plantations by fusing spectral and textural information from UAV-based RGB imagery. **Ecological Indicators**, v. 142, n. May, p. 109286, 2022.

LU, D. et al. Aboveground Forest Biomass Estimation with Landsat and LiDAR Data and Uncertainty Analysis of the Estimates. **International Journal of Forestry Research**, v. 2012, n. 1, p. 1–16, 2012.

MACDICKEN, K. G.; WOLF, G. V.; BRISCOE, C. B. **Standard Research Methods for Multipurpose Trees and Shrubs**. [s.l.] Winrock International, 1991.

MERANER, A. et al. Cloud removal in Sentinel-2 imagery using a deep residual neural network and SAR-optical data fusion. **ISPRS Journal of Photogrammetry and Remote Sensing**, v. 166, n. May, p. 333–346, 2020.

MISHRA, V. N. et al. Performance evaluation of textural features in improving land use/land cover classification accuracy of heterogeneous landscape using multi-sensor remote sensing data. **Earth Science Informatics**, v. 12, n. 1, p. 71–86, 2019.

NUTHAMMACHOT, N. et al. Combined use of Sentinel-1 and Sentinel-2 data for improving above-ground biomass estimation. **Geocarto International**, v. 37, n. 2, p. 366–376, 2022.

OLESK, A. et al. Interferometric SAR coherence models for Characterization of hemiboreal forests using TanDEM-X dssata. **Remote Sensing**, v. 8, n. 9, 2016.

OLIVEIRA-FILHO, A. T.; FONTES, M. A. L. Patterns of floristic differentiation among atlantic forests in southeastern Brazil and the influence of climate. **Biotropica**, v. 32, n. 4 B, p. 793–810, 2000.

OSHIRO, T. M.; PEREZ, P. S.; BARANAUSKAS, J. A. How many trees in a random forest? In: P., P. (Ed.). . **Machine Learning and Data Mining in Pattern Recognition**. Berlin, Heidelberg: Springer, 2012. v. 7376p. 154–168.

PIRASTEH-ANOSHEH, H. et al. Stomatal responses to drought stress. **Water Stress and Crop Plants: A Sustainable Approach**, v. 1–2, p. 24–40, 2016.

R CORE TEAM. **R: A language and environment for statistical computing.R Foundation for Statistical Computing,**Vienna, Austria, 2020. Disponível em: <https://www.r-project.org/.>

RÉJOU-MÉCHAIN, M. et al. Biomass: an R package for estimating above-ground biomass and its uncertainty in tropical forests. **Methods in Ecology and Evolution**, v. 8, p. 1163–1167, 2017.

RODRIGUES, A. F. et al. Modeling canopy interception under drought conditions: The relevance of evaporation and extra sources of energy. **Journal of Environmental Management**, v. 292, n. January, 2021.

RODRIGUES, A. F. et al. Throughfall spatial variability in a neotropical forest: Have we correctly accounted for time stability? **Journal of Hydrology**, v. 608, n. February, 2022.

SAFARI, A.; SOHRABI, H. Integration of synthetic aperture radar and multispectral data for aboveground biomass retrieval in Zagros oak forests, Iran: an attempt on Sentinel imagery. **International Journal of Remote Sensing**, v. 41, n. 20, p. 8069–8095, 2020.

SILVEIRA, E. M. DE O. et al. Object-based random forest modelling of aboveground forest biomass outperforms a pixel-based approach in a heterogeneous and mountain tropical environment. **International Journal of Applied Earth Observation and Geoinformation**, v. 78, p. 175–188, 2019.

SOUZA, C. R. et al. Long-term ecological trends of small secondary forests of the atlantic forest hotspot: A 30-year study case. **Forest Ecology and Management**, v. 489, n. February, 2021.

SU, Y. et al. The Development and Evaluation of a Backpack LiDAR System for Accurate and Efficient Forest Inventory. **IEEE Geoscience and Remote Sensing Letters**, v. 18, n. 9, p.

1660–1664, 2021.

TERRA, M. DE C. N. S. et al. Stemflow in a neotropical forest remnant: vegetative determinants, spatial distribution and correlation with soil moisture. **Trees - Structure and Function**, v. 32, n. 1, p. 323–335, 2018.

THAPA, R. B. et al. Potential of high-resolution ALOS-PALSAR mosaic texture for aboveground forest carbon tracking in tropical region. **Remote Sensing of Environment**, v. 160, p. 122–133, 2015.

VAN LOON, A. F. Hydrological drought explained. **Wiley Interdisciplinary Reviews: Water**, v. 2, n. 4, p. 359–392, 2015.

VAN LOON, A. F. et al. Using paired catchments to quantify the human influence on hydrological droughts. **Hydrology and Earth System Sciences**, v. 23, n. 3, p. 1725–1739, 2019.

VICENTE-SERRANO, S. M. et al. Global drought trends and future projections. **Philosophical Transactions of the Royal Society A: Mathematical, Physical and Engineering Sciences**, v. 380, n. 2238, 2022.

WAI, P.; SU, H.; LI, M. Estimating Aboveground Biomass of Two Different Forest Types in Myanmar from Sentinel-2 Data with Machine Learning and Geostatistical Algorithms. **Remote Sensing**, v. 14, n. 9, 2022.

WILLIAMS, A. P. et al. Temperature as a potent driver of regional forest drought stress and tree mortality. **Nature Climate Change**, v. 3, n. 3, p. 292–297, 2013.

XIE, Z. et al. Classification of land cover, forest, and tree species classes with Ziyuan-3 multispectral and stereo data. **Remote Sensing**, v. 11, n. 2, p. 1–27, 2019.

XU, C. et al. Increasing impacts of extreme droughts on vegetation productivity under climate

change. **Nature Climate Change**, v. 9, n. 12, p. 948–953, 2019.

XUE, J.; SU, B. Significant remote sensing vegetation indices: A review of developments and applications. **Journal of Sensors**, v. 2017, 2017.

ZANNE, A. E. et al. **Data from: Towards a Worldwide Wood Economics Spectrum.** Disponível em: <https://doi.org/10.5061/dryad.234>.

Supplementary Material

Table S1. Study area hydrological year. Intervals used to the image collection acquisition.

Ano	Season	Date
2015	Wet	October 01, 2015 until March 31, 2016
	Dry	April 01, 2016 until September 30, 2016
2017	Wet	October 01, 2017 until March 31, 2018
	Dry	April 01, 2018 until September 30, 2018

Table S2. Remaining predictors used to model the aboveground biomass in 2015 and 2017.

Plot	Ponto_X	Ponto_Y	AGB_2015	2015 variables							
				VH_dry_dent	VH_dry_imcorr1	VH_dry_sent	VH_wet_corr	VH_wet_dent	VH_wet_ent	VH_wet_sent	VH_wet_shade
1	-44.9702	-21.2272	6.192422915	3.653888369	-0.849348629	3.660594225	0.604480278	3.626785421	4.353741646	3.660594225	48303024538
2	-44.9702	-21.2274	4.875025253	3.656064034	-0.843569994	3.660594225	0.650922537	3.64266324	4.353741646	3.656072617	56350961664
3	-44.9701	-21.2276	5.053468709	3.652038336	-0.848838508	3.660594225	0.37000671	3.64328146	4.353741646	3.651322126	5589997056
4	-44.9701	-21.2278	4.391235504	3.649905729	-0.855461156	3.660594225	0.531874472	3.647124386	4.352152824	3.656008434	1221659955
5	-44.9701	-21.2279	3.714661187	3.632879734	-0.854345143	3.660594225	0.537233114	3.648305178	4.353741646	3.660594225	-1508606464
6	-44.9701	-21.2281	3.156022353	3.632570028	-0.847316921	3.652851582	0.436913967	3.632579565	4.353741646	3.650967121	-419097376
7	-44.97	-21.2283	7.409678541	3.622703505	-0.844246626	3.652484226	0.387466043	3.628859043	4.353741646	3.65706377	-319564647.2
8	-44.97	-21.2285	6.052482234	3.609464169	-0.84452641	3.660594225	0.491972834	3.651138544	4.353741646	3.660594225	1101393280
9	-44.97	-21.2286	4.299740987	3.587500095	-0.83976239	3.660594225	0.373835802	3.658900976	4.353741646	3.652112007	994601536
10	-44.9699	-21.2288	8.94648895	3.615721941	-0.835294604	3.660594225	0.444587499	3.660021782	4.353741646	3.650967121	2246278912
11	-44.9701	-21.2289	7.446989298	3.623191595	-0.842968404	3.658675194	0.360939324	3.650967121	4.353741646	3.650584459	221791232
12	-44.9701	-21.2287	4.402750313	3.607002735	-0.84887284	3.650967121	0.249554649	3.651130199	4.353741646	3.651774406	204092272
13	-44.9702	-21.2285	6.643855174	3.607385159	-0.844752669	3.651019096	0.41959843	3.650356531	4.353741646	3.660594225	490555328
14	-44.9702	-21.2283	4.167308528	3.618552923	-0.84648335	3.642390251	0.498357981	3.651932001	4.34967804	3.652818918	74840376
15	-44.9702	-21.2281	4.727732841	3.62528944	-0.842112958	3.644090891	0.498905301	3.626098394	4.345550537	3.65246439	283493792
16	-44.9703	-21.228	6.613835029	3.616507292	-0.850818455	3.645875454	0.516626358	3.626736403	4.349615574	3.660594225	-344960512
17	-44.9703	-21.2278	5.358324146	3.639028788	-0.847292483	3.652420521	0.550720215	3.632274151	4.349615574	3.660594225	1880093312
18	-44.9703	-21.2276	7.863807551	3.654483557	-0.846381724	3.646326303	0.540381372	3.648036718	4.352228642	3.654496908	4280882688
19	-44.9704	-21.2274	5.05918273	3.656803608	-0.846903265	3.64731288	0.531890094	3.660594225	4.353741646	3.650967121	36880859136
20	-44.9704	-21.2272	4.405132146	3.650587749	-0.853763044	3.652731037	0.71298939	3.641837835	4.353741646	3.660594225	80178809242

21	-44.9706	-21.2273	5.434099611	3.647979259	-0.852257967	3.656705856	0.729650795	3.645471096	4.353388309	3.660240889	63370690560
22	-44.9706	-21.2275	4.89926314	3.639231443	-0.861632228	3.660594225	0.729856014	3.646554947	4.353741646	3.650967121	36055879680
23	-44.9705	-21.2276	5.637857078	3.643220186	-0.861632228	3.660594225	0.601753414	3.648513079	4.347327709	3.650925636	-4500063744
24	-44.9705	-21.2278	7.523744199	3.647225857	-0.857496738	3.660594225	0.471322089	3.64095211	4.344569683	3.651799917	479764704
25	-44.9705	-21.228	4.49363986	3.63918066	-0.849613965	3.660594225	0.561763644	3.634408712	4.349459171	3.660325766	1596255744
26	-44.9704	-21.2282	6.207719226	3.609003544	-0.827831447	3.644356012	0.492750764	3.626305342	4.345489502	3.652342558	-204380768
27	-44.9704	-21.2283	4.724560133	3.602884769	-0.828617752	3.634366035	0.398397863	3.644701242	4.341363907	3.644102097	-238670112
28	-44.9704	-21.2285	4.870769271	3.607289982	-0.836825693	3.6293293	0.460049421	3.623697424	4.341363907	3.644194126	-22664981.6
29	-44.9703	-21.2287	5.345265693	3.615241528	-0.854049265	3.63073802	0.292680681	3.609470844	4.341363907	3.635601521	52826720
30	-44.9703	-21.2289	10.799393	3.637581396	-0.84822638	3.649535227	0.439015269	3.631100607	4.353741646	3.65205698	113594514.4
32	-44.9705	-21.2287	5.429549042	3.649973154	-0.849852681	3.623653412	0.337039232	3.608333111	4.351782799	3.644496918	-253705648
33	-44.9706	-21.2286	4.036119421	3.614964962	-0.829355896	3.616862774	0.421213508	3.60964179	4.341363907	3.652342558	-791567360
34	-44.9706	-21.2284	6.29735304	3.62371707	-0.83424902	3.643362284	0.553147495	3.642593145	4.341363907	3.652340174	-2398903552
35	-44.9706	-21.2282	4.73479943	3.607992887	-0.834274173	3.652342558	0.570574343	3.633801222	4.345439434	3.652297258	-618203520
36	-44.9707	-21.228	5.068797995	3.628192186	-0.848269358	3.659912467	0.450953208	3.640743554	4.342977166	3.648346901	1497986080
37	-44.9707	-21.2278	4.509893776	3.655226946	-0.853210211	3.660594225	0.29532671	3.634219646	4.336550236	3.644090891	-763333696
38	-44.9707	-21.2277	6.772192186	3.641031504	-0.85494417	3.660594225	0.609172821	3.633157969	4.339160442	3.649311304	-6404155904
39	-44.9707	-21.2275	9.073246779	3.639017344	-0.861632228	3.660594225	0.680755436	3.621757746	4.345489502	3.652342558	914644352
40	-44.9708	-21.2273	6.050121453	3.648938417	-0.851915538	3.656708717	0.320955396	3.633838654	4.349375248	3.656228065	1873440000
41	-44.9709	-21.2275	5.158931168	3.644245386	-0.851259315	3.660594225	0.621387446	3.643074226	4.34437933	3.649172068	699700435.2
42	-44.9709	-21.2277	6.021238977	3.660594225	-0.843920171	3.660594225	0.592015803	3.634463787	4.336550236	3.644090891	-4055079168
43	-44.9709	-21.2279	5.721134382	3.634463787	-0.849384665	3.660594225	0.344002008	3.637735605	4.338584423	3.64612484	-2859976448
44	-44.9708	-21.228	5.533113732	3.617529631	-0.848292589	3.659400702	0.257431269	3.631178141	4.345598698	3.644081354	456298048

45	-44.9708	-21.2282	5.681232585	3.610798597	-0.841176689	3.653380394	0.304680318	3.629166126	4.353042603	3.65018034	76312592
46	-44.9708	-21.2284	5.611514515	3.618340731	-0.841150343	3.646156549	0.416468978	3.617698908	4.345489502	3.651275396	-861353024
47	-44.9708	-21.2286	5.164016417	3.626423359	-0.837186366	3.647898555	0.577337831	3.608596206	4.343636274	3.643574953	-1954819712
48	-44.9707	-21.2288	6.74413558	3.657988787	-0.850172043	3.660594225	0.480477273	3.615414143	4.351853371	3.627514601	-617916096
49	-44.9709	-21.2288	8.862104199	3.659487009	-0.860908329	3.660594225	0.506907821	3.642031431	4.352119446	3.62648201	-977813696
50	-44.9709	-21.2286	8.242012954	3.649725199	-0.857250011	3.660086584	0.580814362	3.639315224	4.349525356	3.635792351	-1875947827
51	-44.971	-21.2284	4.141806738	3.651210308	-0.854703188	3.660594225	0.315528005	3.63438797	4.353741646	3.652313471	-465977824
52	-44.971	-21.2283	7.385361219	3.638712883	-0.855776966	3.660594225	0.178302571	3.640805483	4.353741646	3.650265217	-144435648
53	-44.971	-21.2281	6.029008699	3.643568993	-0.852398694	3.660594225	0.52789712	3.651241541	4.349615574	3.650653124	-1145459712
54	-44.9711	-21.2279	5.119535526	3.651874542	-0.842208862	3.660594225	0.642185688	3.644502878	4.344624519	3.65560317	-3704826624
55	-44.9711	-21.2277	9.948364797	3.660594225	-0.83472538	3.660594225	0.617519081	3.652342558	4.342991829	3.65397048	-135109328
56	-44.9711	-21.2275	9.191336116	3.651540756	-0.849933326	3.660594225	0.583414435	3.648970604	4.353741646	3.655714512	3577652480
58	-44.9713	-21.2277	9.33085571	3.65857935	-0.844111502	3.660594225	0.559246898	3.652342558	4.353741646	3.660594225	2686461184
59	-44.9713	-21.2279	6.643895335	3.64033556	-0.850210547	3.660594225	0.75837189	3.637381554	4.353741646	3.658214569	-4093017088
60	-44.9712	-21.2281	6.148371819	3.638436913	-0.853751659	3.660594225	0.539299451	3.650933444	4.352233529	3.645353258	-2986902592
61	-44.9712	-21.2283	5.833904587	3.638515949	-0.861265123	3.660594225	0.391199529	3.643266201	4.353741646	3.635539293	-80176832
62	-44.9712	-21.2285	6.486018114	3.642646074	-0.85098201	3.660594225	0.367259979	3.625779629	4.353741646	3.642715454	-583821632
63	-44.9711	-21.2286	6.239528745	3.623972654	-0.853175759	3.652089596	0.512645662	3.630580425	4.350096703	3.64287591	-1171408000
64	-44.9711	-21.2288	16.59230696	3.64157629	-0.861632228	3.650967121	0.330881685	3.642245531	4.348811626	3.634941816	-248982032
65	-44.9697	-21.2288	6.532508688	3.631573296	-0.847157097	3.660594225	0.529027164	3.652817106	4.353741646	3.653972197	3057040552
66	-44.9698	-21.2286	5.074571577	3.629688025	-0.842469573	3.660594225	0.482614309	3.635730505	4.353741646	3.660594225	1007222912
67	-44.9698	-21.2284	8.019491924	3.620069504	-0.84246856	3.660594225	0.499871373	3.617992163	4.353741646	3.660594225	-6345270272
68	-44.9698	-21.2283	6.64606967	3.648356628	-0.844638538	3.657269049	0.60386464	3.628407097	4.353741646	3.659020567	-45242133299

69	-44.9699	-21.2281	8.73512658	3.660594225	-0.860729575	3.660594225	0.751030207	3.643959761	4.353741646	3.659188986	-52807282688
70	-44.9699	-21.2279	6.239913612	3.660594225	-0.861362815	3.660594225	0.720519841	3.658494473	4.353741646	3.660594225	-37520261120
71	-44.9699	-21.2277	6.864029771	3.654428005	-0.861038923	3.660594225	0.72167027	3.660594225	4.353741646	3.652342558	-26108411904
72	-44.97	-21.2275	8.543384379	3.652342558	-0.850841045	3.660594225	0.490482718	3.650967121	4.353741646	3.652342558	4671253504
73	-44.97	-21.2274	14.23501047	3.656362057	-0.844358563	3.660594225	0.6311028	3.646046877	4.353741646	3.652342558	49338740736
74	-44.9696	-21.2286	5.146531561	3.659940481	-0.852434635	3.660594225	0.561632097	3.643844604	4.353741646	3.660594225	-5243506688
75	-44.9696	-21.2284	8.167016675	3.652342558	-0.852433622	3.660594225	0.607271016	3.634227276	4.353741646	3.660594225	-19617093632
76	-44.9696	-21.2282	6.29705113	3.643508434	-0.852432609	3.660594225	0.777123928	3.626966	4.353741646	3.660594225	-1.54E+11
77	-44.9697	-21.2281	12.67482413	3.657740116	-0.860731602	3.660594225	0.833314836	3.650769949	4.353741646	3.660594225	-1.43E+11
78	-44.9697	-21.2279	9.039413335	3.660594225	-0.856282651	3.660594225	0.793901622	3.660594225	4.353741646	3.660594225	-84556603392
79	-44.9694	-21.2286	7.586446568	3.648587227	-0.861632228	3.660594225	0.726981461	3.658410311	4.353741646	3.660594225	-27870773248
80	-44.9694	-21.2284	11.95457624	3.654197693	-0.861632228	3.660594225	0.660471141	3.660591602	4.353741646	3.660594225	-16472992768
81	-44.9694	-21.2282	7.648941577	3.647368431	-0.861632228	3.660594225	0.71936655	3.660594225	4.353741646	3.658596277	-89217187840
82	-44.9695	-21.228	7.227807223	3.650773525	-0.861202896	3.660594225	0.762397647	3.659342527	4.353741646	3.660594225	-25374357504
83	-44.9692	-21.2285	11.79712398	3.6580863	-0.861632228	3.660594225	0.633820426	3.657656193	4.353741646	3.660594225	-10938882867
84	-44.9692	-21.2284	8.260149872	3.65796423	-0.861632228	3.660594225	0.592495143	3.652342558	4.353741646	3.660594225	-33551013888
85	-44.9693	-21.2282	6.175290204	3.657968044	-0.861632228	3.660594225	0.788299501	3.652342558	4.353741646	3.659419537	-1.16E+11
86	-44.969	-21.2285	9.727264898	3.638695478	-0.861632228	3.660594225	0.661439896	3.657619715	4.353741646	3.660594225	-15726508032
87	-44.969	-21.2283	13.8912324	3.64244318	-0.861632228	3.660594225	0.650339127	3.652234554	4.353741646	3.660594225	-5919519744
88	-44.9713	-21.229	9.701660025	3.635702133	-0.859923661	3.650967121	0.446889907	3.6324718	4.345489502	3.647736788	1820356608
89	-44.9713	-21.2288	10.85154929	3.632565022	-0.859921038	3.650967121	0.264034688	3.624584675	4.345489502	3.637717724	8998640
90	-44.9713	-21.2287	7.471129808	3.62860775	-0.853391588	3.652086258	0.304936856	3.626104116	4.350095272	3.648286104	-478073952
91	-44.9714	-21.2285	7.896006482	3.653903723	-0.855718255	3.660594225	0.259893268	3.63151598	4.353741646	3.653437138	-275012864

92	-44.9714	-21.2283	6.529040304	3.633250475	-0.861452699	3.660594225	0.300586164	3.635073662	4.353741646	3.653414965	-231976640
93	-44.9714	-21.2281	8.206193093	3.649448395	-0.856406033	3.660594225	0.546034098	3.640515089	4.353741646	3.648875237	-4174639616
94	-44.9714	-21.228	6.404972508	3.642715454	-0.844221115	3.660594225	0.764377296	3.639945984	4.353741646	3.648569822	-19232811008
95	-44.9715	-21.2278	8.941905564	3.649570465	-0.834757924	3.658193827	0.628416717	3.648281574	4.353741646	3.659903049	1197685376
96	-44.9714	-21.2292	9.874196272	3.645128012	-0.859433115	3.660594225	0.603038728	3.647862434	4.347970009	3.654717207	-1061087680
97	-44.9715	-21.2291	4.384188341	3.624985933	-0.851969421	3.657532215	0.612250447	3.648096323	4.345489502	3.655832291	1267506816
98	-44.9715	-21.2289	7.699856319	3.640164089	-0.851969421	3.652168894	0.322390532	3.64560318	4.346004581	3.64761281	679231843.2
99	-44.9715	-21.2287	8.411514945	3.63881588	-0.856757939	3.654742956	0.136754707	3.640220642	4.350093842	3.660594225	47998064
100	-44.9715	-21.2285	3.985968563	3.652004719	-0.861632228	3.660594225	0.188776582	3.645846367	4.353741646	3.660150766	-163364944
101	-44.9716	-21.2283	8.178538709	3.633528471	-0.861632228	3.660594225	0.313500255	3.640191793	4.353741646	3.657138348	-982102464
102	-44.9716	-21.2282	5.395187989	3.652358532	-0.861632228	3.660594225	0.697193801	3.65734911	4.352350712	3.647006035	-14185594880
103	-44.9716	-21.228	10.33746553	3.64081502	-0.85283041	3.660594225	0.746094465	3.653012753	4.352349281	3.652342558	-10172456960
104	-44.9717	-21.2278	14.10861368	3.644000292	-0.841790736	3.652342558	0.581427336	3.652617216	4.352347851	3.658215284	1121278976
105	-44.9718	-21.228	7.212689052	3.630634785	-0.857758164	3.65887928	0.68877548	3.63308835	4.339988708	3.642715454	-3425773312
106	-44.9718	-21.2282	5.985640843	3.652342558	-0.861632228	3.660594225	0.728323281	3.636902571	4.349973202	3.650967121	-30931779584
107	-44.9718	-21.2284	8.185008404	3.652339792	-0.861632228	3.660594225	0.408571929	3.64062109	4.353741646	3.649486351	-3591615718
108	-44.9717	-21.2285	8.498956483	3.655050039	-0.861632228	3.660594225	0.362855166	3.615744114	4.353741646	3.656512022	-202871872
109	-44.9717	-21.2287	10.77448118	3.652127981	-0.853524387	3.660594225	0.27393961	3.632143259	4.353741646	3.656131744	-26260306
110	-44.9717	-21.2289	8.876153569	3.643374777	-0.852340662	3.660594225	0.340215874	3.641133261	4.352096462	3.650237513	538059097.6
111	-44.9716	-21.2291	8.347771532	3.634463787	-0.851969421	3.660594225	0.574965715	3.645977259	4.350997925	3.657972336	2328125952
112	-44.9716	-21.2293	7.030570832	3.64461422	-0.859435022	3.660594225	0.633121192	3.646025419	4.350165844	3.660594225	970285696
113	-44.9718	-21.2293	7.168312256	3.65549159	-0.856730759	3.660594225	0.613482535	3.651651382	4.35220623	3.660594225	1231625216
114	-44.9718	-21.2291	8.369829664	3.635448217	-0.853566468	3.660594225	0.453543484	3.646571398	4.353741646	3.660594225	317954976

115	-44.9719	-21.2289	8.556891564	3.632970333	-0.861632228	3.660594225	0.475072086	3.637714624	4.353741646	3.660594225	1030416320
116	-44.9719	-21.2288	11.04440729	3.65362668	-0.861632228	3.660594225	0.342783183	3.619741678	4.353741646	3.660072803	225788784
117	-44.9719	-21.2286	11.87150852	3.660166979	-0.861632228	3.660594225	0.474335372	3.61399889	4.353741646	3.647612572	-5109998592
118	-44.972	-21.2284	14.13784852	3.65592289	-0.861632228	3.660594225	0.716126263	3.650878906	4.353741646	3.642715454	-54074179584
119	-44.972	-21.2282	6.202283323	3.647645235	-0.861632228	3.660594225	0.766753614	3.655590534	4.349974632	3.650967121	-30511581184
120	-44.972	-21.228	4.861758123	3.652945518	-0.861632228	3.660594225	0.706214428	3.645490408	4.339988708	3.646272898	13458518016
121	-44.972	-21.2295	5.609789213	3.632561922	-0.861632228	3.660594225	0.586642504	3.660594225	4.353741646	3.652342558	683226688
122	-44.972	-21.2293	9.528795038	3.646250486	-0.861632228	3.660594225	0.651982725	3.65637517	4.353741646	3.660594225	2749051136
123	-44.972	-21.2291	9.839396492	3.647748888	-0.861632228	3.660594225	0.480791859	3.64549309	4.353741646	3.660594225	-167621549
124	-44.9721	-21.229	8.993143304	3.634711409	-0.861632228	3.657367516	0.466221726	3.638388872	4.353741646	3.660594225	876621606.4
125	-44.9721	-21.2288	9.561751873	3.637239695	-0.861632228	3.655329466	0.415929079	3.63662529	4.353741646	3.659312963	-3853359616
126	-44.9723	-21.2288	9.817151276	3.647527695	-0.861632228	3.660594225	0.695637703	3.653013945	4.353741646	3.660594225	-19013750784
127	-44.9722	-21.229	12.09936128	3.650009394	-0.861632228	3.660594225	0.713056624	3.648861647	4.353741646	3.660594225	-7675113984
128	-44.9722	-21.2292	7.46939068	3.638396263	-0.861632228	3.660594225	0.698386908	3.644350767	4.353741646	3.660594225	-1586833408

Cont…

VV_dry	VV_dry_corr	VV_dry_dent	VV_dry_ent	VV_dry_idm	VV_dry_imcorr2	VV_dry_sent	VV_dry_shade	VV_wet_corr	VV_wet_dent	VV_wet_imcorr2
-7432.727539	0.648745263	3.66041522	4.353741646	0.000628404	0.999311924	3.660594225	7342222336	0.683488321	3.649307108	0.999163973
-9019.177734	0.704978704	3.660439968	4.353741646	0.001002227	0.999311924	3.660594225	10857698304	0.66402173	3.620069504	0.999104679
-10342.41504	0.656437278	3.660594225	4.353741646	0.001020103	0.999311924	3.660594225	-8958347264	0.512158513	3.612313509	0.999116361
-9311.341309	0.694183111	3.652342558	4.353741646	0.000841719	0.999311924	3.657870293	-9089419674	0.636239469	3.618861532	0.999185932
-9104.138672	0.693276525	3.652342558	4.353741646	2.63E-05	0.999311924	3.660594225	-21339209728	0.569648087	3.654432297	0.999308944

-9541.112305	0.463360697	3.636413813	4.353741646	3.78E-05	0.999311924	3.660594225	-4091620608	0.583817661	3.659500122	0.999311924
-7848.195898	0.356569076	3.65191617	4.353741646	9.11E-05	0.999311924	3.660594225	-118570652.8	0.616419113	3.646762896	0.999310517
-9119.734375	0.533704758	3.643476725	4.353741646	0.000382017	0.999311924	3.660594225	1082601728	0.683787584	3.634830475	0.999263585
-9475.237305	0.447900712	3.643927336	4.353741646	0.00093963	0.999311924	3.660594225	1461241472	0.70817548	3.6364851	0.999311924
-10501.1875	0.580024183	3.643375397	4.353741646	0.003749605	0.999311924	3.660594225	830240000	0.485467345	3.642596245	0.999311924
-9180.615234	0.564397752	3.592344522	4.353741646	0.004736473	0.999240935	3.660594225	1949587072	0.430257559	3.628243685	0.999311924
-10412.95215	0.306982458	3.652397633	4.353741646	0.001933907	0.999311924	3.660594225	266377632	0.496952683	3.637024164	0.999311924
-10011.59375	0.536453485	3.651669741	4.353741646	0.001281995	0.999311924	3.660594225	1994682240	0.669762075	3.61694479	0.99930954
-9546.34375	0.480195671	3.630631208	4.353741646	0.000161464	0.999230742	3.652699232	-569405120	0.537391901	3.634091377	0.9992401
-8686.834961	0.277075499	3.632498741	4.353741646	3.97E-05	0.999233842	3.644090891	-296108896	0.520278871	3.65854454	0.99927187
-8555.55957	0.353746116	3.644520044	4.353741646	2.75E-05	0.999262631	3.65065217	-3098737664	0.520815909	3.654032946	0.999311924
-8294.212891	0.405294627	3.647245169	4.353741646	0.000335175	0.999311924	3.654645443	-765742400	0.640674591	3.608722687	0.999102175
-8676.595703	0.596815646	3.65227747	4.351128101	0.004203199	0.999288917	3.657487631	-6543100928	0.694995999	3.618988991	0.999097288
-9416.282227	0.681659341	3.65221405	4.349615574	0.006383193	0.999238729	3.660556555	-5412270080	0.587614536	3.635740519	0.999114215
-8811.741406	0.780368745	3.659772682	4.349615574	0.006486511	0.99922843	3.659146404	41484637696	0.753144836	3.655266094	0.999234366
-13200.55566	0.658545673	3.650285244	4.349615574	0.006336391	0.99921298	3.660594225	49897308160	0.626660585	3.650967121	0.999213636
-11565.51953	0.768642306	3.640419006	4.349615574	0.006409707	0.99921298	3.660594225	1532976896	0.642163992	3.643933535	0.999092877
-9810.726563	0.711928248	3.646040201	4.351129532	0.004244418	0.999275625	3.657737732	-5634995712	0.602874815	3.627545118	0.999114633
-10212.11914	0.537807286	3.648894072	4.35256052	0.002068425	0.999301255	3.655036211	919211072	0.610035002	3.6226964	0.999125481
-9207.02832	0.464623541	3.636157036	4.353607178	0.00022232	0.99930954	3.641022205	118473040	0.699796617	3.644095659	0.99921298
-8469.544922	0.426422656	3.642715454	4.353608608	0.00022907	0.999309599	3.633437157	-335651520	0.60122174	3.624791622	0.999147594
-7923.967285	0.588952303	3.633494854	4.353610516	0.00034626	0.999306202	3.634823561	-881930944	0.501226187	3.631739378	0.99921298
-9116.436133	0.649720323	3.647378302	4.353740692	0.002016667	0.999231493	3.660193872	618485612.8	0.416553861	3.614352083	0.999192476

-9519.896484	0.609839499	3.635201454	4.353741646	0.005058205	0.999311924	3.652105093	1613473152	0.390363634	3.618090153	0.999091625
-9080.975781	0.626266313	3.601500177	4.353741646	0.009892813	0.999219143	3.656743383	1624795750	0.477829438	3.630032873	0.999105501
-9434.457031	0.538129628	3.636627197	4.353741646	0.006042071	0.999311924	3.650967121	938607360	0.387885332	3.629269838	0.999015749
-8157.562012	0.537145436	3.650516272	4.353741646	0.002422116	0.999305785	3.660594225	65173724	0.38687554	3.618495226	0.999082923
-7298.640137	0.588554442	3.642715454	4.349630356	0.007072513	0.999163866	3.651001453	-1129456896	0.386994511	3.623506546	0.999214828
-9105.924805	0.642243862	3.650879622	4.349615574	0.005989216	0.999205828	3.643411636	-439030752	0.532057643	3.624718666	0.999155343
-9533.218018	0.570791855	3.647889316	4.349615574	0.006027993	0.999209806	3.650285363	1330064912	0.477473147	3.623679638	0.999210164
-10273.5752	0.384581417	3.657377481	4.35255909	0.001882229	0.999295473	3.659600019	363242976	0.260312498	3.630897045	0.999215662
-9913.302734	0.63256228	3.655373812	4.351131439	0.003955403	0.999277055	3.660594225	-10694561792	0.412116975	3.64296937	0.999245942
-11717.74805	0.700954378	3.647029877	4.349615574	0.006054994	0.999215662	3.660594225	-1850364160	0.602894425	3.64334321	0.999213636
-12929.65039	0.365848184	3.640086889	4.350142956	0.005254695	0.999248326	3.660594225	3332955904	0.434154034	3.660594225	0.999213636
-11923.00371	0.647519445	3.651917839	4.353741646	0.000630522	0.999311924	3.660594225	-6517682541	0.493182856	3.657423782	0.999237466
-9472.532227	0.458322406	3.660594225	4.353741646	0.000283151	0.999309838	3.647816181	-8233319936	0.291770548	3.645521641	0.999311924
-10562.81836	0.345957726	3.653580189	4.349615574	0.006214969	0.999222815	3.643713236	121194520	0.231885746	3.631648064	0.999311924
-10241.37012	0.469557732	3.643744946	4.349615574	0.006067447	0.99919802	3.649400473	1587091968	0.495097399	3.616481781	0.999248207
-9650.169922	0.642971456	3.649380684	4.349615574	0.006035277	0.999092042	3.644230127	4148432640	0.477627575	3.632938147	0.999283016
-9986.750977	0.578491569	3.651107311	4.349631786	0.006020654	0.999124408	3.660594225	1476799616	0.361397594	3.633158445	0.999311924
-8839.805176	0.550336808	3.643277645	4.353741646	0.001302601	0.999307573	3.660594225	-1123041472	0.407445222	3.64383924	0.999150962
-7944.550781	0.444145977	3.636315823	4.353741646	0.005079417	0.999311924	3.660594225	25296082	0.40112859	3.644925833	0.998907804
-7782.46875	0.432418287	3.641289473	4.353741646	0.001965612	0.999310672	3.660594225	-528894144	0.4067159	3.659372091	0.999071896
-8811.616895	0.488111699	3.644359684	4.353741646	0.001487628	0.999276733	3.660594225	782964640	0.314434057	3.652006817	0.999207819
-9740.519531	0.369414836	3.653729439	4.35034132	0.005071367	0.999102652	3.660594225	713582016	0.296449453	3.632914543	0.999311924
-9533.738281	0.405254006	3.642134666	4.350327969	0.005065802	0.999027252	3.645540237	681503808	0.274922848	3.622036934	0.999311924

-10915.48828	0.279582798	3.642715454	4.353741646	0.000180392	0.999197423	3.644830704	551294144	0.482142091	3.632343531	0.999311924
-9483.589844	0.285879225	3.660594225	4.353741646	0.000252147	0.999090791	3.643235922	234059520	0.266581893	3.640197754	0.999311924
-9226.445313	0.472065598	3.660594225	4.352927685	0.001528659	0.999273658	3.648435116	-6727367168	0.392242283	3.65806222	0.999311924
-10303.74707	0.686746359	3.660594225	4.349615574	0.006352653	0.999233246	3.660594225	-12847689728	0.562260032	3.660594225	0.999311924
-10271.4541	0.505558312	3.660594225	4.349615574	0.009386436	0.999174953	3.660594225	-4121015552	0.490734756	3.660594225	0.999311924
-10575.20605	0.402092427	3.660096884	4.353741646	0.003322672	0.999120474	3.660594225	-4619333120	0.457990795	3.65413475	0.999311924
-10279.73438	0.521477662	3.649006188	4.353741646	0.002039726	0.999266922	3.659029007	828891712	0.620009974	3.640232325	0.999311924
-9937.194336	0.550857723	3.643343687	4.353741646	0.000941702	0.999112964	3.660512686	-377279680	0.600391269	3.633893251	0.999298453
-9042.852539	0.325984865	3.642507792	4.353741646	0.001243583	0.999210179	3.657043695	-181474608	0.399820149	3.641684771	0.999300182
-9640.211914	0.264415503	3.642715454	4.353741646	0.001625106	0.999233902	3.656985283	99280920	0.286673993	3.647984982	0.999311924
-8707.029297	0.486707538	3.626523733	4.353741646	0.004215111	0.9992975	3.660594225	-620045248	0.397282571	3.651677847	0.999218106
-8817.102441	0.496294141	3.639412689	4.353741646	0.000494696	0.999311924	3.660594225	-880688345.6	0.477182859	3.644364977	0.999276841
-7990.717285	0.441927016	3.634016752	4.353741646	0.000306464	0.999311924	3.660594225	-878265856	0.573540032	3.652342558	0.999311924
-9367.362305	0.441372871	3.649772882	4.353741646	4.66E-05	0.999311924	3.660594225	-5531349504	0.62286979	3.652342558	0.999311924
-8325.225391	0.540372992	3.655899048	4.353541374	0.000310827	0.99931016	3.660594225	-58035593216	0.696432638	3.656387281	0.999311924
-9195.921875	0.714033425	3.653237104	4.353741646	2.19E-05	0.999311924	3.660594225	-50081972224	0.71682936	3.660594225	0.999311924
-11734.97559	0.655903518	3.653233767	4.353741646	0.00046099	0.999311924	3.660594225	-15206751232	0.583828628	3.660594225	0.999212801
-12437.91699	0.612057984	3.653230667	4.353741646	0.002738581	0.999311924	3.660594225	-6812766720	0.564094186	3.653762102	0.999206364
-11430.0498	0.662299335	3.652342558	4.353741646	0.003614863	0.999311924	3.660594225	-2470855680	0.513405442	3.637987375	0.999246299
-9173.657227	0.747878194	3.652342558	4.353741646	0.003636574	0.999311924	3.660594225	9956240384	0.702278852	3.646277666	0.999282539
-8130.384766	0.496116936	3.626865864	4.353741646	0.000307908	0.999311924	3.660594225	-6261813760	0.721723199	3.660594225	0.999311924
-8251.90625	0.642403483	3.633090496	4.353741646	5.05E-05	0.999311924	3.660594225	-25843003392	0.782641053	3.660594225	0.999311924
-9469.37207	0.797145486	3.63229537	4.349955559	0.005485564	0.999259353	3.660594225	-1.98E+11	0.84536469	3.652342558	0.999311924

-10297.62598	0.835438907	3.652218103	4.349615574	0.005973788	0.999234974	3.660594225	-1.71E+11	0.835216761	3.660594225	0.999311924
-12875.78516	0.775768399	3.653831959	4.349615574	0.006792884	0.999234974	3.660594225	-60575981568	0.789470255	3.659315825	0.999250412
-10202.04102	0.724068761	3.650967121	4.353741646	0.000116431	0.999311924	3.660594225	-44915277824	0.739666224	3.644587517	0.999311924
-9890.34668	0.69802624	3.643529415	4.353741646	4.01E-05	0.999311924	3.660594225	-25571340288	0.736608267	3.654199839	0.999311924
-11545.02637	0.739988089	3.646757364	4.349954128	0.005483796	0.999259293	3.660594225	-1.08E+11	0.759955049	3.660070658	0.999311924
-16324.28613	0.806840897	3.659025192	4.349615574	0.005971948	0.99921298	3.660594225	-34485923840	0.776682317	3.660594225	0.999311924
-13806.81328	0.623620379	3.650967121	4.353741646	0.000368829	0.999311924	3.660594225	-3794616115	0.632818437	3.638237762	0.999311173
-10390.57227	0.605487883	3.652285814	4.353741646	0.000253547	0.999311924	3.660594225	-33865867264	0.638282776	3.648712873	0.999292433
-11563.86719	0.794970393	3.652342558	4.35074091	0.004580519	0.999262154	3.660594225	-1.33E+11	0.780018866	3.652174711	0.999292016
-13110.86133	0.574264109	3.648005009	4.353741646	0.000525705	0.999311924	3.660594225	-11225545728	0.52583468	3.625644445	0.999309599
-10112.19824	0.532153547	3.660201073	4.353741646	0.000523093	0.999311924	3.660594225	-9156651008	0.577502131	3.634463787	0.999214709
-8435.224609	0.575518787	3.627777338	4.353741646	0.004033417	0.999225318	3.660594225	2466510592	0.405621678	3.660594225	0.999268472
-9343.454102	0.413665295	3.638421774	4.353741646	0.005296982	0.99921155	3.657732964	9203752	0.352878094	3.641004562	0.999271631
-9252.587891	0.254032791	3.628981352	4.353741646	0.002311491	0.99930197	3.65453434	14391314	0.293315738	3.649072647	0.999311924
-8936.136719	0.41956681	3.625172138	4.353741646	0.002346193	0.999311924	3.654537201	-716961856	0.508197427	3.6562047	0.999266982
-8585.072266	0.581994295	3.625252247	4.353741646	0.000909794	0.999311924	3.660319567	-2244169984	0.554476082	3.641229153	0.999272466
-8653.097656	0.495977521	3.659378052	4.353741646	0.003479957	0.999311924	3.65955162	-2069065216	0.613671839	3.626405954	0.999311924
-9810.161133	0.671930611	3.650967121	4.353741646	0.003458731	0.999224544	3.660594225	-25577666560	0.750721514	3.642715454	0.999311924
-10929.88965	0.550387204	3.648166656	4.350803852	0.007767424	0.999135673	3.660594225	-26002890752	0.497054756	3.654027462	0.999311924
-6183.719238	0.655496657	3.650967121	4.351261139	0.005130507	0.999286532	3.660594225	2621657088	0.527088463	3.650407791	0.999311924
-8458.922852	0.695433438	3.655640602	4.353741646	0.003617797	0.999300003	3.660594225	5245538304	0.535902858	3.650721073	0.999311924
-8921.716602	0.338271058	3.643003178	4.353741646	0.004737348	0.999262774	3.658972025	581230956.8	0.350527883	3.639405203	0.999311924
-8608.189453	0.277767122	3.616013765	4.353741646	0.002269278	0.999311924	3.660594225	189526320	0.383547008	3.645076752	0.999311924

-8726.193359	0.189702824	3.619102716	4.353741646	0.002316312	0.999311924	3.660594225	31983230	0.423423886	3.641128778	0.999311924
-8623.416992	0.251190275	3.633309603	4.353741646	0.000885712	0.999311924	3.660594225	-627522624	0.418221802	3.638543606	0.999311924
-9129.913086	0.648377538	3.64974761	4.353741646	0.003459128	0.999311924	3.659548759	-18942154752	0.715664268	3.630110025	0.999311924
-8860.777344	0.732513547	3.657809734	4.353741646	0.003476513	0.999311924	3.660594225	-27447732224	0.781033397	3.642715454	0.999311924
-12174.05273	0.566236258	3.644290686	4.351797104	0.006292307	0.999294877	3.660594225	-7984156160	0.53827697	3.652342558	0.999311924
-11646.83496	0.711199999	3.652342558	4.353741646	0.000392563	0.999311924	3.660594225	-3698284032	0.7177912	3.650967121	0.999311924
-8610.844727	0.683038056	3.651801348	4.353741646	5.96E-05	0.999311924	3.660594225	-33342656512	0.641494215	3.651187181	0.999311924
-8600.325781	0.432000571	3.640675926	4.353741646	0.000156378	0.999311924	3.660594225	-4226490650	0.394946069	3.63184042	0.999311924
-8121.703125	0.369479865	3.605787516	4.353741646	0.001100288	0.999311924	3.660594225	-373511680	0.489331454	3.631750822	0.999311924
-9015.102539	0.363338202	3.629607439	4.353741646	0.001160924	0.999311924	3.660594225	277775168	0.35632053	3.641424894	0.999259472
-9406.810156	0.327218753	3.640485573	4.353741646	0.001424841	0.999311924	3.656815958	661164518.4	0.324987417	3.631537962	0.99926188
-8856.568359	0.73780781	3.657681942	4.353741646	0.000151872	0.999311924	3.660594225	7149788160	0.607078254	3.641913891	0.999275982
-7445.484863	0.694312751	3.660594225	4.351259708	0.003738148	0.999277472	3.660594225	1026650304	0.585552454	3.630312204	0.999230266
-7443.694336	0.644441843	3.648805141	4.351258278	0.003794333	0.9992823	3.660594225	467863392	0.617094815	3.631392956	0.99921298
-8912.643555	0.646248996	3.651145697	4.353741646	0.000193543	0.999311924	3.660594225	3468675840	0.530035079	3.631886482	0.99924767
-9484.196289	0.477165401	3.629181862	4.353741646	0.00041903	0.999311924	3.654293299	-59717268	0.531337142	3.634161472	0.999217033
-9027.134766	0.471787721	3.631014824	4.353741646	0.000368891	0.999311924	3.660594225	598736704	0.494857728	3.637761354	0.999251425
-9622.639648	0.451429754	3.621103525	4.353741646	0.000307846	0.999311924	3.656680346	-2329418240	0.473762214	3.635046005	0.999311924
-8608.849609	0.708948612	3.644031286	4.353741646	0.001337389	0.999311924	3.660534859	-54066991104	0.623353064	3.64710474	0.999277771
-8801.457031	0.782242358	3.648056507	4.353741646	0.001324039	0.999311924	3.653060198	-43442384896	0.732036531	3.642551899	0.999309957
-11808.76074	0.7406708	3.651423693	4.353741646	0.000337397	0.999311924	3.652342558	20351793152	0.72139132	3.640552521	0.999311924
-7354.797363	0.650056839	3.637409687	4.353741646	0.00018132	0.999311924	3.648373842	-808216128	0.569173753	3.660594225	0.999224126
-6851.650879	0.614896357	3.634817362	4.353741646	0.000231292	0.999311924	3.655958891	564598208	0.529012918	3.658787012	0.999224126

-8408.666382	0.593122214	3.644553602	4.353741646	0.000181839	0.999311924	3.660594225	828731768	0.446358055	3.648814023	0.999271333
-8527.985645	0.546883368	3.624444914	4.353741646	0.000384607	0.999311924	3.658894873	311429356.8	0.539765471	3.638602829	0.999286985
-9969.470703	0.562677324	3.637963057	4.353741646	0.000424705	0.999311924	3.660594225	-1613321856	0.420921922	3.642967939	0.999239445
-9104.423828	0.589298427	3.644340992	4.353741646	0.000372356	0.999311924	3.660594225	168857184	0.630036116	3.636344194	0.999284983
-7565.646973	0.632582009	3.645948172	4.353741646	0.000164805	0.999311924	3.660594225	-5136497664	0.731495321	3.640436888	0.999311924
-8570.765625	0.580476522	3.650967121	4.353741646	0.000118388	0.999311924	3.660594225	733407744	0.622004688	3.637715578	0.999311924

Cont…

VV_wet_sent	VV_wet_shade	B2_dry_corr	B3_dry	B4_dry_shade	B8_dry	B8_dry_corr	B8_dry_dvar	B8_dry_savg	B8_dry_shade	EVI_dry_shade	SAVI_dry_ent
3.658851576	23758395802	0.569097733	1465.99585	-13799922.8	2793.402588	0.486094403	65098.56328	4739.495508	-235047779.2	1165527194	4.353024483
3.652342558	29463513088	0.721455038	976.6102295	105980056	2581.876465	0.468479186	56643.65234	4804.02832	-189711952	1612948096	4.353741646
3.652342558	3637185024	0.746287346	850.9934082	250038896	2623.098389	0.499410629	39945.08984	4645.580566	-92634176	757933696	4.353741646
3.653556681	-1265501491	0.774353051	656.8512329	-14175664.3	2571.1875	0.486767912	25719.95586	4548.287891	12058249.04	-239850380.8	4.353741646
3.660594225	-690641728	0.814554989	510.7658997	56363204	2549.623779	0.399394661	31743.61719	4474.231445	38789164	-2336508160	4.353741646
3.651561022	799295296	0.721376777	355.0689392	71159248	1756.207153	0.264951915	32410.17383	4497.718262	4060036.25	-1197834752	4.353741646
3.657059526	-1991403282	0.341846946	465.0533447	17512426.1	2287.801221	0.27685571	37253.07109	4523.888574	11520746.9	-69478547.2	4.353741646
3.660594225	-1403367424	0.111607157	398.7375793	16770.9668	2296.932373	0.235574514	25422.82422	4526.737305	31885140	91789520	4.353741646
3.660594225	2389582848	0.147982374	421.5266724	9312.887695	2224.481689	0.314416409	16177.30371	4556.369629	33410698	119637464	4.353741646
3.660594225	1016178560	0.172520846	430.3105774	14108.51367	2197.726563	0.342627883	13807.1582	4344.513184	-6940635	-93103376	4.353741646
3.648811579	608820224	0.165546805	457.2123108	917.1696167	2413.812988	0.435934305	11619.81152	4465.044922	-8612974	-119713632	4.353741646
3.638607979	544081984	0.160870835	423.1967163	2363.280762	2157.451904	0.237241715	11493.64746	4564.178223	2855970	2722409.5	4.353741646
3.639080048	3092396800	0.21684821	420.4918518	10300.40918	2158.087402	0.145502329	17709.16602	4556.349121	797471.6875	-10495648	4.353741646

3.660038471	1433150336	0.273032129	446.0952454	152215.0781	2374.422852	0.41261068	24280.95703	4583.681641	-16698075	-156474016	4.353741646
3.650967121	1751296896	0.531871855	442.3822937	27520596	2254.720459	0.349189162	29108.55469	4521.164551	-9675733	-323750528	4.353741646
3.651105642	206745168	0.715604722	402.6730652	70601048	2039.613525	0.377100766	29561.875	4516.686035	24563142	-1159387008	4.353741646
3.654701233	-549501248	0.680183709	470.0877075	93481128	2105.976074	0.449209124	25011.59961	4548.660156	48999264	-858563200	4.275349617
3.652342558	4949073408	0.785256684	455.1110229	133287760	1928.685425	0.601785839	32151.07422	4478.79541	-57924744	-3761948160	4.275349617
3.652342558	15227961344	0.754637063	804.3208008	746344448	1987.575806	0.676270008	50440.84766	4399.356445	-87871016	137855664	4.275349617
3.65797863	73529294848	0.65803076	1106.314673	353065840	2050.597217	0.691036904	64504.53203	4210.680811	150839843.2	1596741274	4.275349617
3.660594225	39043973120	0.674233258	765.0808716	388170144	1700.654175	0.201777115	58287.53125	3473.955566	78348224	860323008	4.275349617
3.652813911	10646514688	0.724880099	823.1484375	956020800	1757.012329	0.47381559	54000.30078	3868.226563	93583984	1201841024	4.275349617
3.652810812	5230601728	0.733534515	502.1182556	230633392	2180.179932	0.432885736	34527.37109	4079.070068	-96023320	-4410084352	4.275349617
3.655036211	2467402752	0.388065517	462.1414185	41612984	2286.134766	0.178029671	17386.80859	4361.242188	3531296.25	-1266548736	4.275349617
3.660281181	1610735488	0.33103928	447.5558472	2965871	2242.607666	0.445017427	20424.54297	4568.691895	16992790	-12595025	4.275349617
3.660284758	260969024	0.503638864	455.3888855	72343.64063	2422.436279	0.522675872	17588.70117	4680.994629	-970702.375	-55948768	4.275349617
3.660301685	406769952	0.643407166	435.9743042	36179.3125	2357.261475	0.548713088	15127.25977	4828.624023	-5006911	-67271096	4.275349617
3.643342781	719619225.6	0.627537954	454.439447	26723.03828	2456.051709	0.55503211	13323.09121	4801.930762	15640875.6	33826807.6	4.275349617
3.630529881	307326336	0.615576446	423.7692566	28075.60742	2252.523926	0.524467766	12104.01855	4739.832031	19936092	49536584	4.275349617
3.642669725	1481719078	0.192153567	442.5050476	3872.91958	2371.683984	0.445519263	10920.45898	4565.84375	-12877597.6	-108736113.6	4.322384834
3.650967121	97154584	0.455774844	451.0569763	67184.10938	2464.905029	0.256318033	12353.34961	4791.061035	8607988	5522156	4.275349617
3.650967121	251121280	0.493953258	487.5419617	30168.22461	2485.001709	0.370507956	15961.28027	4868.314453	16630136	14843080	4.275349617
3.65991497	470508128	0.403589308	519.8999634	32606.90625	2797.262695	0.419576675	16231.84863	4905.459473	3199719.25	-29193226	4.275349617
3.650371313	1306593280	0.47746703	468.1943054	57623.16016	2571.156494	0.437291443	16097.69434	4849.472168	8571084	-5791642.5	4.275349617
3.646513999	-572299440	0.229663573	454.1856079	101240.019	2313.12439	0.491796307	11256.29541	4649.415649	-2254872.219	-27279077.06	4.275349617
3.652342558	-380228416	0.361055225	454.8747253	57064924	2235.384277	0.447197706	11048.57227	4384.751953	1914342.75	-2052905088	4.275349617

3.660594225	-2957746176	0.697079718	494.7829895	175090272	2102.312744	0.536643505	22900.1875	4010.664551	-88805288	-3324995840	4.275349617
3.660594225	-6937924608	0.619951725	639.4753418	43940468	1560.850098	0.498948067	29130.75586	3639.716309	-38019452	2396758528	4.275349617
3.660594225	478004448	0.579641998	556.8215332	84489512	1425.651855	0.405519128	44154.47266	3456.675049	27358438	741656192	4.285373211
3.660594225	-3739030669	0.681470716	728.5991089	178858004.8	1959.814478	0.482779998	32342.45352	3894.645361	-74136340.8	2528068045	4.353166294
3.657893419	-4284423936	0.74624294	458.7237854	399305696	1985.348633	0.392076224	22456.17578	4218.946777	-31753274	-5772137472	4.353741646
3.642073631	-1259821056	0.612271667	452.2364197	73591064	2296.879883	0.395499945	16611.53516	4457.884766	3156459.25	-1537274624	4.353741646
3.64167428	-160861168	0.386449188	449.4143677	127324.5859	2517.19873	0.45467782	12846.02441	4627.04248	1635664.625	7623898	4.285240173
3.643414497	1334158464	0.601391494	443.0726318	78353.98438	2292.350098	0.531825423	14216.99219	4730.057617	11896409	10915802	4.285210609
3.637908697	561460928	0.588355958	467.264801	54794.25391	2255.4375	0.541004419	14305.97461	4780.992188	1463624.375	-6429297	4.285181046
3.651424646	17280626.25	0.46226421	470.3234253	37481.50195	2353.207153	0.436629951	15209.59033	4829.292236	8017976.75	22210017	4.280250549
3.658924341	112586784	0.352350712	435.177002	51846.60938	2198.579346	0.294895738	11839.64746	4848.091309	2056257.75	-9838638	4.275349617
3.653564692	133495552	0.315484941	454.6337891	50358.51953	2382.759277	0.211391538	11435.25977	4877.504395	-3601972.75	-25073374	4.353741646
3.656378078	-82898901.2	0.3666152	453.2009827	54735	2449.741943	0.23413718	13042.45371	4780.410645	-3187225.75	-15583102.6	4.353741646
3.660594225	-45576600	0.324720055	447.9618225	50686.52734	2190.17749	0.319346309	13153.17969	4663.804199	-9517750	-37127448	4.353741646
3.653044462	78334800	0.263373971	425.0526123	68170.5625	2117.508545	0.320358425	13868.1377	4601.927246	-7618838	-28475390	4.353741646
3.645712614	609900288	0.288205922	437.4378967	13807762	2075.133789	0.344073862	16677.16211	4564.134277	-9545417	-129306616	4.353741646
3.645715714	-1928387072	0.701093376	418.7032776	168681984	1958.628662	0.334714174	20414.45508	4479.404297	-9666236	-4290490368	4.353741646
3.658423901	9159083008	0.769085705	618.0822754	244183952	2450.187744	0.443787664	22488.13477	4227.979492	-12208578	-3912326912	4.345489502
3.660594225	21639530496	0.69732523	799.461731	-148146928	1836.111694	0.502459347	27531.47852	3987.125244	12864089	6825145344	4.345489502
3.660594225	18294155264	0.796048343	777.9902954	-37625116	2193.233643	0.60945034	29337.86133	4180.601563	-32623668	1021149440	4.344482422
3.654354572	-7464198656	0.792867482	465.0653687	337002208	2326.671387	0.408586353	28431.27734	4509.166992	-54726420	-10277864448	4.353741646
3.653802872	741999736	0.446305752	460.1651764	60988954.16	2401.627075	0.369255021	17522.18091	4629.765869	-13235714.5	-705235891	4.353741646
3.660594225	-83324352	0.307992339	468.1060791	33597.27734	2389.983398	0.377912104	11059.3418	4705.034668	-15312402	-51808528	4.353741646

3.660594225	-10260246	0.255972177	457.6324463	-3677.56543	2448.849854	0.318388969	11461.73145	4733.567383	-14046019	-46540072	4.353741646
3.660594225	408855008	0.119682431	476.7437744	-483.0000305	2465.913818	0.171465769	12024.42676	4833.586426	-3576905.75	-9981404	4.353741646
3.652869225	298408096	0.288566232	459.9744873	34570.35938	2535.185059	0.228593543	11328.93555	4966.421387	-4572576.5	-10642076	4.353741646
3.653119898	296449811.2	0.218625557	450.2703369	40263.10313	2312.360791	0.391556942	21020.77969	4398.16377	-15653657.3	-370031513.6	4.353741646
3.652342558	15390650	0.140207306	419.4417419	12792.32227	2283.108887	0.327949882	40724.46484	4599.35791	-66004416	-669843712	4.353741646
3.652342558	-22998388736	0.125953764	482.7411194	6922021	2603.200439	0.27350229	58248.70703	4523.427734	-54512252	-675302528	4.353741646
3.660516739	-65961486746	0.534166127	434.5218628	30901941	2078.546484	0.283959121	54502.29375	4614.197461	-54595253.6	-400011720	4.353741646
3.660594225	-36034564096	0.799098849	526.713562	27844374	2621.570068	0.300589412	42401.37891	4505.986328	40348108	-1323891456	4.353741646
3.660594225	-22803822592	0.771838605	697.2477417	1163357.5	2073.560303	0.54624927	32855.72656	4465.581055	38239116	4755190.5	4.353741646
3.660594225	-12906775552	0.678123832	660.0286255	13843605	1807.840332	0.646479905	20521.59766	4316.770996	75050768	1575869312	4.353741646
3.660594225	4356282368	0.619702399	834.0432129	138069120	2160.580322	0.706736565	22002.29688	4548.026855	-27136700	3524537856	4.353741646
3.655656815	20525819904	0.692629099	944.7474365	191404432	2522.264404	0.666196048	23312.5625	4759.20459	-89762808	1651292672	4.353741646
3.660594225	-7509975552	0.298104227	449.8364868	-105495.2422	2519.414063	0.68270123	58008.17969	4324.061523	-976388800	-6703473152	4.346493721
3.660594225	-52632293376	0.241143167	493.5873108	8312880.5	2193.536621	0.620183587	69057.03125	4120.953125	-633578432	-3678823936	4.350774765
3.660594225	-2.31E+11	0.620746434	445.8435974	47375384	2135.802002	0.6533041	63591.92188	4101.842773	-521474240	-40457732	4.353680611
3.660594225	-2.46E+11	0.799702525	592.3423462	-9706108	2627.5979	0.44614017	49344.72656	4298.439453	-77974960	158099712	4.353741646
3.660594225	-1.76E+11	0.761098981	713.0620728	27334746	2106.729248	0.579274058	29558.16406	4226.371094	111414200	2623268352	4.353741646
3.660594225	-38913306624	0.453404963	483.9677734	-359264.6875	2228.955566	0.744862139	69777.53906	3864.302979	-832667136	-4846955008	4.273974419
3.660594225	-6675036160	0.407474369	349.9143372	9154892	840.0026245	0.662971914	78517.35156	3572.663574	-113042312	-68189952	4.273974419
3.660594225	-81787437056	0.649621546	298.5145264	65599900	1455.800171	0.674090683	65543.26563	3476.408691	43116236	1438625664	4.275237083
3.660594225	-61996892160	0.770262837	632.4146118	11418588	2101.508301	0.578589082	47011.42969	3923.823975	-26258292	541960576	4.337888718
3.660364866	2718410457	0.512448144	404.5008118	64247.46367	1323.720679	0.656690598	65105.01953	3083.234277	379883123.2	1724649856	4.273974419
3.650967121	-20523319296	0.502422333	308.1130371	24648114	1205.014648	0.533688366	62237.58203	2986.454102	168986192	1289257984	4.273974419

3.650967121	-1.28E+11	0.687092841	348.464325	100083152	1847.190308	0.716091752	55105.80078	3447.609863	909574976	4357683712	4.275349617
3.660332918	-6088036864	0.465318441	353.3653259	128735.4922	982.3700562	0.588849247	57293.17969	3059.232178	222726624	1079843328	4.286158085
3.65404892	2451552512	0.34997806	323.6618347	193595.0156	1321.833618	0.666055679	64646.13672	3178.576172	1001897536	4181016320	4.278538704
3.650967121	190868448	0.145986795	460.8491516	3372.693115	2602.083252	0.360017508	19466.69727	4946.997559	-37415124	-144094096	4.344114304
3.652865887	251694672	0.183799654	445.6689453	859.4962158	2258.530273	0.361740947	13357.32617	4933.910645	-10294813	-39423276	4.346013069
3.652342558	346605920	0.17592597	438.9207153	-1742.679321	2344.521729	0.219007894	13092.88965	4818.01123	-101967.4922	12961678	4.353741646
3.660594225	-275108256	0.23396866	480.2435608	-5940.333984	2445.108154	0.238129377	9677.905273	4783.271484	-6199559.5	-28460074	4.353741646
3.660594225	-1179610496	0.194662675	463.2481079	14656.1123	2431.544189	0.170077845	9402.724609	4822.621094	-9303786	-24340804	4.353741646
3.660594225	-4737221632	0.509050012	466.7501526	32392538	2356.716553	0.212638855	15975.90527	4890.475098	2289000.75	-686622144	4.353741646
3.652961493	-17763006464	0.765689135	500.2757568	359982368	2436.568115	0.393165499	25150.57422	4758.83252	-56167392	-11355490304	4.353741646
3.650967121	1424729728	0.797235072	882.019104	-297084.0938	2393.23584	0.708943427	28095.15234	4308.929688	-100010616	-99481840	4.344927788
3.654717207	-1491377536	0.482503861	489.0828247	8433627	2490.521484	0.634800673	22003.85547	4715.851563	-91835992	-1741134976	4.349901199
3.660594225	108693112	0.160553902	452.0790405	13965.52051	2455.334717	0.273585856	20149.72461	4985.067383	-31356138	-209896864	4.344114304
3.660594225	71308805.6	0.255447832	473.0907654	3183.949561	2554.433789	0.352078497	14026.89824	4915.915625	-7742162.6	-49987178.4	4.345251179
3.652342558	155787152	0.24879238	423.4622803	34.06584549	2240.927246	0.28397727	13570.10938	4840.705566	-1509453	-2958408.5	4.353741646
3.660594225	-200355792	0.185045883	476.324646	-4453.933105	2471.917969	0.316728473	8819.013672	4841.015625	-3596683.5	-20342086	4.353741646
3.660594225	-1295045120	0.063497841	461.0315552	70517.94531	2464.868408	0.12896359	9015.586914	4912.020996	407908.625	-2697876.25	4.353741646
3.660594225	-17541801984	0.639880538	468.9594116	51032536	2518.77002	0.313562155	22525.5918	4887.419922	-25405740	-3115833088	4.327316284
3.660594225	-8603511808	0.770859301	548.9034424	239380784	2706.532227	0.544429362	31643.36914	4638.086914	-121079840	-6888371200	4.327287674
3.660594225	8766507008	0.749711037	929.8096313	45572428	2150.604492	0.663920343	41888.16797	4161.010254	34532592	3165242368	4.320433617
3.656893969	5714969600	0.754174054	652.3720703	98114416	2194.209717	0.672076106	34542.74219	4439.422363	-86184296	-788084672	4.275349617
3.660594225	-26300942336	0.577661037	497.8941956	52490704	2516.969482	0.350149542	23642.24414	4933.992676	-25277000	-3594264832	4.275349617
3.660594225	-2828421888	0.356457901	460.9867798	1408842.059	2424.921729	0.192919326	18342.27695	4968.148535	4452972.1	-61198541.45	4.275349617

3.652962685	-533209824	0.242828816	480.4482422	411.3180237	2606.697266	0.211475134	13002.99316	4905.893555	-3349837.75	-23266256	4.275349617
3.65930748	120606632	0.253689766	429.8253174	3756.530273	2417.300781	0.303135693	11798.98926	4897.665039	-4564854	-34235816	4.275349617
3.660594225	288073037.2	0.308532435	461.4000305	7493.109229	2434.483447	0.296094459	12619.64648	4897.663086	-5184683.55	-39956545.2	4.303017616
3.660594225	1149680640	0.275508195	479.2258606	13845.04688	2500.358154	0.166241691	17785.49219	4976.009766	-8317836	-46307176	4.321073532
3.660594225	-925528640	0.283103794	486.4829712	1978307.5	2644.015869	0.531771302	19433.24414	4787.911621	-49360000	-416882464	4.324950695
3.656920195	-436965728	0.203392908	485.3989258	6363.142578	2558.624023	0.477376103	21001.94727	4796.918457	-51151432	-299392384	4.275349617
3.660594225	522686144	0.285388678	482.5449219	9724.783203	2399.621582	0.197247475	17320.86523	4906.24707	-4458368.5	-23212134	4.275349617
3.660594225	-272871392	0.28843829	460.2174072	14197.93066	2336.372314	0.126754031	12282.50293	4870.265625	-3068938.5	-13561741	4.275349617
3.660594225	108206192	0.244151935	453.42099	4810.947266	2581.860107	0.240923166	15663.93652	4852.88623	-11140694	-52976616	4.275349617
3.660594225	-2249469440	0.303598166	421.6181946	29184.76172	2454.216553	0.201435879	18299.42188	4891.909668	-14384147	-85114816	4.275349617
3.660594225	-44866453504	0.420820355	447.5462952	92683424	2362.556885	0.338438332	38366.71875	4812.29248	-38702424	-3310273792	4.275349617
3.660594225	-43105611776	0.667130172	531.046875	318766688	2836.793945	0.377264172	38646.09766	4720.452637	-31244750	-8699966464	4.275349617
3.652582407	15534130176	0.679987133	553.0990601	139160752	2206.516357	0.618280947	42528.82031	4368.821777	2427499.75	314968800	4.275349617
3.660594225	384508032	0.203978136	493.6782227	213874.125	2456.544922	0.341932476	22217.26758	4667.078125	-14510486	-72224152	4.275349617
3.65637517	-261181520	0.192856103	495.5396729	-257.265625	2373.118652	0.262661695	21264.86328	4786.426758	-20686522	-103554816	4.275349617
3.651115298	-1286894832	0.155395959	481.2364502	8684.624268	2507.893982	0.220067475	18422.9939	4772.884521	-6938569.5	-61805013	4.275349617
3.654407358	-385692579.2	0.169204603	462.4557312	20326.00137	2303.85459	0.112915005	15495.25098	4845.345703	-3149010.8	-19663346.4	4.275349617
3.650967121	436339712	0.229490265	440.0582581	904850.125	2481.471924	0.232546061	18863.62109	4747.51709	-7815436.5	-103745648	4.275349617
3.650967121	-10455340032	0.287094653	481.3255615	91470160	2478.706543	0.402452022	27858.36328	4532.708008	-36723628	-5635420672	4.353741646
3.657935858	-8074277888	0.174043298	460.947113	17693168	2179.073975	0.309047163	33130.46094	4647.39209	-42292920	-1911848064	4.353741646
3.654405117	-2834092544	0.194587424	459.2492676	8052.243164	2453.039063	0.210147083	28989.94141	4674.194336	-5863418	-74605056	4.310115337

Cont…

Plot	**Ponto_X**	**Ponto_Y**	**AGB_2017**	**2017 variables**

				VH_dry	VH_dry_corr	VH_dry_dent	VH_dry_ent	VH_dry_sent	VH_dry_shade	VH_wet_dent	VH_wet_imcorr1	VH_wet_sent	VV_dry_asm
1	-44.9702	-21.2272	6.447519	-11023.2	0.635958	3.648467	4.353742	3.660594	4.27E+10	3.650548	-0.86163	3.658509	0.01308
2	-44.9702	-21.2274	5.055043	-15463.7	0.754382	3.646738	4.353742	3.660594	6.64E+10	3.644091	-0.86163	3.660594	0.013002
3	-44.9701	-21.2276	5.170532	-17323.5	0.559152	3.647735	4.349616	3.660594	1.77E+10	3.648806	-0.86163	3.660594	0.013039
4	-44.9701	-21.2278	4.562179	-15622.6	0.62426	3.657417	4.349616	3.660594	-1.2E+10	3.645152	-0.86163	3.660594	0.012996
5	-44.9701	-21.2279	3.391004	-15544.7	0.606974	3.652343	4.34549	3.660594	-2.2E+10	3.652848	-0.86163	3.660594	0.012953
6	-44.9701	-21.2281	3.416768	-16252.9	0.413059	3.652343	4.349616	3.660594	1.36E+08	3.660594	-0.86032	3.660594	0.012897
7	-44.97	-21.2283	7.733483	-14719.2	0.547308	3.647117	4.349616	3.654498	1.61E+09	3.656221	-0.8505	3.660594	0.012897
8	-44.97	-21.2285	6.396627	-16215.4	0.636725	3.636153	4.349616	3.642503	1.67E+09	3.632907	-0.85137	3.660594	0.012897
9	-44.97	-21.2286	4.339548	-15866.3	0.481794	3.644091	4.353742	3.649921	1.63E+09	3.61654	-0.84641	3.64134	0.012897
10	-44.9699	-21.2288	9.622515	-16329.1	0.597367	3.645771	4.35044	3.652343	-2.7E+08	3.61796	-0.85043	3.649045	0.012968
11	-44.9701	-21.2289	6.085101	-15750.8	0.556988	3.659621	4.350438	3.660594	-1.8E+09	3.64192	-0.86067	3.658292	0.013229
12	-44.9701	-21.2287	4.725702	-14244.3	0.446772	3.643766	4.353742	3.649826	-5E+08	3.633338	-0.85238	3.650588	0.012965
13	-44.9702	-21.2285	6.612984	-16037.5	0.513197	3.643781	4.349616	3.641704	-5.6E+08	3.643337	-0.83277	3.660594	0.012965
14	-44.9702	-21.2283	3.967721	-15267.2	0.481284	3.627125	4.349616	3.650967	2.25E+08	3.652051	-0.85054	3.660594	0.0129
15	-44.9702	-21.2281	4.718428	-15227.8	0.341325	3.634606	4.349616	3.660594	1.57E+08	3.659444	-0.86061	3.652279	0.012897
16	-44.9703	-21.228	7.009488	-14683	0.328684	3.634602	4.34549	3.660594	-2.5E+09	3.652085	-0.86163	3.652461	0.012953
17	-44.9703	-21.2278	5.206742	-16408.5	0.397426	3.649962	4.349655	3.650967	-1.4E+09	3.644169	-0.86163	3.660594	0.013089
18	-44.9703	-21.2276	8.066001	-15903.5	0.311437	3.652343	4.349656	3.650967	-4.1E+07	3.649296	-0.86163	3.660594	0.013579
19	-44.9704	-21.2274	5.370659	-16338.3	0.622569	3.660594	4.351914	3.660594	9.12E+10	3.656864	-0.86163	3.660594	0.013617
20	-44.9704	-21.2272	4.897013	-11793.4	0.706664	3.660497	4.353742	3.660511	9.38E+10	3.65555	-0.86163	3.659171	0.013468
21	-44.9706	-21.2273	5.567301	-17649.8	0.742313	3.655743	4.353742	3.656706	1.11E+11	3.655563	-0.86163	3.660594	0.013444
22	-44.9706	-21.2275	4.764913	-16745.3	0.699869	3.660594	4.353742	3.660594	9.73E+10	3.644952	-0.86163	3.660594	0.013476

23	-44.9705	-21.2276	5.662465	-16117.5	0.398794	3.652343	4.353742	3.651514	-2.1E+09	3.630616	-0.8596	3.650967	0.013437
24	-44.9705	-21.2278	7.959734	-16477.3	0.364082	3.647154	4.353742	3.65151	5.39E+08	3.65221	-0.85363	3.650967	0.013039
25	-44.9705	-21.228	4.924686	-15490.7	0.409757	3.645784	4.353742	3.652943	-1.3E+09	3.647016	-0.86163	3.652343	0.013024
26	-44.9704	-21.2282	6.611418	-15068.2	0.437205	3.645073	4.353228	3.660594	-4E+08	3.631884	-0.86063	3.653336	0.012899
27	-44.9704	-21.2283	5.289209	-13842.4	0.522802	3.652245	4.349609	3.659912	-9E+08	3.6331	-0.85097	3.659984	0.012902
28	-44.9704	-21.2285	5.426082	-15302.1	0.50641	3.640868	4.346332	3.654545	-5.4E+08	3.64041	-0.8507	3.658789	0.012968
29	-44.9703	-21.2287	6.049001	-14586	0.43595	3.643123	4.34549	3.65104	-5.4E+08	3.642805	-0.86061	3.660594	0.012968
30	-44.9703	-21.2289	7.027927	-14455.2	0.508547	3.650628	4.349454	3.65913	3.21E+08	3.64597	-0.86163	3.65691	0.013231
32	-44.9705	-21.2287	6.174042	-15305.5	0.400208	3.641092	4.337203	3.659289	1.75E+08	3.651113	-0.85541	3.653577	0.012968
33	-44.9706	-21.2286	4.36059	-14905.2	0.432472	3.635848	4.340996	3.652343	-8.8E+07	3.642791	-0.85159	3.659499	0.012968
34	-44.9706	-21.2284	5.113152	-13764.2	0.549895	3.650942	4.344802	3.643503	-1.8E+09	3.624903	-0.86163	3.651663	0.013033
35	-44.9706	-21.2282	4.99057	-15002	0.625206	3.650932	4.349616	3.659898	-3.1E+08	3.624782	-0.85467	3.651692	0.012968
36	-44.9707	-21.228	4.990641	-16201.9	0.475354	3.638886	4.353742	3.660594	1.54E+09	3.630614	-0.85315	3.649714	0.013033
37	-44.9707	-21.2278	4.3881	-16859.3	0.325097	3.640173	4.353742	3.660594	5.65E+08	3.649978	-0.84481	3.650967	0.013039
38	-44.9707	-21.2277	6.667931	-17169	0.50895	3.653198	4.353742	3.659596	-9.2E+09	3.63638	-0.85864	3.650967	0.013396
39	-44.9707	-21.2275	7.924532	-18965.8	0.618623	3.657281	4.353742	3.659593	4.72E+09	3.65303	-0.86163	3.660594	0.013426
40	-44.9708	-21.2273	5.214948	-19338.6	0.358008	3.652673	4.353742	3.652112	4.03E+09	3.648304	-0.86163	3.660594	0.012959
41	-44.9709	-21.2275	5.103967	-17944.8	0.562003	3.660178	4.353742	3.650967	-1.4E+09	3.647837	-0.86163	3.655212	0.012897
42	-44.9709	-21.2277	6.08299	-16522	0.491675	3.6583	4.353742	3.654118	-1E+10	3.639793	-0.85111	3.651174	0.012897
43	-44.9709	-21.2279	5.754056	-16312.5	0.318658	3.646326	4.353742	3.660594	3.36E+08	3.659506	-0.84603	3.653191	0.012968
44	-44.9708	-21.228	5.722723	-16246.7	0.440027	3.645132	4.353742	3.660594	1.01E+09	3.628173	-0.85147	3.650977	0.013019
45	-44.9708	-21.2282	4.502228	-16300.8	0.542394	3.6282	4.350134	3.659983	7.52E+08	3.627598	-0.85227	3.644091	0.012968
46	-44.9708	-21.2284	6.008705	-15558.8	0.556925	3.635508	4.345319	3.653377	-9.6E+08	3.62832	-0.86081	3.652337	0.012976

47	-44.9708	-21.2286	4.282676	-14848.2	0.535885	3.628271	4.343349	3.652858	-1.9E+08	3.643495	-0.86161	3.656146	0.012901
48	-44.9707	-21.2288	3.800565	-14860.6	0.518575	3.627236	4.337619	3.659292	7.98E+08	3.654348	-0.86163	3.644926	0.012897
49	-44.9709	-21.2288	9.118458	-13543.7	0.383065	3.645583	4.345452	3.660594	2.9E+08	3.650917	-0.86163	3.652343	0.012968
50	-44.9709	-21.2286	8.132903	-14128	0.438171	3.652841	4.349259	3.660594	-5E+08	3.645687	-0.86152	3.657237	0.012968
51	-44.971	-21.2284	4.29812	-14467.9	0.562166	3.639763	4.349758	3.660594	-4.8E+08	3.653735	-0.86163	3.650685	0.013026
52	-44.971	-21.2283	7.425472	-15618.6	0.50321	3.639678	4.353742	3.660594	5.22E+08	3.653768	-0.85276	3.649376	0.012961
53	-44.971	-21.2281	6.093324	-15912.6	0.400107	3.649075	4.353742	3.660594	-1.2E+08	3.660594	-0.85484	3.649374	0.012897
54	-44.9711	-21.2279	5.270318	-15637.2	0.419124	3.658699	4.353742	3.660594	-3.4E+09	3.653344	-0.85595	3.652343	0.012897
55	-44.9711	-21.2277	10.11734	-15044.5	0.579529	3.652343	4.353742	3.655399	-1.3E+10	3.642715	-0.86076	3.652343	0.012897
56	-44.9711	-21.2275	9.288309	-18857.7	0.554569	3.652343	4.353742	3.660594	2.79E+09	3.643384	-0.86163	3.652343	0.012897
58	-44.9713	-21.2277	7.100712	-16872.1	0.657735	3.645102	4.352734	3.657437	-1.7E+10	3.648261	-0.86163	3.653697	0.012897
59	-44.9713	-21.2279	6.726186	-16489.6	0.700842	3.646608	4.348609	3.650967	-3.9E+10	3.64372	-0.86163	3.652343	0.012897
60	-44.9712	-21.2281	5.541135	-15075.9	0.411246	3.6431	4.350754	3.655092	-1.3E+09	3.654722	-0.85812	3.644922	0.012897
61	-44.9712	-21.2283	5.481215	-14703.1	0.447888	3.633692	4.352836	3.658482	1.35E+08	3.660594	-0.86163	3.644828	0.012968
62	-44.9712	-21.2285	6.792843	-13940.1	0.463406	3.64094	4.353709	3.658485	-4.1E+08	3.651312	-0.86163	3.66003	0.012983
63	-44.9711	-21.2286	5.188354	-14976.4	0.389569	3.657617	4.353742	3.658489	-3.3E+08	3.6448	-0.86163	3.654899	0.012983
64	-44.9711	-21.2288	16.5369	-13909.2	0.357215	3.638474	4.35043	3.652343	3.64E+08	3.642715	-0.85687	3.644591	0.012911
65	-44.9697	-21.2288	6.556011	-16292.2	0.591977	3.660366	4.351969	3.644594	6.8E+08	3.617909	-0.84175	3.651015	0.012897
66	-44.9698	-21.2286	4.94311	-15075.6	0.605991	3.653354	4.353742	3.660594	1.5E+09	3.626754	-0.84267	3.651726	0.012897
67	-44.9698	-21.2284	8.25591	-13813	0.558792	3.652343	4.353742	3.660594	-5.9E+09	3.641423	-0.8453	3.660594	0.012897
68	-44.9698	-21.2283	5.960035	-13607.2	0.640138	3.650283	4.352271	3.658736	-4.1E+10	3.646867	-0.84719	3.660594	0.012897
69	-44.9699	-21.2281	8.067188	-15125.3	0.720876	3.646938	4.346986	3.660594	-7.6E+10	3.660594	-0.86163	3.660594	0.012897
70	-44.9699	-21.2279	5.75003	-16280.4	0.627201	3.651434	4.349161	3.660594	-4.2E+10	3.660594	-0.86163	3.660594	0.012897

71	-44.9699	-21.2277	5.417591	-19204.5	0.528283	3.660594	4.35006	3.660594	-1.6E+10	3.660594	-0.86163	3.660594	0.012897
72	-44.97	-21.2275	8.699905	-18636.6	0.58578	3.651774	4.349616	3.660594	2.53E+10	3.652343	-0.86163	3.660594	0.013027
73	-44.97	-21.2274	14.09278	-13749	0.727112	3.65177	4.353742	3.660594	8.07E+10	3.652343	-0.86163	3.660594	0.012993
74	-44.9696	-21.2286	5.179711	-14218.8	0.66737	3.658326	4.353742	3.660594	-7.5E+09	3.636266	-0.85217	3.660594	0.012929
75	-44.9696	-21.2284	8.700023	-14220.1	0.746459	3.652096	4.353742	3.660594	-2E+10	3.633101	-0.85475	3.660594	0.012897
76	-44.9696	-21.2282	6.918465	-15837	0.803773	3.634428	4.353742	3.660594	-1.88E+11	3.640661	-0.86163	3.660594	0.012897
77	-44.9697	-21.2281	12.32815	-16667.5	0.818479	3.648124	4.353742	3.660594	-3.23E+11	3.650967	-0.86163	3.660594	0.012897
78	-44.9697	-21.2279	8.96122	-20219.5	0.716006	3.660594	4.353742	3.660594	-1.86E+11	3.658244	-0.85374	3.660594	0.012897
79	-44.9694	-21.2286	5.117404	-16689.4	0.758563	3.650967	4.353742	3.660594	-4.8E+10	3.637626	-0.85632	3.660594	0.013074
80	-44.9694	-21.2284	11.40248	-17196	0.747666	3.650967	4.353742	3.660594	-2.2E+10	3.644886	-0.85844	3.660594	0.012897
81	-44.9694	-21.2282	8.25269	-18464.6	0.691488	3.633292	4.353742	3.660594	-8.8E+10	3.652467	-0.86163	3.658418	0.012968
82	-44.9695	-21.228	7.414699	-21087.6	0.784616	3.639771	4.353742	3.660594	-1.39E+11	3.651245	-0.86163	3.660594	0.012911
83	-44.9692	-21.2285	11.52005	-20979.5	0.642697	3.643451	4.353742	3.660594	-8.6E+09	3.65153	-0.8584	3.660594	0.012957
84	-44.9692	-21.2284	8.246861	-17741.9	0.644034	3.640194	4.353742	3.660594	-1.8E+10	3.660486	-0.85385	3.653886	0.012965
85	-44.9693	-21.2282	6.091279	-16251.8	0.766689	3.637707	4.353742	3.660594	-2.27E+11	3.660594	-0.85385	3.643966	0.012968
86	-44.969	-21.2285	10.21862	-20521.2	0.611419	3.649604	4.353742	3.660594	-1.4E+10	3.646575	-0.85366	3.660594	0.012897
87	-44.969	-21.2283	13.85901	-17182.5	0.682212	3.643217	4.353742	3.660594	-1.6E+10	3.654918	-0.84966	3.660594	0.012965
88	-44.9713	-21.229	9.787868	-14692.8	0.498232	3.648772	4.347633	3.652343	2.08E+08	3.646179	-0.85545	3.660594	0.012897
89	-44.9713	-21.2288	11.18572	-15380.6	0.443688	3.654734	4.35123	3.650444	1.81E+08	3.64465	-0.85781	3.660594	0.012982
90	-44.9713	-21.2287	7.392263	-14408.4	0.45117	3.649465	4.353742	3.649848	-4.6E+08	3.644795	-0.86163	3.659635	0.013039
91	-44.9714	-21.2285	7.855295	-14006.9	0.303714	3.619628	4.353595	3.64134	-7.7E+07	3.641232	-0.86163	3.652343	0.013039
92	-44.9714	-21.2283	7.042004	-15391.8	0.408806	3.635465	4.349616	3.650531	-3.8E+08	3.660594	-0.86163	3.652343	0.012971
93	-44.9714	-21.2281	8.657125	-14773.2	0.413548	3.634837	4.346011	3.654624	-1.7E+09	3.650967	-0.8591	3.652343	0.012897

94	-44.9714	-21.228	5.073911	-14959.5	0.701165	3.639658	4.34549	3.653764	-3.5E+10	3.650967	-0.8599	3.650633	0.012897
95	-44.9715	-21.2278	8.226853	-17939	0.733037	3.646235	4.348427	3.653768	-1.8E+10	3.653656	-0.86163	3.652343	0.012897
96	-44.9714	-21.2292	9.146012	-13821	0.750442	3.651723	4.349616	3.660594	6.05E+09	3.629793	-0.85593	3.660594	0.012897
97	-44.9715	-21.2291	4.337543	-15064.6	0.595882	3.651652	4.349616	3.660594	2.93E+09	3.636169	-0.85284	3.659712	0.012897
98	-44.9715	-21.2289	7.925062	-15574.6	0.43778	3.651259	4.353742	3.659576	1.51E+08	3.646088	-0.8516	3.655076	0.01295
99	-44.9715	-21.2287	8.727682	-14168	0.531068	3.651685	4.353742	3.653209	-4.9E+08	3.631885	-0.8581	3.650967	0.012968
100	-44.9715	-21.2285	4.154346	-13875.9	0.405392	3.63819	4.353597	3.647365	16961230	3.629554	-0.86163	3.660594	0.012968
101	-44.9716	-21.2283	7.513078	-14045.9	0.326405	3.649068	4.349616	3.653681	-6.4E+07	3.650849	-0.85217	3.660594	0.0129
102	-44.9716	-21.2282	5.402737	-13824.2	0.538421	3.653036	4.346013	3.660594	-4.3E+09	3.652572	-0.85089	3.655124	0.012897
103	-44.9716	-21.228	9.326141	-14382.8	0.753552	3.645803	4.34549	3.660594	-2.9E+10	3.651878	-0.8484	3.651208	0.012897
104	-44.9717	-21.2278	14.5859	-17846.1	0.726745	3.655836	4.348426	3.660594	-3.1E+09	3.655767	-0.85256	3.652343	0.012897
105	-44.9718	-21.228	7.9088	-16327.8	0.74686	3.654058	4.349616	3.660594	-9.2E+09	3.647267	-0.84638	3.660594	0.012897
106	-44.9718	-21.2282	5.128927	-15396.1	0.636947	3.646543	4.353742	3.660594	-1.3E+10	3.651481	-0.85111	3.660594	0.012897
107	-44.9718	-21.2284	8.493005	-14836.3	0.57598	3.64569	4.352163	3.660594	-5.4E+08	3.65393	-0.85852	3.660594	0.012935
108	-44.9717	-21.2285	7.898674	-13309.3	0.511181	3.641123	4.353742	3.660594	-7.2E+08	3.634621	-0.86163	3.651691	0.012968
109	-44.9717	-21.2287	11.91944	-14223.3	0.520846	3.656805	4.353742	3.657675	1.36E+08	3.64231	-0.85262	3.642715	0.012968
110	-44.9717	-21.2289	9.365967	-15125.9	0.389069	3.647249	4.353742	3.659739	2.85E+08	3.643589	-0.84412	3.64811	0.012935
111	-44.9716	-21.2291	8.600329	-15527.8	0.540975	3.638348	4.353742	3.660594	3.58E+09	3.644131	-0.84212	3.657536	0.012897
112	-44.9716	-21.2293	6.999678	-13901.4	0.745412	3.640254	4.353742	3.660594	5.9E+09	3.64649	-0.85128	3.660594	0.012897
113	-44.9718	-21.2293	6.526316	-14075.1	0.701572	3.638362	4.353742	3.660594	5.07E+09	3.644358	-0.85129	3.660594	0.012897
114	-44.9718	-21.2291	8.016942	-14925.5	0.497995	3.642715	4.353742	3.660594	2.4E+09	3.639504	-0.84212	3.658706	0.012897
115	-44.9719	-21.2289	8.791711	-15277.3	0.563326	3.646622	4.353742	3.658318	-1.2E+09	3.647532	-0.84548	3.658643	0.012897
116	-44.9719	-21.2288	11.74277	-14989.9	0.659098	3.644522	4.353742	3.652465	4.81E+08	3.644569	-0.85364	3.652343	0.012897

117	-44.9719	-21.2286	12.04848	-15173.4	0.693119	3.620052	4.353742	3.660594	13431198	3.636443	-0.86163	3.660594	0.012897
118	-44.972	-21.2284	15.03292	-15497	0.691341	3.637935	4.353742	3.660594	-3.1E+10	3.655077	-0.85859	3.660594	0.012897
119	-44.972	-21.2282	6.577621	-15085.9	0.726226	3.654651	4.353742	3.660594	-9.2E+10	3.655114	-0.85556	3.660594	0.012897
120	-44.972	-21.228	5.133134	-16568.6	0.69735	3.660594	4.349616	3.660594	-4.9E+10	3.649641	-0.85699	3.660594	0.012897
121	-44.972	-21.2295	5.381033	-13358.2	0.505644	3.648374	4.349616	3.651996	-8.7E+08	3.640559	-0.86015	3.660594	0.012897
122	-44.972	-21.2293	9.105654	-13313.1	0.559621	3.652343	4.351424	3.660594	46540476	3.652343	-0.86081	3.660594	0.012897
123	-44.972	-21.2291	9.483385	-14260.5	0.559213	3.652786	4.353742	3.660594	-7.1E+07	3.649514	-0.85836	3.660594	0.012897
124	-44.9721	-21.229	9.226115	-15104.1	0.58876	3.6484	4.353742	3.65923	-7.9E+08	3.648272	-0.85741	3.660149	0.012897
125	-44.9721	-21.2288	9.523708	-16486	0.457658	3.624743	4.353742	3.652462	16126615	3.656275	-0.85672	3.660594	0.012897
126	-44.9723	-21.2288	8.690359	-15814	0.576417	3.644707	4.353742	3.660594	-7.2E+09	3.634969	-0.86056	3.650967	0.012897
127	-44.9722	-21.229	12.68859	-15118.2	0.68811	3.653497	4.353742	3.660594	-3.5E+09	3.636244	-0.86163	3.660594	0.012897
128	-44.9722	-21.2292	7.925126	-14585.4	0.691141	3.640653	4.353742	3.660594	-6E+08	3.647506	-0.86163	3.660594	0.012897

Cont…

VV_dry_corr	VV_dry_dent	VV_dry_sent	VV_wet	VV_wet_asm	VV_wet_dent	VV_wet_sent	VV_wet_shade	B2_wet	B4_dry_shade	B8_dry
0.570322	3.641072	3.657336	-6998.69	0.012968	3.653685	3.660594	3.38E+09	923.5042	-4.9E+07	2458.072
0.598434	3.646945	3.656718	-9181.72	0.012968	3.660594	3.660594	5.8E+09	653.5441	1.09E+08	2398.375
0.509401	3.649111	3.655879	-9242.73	0.012968	3.654882	3.660594	-2.1E+09	469.0497	1.8E+08	2453.508
0.561016	3.653534	3.660594	-7983.75	0.012928	3.647268	3.660594	-3.5E+09	336.7887	-1.2E+07	2458.623
0.543571	3.642715	3.658626	-8131.17	0.012897	3.644597	3.660474	-2.9E+09	298.0923	54913964	2497.176
0.364223	3.651749	3.652158	-9829.85	0.012897	3.635157	3.648139	-1.4E+09	188.5527	71899216	1701.016

0.42937	3.651553	3.660251	-8985.6	0.012897	3.629593	3.644629	-9.1E+08	216.5842	14334257	2056.399
0.521217	3.660228	3.660563	-10018.1	0.012897	3.632806	3.660594	-4.7E+08	214.478	18556.41	2098.035
0.45331	3.635796	3.653951	-9058.98	0.012897	3.649986	3.660594	-4.5E+08	221.6015	6448.012	2137.526
0.346013	3.636405	3.653058	-8831.93	0.012897	3.637061	3.654563	6.64E+08	227.1505	-10729	2046.853
0.278207	3.613549	3.642715	-9034.51	0.012897	3.623753	3.653987	5.34E+08	221.7259	-8638.67	2255.725
0.363056	3.64106	3.653321	-8964.75	0.012897	3.648724	3.660594	-3.6E+08	211.4477	-3851.98	2161.793
0.309436	3.651692	3.660594	-9894.84	0.012899	3.635085	3.660594	3.76E+08	218.2764	-2279.22	2098.317
0.372331	3.660243	3.652467	-7845.58	0.012968	3.644302	3.642173	-4.6E+07	224.3367	27991.68	2287.034
0.258221	3.660472	3.644032	-8226.19	0.012968	3.643951	3.658064	-9.2E+07	228.3781	15810621	2134.438
0.321767	3.644287	3.656956	-8768.98	0.012968	3.644091	3.660594	1.49E+08	202.0657	48408440	1769.348
0.576634	3.619077	3.660594	-8586.25	0.012917	3.644091	3.660516	-6.8E+08	213.0448	58665744	2116.932
0.661373	3.571146	3.645681	-8028.23	0.012968	3.639523	3.660564	14915143	262.0281	1.02E+08	2052.879
0.607638	3.573946	3.642715	-9720.83	0.012968	3.652472	3.660594	5.29E+09	579.0959	6.25E+08	1878.111
0.683759	3.604369	3.644376	-9234.51	0.012968	3.644696	3.660594	2.16E+10	777.681	2.69E+08	1840.923
0.651879	3.608567	3.642715	-11591.7	0.012897	3.643637	3.652343	1.25E+10	543.9496	2.99E+08	1829.573
0.617676	3.593907	3.642715	-10298.9	0.012964	3.632587	3.660594	2.25E+09	496.4617	6.37E+08	1742.268
0.495057	3.601615	3.63965	-9788.62	0.012964	3.606111	3.657738	-4.7E+09	272.3744	1.25E+08	2091.65
0.584708	3.627991	3.660594	-9676.3	0.012937	3.629299	3.652808	-3.6E+09	227.1414	26160822	2247.377
0.476529	3.630457	3.660594	-9039.25	0.01297	3.652074	3.652343	-2.3E+08	214.716	1433158	2146.139
0.191007	3.652304	3.652343	-8851.22	0.01297	3.660329	3.652343	59189852	224.4693	1930.165	2295.233
0.351632	3.643498	3.652343	-8607.3	0.013041	3.643992	3.660594	1.1E+08	219.4691	-7436.73	2134.98
0.39282	3.633934	3.652343	-9524.92	0.012927	3.635571	3.660594	3.55E+08	230.0258	531.6664	2225.957
0.4828	3.648865	3.652397	-9074.58	0.012897	3.641751	3.653318	2.35E+08	194.8181	3400.413	2196.843

0.435999	3.612097	3.642739	-8977.76	0.012897	3.634455	3.653	9.99E+08	228.8386	3789.435	2278.182
0.421778	3.652343	3.660594	-8595.88	0.012968	3.644957	3.660146	-2.5E+08	249.5823	3120.106	2232.335
0.35552	3.641996	3.651891	-7834.48	0.012968	3.644091	3.660143	1.57E+08	228.542	1711.913	2227.31
0.526523	3.618663	3.644091	-9290.07	0.013103	3.641874	3.65299	9.07E+08	256.0021	4268.058	2210.62
0.538559	3.625204	3.644091	-8841.75	0.013039	3.634176	3.659953	1.38E+08	220.9738	7389.295	2425.709
0.565935	3.631685	3.659912	-8858.27	0.013	3.642534	3.658334	-2E+09	221.7156	113101.4	2183.134
0.473671	3.63507	3.660594	-10224.9	0.012917	3.636271	3.649973	-2.3E+09	221.1387	59060316	2147.886
0.437613	3.61114	3.641827	-10874.6	0.012897	3.619744	3.650601	-3.7E+09	293.8953	1.98E+08	2070.969
0.600171	3.599906	3.644576	-12416.6	0.012897	3.626451	3.660594	-9.4E+08	441.9215	88952416	1540.214
0.414701	3.642481	3.660594	-13287.4	0.012897	3.651846	3.653398	-3.7E+08	426.6178	1.21E+08	1500.106
0.520215	3.658471	3.660477	-12047.8	0.012897	3.624697	3.65926	6.78E+09	457.9178	1.69E+08	2006.71
0.390675	3.660594	3.660594	-10493.7	0.012897	3.625221	3.640087	-6.1E+07	227.9258	3.48E+08	2007.486
0.338642	3.65856	3.660594	-9784.43	0.012968	3.622661	3.634532	-3.7E+09	225.3313	58111312	2325.24
0.459853	3.634303	3.659401	-8870.95	0.012968	3.624418	3.659553	-1.3E+09	222.5694	171548.5	2359.942
0.633135	3.635711	3.645129	-9684.72	0.012974	3.623893	3.659644	-7.5E+07	230.6014	10035.48	2142.174
0.667247	3.6499	3.645126	-9821.82	0.013038	3.644095	3.660594	1.04E+09	243.2782	7758.222	2073.231
0.553081	3.646777	3.644607	-8571.91	0.012968	3.6409	3.660594	1.65E+08	225.1066	6060.889	2169.346
0.501747	3.644104	3.660594	-8041.25	0.012968	3.635983	3.660594	-5.9E+08	247.0947	-5697.71	1992.191
0.51047	3.641101	3.659294	-8302.16	0.012957	3.626353	3.660594	-4E+08	230.942	1419.104	2325.351
0.52357	3.629581	3.652593	-9211.56	0.012933	3.646129	3.660403	1.15E+08	237.3033	2791.869	2275.969
0.639779	3.633075	3.653759	-9233.48	0.012955	3.644131	3.650967	1.25E+09	226.8365	3009.658	2229.057
0.524335	3.649885	3.653768	-9408.36	0.012955	3.6204	3.643417	3.06E+08	223.6491	23869.01	2047.525
0.573286	3.64251	3.660594	-8942.97	0.012897	3.648061	3.652366	-9.2E+08	217.8018	22302310	2088.189

0.391165	3.649904	3.65438	-8506.51	0.012897	3.618106	3.64434	-4.4E+09	225.0935	1.57E+08	2046.582
0.446668	3.652343	3.652343	-9316.11	0.012897	3.625361	3.648797	3.92E+09	321.0654	1.86E+08	2287.64
0.629303	3.660594	3.657222	-10009.6	0.012897	3.645906	3.660594	2.27E+10	493.6182	-1.1E+08	1811.581
0.500751	3.652343	3.652343	-10442	0.012897	3.642024	3.660594	1.17E+08	456.249	-2.6E+07	2104.256
0.528289	3.648263	3.654382	-8482.6	0.012897	3.630264	3.660594	-1.6E+10	244.1903	3.46E+08	2216.121
0.617773	3.643273	3.660594	-8258.93	0.012897	3.637216	3.65498	-9.3E+08	238.7134	68468908	2390.788
0.666442	3.639448	3.660513	-8409.71	0.012897	3.628525	3.648855	6.12E+08	230.6261	40090.85	2319.572
0.557557	3.620486	3.654316	-8746.5	0.012897	3.640794	3.648858	2.17E+08	239.8486	-850.653	2258.588
0.489425	3.620547	3.659842	-7359.45	0.012897	3.650538	3.660594	5.06E+08	238.1955	-6385.06	2599.898
0.496602	3.650712	3.660594	-8538.07	0.012897	3.645699	3.660594	1.91E+08	239.3039	-5645.2	2333.05
0.491251	3.653787	3.660594	-8458.23	0.013003	3.656825	3.654719	-2E+08	231.5212	1656.15	2317.446
0.536527	3.645571	3.660594	-8157.05	0.012993	3.652594	3.660594	-8E+08	214.4266	16992.27	2143.644
0.555605	3.659484	3.660594	-8770.29	0.012993	3.63448	3.660594	-5.3E+09	227.0481	3485819	2319.962
0.619468	3.655159	3.658736	-8263.08	0.012898	3.644303	3.655296	-6.1E+10	217.942	37218650	1950.454
0.637577	3.636402	3.660594	-8547.12	0.012897	3.659243	3.649391	-5.9E+10	229.5634	35810904	2547.515
0.624132	3.650207	3.660594	-10183.6	0.012897	3.655034	3.660594	-4E+10	367.5753	-2E+07	1998.767
0.623351	3.657799	3.660594	-10017.5	0.012897	3.653231	3.660594	-1.9E+10	364.9464	6646710	1851.024
0.609844	3.644213	3.660594	-11684.5	0.012903	3.655358	3.650967	2.31E+09	495.2866	1.32E+08	2167.539
0.665502	3.65691	3.660594	-10206.1	0.012903	3.655206	3.655905	8.8E+09	523.8363	1.77E+08	2402.8
0.62159	3.651578	3.656751	-8090.85	0.012993	3.660058	3.660594	-5.7E+09	230.7629	-393253	2438.223
0.740941	3.652332	3.650965	-8301.59	0.012993	3.647065	3.660594	-3.1E+10	253.7157	5529627	2184.357
0.800276	3.645091	3.660594	-9535.34	0.012897	3.653263	3.660594	-2.30E+11	221.7608	64744232	1832.713
0.828902	3.652098	3.660594	-10252.9	0.012897	3.649619	3.659266	-2.45E+11	296.9063	-1.3E+07	2705.264

0.788761	3.660594	3.660594	-12913.7	0.012897	3.660594	3.660594	-1.60E+11	359.7433	20002286	2035.021
0.758906	3.651077	3.642889	-10276.5	0.012993	3.660594	3.660594	-3.8E+10	253.7711	-1007912	2004.917
0.733636	3.652343	3.653138	-9844.95	0.012993	3.660594	3.660594	-2.7E+10	260.316	6655678	960.715
0.699573	3.652343	3.660594	-12069.9	0.012897	3.660594	3.660594	-1.16E+11	170.4726	91301480	1381.278
0.802469	3.652343	3.660594	-16448	0.012897	3.660594	3.660594	-4.8E+10	303.4907	-4561643	2023.536
0.684311	3.641468	3.657578	-14079.7	0.012897	3.65381	3.660555	-2.1E+10	284.454	94329.26	1323.536
0.63084	3.660594	3.660594	-10123.3	0.012897	3.660486	3.660594	-3.5E+10	185.504	38216232	918.4667
0.777999	3.658618	3.660594	-11113.9	0.012897	3.660594	3.660594	-1.37E+11	192.8542	1.24E+08	1767.928
0.605336	3.641665	3.660594	-14543.6	0.012897	3.651352	3.660264	-2.4E+10	254.6619	267438	989.3425
0.640735	3.649598	3.660594	-10655.9	0.012897	3.658061	3.660257	-2.3E+10	191.2098	449554.5	1006.964
0.596902	3.644363	3.660594	-8277.94	0.012897	3.626867	3.660594	1.93E+09	239.6406	-7058.04	2527.956
0.529438	3.645617	3.660135	-9091	0.012897	3.650474	3.660594	44126208	227.8902	-7246.75	2235.089
0.278352	3.62596	3.650967	-7813.51	0.012897	3.644346	3.658402	7882207	224.4565	-7016.49	2091.075
0.258516	3.628963	3.650675	-8497.15	0.012897	3.639261	3.641784	-5.4E+07	243.5997	6938.216	2463.518
0.323463	3.651968	3.650593	-8110.25	0.012897	3.625795	3.643904	1.03E+08	223.5416	50608.56	2301.344
0.41806	3.654031	3.660594	-8504.86	0.012897	3.649208	3.660594	-1.7E+09	238.1207	30522752	2214.62
0.709602	3.65474	3.660594	-9102.99	0.012897	3.647739	3.660594	-2.4E+10	256.9582	3.29E+08	2421.683
0.558148	3.660594	3.654743	-11371.2	0.012917	3.643424	3.660594	-1.2E+10	496.5543	13822692	2317.087
0.53997	3.610107	3.650967	-6477.59	0.012897	3.639702	3.660594	1.17E+09	237.8478	7797619	2201.47
0.624426	3.616398	3.654029	-8008.11	0.012897	3.612488	3.660594	1.28E+09	231.8665	-755.135	2327.728
0.39193	3.637726	3.658033	-8901.58	0.012897	3.62699	3.656614	74142306	240.2195	-5993.49	2548.748
0.347905	3.641651	3.643145	-8268.01	0.012897	3.642468	3.654573	-2.8E+08	234.9991	-6637.12	2188.395
0.242779	3.640549	3.642947	-7592.87	0.012897	3.641889	3.642484	-9.6E+07	237.3843	6295.957	2267.82

0.148424	3.640131	3.653229	-8859.34	0.012897	3.644468	3.650829	-7.3E+08	239.7257	162553.2	2318.69
0.60033	3.643242	3.660594	-8914.47	0.012897	3.652343	3.660594	-9.9E+09	251.4074	45066488	2385.873
0.74351	3.646309	3.660594	-8823.96	0.012921	3.643451	3.660594	-8.9E+09	270.6449	2.27E+08	2487.678
0.550137	3.656404	3.660594	-12148.3	0.012992	3.645601	3.660594	8.41E+09	597.978	69924600	2012.683
0.740801	3.630009	3.660594	-10919.2	0.012968	3.652937	3.660594	1.88E+09	368.4315	77266360	2039.501
0.61388	3.622493	3.658926	-8274.39	0.012897	3.642156	3.660594	-3.1E+10	244.6375	66019704	2180.774
0.233197	3.607942	3.643601	-8231.19	0.012897	3.642964	3.65464	-6.4E+09	235.5315	2711479	2223.737
0.283194	3.639285	3.637166	-8251.43	0.012897	3.63061	3.650967	-2.6E+08	244.4992	10609.34	2486.775
0.293992	3.643463	3.643551	-8318.18	0.012897	3.629767	3.653629	-2.7E+08	234.4964	542.5472	2197.883
0.401654	3.640169	3.651694	-8486.74	0.012897	3.621674	3.656121	76489563	233.9318	1003.736	2284.161
0.58659	3.64548	3.660594	-7542.52	0.012897	3.62189	3.660594	1.69E+09	249.879	7229.44	2328.839
0.566428	3.639153	3.658656	-7328.45	0.012897	3.63558	3.660594	1.86E+09	256.6653	1543840	2372.753
0.478834	3.642843	3.649873	-7587.73	0.012897	3.648056	3.657445	1.08E+09	237.8541	4373.617	2320.997
0.373368	3.654962	3.655932	-8582.9	0.012897	3.652243	3.657442	6.46E+08	238.5175	10186.66	2292.672
0.509655	3.645256	3.648436	-7917.09	0.012904	3.626066	3.648436	92205568	233.6359	16356.01	2330.057
0.438196	3.622917	3.639291	-8180.07	0.012926	3.626813	3.649716	-6.5E+08	236.8673	4622.714	2425.931
0.345283	3.633191	3.625088	-8987.69	0.012926	3.624108	3.650967	-3.8E+09	233.7008	57590.8	2396.685
0.652197	3.638015	3.641311	-8546.86	0.012968	3.643307	3.6414	-3.8E+10	237.8673	71856904	2320.194
0.783933	3.627239	3.65892	-8987.61	0.012903	3.644332	3.660594	-4.2E+10	260.1471	3.55E+08	2357.269
0.746738	3.630906	3.660594	-12325.5	0.012956	3.640184	3.659898	1.38E+10	291.5121	1.55E+08	2193.349
0.485863	3.630091	3.650967	-6640.36	0.012897	3.649207	3.660594	-6.1E+07	237.9791	45587.21	2214.135
0.460135	3.616659	3.646105	-6771.42	0.012897	3.633521	3.652343	60307748	249.0707	3735.871	2150.612
0.417778	3.646172	3.645284	-8276.81	0.012897	3.627292	3.650817	6.42E+08	244.1401	-416.429	2329.024

0.546637	3.645254	3.642493	-8038.84	0.012907	3.615148	3.64344	-4.3E+08	236.3704	9006.025	2258.696
0.517725	3.63532	3.650967	-8518.17	0.012968	3.639654	3.650967	-8E+08	248.9486	1723612	2260.241
0.520203	3.657371	3.648033	-9245.21	0.013025	3.617865	3.655779	-7E+09	243.3463	69633816	2364.347
0.68037	3.652343	3.646149	-9252.54	0.012968	3.629384	3.651646	-1.2E+10	223.2711	10565829	2187.997
0.546373	3.650967	3.657156	-8880.63	0.012931	3.630142	3.652343	2.17E+09	231.2972	-1193.28	2245.669

Cont…

B8_dry_corr	B8_dry_savg	B8_dry_shade	B8_wet_corr	B8_wet_dvar	B8_wet_shade	EVI_wet_shade	SAVI_dry_ent
0.50351	4439.561	-1.7E+08	0.473095	56312.19	-9.6E+07	2.13E+09	4.353742
0.495586	4524.376	-1.5E+08	0.359184	49549.77	-7.6E+07	3.93E+09	4.353742
0.5521	4438.8	-7.2E+07	0.446158	37360.84	-3.4E+07	1.13E+09	4.35368
0.446003	4387.596	8087872	0.368374	27743.94	18772888	3.22E+08	4.351204
0.40015	4283.492	42631784	0.327111	22925.58	23118306	-1.5E+09	4.349616
0.352127	4233.911	37759076	0.383134	21551.47	6766654	-2.7E+09	4.353742
0.343111	4221.375	35890791	0.420323	23314.34	13067880	-9.4E+08	4.353742
0.282007	4229.51	19999176	0.251864	24255.16	21659102	-1.1E+07	4.353742
0.317158	4300.794	16897252	0.360408	16299.8	23925846	40294124	4.353742
0.316457	4183.817	-5206005	0.123362	16629.39	1461576	14375020	4.353742
0.490905	4267.87	-5915559	0.242642	8430.414	-1039876	-972495	4.353742
0.353831	4292.231	320000.1	0.225499	9016.562	4254150	-3886352	4.353742
0.33039	4265.048	-38423.6	0.115655	14826.68	6019186	-5064743	4.353742

0.427717	4255.459	-2.2E+07	0.356957	17099.25	-1.4E+07	-4.1E+08	4.353742
0.394623	4239.383	1901691	0.286629	20943.95	-9492028	-1.9E+09	4.353742
0.400897	4303.308	12385068	0.249445	23420.96	-422165	-2.8E+09	4.353742
0.483455	4340.374	21741506	0.408398	21786.58	-7121899	-1.9E+09	4.265723
0.627395	4318.267	-4E+07	0.599459	28615.56	-2.7E+07	-4.9E+09	4.27535
0.662195	4199.887	-8.2E+07	0.632617	44165.71	-3.8E+07	2.22E+09	4.27535
0.625751	4003.765	31779919	0.658222	56604.88	25086589	2.3E+09	4.275293
0.132066	3475.182	29223218	0.308749	48217.23	80388208	1.73E+08	4.271224
0.442838	3788.188	-1.9E+07	0.542275	40592.77	87180256	4.16E+09	4.273071
0.486766	3990.684	-8.3E+07	0.573215	21516.71	-2.3E+07	-5.9E+09	4.27535
0.233243	4198.506	-2245094	0.487346	11960.78	-7551709	-3.5E+09	4.265723
0.471383	4332.315	-9391135	0.284567	14468.17	742527.9	-2.4E+07	4.265723
0.476399	4333.413	-2.4E+07	0.242081	10497.64	-4447749	-3.3E+07	4.266921
0.427498	4420.733	-1.6E+07	0.286486	7928.521	-2704115	-7483562	4.27514
0.282763	4395.453	-1465212	0.175189	9705.003	-635710	-2466952	4.273402
0.254668	4387.865	-2280114	0.237842	9488.145	-1235380	1835105	4.275313
0.326472	4356.29	-6349266	0.160578	10140.62	-3160284	-1.3E+07	4.322376
0.170294	4408.146	186727.8	0.20773	11606.29	-6009643	-2.5E+07	4.270536
0.325024	4380.567	-1032347	0.241931	8932.939	-4299317	-2.2E+07	4.270536
0.398013	4439.53	3461725	0.38848	6235.044	-3994439	-5187235	4.270536
0.377611	4445.787	2727020	0.372948	7998.52	-4321714	-9782011	4.27535
0.378961	4425.644	1391323	0.421185	12129.51	-7441842	-3.5E+07	4.266218
0.37917	4245.893	3205029	0.540618	14371.14	557196.8	-4E+09	4.266717

0.484333	3973.825	-7.1E+07	0.61927	15296.02	214034.3	-3.2E+09	4.27535
0.430875	3678.894	-4.1E+07	0.475363	16645.62	-7915849	5E+09	4.273073
0.403381	3533.259	24777542	0.504194	21846.74	24396272	-1E+08	4.281248
0.432261	3908.176	-5.7E+07	0.495271	16201.8	-1.7E+07	4.77E+09	4.352832
0.333839	4139.149	-2.8E+07	0.55925	14885.62	17147472	-6.7E+09	4.353742
0.343275	4339.407	820018.2	0.493445	14036.1	1368820	-3.4E+09	4.353742
0.302834	4427.551	2743488	0.369318	13834.58	-5587214	-2.4E+07	4.28524
0.319033	4439.286	2632142	0.401358	8637.191	-2622478	14462117	4.285211
0.27545	4410.407	4676302	0.534993	6703.615	-440505	17214370	4.280367
0.326043	4407.192	7639270	0.479307	9559.599	3261863	48528913	4.275437
0.425012	4485.497	11214651	0.429919	12270.26	-4436249	39644588	4.270536
0.441834	4605.941	858152.3	0.612611	10307.3	-9749124	-5.1E+07	4.349641
0.349806	4515.309	6529680	0.59962	9926.762	-573200	-3E+07	4.351282
0.286915	4469.31	5610699	0.594264	7523.775	-1806766	-1.5E+07	4.353742
0.283696	4458.864	-268269	0.39597	10088.16	-972689	12187702	4.353742
0.270396	4472.632	-955464	0.329194	14618.59	-1297704	-5.3E+08	4.353742
0.321396	4378.357	-7101191	0.586423	15013.42	-2.2E+07	-8.6E+09	4.353742
0.423842	4147.689	-1.5E+07	0.618887	16064.25	28293414	-3.4E+09	4.353742
0.527618	3936.186	-8431201	0.562485	15632.57	7647939	8.57E+09	4.353742
0.621096	4078.148	-4.3E+07	0.725064	16609.93	17429500	5.03E+09	4.353742
0.398108	4383.929	-3.9E+07	0.668988	15846.04	-7.9E+07	-1.5E+10	4.353742
0.259301	4517.386	-1175013	0.223586	14823.32	-1240534	-1.6E+09	4.353742
0.205074	4558.139	-5308421	0.355232	10035.62	-3903655	-2.1E+07	4.353742

0.182745	4564.346	-1670712	0.453855	10803.81	-3194605	-3.6E+07	4.353742
0.191307	4691.208	-645414	0.417371	10508.63	-1806402	-2.1E+07	4.353742
0.217443	4792.758	-7747949	0.35236	10525.44	-4955750	-1.4E+07	4.353742
0.46063	4234.49	-5.4E+07	0.31468	20367.78	4070626	-1.8E+08	4.353742
0.39756	4326.459	-4.9E+07	0.380276	25729.18	-1.6E+07	-3.3E+08	4.353742
0.368656	4207.605	-3.1E+07	0.508779	31072.88	-6.3E+07	-9.1E+08	4.353742
0.386087	4303.015	4307220	0.513456	28351.21	12093262	-1.4E+09	4.353742
0.388785	4309.394	65291364	0.254849	22577.5	18339344	-2E+08	4.350291
0.490868	4334.72	47899664	0.362733	20500.07	33620996	-4.4E+07	4.349616
0.574632	4234.111	64155240	0.5244	22333.85	50362884	37813584	4.349616
0.618005	4389.829	-2.2E+07	0.594482	24576.54	6451434	2.2E+09	4.352065
0.571145	4550.773	-6.3E+07	0.611842	21038.97	-2.3E+07	2.32E+09	4.353742
0.704776	4154.746	-9E+08	0.641879	25319.12	-2.1E+08	-1.8E+09	4.346494
0.644757	3888.054	-5.8E+08	0.714603	28967.07	-1.2E+08	-6.4E+08	4.350775
0.65117	3891.771	-4.6E+08	0.726994	31522.96	-6.4E+07	5.85E+08	4.353681
0.533553	4078.426	-6E+07	0.621165	24331	-1.1E+08	8.44E+08	4.350289
0.579794	4085.809	1.27E+08	0.535103	22326.91	-8.9E+07	3.97E+08	4.349616
0.793231	3737.278	-9.9E+08	0.738193	24123.83	-8.2E+07	-5.6E+08	4.273974
0.702499	3359.973	-1.7E+08	0.687894	26997.45	1.68E+08	1.12E+09	4.273974
0.692191	3297.607	-9.6E+07	0.592197	32580.48	1.35E+08	5.69E+08	4.275237
0.621521	3716.164	-8.5E+07	0.648262	32095.6	-4.9E+07	23900778	4.335134
0.702108	2906.44	3.85E+08	0.604078	35572.84	1.1E+08	9.05E+08	4.273974
0.614048	2802.493	1.62E+08	0.429362	28590.43	32377758	1.01E+08	4.273974

0.759756	3236.82	8.7E+08	0.448003	34567.8	77178880	-1.2E+09	4.27535
0.658769	2890.207	3.35E+08	0.476384	37254.61	46683720	2.05E+08	4.286158
0.693585	2984.416	8.92E+08	0.474187	32810.24	81405192	1.68E+08	4.278539
0.369455	4765.794	-1E+07	0.358156	12212.65	-7009201	-1.7E+07	4.353742
0.309252	4784.258	-1.2E+07	0.417469	10883	-8365870	-3.7E+07	4.353742
0.229944	4657.663	3614987	0.272751	14159.48	-67188.1	-1.6E+07	4.353742
0.126687	4585.691	1021610	0.330152	12430.26	1027090	-1.3E+07	4.353742
0.064004	4616.506	-1017084	0.169182	12674.15	1130359	-1.4E+07	4.353742
0.156407	4645.5	2759539	0.204373	16892.34	-9457594	-1.7E+09	4.353742
0.330988	4552.55	-2.9E+07	0.605536	18222.8	-9.2E+07	-1.6E+10	4.353742
0.680054	4170.25	-7.6E+07	0.750505	19281.92	10092956	3.01E+09	4.353742
0.602905	4426.583	-2.8E+07	0.250526	17553.37	-2604216	-5.9E+08	4.353742
0.417983	4700.047	-1.7E+07	0.171989	12727.86	-1478906	-1.6E+07	4.353742
0.363698	4712.849	-3035606	0.244504	12575.42	-718393	-7923816	4.353742
0.282128	4640.959	4185093	0.196932	13262.36	2973138	16126902	4.353742
0.19489	4581.035	1292917	0.296788	11456.73	4366006	-2761377	4.353742
0.151437	4634.528	1231527	0.172703	13678.87	2431133	-1.9E+07	4.353742
0.312829	4565.142	-1E+07	0.367321	21009.84	-2.7E+07	-3.1E+09	4.327316
0.486928	4399.666	-3.3E+07	0.522876	23352.35	-4.2E+07	-1E+10	4.327288
0.620106	4057.011	10450288	0.618929	26686.73	19433146	1.49E+09	4.327259
0.611732	4211.334	-6650295	0.475393	24761.17	1614710	-3.5E+09	4.27535
0.259811	4576.826	-1.3E+07	0.460606	17703.59	-3E+07	-3.2E+09	4.27535
0.2556	4628.395	-1993610	0.351683	12653.18	2217677	-1.4E+08	4.27535

0.284104	4654.982	-2757807	0.278855	11389.67	9039583	1850197	4.27535
0.353875	4685.029	-1849469	0.164165	10400.32	1961947	13082834	4.27535
0.337242	4679.779	-380655	0.23003	11980.5	4583108	2760271	4.306604
0.355387	4669.284	-3161049	0.294776	14026.42	5952766	-1.3E+07	4.327475
0.580449	4442.047	-3.1E+07	0.345372	16223.26	3327074	-7.3E+07	4.327503
0.543926	4450.229	-3.5E+07	0.39971	14406.89	-5505068	-4.5E+07	4.27535
0.204422	4606.833	-6590506	0.329416	13305.87	3921607	-1.2E+07	4.27535
0.17378	4614.457	-2132053	0.396494	9213.354	6478707	-2339892	4.27535
0.3686	4622.026	-4083796	0.322128	7989.25	2385373	5696878	4.27535
0.320669	4621.116	-8764592	0.244553	11616.76	-2140232	-1E+08	4.27535
0.374808	4497.581	-2.9E+07	0.349471	23813.52	-7.2E+07	-3.7E+09	4.27535
0.289135	4416.884	-2.4E+07	0.466377	28833.29	-5.9E+07	-1E+10	4.27535
0.506794	4110.489	-2.9E+07	0.522512	27734.84	-17820.2	-2.6E+09	4.27535
0.309619	4360.665	-426358	0.325852	18527.27	-7548778	-1.2E+07	4.269844
0.325322	4442.15	-7725408	0.333762	17562.71	-1.3E+07	-1.5E+07	4.272259
0.318435	4497.803	-7976451	0.256518	15711.76	1231564	-9099209	4.27535
0.13109	4591.724	-2886643	0.378814	12129.42	5439741	-2.1E+07	4.27535
0.376381	4525.646	-4171002	0.425624	11975.99	-8270802	-3.3E+08	4.27535
0.559116	4286.258	-5.4E+07	0.628649	17366.76	-8.3E+07	-6.5E+09	4.352936
0.378837	4383.635	-3.5E+07	0.409051	21098.03	-6.2E+07	-2.2E+09	4.353742
0.278291	4412.509	-5298972	0.150287	18965.54	1436459	-3.9E+07	4.312639

Table S3. Selected variables by the random forest model to the estimates above ground biomass (AGB) for each interval in the Forest Atlantic remnant, southeast Brazil. Em que %IncMSE é o valor de importância da variável.

Year	Variable	%IncMSE
2015	B2_dry_corr	56.81951
	VH_wet_dent	56.74262
	VV_wet_shade	53.2442
	VH_dry_imcorr1	52.17015
	B8_dry_shade	49.80094
2017	B8_dry_savg	64.04825
	B8_dry_shade	61.40845
	B8_dry	59.0149
	B8_dry_corr	56.15543

Figure S1. Diameters' distribution of the arboreal tree individuals for each interval in the Forest Atlantic remnant, southeast Brazil. The tree individuals were classified into three categories: Small (5 < DBH < 10 cm), Medium (10 < DBH < 35 cm), and Larger (greater than 35 cm).

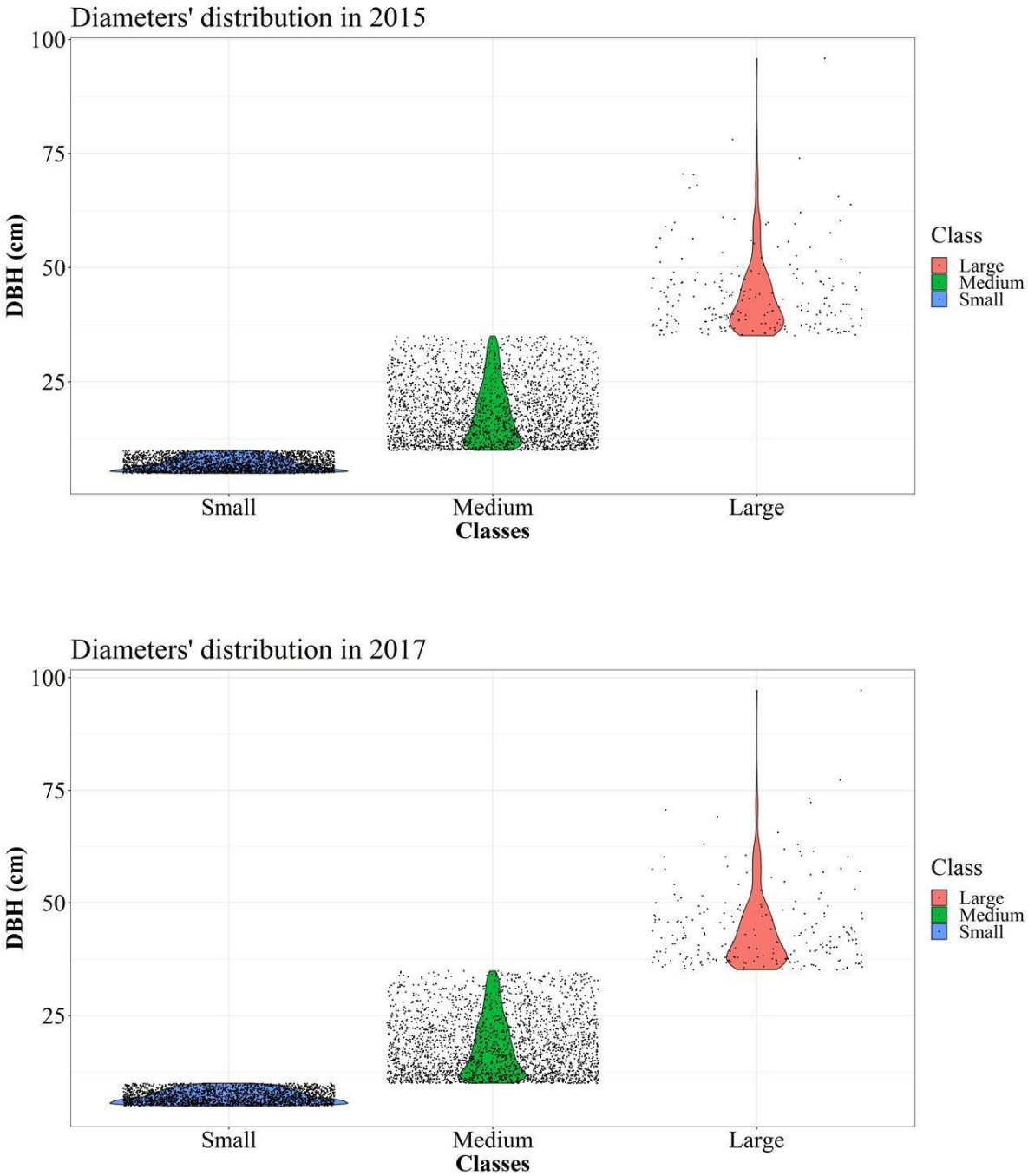

Figure S2. Above ground biomass distribution into the Atlantic Forest remnant.

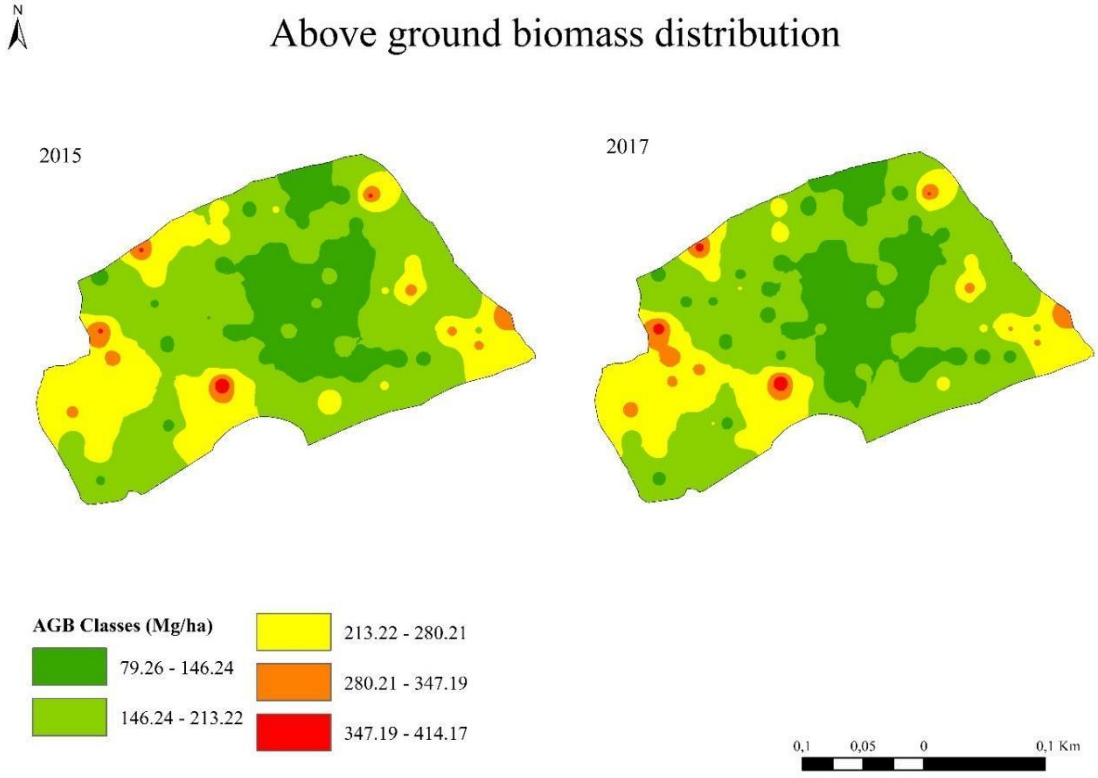

ARTIGO II

The role of environmental filters in Brazilian savanna vegetation dynamics

Natielle Gomes Cordeiro, Kelly Marianne Guimarães Pereira, Marcela de Castro Nunes Santos Terra, Eduarda Martiniano de Oliveira Silveira, Ivy Mayara Sanches de Oliveira, Fausto Weimar Acerbi Júnior, Eduardo van den Berg, José Márcio de Mello

Artigo publicado na revista Forest Ecology and Management
Volume 500, 2021

https://doi.org/10.1016/j.foreco.2021.119645

The role of environmental filters in Brazilian savanna vegetation dynamics

Natielle Gomes Cordeiro[a,*], Kelly Marianne Guimarães Pereira[b], Marcela de Castro Nunes Santos Terra[a], Eduarda Martiniano de Oliveira Silveira[c], Ivy Mayara Sanches de Oliveira[d], Fausto Weimar Acerbi Júnior[a], Eduardo van den Berg [b], José Márcio de Mello[a]

[a] *Department of Forest Sciences, Federal University of Lavras, Minas Gerais, Brazil.*

[b] *Department of Ecology and Conservation, Federal University of Lavras, Minas Gerais, Brazil.*

[c] *Department of Forest & Wildlife Ecology, University of Wisconsin-Madison, WI, United States of America.*

[d] *Forest Engineer, Forest Expansion sector, Bracell Cellulose Company, São Paulo, Brazil.*

* **Corresponding author**

E-mail addresses:

natiellegcordeiro@gmail.com (Cordeiro, N.G.); kellyguimaraes10@gmail.com (Pereira, K.M.G.); marcelacns@gmail.com (Terra, M.C.N.S.); dudalavras@hotmail.com (Silveira, E.M. de O); ivymayara07@gmail.com (Oliveira, I.M.S.); fausto@ufla.br (Acerbi Júnior, F.W.); evandenb@ufla.br (van den Berg, E.); josemarcio.florestal@gmail.com (Mello, J.M. de).

Abstract

Climate, topography and edaphic characteristics are important factors for plant community dynamics when considering spatial and temporal scales. Efforts on vegetation dynamics in tropical regions are mostly focused on forests, with far less attention dedicated to open vegetation ecosystems. This study aimed to understand how demographic rates (based on models and maps) are affected by climate, soil and terrain variables in the Brazilian savanna, the Cerrado, which is a hotspot for the world biodiversity conservation. To do so, we used forest inventory data collected from 354 plots (10 x 100m) distributed in the savanna of Minas Gerais State, southeast of Brazil, in the years of 2005-2006 and 2010-2011. Next, we calculated the rates of mortality, recruitment, net change in number of individuals, basal area loss and gain, and net change in basal area for the plots. We used the Random Forest (RF) algorithm to model the demographic rates in function of climate, soil and terrain variables obtained from the WorldClim 2, Harmonized World Soil Database and Shuttle Radar Topography Mission (SRTM), respectively. The models presented good performance with coefficient of determination (R^2) values ranging from 0.68 to 0.84, mean absolute errors (MAE) between 0.32 and 0.96 $\%.year^{-1}$, and root mean square error (RMSE) ranging from 60 a 160%. The recruitment was higher than mortality, and the basal area gain was greater than the basal area loss, resulting in positive net change rates. The most important variables for the model and best predictors of vegetation dynamics rates of Brazilian savanna were the terrain variables, since they encompass characteristics such as soil water content, erosion, altitudes and slope. We showed that the gain in number of individuals and basal area were greater at low regions, that is, near drainage lines and with higher humidity. The losses in number of individuals and basal area were higher in boundary regions of the savanna vegetation, that is, regions of higher altitude and consequently, low humidity. Therefore, our findings provide support for conservation and management strategies of the biome, since from the vegetation dynamics drivers identification, we may identify priority areas as well as the vegetation vulnerability.

Keywords: Cerrado; Environment variables; Mortality; Random Forest algorithm; Recruitment.

1. Introduction

Climate has been pointed out as the main driver of the vegetation structure and spatial distribution at global scales (Pausas and Dantas, 2017), and special attention has been given to climate change impact on vegetation attributes such as species composition and demographic rates (Bowler et al. 2017; Esquivel-Muelbert et al. 2018; Sullivan et al. 2020). As an example, temperature and precipitation variables control overall vegetation distribution and structure over the time and space, and also play an important role in the individuals' establishment, reproduction, survival and interaction in the habitat (Jin et al. 2016; Valadão et al. 2010).

Terrain and edaphic characteristics as well as disturbances have shown great influence on biodiversity and vegetation dynamics at regional scales (Bell et al. 2016). Terrain variables are important components and are related to the water dynamics and soil properties in local and regional scales (Forkuor et al. 2017; Pelegrino et al. 2016; Silveira et al. 2019a). The terrain-related characteristics such as topography, slope and proximity to water are intrinsically linked to soil fertility, water availability, altitude, shading, and the microclimate. Therefore, they are known as good indicators of tree growth and productivity (Forkuor et al. 2017; Hengl et al. 2015; Pelegrino et al. 2016; Silveira et al. 2019a), and consequently good predictors of vegetation structure and dynamics (Silveira et al. 2019a; Sun et al. 2013).

Most studies on vegetation dynamics in the tropics are focused on the forests (Lewis et al. 2004; Qin et al. 2017), with far less attention dedicated to open vegetation ecosystems, such as Savannas (Oliveira et al. 2014; Roitman et al. 2016). Savannas differ from tropical forests in terms of species strategies and adaptations, as well as in relation to the importance of the light for their structure and dynamics (Gignoux et al. 2016). Therefore, the drivers of savannas' dynamics must be different from the drivers of forest dynamics, and need to be evaluated to

better understand their functioning, allowing more effective strategies for their management and conservation (Murphy and Bowman, 2012; Terra et al. 2021).

The Savannas are situated in tropical and subtropical regions throughout the world, covering around 20% of the Earth's surface (Pennington et al. 2018; Scholes and Archer, 1997). They occupy areas in Asia, Australia, Africa, and South America, with the latter being one of the richest savannas in the world (Borghetti et al. 2019; Müller et al. 2015). These vegetation types provide multiple ecosystem services like water regulation, food production, nutrient cycling, carbon stocking, soil formation, and climate regulation (Pereira et al. 2020; Pennington et al. 2018; Resende et al. 2019).

The Brazilian savanna (also known as Cerrado) is considered a global hotspot due its high biodiversity and endemism, as well as due to the alarming habitat losses due to farming, but also to other activities like mining (Myers et al. 2000; Pereira et al. 2020; Silveira et al. 2019b). The Cerrado originally covered an area of 2 million km^2, harboring major biological diversity with high fauna and flora endemism (Silva et al. 2011; Strassburg et al. 2017). However, only 55% currently remains mostly intact and 45% has been converted to other types of land use (Alencar et al. 2020). The Cerrado loses about 1% of its native coverage every year and it is legally under-protected (only 7.5% in protected areas) in comparison to the forests in Brazil (Alencar et al. 2020; Strassburg et al. 2017). The Cerrado comprises a very diverse flora distributed in different vegetation types, from grasslands and rupestrian grasslands to woodlands and forests, which may be explained by soil characteristics, climate seasonality and fire regimes (Barbosa et al. 2015; Eiten, 1972; Lehmann et al. 2014; Pausas and Dantas, 2017; Ribeiro and Walter, 2008). The frequency of fire events as well as availability of water and nutrients in soils may influence the vegetation composition, since these filters locally promote or suppress species with favorable or unfavorable strategies, respectively, according to the local conditions (Batalha et al. 2011; Coutinho, 1990; Ferreira et al. 2007).

Studies on Brazilian savanna vegetation dynamics have shown that the recruitment rate is greater than mortality rate in areas which are free from disturbance (Gomes et al. 2016; Henriques and Hay, 2002; Mews et al. 2011). However, most of the Brazilian savanna dynamics studies have been conducted on a local scale (Cordeiro et al. 2020; Durigan and Ratter, 2006; Mews et al. 2011; Pinheiro and Durigan, 2009), with fewer in regional scales (Ferreira and Huete, 2004; Ledru et al. 1998). Therefore, the knowledge regarding the drivers of community fluctuations in number of individuals and basal area, species composition and diversity at a regional scale is still scarce for the Cerrado.

The complex synergy among the environmental conditions, together with the landscape processes, genetic variability, functional and phylogenetic aspects, floristic composition and disturbance may promote vegetation structure fluctuations, and can induce different tree recruitment and mortality rates in seasonally dry ecosystems such as the savannas (Franco et al. 2014). In this sense, modeling how climate, soil and terrain variables drive the demographic rates is fundamental to understand the changes at the spatial and temporal scales in the vegetation, thereby enabling more efficient conservation strategies.

Regression analysis is the most popular among the several methods applied to model environmental effects on vegetation features (Abreu et al. 2014; Grömping, 2009; Terra et al. 2018). Nevertheless, new approaches such as generalized linear models, computational intelligence methods such as artificial neural networks, support vector machine and the random forest algorithm (RF) have been used for this purpose (Carvalho et al. 2019; Pyles et al. 2018). The RF algorithm has been successfully used in different fields and has been shown to be a less sensitive technique to noise in the training data and with good generalization capacity, resulting in accurate models (Carvalho et al. 2019; Li et al. 2018; Oshiro et al. 2012; Silveira et al. 2019c).

Thus, our study aimed to understand which environmental variables better explain the demographic rates in Brazilian savanna. Specifically, we modeled and mapped tree

community rates of mortality, recruitment, net change in number of individuals, basal area loss and gain, and net change in basal area as a function of climate, soil and terrain variables in an extensive region of the Brazilian savanna in southeast Brazil. The local ecological processes in the Brazilian savanna are subjected to strong environmental filters related to climate seasonality, relief, low-nutrient and moisture soil (Bueno et al. 2018). Thus, we hypothesize that terrain variables will stand out as better predictors for demographic rates than climate and soil variables, as terrain features encompass local detailed information of soil and water availability.

2. Material and methods

2.1. Study Area

Our study covered the Brazilian savanna area in Minas Gerais State, located in the southeast Brazil. Although three large biomes (Brazilian savanna - Cerrado, Tropical Forest – Floresta Atlântica, and Semiarid woodland – Caatinga) exist in this state, the Cerrado originally occupied ~50% of its territory, which represents 335,378.7 km^2 (IBGE, 2004) (Figure 1), encompassing all variations of Cerrado physiognomy (Silveira et al. 2019c; Terra et al. 2018). In this study, we used the database collected in the Savanna's permanent plot network sampled during the "Forest Inventory of Minas Gerais" Project (Morais et al. 2013; Scolforo et al. 2008).

The climate in the study area can be classified as Cwa, Cwb, Aw, and As across the region according to the Köppen classification (Alvares et al. 2014). All of these categories are strongly seasonal, with a dry winter. The mean annual temperature in the region ranges between 20.38 ºC to 24.18 ºC, and mean annual precipitation between 867.11 to 1801.92 mm (Scolforo et al. 2008).

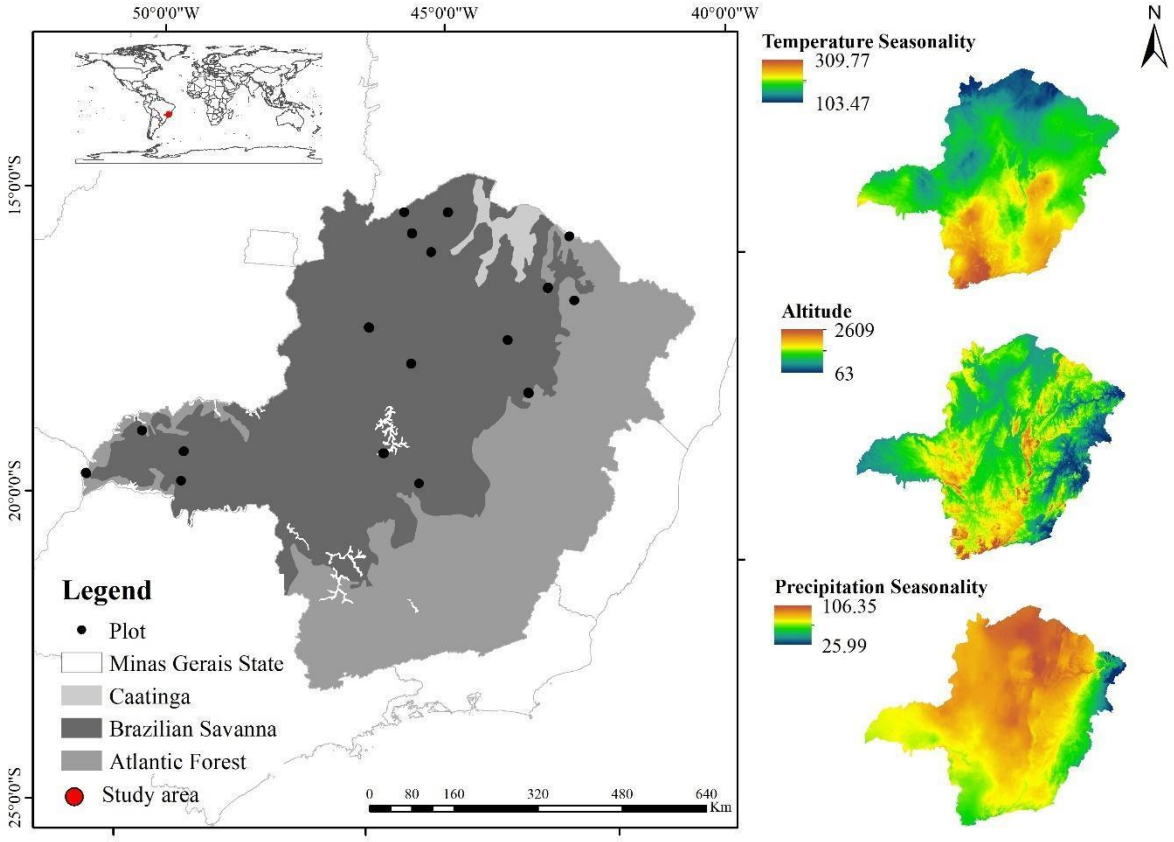

Figure 1 – Study area in the Brazilian savanna vegetation located in Minas Gerais State, southeast Brazil, with boundary regions to other Brazilian biomes (Caatinga and Atlantic Forest).

The Cerrrado vegetation in the area varies from Grassland savanna ("Campo Cerrado") to Densely wooded savanna ("Cerradão"), then passing to Woodland savanna ("Cerrado *sensu stricto"*) (sensu Eiten, 1972). These vegetation areas are also under different levels of human impact and different successional stages (Scolforo et al. 2008). The Grassland savanna has an herbaceous stratum composed by grasses and other herbs, with dwarf shrubs, and a few tree individuals. Although the Woodland savanna still has a conspicuous herbaceous stratum, it is dominated by closed shrubs as well as spaced trees with height between 5 to 8 meters. Finally, the Densely wooded savanna is a forest-like physiognomy with closed canopy dominated by savanna trees of 8 to 15 meters in height (Eiten, 1972; Ribeiro and Walter, 2008).

2.2. Data collection

We used a total of 354 plots of 1,000 m² (10 × 100m) which are distributed in 17 fragments of Cerrado (Scolforo et al. 2008). The plots were systematically sampled considering a distance of 25 meters between each plot. Overall, a total of 51 plots were allocated to the Densely wooded savanna, 102 plots to the Grassland savanna and 201 to Woodland savanna (Table S1, Supplementary Information). The plots were established in 2005 and 2006 (Table S2, Supplementary Information). All arboreal individuals with diameter at breast height (DBH) equal or greater than 5 cm were identified and had their diameter measured during the first survey (Scolforo et al. 2008). The plants which showed tillering had their diameter transformed to one value using the following equation (Macdicken et al. 1991):

$$D = \sqrt{d_{n1}^2 + d_{n2}^2 + \cdots + d_n^2}$$

Where: D is the transformed diameter and d_n is the tillered tree diameter.

In addition, all the trees were labeled with metal tree tags with the plot number and the plant number. Next, all surviving and recruited trees were measured, the recruits were identified, and the dead ones were registered during the second survey (2010 and 2011 - Table S2, Supplementary Information). The interval between the measurements varied from 3.84 to 5.08 years (Table S2, Supplementary Information). Botanical material regarding the species identification was collected and produced exsiccates which were deposited into the Federal University of Lavras herbarium (Herbarium ESAL) (Scolforo et al. 2008). The taxonomy was standardized using the “Flora do Brasil” according to the APG IV classification system (APG IV, 2016; BFG, 2021).

2.3. Vegetation dynamics

We calculated the rates of mortality (M), recruitment (R) and net change in number of individuals (ChN), as well as basal area loss (L), basal area gain (G) and net change in basal area (ChBA) for each plot. We used the algebraic models proposed by Korning and Balslev (1994), Sheil et al. (2000) and Sheil and May (1996):

$$M = [1 - ((N_0 - N_m) / N_0)^{1/t}] * 100$$

$$R = [1 - (1 - N_r/N_t)^{1/t}] * 100$$

$$ChN = [(N_t/N_0)^{1/t}-1] *100$$

$$L = \{1 - [(BA_0 - (BA_m + BA_d))/ BA_0]^{1/t}\} * 100$$

$$G = \{1 - [1 - (BA_r + BA_g)/ BA_t]^{1/t}\} * 100$$

$$ChBA = [(BA_t/BA_0)^{1/t}-1] *100$$

Where: t is the number of years (interval) between the inventories; N_0, N_m, N_r and N_t are the initial number of trees, number of dead trees, number of recruited and final number of trees in the interval, respectively; BA_0 is the initial basal area; BA_m is the basal area of dead trees; BA_d is the decrement in basal area; BA_r is the basal area of recruited trees; BAg is the basal area gain with the tree growth; BA_t is the final basal area considering the interval.

We calculated the demographic rates (mortality, recruitment, net change in number of individuals, basal area loss, basal area gain and net change in basal area) using the “forest.din” function (Higuchi, 2018) in the R software program (R Core Team, 2020).

2.4. Predictive variables

Next, we used climate, soil and terrain variables in order to model the demographic rates (Table 1). The climate variables selected were obtained from the WorldClim 2 with 1 km spatial resolution (Fick and Hijmans, 2017). Previous studies have shown these variables as good predictors for the fluctuation in species richness and composition, as well as the species distribution, justifying the application of these variables for our study (Silveira et al. 2019c; Terra et al. 2018). We subsequently calculated soil variables through the R software program (R Core Team, 2020) using the data from the Harmonized World Soil Database v 1.2 with 1 km spatial resolution (FAO, 2020). Moreover, we calculated terrain variables from a digital elevation model (DEM) with 30 meters spatial resolution from the Shuttle Radar Topography Mission (SRTM). We used the terrain variables that represent soil water content, erosion, altitudes and slope. These features are known to affect the vegetation structure (Matasci et al. 2018; Silveira et al. 2019a). All variables were resampled at 100 × 100 m (1 hectare) and projected to 'Albers Equal Area Conic projection', aiming to have the same spatial resolution.

Table 1. Climate, soil and terrain variables selected to model the demographic rates for the Brazilian savanna, Minas Gerais State, southeast Brazil.

Category	Variables	Description
Climate	BIO1	Annual mean temperature
	BIO4	Temperature seasonality
	BIO12	Annual precipitation
	BIO15	Precipitation seasonality
Soil	T_SAND	Topsoil Sand Fraction
	T_SILT	Topsoil Silt Fraction
	T_CLAY	Topsoil Clay Fraction
	T_PH_H2O	Topsoil pH (H_20) - a measurement of the soil acidity and alkalinity
	T_CEC_SOIL	Topsoil Cation Exchange Capacity
	T_BS	Topsoil Base Saturation
	T_TEB	Topsoil Total Exchangeable Bases
Terrain	Analytical Hillshade (HILS)	Represents the angle between the natural light and the Earth's surface
	Aspect (ASP)	The slope direction in relation to North
	Channel Network Base Level (CNBL)	Vertical distance to a channel network base level

Digital Elevation Model (DEM)	Digitally represents the altitude of the study area
LS Factor (LSF)	Combination of slope and slope length used to predict erosion potential
Multiresolution index of Ridge Top Flatness (MRRTF)	Topographic index used to identify high flat areas at a range of scales
Multiresolution index of Valley Bottom Flatness (MRVBF)	Topographic index used to identify low flat areas at a range of scales
Relative Slope Position (Slope)	Represents the cell slope position and its relative position between the top and bottom areas
Topographic Position Index (TPI)	Represents the difference between a central pixel and the mean of its surrounding cells
Topographic Wetness Index (TWI)	Related to the area's capacity to accumulate water
Valley Depth (VD)	Vertical distance in relation to valley bottom
Vertical Distance to Channel Network (VDCN)	Vertical distance of each pixel to the channel network base level

2.5. Random forest model

We used the Random Forest (RF) algorithm to model the demographic rates considering all climate, soil and terrain variables as predictors (Breiman, 2001). The RF algorithm is a computational technique less sensitive to noise in the training data and that searches to minimize the prediction errors (Oshiro et al. 2012; Silveira et al. 2019a). Also, the random forest stands out from other machine learning algorithms because of its capacity in selecting and ranking the most important variables and for its application to big dataset (Oshiro et al. 2012; Silveira et al. 2019a). We processed the data using the *randomforest* package (Liaw and Wiener, 2002) in the R software program (R Core Team, 2020). We grouped the data into classes to ensure that the training and validation process have values from all dataset intervals (Silveira et al. 2019a). We analyzed the data composition using a frequency histogram, verifying the distribution of values in each class (Gislason et al. 2006). The classes were defined following the dataset range, meaning that we observed the minimum and maximum value of each demographic rate. Thus, six classes were established for mortality, basal area gain, net change in number of individuals and basal area, five classes for recruitment, and four classes for basal area loss (Figure S1, Supplementary Information).

The data was randomly split into training (70%) and validation (30%) sets (Silveira et al. 2019a) of the predefined classes, and the decision tree number (ntree) was fixed at 1,000, since this tree number is considered good enough to avoid the increase in number of errors (Lawrence et al. 2006). The *mtry*, a parameter that represents the number of predictors sampled for splitting at each node, was obtained by the "tuneRF" function that searches the best value of *mtry* to achieve the lowest OOB error (Out of Bag). The environmental variables were selected using a recursive feature elimination by the random forest algorithm, considering their importance order (Gregorutti et al. 2017). Thus, the variables with the lowest importance value (%IncMSE) in each iteration were excluded and a new Random Forest model with the

remaining variables was processed (Silveira et al. 2019a, 2019c). We used the OOB (Out of Bag) error as a minimization criterion, thus identifying the smaller number of variables for the final model and excluding variables with the lowest importance value (Figure S2, Supplementary Information) (Silveira et al. 2019c). Next, we computed the coefficient of determination (R^2), root mean square error (RMSE) and mean absolute error (MAE) analysis to evaluate the modelling performance. In addition, we established correlations of variable pairs using the Pearson's correlation (r) since the dataset showed normality.

2.6. Deriving demographic rates maps

We generated six maps for the demographic rates of the Brazilian savanna in Minas Gerais State, southeast Brazil. To do so, we used a Brazilian savanna mask (Scolforo, 2006) to predict the demographic rates. We created continuous cells with a dimension of 1 hectare for the whole study area and applied the random forest model using the selected variables' values of each cell to predict its demographic rates (Silveira et al. 2019a).

3. Results

The number of individuals increased from 27,371 in the first sampling interval (2005 and 2006) to 30,725 in the second sampling interval (2010 and 2011). This fluctuation is reflected in the demographic rates, in which the mean recruitment rate (3.72 %.year^{-1}, with standard deviation equal to 1.52 %.year^{-1}) was greater than mean mortality rate (1.33 %.year^{-1}, with standard deviation equal to 1.07 %.year^{-1}). Furthermore, the basal area gain (4.84 %.year^{-1}, with standard deviation equal to 1.49 %.year^{-1}) was greater than the basal area loss (1.08 %.year^{-1}, with standard deviation equal to 0.71 %.year^{-1}). As a result, we found a net change rate in number of individuals of 2.54 %.year^{-1} (with standard deviation equal to 1.72 %.year^{-1}) and a net change in basal area of 4.01 %.year^{-1} (with standard deviation equal to 1.61 %.year^{-1}) (Table S3 and S4, Supplementary Information).

The RF models had a coefficient of determination (R^2) between 0.68 and 0.84 and the MAE was between 0.32 and 0.96 %.year^{-1}. The RMSE (in percentage) showed the largest difference between the models for net change in number of individuals and basal area (Table 2, see also the scatterplots in the Figure S3 Supplementary information for the bias distribution of the demographic rates).

Table 2. Model accuracy for the demographic rates in the Brazilian savanna, Minas Gerais State, southeast Brazil.

Demographic rates	Mean (%.year^{-1})	CV (%)	R^2	RMSE (%)	MAE (%.year^{-1})
Mortality	1.33	80.77	0.68	80	0.39
Recruitment	3.72	40.90	0.84	89	0.46
Basal area loss	1.08	65.78	0.72	60	0.32
Basal area gain	4.84	30.71	0.84	80	0.37
Net change in number of individuals	2.54	67.84	0.77	160	0.96
Net change in basal area	4.01	40.32	0.68	148	0.84

In which: CV is the coefficient of variance; R^2 is the coefficient of determination; RMSE is the root mean square error; MAE is the mean absolute error.

The mortality rate showed greater values at boundary regions between the Brazilian savanna and Atlantic Forest biome close to the mountain range known as "*Cadeia do Espinhaço*" (Espinhaço mountain range), in the north region of Minas Gerais State, as well as close to the "*Serra da Canastra*" mountain in the southwest, and "*Chapada do Rio São Francisco*" (São Francisco River tablelands) in central-west and west regions (Figure 2; see also the Figure S4, Supplementary information for the vegetation type distribution in Minas Gerais state, southeast Brazil). The predictor variables for mortality rates were aspect (ASP) with a negative influence, and LS-factor (LSF), valley depth (VD) and vertical distance to

channel network (VDCN) all with a positive influence (Figure 3). All variables showed similar importance values (%IncMSE = 42.10% to 55.42%) (Table S5 and Figure S5, Supplementary information).

The recruitment rate presented higher values in the north and northwest regions and medium-high rates in the southwest region of Minas Gerais State (Figure 2; see also the Figure S4, Supplementary information for the vegetation type distribution in Minas Gerais state, southeast Brazil). The main recruitment drivers were aspect (ASP), channel network base level (CNBL) and multiresolution index of ridge top flatness (MRRTF) with a negative correlation, and precipitation seasonality (BIO15) with a positive correlation (Figure 3). The variables showed importance values ranging from 95.26 to 102.29% (Table S5 and Figure S5, Supplementary information).

The basal area loss had higher values in the center region of Minas Gerais State and some boundary areas with the Semi-arid woodland. Meanwhile, low values of basal area loss were recorded in the south and southwest regions (Figure 2; see also the Figure S4, Supplementary information for the vegetation type distribution in Minas Gerais state, southeast Brazil). This rate was predicted by the following variables: aspect (ASP), precipitation seasonality (BIO15), relative slope position (Slope) and valley depth (VD), all of them presenting a positive correlation (Figure 3). The predictors showed importance values varying from 62.89 to 71.90% (Table S5 and Figure S5, Supplementary information).

The basal area gain rate showed a similar pattern to the recruitment rate, meaning greater values in the north and northwest regions. Also, higher gains were found for the west region of Minas Gerais State (Figure 2; see also the Figure S4, Supplementary information for the vegetation type distribution in Minas Gerais state, southeast Brazil). The basal area gain had the channel network base level (CNBL) and topographic wetness index (TWI) as predictors,

both with a negative influence on the rate (Figure 3) and importance values of 266.57 and 154.59%, respectively (Table S5 and Figure S5, Supplementary information).

The net change in the number of individuals' rate followed the gain pattern for the north, northwest and center regions, while the loss pattern was found for the south and boundary regions between the Brazilian savanna and Atlantic Forest (Figure 2), representing an area of 28,8095.11 Km^2 of positive values (86.50% of the total area) and 44,956.96 Km^2 of negative values (13.50% of the total area). This rate was mainly predicted by precipitation seasonality (BIO15) and channel network base level (CNBL) with a positive correlation, in addition to analytical hillshade (HILS), valley depth (VD) and vertical distance to channel network (VDCN) with a negative correlation (Figure 3). The importance values for all variables varied from 64.11 to 66.05% (Table S5 and Figure S5, Supplementary information).

The net change in basal area presented greater gain in the central-north, south and southwest regions, and major losses for the west and boundary regions of Brazilian savanna to Atlantic Forest (Figure 2), representing an area of 31,3849.77 Km^2 of positive values (94.23% of the total area) and 19,202.16 Km^2 of negative values (5.77% of the total area). This rate showed a negative correlation to precipitation seasonality (BIO15), channel network base level (CNBL) and analytical hillshade (HILS) (Figure 3), in which the importance values ranged from 117.29 to 132.94% (Table S5 and Figure S5, Supplementary information).

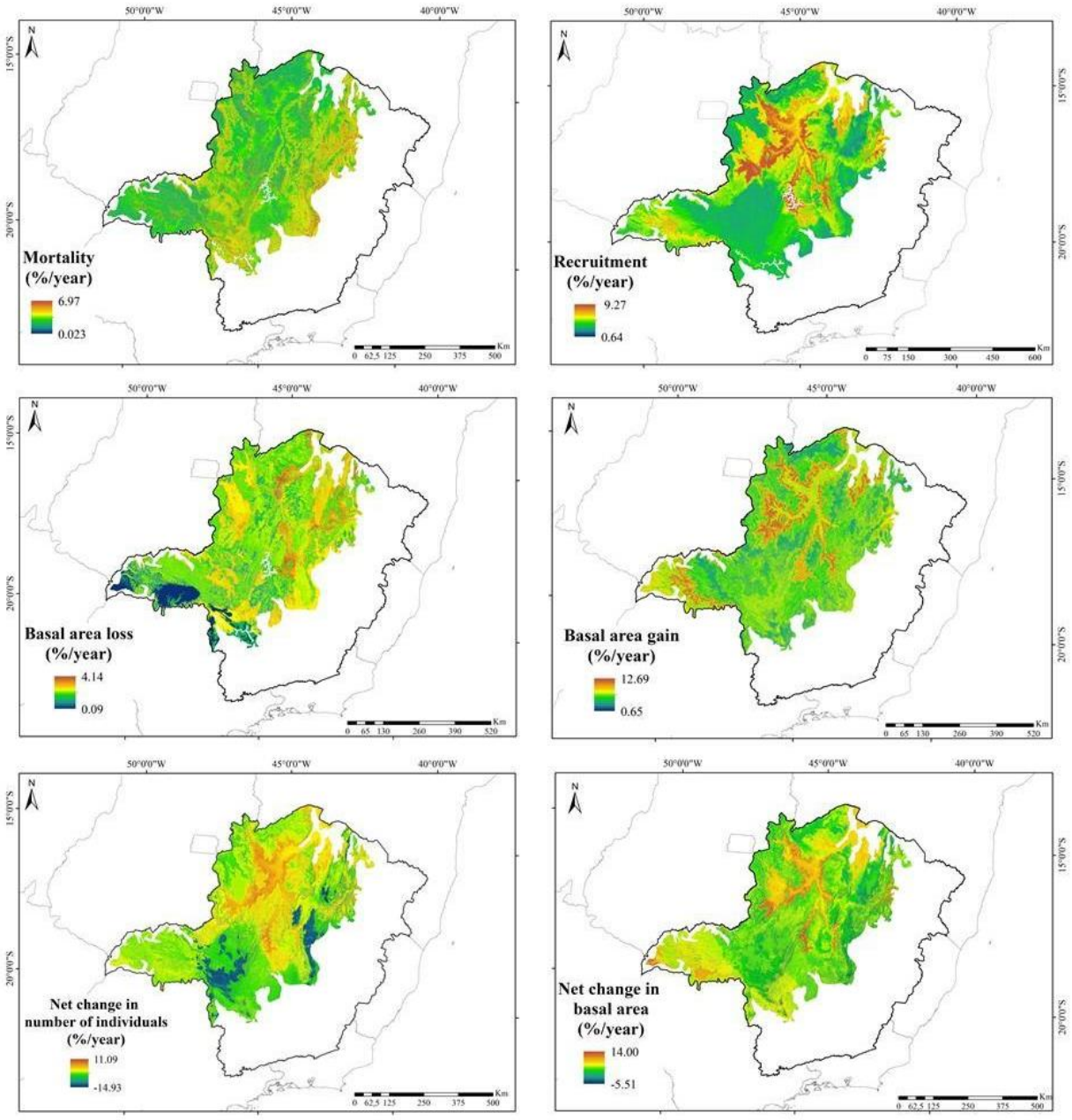

Figure 2 - Spatial distribution of mortality, recruitment, basal area loss, basal area gain, net change in number of individuals and net change in basal area rates considering the Brazilian savanna, Minas Gerais State, southeast Brazil.

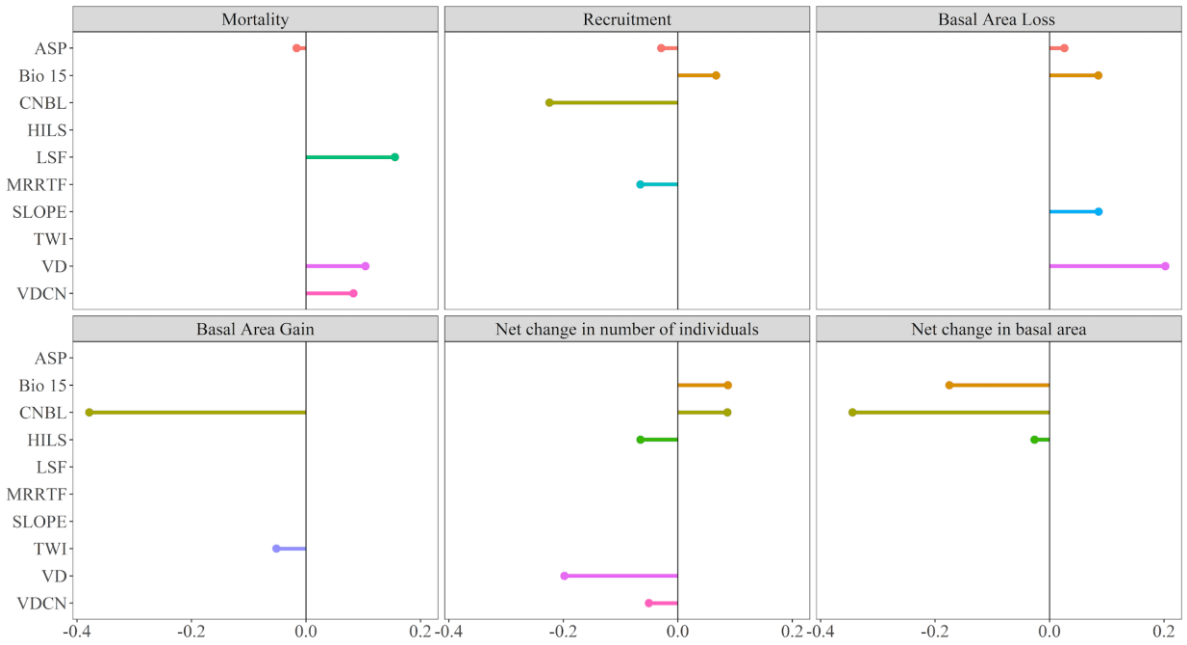

Figure 3 - Pearson correlation between the mortality (M), recruitment (R), basal area loss (L), basal area gain (G), net change in number of individuals (ChN) and net change in basal area (ChBA) rates with the climate and terrain variables selected by the Random Forest algorithm. In which: ASP is aspect; BIO15 is precipitation seasonality; CNBL is channel network base level; HILS is analytical hillshade; LSF is LS factor; MRRTF is multiresolution index of ridge top flatness; Slope is relative slope position; TWI is topographic wetness index; VD is valley depth; VDCN is vertical distance to channel network.

4. Discussion

We assessed to what extent climatic, soil and terrain variables may influence the demographic rates for the Brazilian savanna. Our hypothesis that terrain variables were the most important drivers of tree demographic rates was confirmed. Only the precipitation seasonality among the climate variables showed significant influence in modeling some of the demographic rates. On the other hand, soil variables were not selected as predictors of the demographic rates.

4.1. Vegetation dynamics

Overall, we found that recruitment and basal area gain overcame mortality and basal area loss in most of the Brazilian savanna area in the studied interval. The great recruitment to the Brazilian savanna may be related to the woody plant encroachment, which is an increase in stem density and biomass, decreasing the number of grasses and herbs in the area (Wiegand et al. 2006; Stevens et al. 2017). The encroachment process in Savannas occurs due to fire frequency and temperature decrease, rainfall increase, alien plant invasion, and rising carbon dioxide (Honda and Durigan, 2016; Le Maitre et al. 2015; Stevens et al. 2017). Furthermore, the Brazilian savanna woody encroachment is found in the biome core area, which corroborates the recruitment rates found for the studied Brazilian savanna vegetation (Moreira, 2000; Pellegrini et al. 2016).

Two plots in particular (F94P3 and F104P9 – see Table S4, supplementary information) showed high mortality in our study area. These plots are located next to a road, being more sensitive to edge effects, alien grass invasion which inhibits the native species' regeneration, in turn affecting the structure and community dynamics (Hoffmann et al. 2004, Mendonça et al. 2015). Higher mortality and basal area loss, as well as low recruitment and basal area gain were concentrated in boundary regions of Brazilian savanna with Atlantic Forest, where precipitation is less seasonal and topography is hillier (Scolforo et al. 2016; Silveira et al. 2019a). As a consequence, these regions are classified as colder and less propitious to the Cerrado arboreal vegetation, thus implying in higher mortality and basal area loss rates (Oliveira et al. 2020; Silveira et al. 2019a). In addition, these transitional areas are under orographic effects, presenting gradients in temperature and humidity, thus reduced favorability for Brazilian savanna species and implying in higher mortality rates (Coelho et al. 2016; Silveira et al. 2019d).

Considering the balance between mortality and recruitment, the net change in number of individuals was positive. Following the same pattern related to the balance between the basal area loss and gain, the net change in basal area showed the greatest positive changes. The gains in number of individuals and basal area are concentrated in the core area of the studied Brazilian savanna, where there is strong precipitation seasonality and higher temperatures (Bustamante et al. 2012). These regions are flat areas close to rivers, thus implying in higher soil water availability (Franco et al. 2014). In addition, the encroachment process in these areas is more intense, possibly due to reduced fire frequency (Maracahipes-Santos et al. 2018). The greatest gain in basal area during the interval pointed out the Savanna vegetation capacity in stocking biomass over the years (Cordeiro et al. 2020; Pereira et al. 2020; Reis et al. 2015).

The demographic rates found in our study correspond to other studies on Brazilian savanna vegetation dynamics, in which the recruitment and basal area gain are greater than mortality and basal area loss (Aquino et al. 2007; Gomes et al. 2016; Mews et al. 2011). This pattern indicates a general increase in tree density and biomass over time for the Cerrado, mainly in protected areas and those free of fire (Aquino et al. 2007; Maracahipes-Santos et al. 2018; Mews et al. 2011; Pereira et al. 2020).

4.2. Predictors of vegetation dynamics

Overall, terrain and precipitation seasonality were the most important variables to explain the variation in demographic rates among the plots. No soil variable was significant in modeling the rates.

The regions with greater gain in number of individuals and basal area are those situated in the Brazilian savanna central-north regions, nevertheless, presenting high temperature. In addition, the greater gains are associated to areas close to the drainage channels, that is, areas with higher humidity. The areas with greater loss in number of individuals and basal area values

are centered in the highest regions, which are consequently the coldest ones, and are at the boundary distribution areas of the Brazilian savanna in Minas Gerais State, southeast of Brazil.

The positive relation between mortality, valley depth (VD) and Ls Factor (LSF) implies that most of the tree mortality is concentrated in regions with deeper valley and greater soil loss (higher LS) (Furley, 1999; Jacquin et al. 2010). The vertical distance to channel network (VDCN), which also had a positive correlation to mortality, describes the elevation difference from the channel network (Horst-Heinen et al. 2021), indicating higher mortality in areas which are more vertically distant from the valley bottom (Wu et al. 2017). All the valley depth (VD), vertical distance to channel network (VDCN) and LS Factor (LSF) variables are associated to hilly regions where the moisture retention is lower, the wind exposition greater and the soils are shallow, which may have influenced the mortality rate (Chalise et al. 2018; Kolbek and Alves, 2008; Souza et al. 2010; Wei et al. 2019). This relation between the variables and mortality explains the patterns observed for net change in number of individuals, meaning areas with lower elevation are those with lower mortality, and consequently with a greater gain in number of individuals (Mota et al. 2018). The Brazilian savanna is characterized by its open vegetation, in which the species need light for growth (Rodrigues et al. 2021; Santos et al. 2019). Thus, areas less exposed to solar radiation present a high mortality, which is explained by the negative correlation found between mortality and aspect (ASP) (Zawawi et al. 2014).

The recruitment and net change in number of individuals presented a positive correlation to precipitation seasonality (BIO15) and a negative and positive correlation to channel network base level (CNBL), respectively. Both variables are related to water availability, in which low values of CNBL indicate close proximity to water resources, something which may favor plant growth and recruitment (Campos et al. 2018; Terra et al. 2018). The precipitation seasonality is a characteristic from the Brazilian savanna, since the rain events are concentrated and the dry season is two months or more in length (Lehmann et al. 2014; Staver et al. 2011). The regions

with high precipitation seasonality and warmer climate presented higher recruitment for the Brazilian savanna area studied (Mello and Viola, 2013). Although Passos et al. (2018) found higher recruitment where the resources availability and precipitation were greater in a forest-cerrado transitional area, our study with a large scale of savanna areas showed greater recruitment in areas with greater precipitation seasonality. Despite the higher precipitation seasonality, these areas are situated close to wetter spots, considering the proximity to the middle "São Francisco" River basin (Alves and Gomes, 2020).

In addition, the recruitment rate showed negative correlation to aspect (ASP) and multiresolution index of ridge top flatness (MRRTF). These parameters are related to a downslope direction from the north and high flat areas, respectively (Adhikari et al. 2018; Eugenio et al. 2016). The major gains in recruitment are for regions with low elevation variation in the studied Brazilian savanna area (Gomes et al. 2016; Wakeling et al. 2012). As a consequence of the balance between the mortality and recruitment rates, the net change in number of individuals showed a negative correlation to analytical hillshade (HILS), indicating that areas with major solar light exposure had a greater gain in number of individuals (Batalha et al. 2001; Hoffmann et al. 2009). In summary, although more seasonal in terms of precipitation, the higher water availability and higher the light exposure in the flatter areas close to the São Francisco River areas seem to favor tree establishment and growth.

Our findings showed that the number of individuals, basal area loss and gain rates results imply that regions with the greatest water available show a bigger increment in basal area, and the losses in basal area are mainly in hilly areas (Assis et al. 2011; McCalip et al. 2019; Terra et al. 2018). As a consequence, the net change in basal area showed a negative relation to precipitation seasonality (BIO15), channel network base level (CNBL) and analytical hillshade (HILS).

4.3. Ecology and Management implications

Our study provides the knowledge and description of the Brazilian savanna demographic rates in areas with different successional stages and under different levels of human impact, allowing to infer as to the vegetation vulnerability and its main drivers. From our findings, we may imply that local characteristic (e.g., precipitation seasonality, soil moisture, topography and water availability) are influencing the tree community fluctuations. In addition, variability in local features such soil and climate may influence the vegetation structure, resulting in an ecosystem loss (Hofmann et al. 2021).

Considering our results, the major gains in number of individuals and basal area are related to regions with great water availability. However, the Intergovernmental Panel on Climate Change (IPCC) projection indicates higher water deficit to the studied area in the upcoming years (Hofmann et al. 2021). If we consider the projection confirmation, the vegetation will present less biomass gain. From this information, our results may lead to vulnerable areas identification to climate change as well as to point out priority areas to conservation. Also, from the mapping of the demographic rates and its drivers is provided insights to the elaboration of public politics, strategies of conservation and restoration, as well as identification of areas fire prone.

5. Conclusion

From the modelling and mapping the tree community rates of mortality, recruitment, net change in number of individuals, basal area loss and gain, and net change in basal area as a function of environmental variables (climate, terrain and soil), our study pointed out the terrain variables as good predictors of the demographic rates, thus highlighting these characteristics as important vegetation drivers. Understanding the demographic rates drivers provides deeper knowledge regarding vegetation establishment and functioning, since we may infer as to the ecosystem tolerance to the environmental filters. Overall, the gains in number of individuals

and basal area in the studied Brazilian savanna area were driven by features related to water availability and the major losses are connected to hilly areas.

Acknowledgments

The authors express gratitude to the Universidade Federal de Lavras (UFLA), *Laboratório de Estudos e Projetos em Manejo Florestal* (*LEMAF*) and the *Programa de Pós-Graduação em Engenharia Florestal* (PPGEF) for the structure necessary to conduct the study. This work was supported by the *Coordenação de Aperfeiçoamento de Pessoal de Nível Superior - Brasil* (*CAPES*) - Finance Code 001. We also thank *CNPq* (National Council for Scientific and Technological Development).

References

Abreu, J.C. de, Guedes, M.C., Guedes, A.C.L., Batista, E. das M., 2014. Estrutura e distribuição espacial de andirobeiras (*Carapa* spp.) em floresta de várzea do Estuário Amazônico. Cienc. Florest., 24, 1009–1019. https://doi.org/10.1590/1980-509 820142404020.

Adhikari, K., Owens, P.R., Ashworth, A.J., Sauer, T.J., Libohova, Z., Richter, J.L., Miller, D.M., 2018. Topographic controls on soil nutrient variation in a silvopasture system. Agrosyst. Geosci. Environ., 1, 1-15. https://doi.org/10.2134/age2018.04.0008.

Alencar, A., Shimbo, J.Z., Lenti, F., Marques, C.B., Zimbres, B., Rosa, M., Arruda, V., Castro, I., Ribeiro, J.P.F.M., Varela, V., Alencar, I., Piontekowski, V., Ribeiro, V., Bustamante, M.M.C., Sano, E.E., Barroso, M., 2020. Mapping three decades of changes in the Brazilian Savanna native vegetation using Landsat data processed in the Google Earth Engine Platform. Remote Sens., 12, 924. https://doi.org/10.3390/rs12060924.

Alvarado, S.T., Fornazari, T., Cóstola, A., Morellato, L.P.C., Silva, T.S.F., 2017. Drivers of fire occurrence in a mountainous Brazilian cerrado savanna: Tracking long-term fire regimes using remote sensing. Ecol. Indic., 78, 270–281. https://doi.org/10.1016/j.ecolind.2017.02.037.

Alvares, C.A., Stape, J.L., Sentelhas, P.C., Gonçalves, J.L.M. de, Sparovek, G., 2014. Köppen's climate classification map for Brazil. Meteorol. Zeitschrift, 22, 711–728. https://doi.org/10.1127/0941-2948/2013/0507.

Alves, L.E.R., Gomes, H.B., 2020. Validação da imputação múltipla via *Predictive Mean Matching* para preenchimento de falhas nos dados pluviométricos da bacia do médio São Francisco. Anu. do Inst. de Geocienc., 43, 199-206. https://doi.org/10.11137/2020_1_199_206.

APG IV., 2016. An update of the Angiosperm Phylogeny Group classification for the orders and families of flowering plants: APG IV. Bot. J. Linn. Soc., 181, 1–20. https://doi.org/10.1111/boj.12385.

Aquino, F. de G., Walter, B.M.T., Ribeiro, J.F., 2007. Dinâmica de populações de espécies lenhosas de Cerrado, Balsas, Maranhão. Rev. Árvore, 31, 793-803. https://doi.org/10.1590/S0100-67622007000500003.

Assis, A.C.C. de, Coelho, R.M., Pinheiro, E. da S., Durigan. G., 2011. Water availability determines physiognomic gradient in an area of low-fertility soils under Cerrado vegetation. Plant Ecol., 212, 1135–1147. https://doi.org/10.1007/s11258-010-9893-8.

Barbosa, H.A., Lakshmi Kumar, T.V., Silva, L.R.M., 2015. Recent trends in vegetation dynamics in the South America and their relationship to rainfall. Nat. Hazards, 77, 883–899. https://doi.org/10.1007/s11069-015-1635-8.

Batalha, M.A., Mantovani, W., Mesquita Júnior, H.N. de, 2001. Vegetation structure in cerrado physiognomies in South-eastern Brazil. Braz. J. Biol, 61, 475-483. https://doi.org/10.1590/S1519-69842001000300018.

Batalha, M.A., Silva, I.A., Cianciaruso, M.V., França, H., Carvalho, G.H. de, 2011. Phylogeny, traits, environment, and space in cerrado plant communities at Emas National Park (Brazil). Flora: Morphol. Distrib. Funct. Ecol. Plants, 206, 946-956. https://doi.org/10.1016/j.flora.2011.07.004.

Bell, F.W., Lamb, E.G., Sharma, M., Hunt, S., Anand, M., Dacosta, J., Newmaster, S.G., 2016. Relative influence of climate, soils, and disturbance on plant species richness in northern temperate and boreal forests. Forest Ecol. Manag., 381, 93–105. https://doi.org/10.1016/j.foreco.2016.07.016.

Borghetti, F., Barbosa, F., Ribeiro, L., Ribeiro, J.F., Walter, B.M.T., 2019. South American Savannas, in: Scogings, P.F., Sankaran, M. (Eds.), Savanna Woody Plants and Large Herbivores. Wiley-Blackwell, Hoboken, pp. 77–122. https://doi.org/10.1002/9781119081111.ch4.

Bowler, D.E., Hof. C., Haase, P., Kröncke, I., Schweiger, O., Adrian, R., Baert, L., Bauer, H-G., Blink, T., Brooker, R.W., Dekoninck, W., Domisch, S., Eckmann, R., Hendrickx, F., Hickler, T., Klotz, S., Kraberg, A., Kühn, I., Matesanz, S., Meschede, A., Neumann, H., O'Hara, R., Russell, D.J., Sell, A.F., Sonnewald, M., Stoll, S., Sundermann, A., Tackenberg, O., Türkay, M., Valladares, F., van Herk, K., van Klink, R., Vermeulen, R., Voigtländer, K., Wagner, R., Welk, E., Wiemers, M., Wiltshire, K.H., Böhning-Gaese, K., 2017. Cross-realm assessment of climate change impacts on species' abundance trends. Nat. Ecol. Evol., 1, 0067. https://doi.org/10.1038/s41559-016-0067.

BFG - Brazil Flora Group, 2021. Brazilian Flora 2020 project - Projeto Flora do Brasil 2020. v393.274. Instituto de Pesquisas Jardim Botânico do Rio de Janeiro. Dataset/Checklist. https://doi.org/10.15468/1mtkaw. (accessed 25 April 2020).

Breiman, L., 2001. Random forests. Machine Learning, 45: 5–32.

Bueno, M.L., Dexter, K.G., Pennington, R.T., Pontara, V., Neves, D.M., Ratter, J.A., Oliveira-Filho, A.T. de, 2018. The environmental triangle of the Cerrado Domain: Ecological factors driving shifts in tree species composition between forests and savannas. J. Ecol., 106, 2109-2120. https://doi.org/10.1111/1365-2745.12969.

Bustamante, M.M.C., Nardoto, G.B., Pinto, A.S., Resende, J.C.F., Takahashi, F.S.C., Vieira, L.C.G., 2012. Potential impacts of climate change on biogeochemical functioning of Cerrado ecosystems. Braz. J. Biol., 72, 655-671. https://doi.org/10.1590/S1519-69842012000400005.

Campos, A.R., Giasson, E., Costa, J.J.F., Machado, I.R., Silva, E.B. da, Bonfatti, B.R., 2018. Selection of environmental covariates for classifier training applied in digital soil mapping. Rev. Bras. Ciênc. Solo, 42, e0170414. https://doi.org/10.1590/18069657rbcs20170414.

Carvalho, M.C., França, L.C. de J., Lopes, I.L. e, Araújo, L.A., Mello, J.M. de, Gomide, L.R., 2019. Algoritmos de aprendizagem de máquina na modelagem da distribuição potencial de habitats de espécies arbóreas. Nativa, 7, 600-606. https://doi.org/10.31413/nativa.v7i5.7214.

Chalise, D., Kumar, L., Shriwastav, C.P., Lamichhane, S., 2018. Spatial assessment of soil erosion in a hilly watershed of Western Nepal. Environ. Earth Sci., 77, 685. https://doi.org/10.1007/s12665-018-7842-3.

Coelho, M.S., Fernandes, G.W., Pacheco, P., Diniz, V., Meireles, A., Santos, R.M. dos, Carvalho, F.A., Negreiros, D., 2016. Archipelago of Montane Forests surrounded by Rupestrian Grasslands: New insights and perspectives, in: Fernandes G. (Ed.), Ecology and Conservation of Mountaintop Grasslands in Brazil, Springer, Switzerland, pp. 129–156. https://doi.org/10.1007/978-3-319-29808-5_7.

Cordeiro, N.G., Pereira, K.M.G., Terra, M. de. C.N.S., Mello, J.M. de, 2020. Structural and compositional shifts in Cerrado fragments in up to 11 years monitoring. Acta Sci. Biol. Sci., 42, e48357. https://doi.org/10.4025/actascibiolsci.v42i1.48357.

Coutinho, L.M., 1990. Fire in the ecology of the Brazilian Cerrado, in: Goldammer, J.G. (Ed.), Fire in the Tropical Biota, Springer, Berlin, pp. 81 – 105.

Durigan, G., Ratter, J.A., 2006. Successional changes in Cerrado and Cerrado/Forest ecotonal vegetation in western São Paulo state, Brazil, 1962–2000. Edinburgh J. Bot., 63, 119-130. https://doi.org/10.1017/S0960428606000357.

Eiten, G., 1972. The Cerrado Vegetation of Brazil. Bot. Rev., 38, 201–341. https://doi.org/10.1007/BF02859158.

Esquivel-Muelbert, A., Baker, T.R., Dexter, K.G., Lewis, S.L., Brienen, R.J.W., Feldpausch, T.R., Lloyd, J., Monteagudo-Mendonza, A., Arroyo, L., Álvarez-Dávila, E., Higuchi, N., Marimon, B.S., Marimon-Junior, B.H., Silveira, M., Vilanova, E., Gloor, E., Malhi, Y., Chave, J., Barlow, J., Bonal, D., Cardozo, N.D., Erwin, T., Fauset, S., Hérault, B., Laurance, S., Poorter, L., Qie, L., Stahl, C., Sullivan, M.J.P., ter Stage, H., Vos, V.A., Zuidema, P.A., Almeida, E., Oliveira, E.A. de, Andrade, A., Vieira, S.A., Aragão, L., Araujo-Murakami, A., Arets, E., Aymard C, G.A., Baraloto, C., Camargo, P.B., Barroso, J.G., Bongers, F., Boot, R., Camargo, J.L., Castro, W., Moscoso, V.C., Comiskey, J., Valverde, F.C., Costa, A.C.L. da, Pasquel, J.D.A., Di Fiori, A., Duque, L.F., Elias, F., Engel, J., Llampazo, J.F., Galbraith, D., Fernández, R.H., Coronado, E.H., Hubal, W., Gimenez-Rojas, E., Lima, A.J.N., Umetsu, R.K., Laurence, W., Lopez-Gonzalez, G., Lovejoe, T., Cruz, O.A.M., Morandi, P.S., Neill, D., Vargas, P.N., Camacho, N.C.P., Gutierrez, A.P., Pardo, G., Peacock, J., Peña-Claros, M., Peñuela-Mora, M.C., Petronelli, P., Pickavance, G.C., Pitman, N., Prieto, A., Quesada, C., Ramírez-Angulo, H., Réjou-Mechain, M., Correia, Z.R., Roopsind, A., Rudas, A., Salomão, R., Silva, N., Espejo, J.S., Singh, J., Stropp, J., Terborgh, J., Thomas, R., Toledo, M., Torres-Lezama, A., Gamarra, L.V., van de Meer, P.J., van der Heijden, G., van der Hout, P., Martinez, R.V., Vela, C., Vieira, I.C.G., Phillips, O.L., 2018. Compositional response of Amazon forests to climate change. Global Change Biol., 25, 39–56. https://doi.org/10.1111/gcb.14413.

Eugenio, F.C., Santos, A.R. dos, Fiedler, N.C., Ribeiro, G.A., Silva, A.G. da, Santos, A.B. dos, Paneto, G.G., Schettino, V.R., 2016. Applying GIS to develop a model for forest fire risk: A case study in Espírito Santo, Brazil. J. Environ. Manage., 173, 65-71. https://doi.org/10.1016/j.jenvman.2016.02.021.

FAO - FAO SOILS PORTAL, 2020. Harmonized World Soil Database v 1.2. http://www.fao.org/soils-portal/soil-survey/soil-maps-and-databases/harmonized-world-soil-database-v12/en/. (accessed 13 June 2020).

Ferreira, L.G., Huete, A.R., 2004. Assessing the seasonal dynamics of the Brazilian Cerrado vegetation through the use of spectral vegetation indices. Int. J. Remote Sens., 25, 1837–1860. https://doi.org/10.1080/0143116031000101530.

Ferreira, J.N., Bustamante, M., Garcia-Montiel, D.C., Caylor, K.K., Davidson, E.A., 2007. Spatial variation in vegetation structure coupled to plant available water determined by two-dimensional soil resistivity profiling in a Brazilian savanna. Oecologia 153, 417–430. https://doi.org/10.1007/s00442-007-0747-6.

Fick, S.E., Hijmans, R.J., 2017. WorldClim 2: new 1-km spatial resolution climate surfaces for global land areas. Int. J. Climatol., 37, 4302–4315. https://doi.org/10.1002/joc.5086.

Forkuor, G., Hounkpatin, O.K.L., Welp, G., Thiel, M., 2017. High resolution mapping of soil properties using Remote Sensing variables in south-western Burkina Faso: A comparison of machine learning and multiple linear regression models. PLoS ONE, 12, e0170478. https://doi.org/10.1371/journal.pone.0170478.

Franco, A.C., Rossatto, D.R., Silva, L. de C.R., Ferreira, C. da, 2014. Cerrado vegetation and global change: the role of functional types, resource availability and disturbance in regulating plant community responses to rising CO2 levels and climate warming. Theor. Exp. Plant Physiol., 26, 19–38. https://doi.org/10.1007/s40626-014-0002-6.

Furley, P.A., 1999. The nature and diversity of neotropical savanna vegetation with particular reference to the Brazilian cerrados. Global Ecol. Biogeogr., 8, 223-241. https://doi.org/10.1046/j.1466-822X.1999.00142.x.

Gignoux, J., Konaté, S., Lahoreau, G., Le Roux, X., Simioni, G., 2016. Allocation strategies of savanna and forest tree seedlings in response to fire and shading: outcomes of a field experiment. Sci. Rep., 6, 38838. https://doi.org/10.1038/srep38838.

Gislason, P.O., Benediktsson, J.A., Sveinsson, J.R., 2006. Random Forests for land cover classification. Pattern Recognit. Lett., 27, 294-300. https://doi.org/10.1016/j.patrec.2005.08.011.

Gomes, L., Maracahipes, L., Reis, S.M., Marimon, B.S., Marimon-Junior, B.H., Lenza, E., 2016. Dynamics of the woody vegetation of two areas of Cerrado *sensu stricto* located on different substrates. Rodriguésia, 67, 859-870. https://doi.org/10.1590/2175-7860201667401.

Gregorutti, B., Michel, B., Saint-Pierre, P., 2017. Correlation and variable importance in random forests. Stat Comput 27, 659–678. https://doi.org/10.1007/s11222-016-9646-1.

Grömping, U., 2009. Variable importance assessment in regression: Linear regression versus random forest. Am. Stat., 63, 308–319. https://doi.org/10.1198/tast.2009.08199.

Hengl, T., Heuvelink, G.B.N., Kempen, B., Leenaars, J.G.B., Walsh, M.G., Shepherd, K.D., Sila, A., MacMillan, R.A., Jesus, J.M. de, Tamene, L., Tondoh, J.E., 2015. Mapping soil properties of Africa at 250 m resolution: Random forests significantly improve current predictions. PLoS ONE, 10, e0125814. https://doi.org/10.1371/journal.pone.0125814.

Henriques, R.P.B, Hay, J.D., 2002. Patterns and dynamics of plant populations, in: Oliveira, P.S., Marquis, R.J. (Eds.), The Cerrados of Brazil. Columbia University Press, New York, 140-158.

Higuchi, P., 2018. forest.din: Função em linguagem de programação estatística R para a determinação da dinâmica de comunidades de espécies arbóreas. https://github.com/higuchip/forest.din. (accessed 23 May 2020).

Hoffmann, W.A., Lucatelli, V.M.P.C., Silva, F.J., Azeuedo, I.N.C., Marinho, M. da S., Albuquerque, A.M.S., Lopes, A. de O., Moreira, S.P., 2004. Impact of the invasive alien grass *Melinis minutiflora* at the savanna-forest ecotone in the Brazilian Cerrado. Divers. Distrib., 10, 99-103. https://doi.org/10.1111/j.1366-9516.2004.00063.x.

Hoffmann, W.A., Adasme, R., Haridasan, M., Carvalho, M.T. de, Geiger, E.L., Pereira, M.A.B., Gotsch, S.G., Franco, A.C., 2009. Tree topkill, not mortality, governs the dynamics of savanna–forest boundaries under frequent fire in central Brazil. Ecology, 90, 1326-1337. https://doi.org/10.1890/08-0741.1.

Hofmann, G.S., Cardoso, M.F., Alves, R.J.V., Weber, E.J., Barbosa, A.A., Toledo, P.M. de, Pontual, F.B., Salles, L. de O., Hasenack, H., Cordeiro, J.L.P., Aquino, F.E., Oliveira, L.F.B. de, 2021. The Brazilian Cerrado is becoming hotter and drier. Glob Chang Biol, 27, 4060-4073. https://doi.org/10.1111/gcb.15712.

Honda, E.A., Durigan, G., 2016. Woody encroachment and its consequences on hydrological processes in the savannah. Phil. Trans. R. Soc. B, 371, 20150313. http://dx.doi.org/10.1098/rstb.2015.0313.

Horst-Heinen, T.Z., Dalmolin, R.S.D., ten Caten, A., Moura-Bueno, J.M., Grunwald, S., Pedron, F. de A., Rodrigues, M.F., Rosin, N.A., Silva-Sangoi, D.V. da., 2021. Soil depth prediction by digital soil mapping and its impact in pine forestry productivity in South Brazil. For. Ecol. Manage., 488, 118983. doi.org/10.1016/j.foreco.2021.118983.

IBGE, 2004. Mapa de biomas do Brasil. Escala 1:5.000.000. http://mapas.ibge.gov.br/biomas2/viewer.htm. (accessed 05 August 2020).

Jacquin, A., Sheeren, D., Lacombe, J-P., 2010. Vegetation cover degradation assessment in Madagascar savanna based on trend analysis of MODIS NDVI time series. Int. J. Appl. Earth Obs. Geoinf., 12, S3–S10. https://doi.org/10.1016/j.jag.2009.11.004.

Jin, X., Liu, J., Wang, S., Xia, W., 2016. Vegetation dynamics and their response to groundwater and climate variables in Qaidam Basin, China. Int. J. Remote Sens., 37, 710–728. https://doi.org/10.1080/01431161.2015.1137648.

Kolbek, J., Alves, R.J.V., 2008. Impacts of cattle, fire and wind in rocky savannas, southeastern Brazil. Acta Univ. Carol. Biol., 22, 111-130.

Korning, J., Balslev, H., 1994. Growth and mortality of trees in Amazonian tropical rain forest in Ecuador. J. Veg. Sci., 5, 77-86.

Lawrence, R.L., Wood, S.D., Sheley, R.L., 2006. Mapping invasive plants using hyperspectral imagery and Breiman Cutler classifications (randomForest). Remote Sens. Environ., 100, 356-362. https://doi.org/10.1016/j.rse.2005.10.014.

Le Maitre, D.C., Gush, M.B., Dzikiti, S., 2015. Impacts of invading alien plant species on water flows at stand and catchment scales. AoB Plants, 7, plv043. https://doi.org/10.1093/aobpla/plv043.

Ledru, M-P., Salgado-Labouriau, M.L., Lorscheitter, M.L., 1998. Vegetation dynamics in southern and central Brazil during the last 10,000 yr B.P. Rev. Palaeobot. Palynol., 99, 131–142. https://doi.org/10.1016/S0034-6667(97)00049-3.

Lehmann, C.E.R., Anderson, T.M., Sankaran, M., Higgins, S.I., Archibald, S., Hoffmann, W.A., Hanan, N.P., Williams, R.J., Fensham, R.J., Felfili, J., Hutley, L.B., Ratnam, J., San Jose, J., Montes, R., Franklin, D., Russell-Smith, J., Ryan, C.M., Durigan, G., Hiernaux, P., Haidar, R., Bowman, D.M.J.S., Bond, W.J., 2014. Savanna vegetation-fire-climate relationships differ among continents. Science, 343, 548-552. https://doi.org/10.1126/science.1247355.

Lewis, S.L., Phillips, O.L., Baker, T.R., Lloyd, J., Malhi, Y., Almeida, S., Higuchi, N., Laurence, W.F., Neill, D.A., Silva, J.N.M., Terborgh, J., Lezama, A.T., Martinez, R.V., Brown, S., Chave, J., Kuebler, C., Vargas, P.N., Vinceti, B., 2004. Concerted changes in tropical forest structure and dynamics: Evidence from 50 South American long-term plots. Philos. T. R. Soc. B, 359, 421–436. https://doi.org/10.1098/rstb.2003.1431.

Li, C., Tao, Y., Ao, W., Yang, S., Bai, Y., 2018. Improving forecasting accuracy of daily enterprise electricity consumption using a random forest based on ensemble empirical mode decomposition. Energy, 165, 1220–1227. https://doi.org/10.1016/j.energy.2018.10.113.

Liaw, A., Wiener, M., 2002. Classification and regression by randomForest. R News, 2, 18–22.

Matasci, G., Hermosila, T., Wulder, M.A., White, J.C., Coops, N.C., Hobart, G.W., Zald, H.S.J., 2018. Large-area mapping of Canadian boreal forest cover, height, biomass and other structural attributes using Landsat composites and lidar plots. Remote Sens. Environ., 209, 90–106. https://doi.org/10.1016/j.rse.2017.12.020.

Macdicken, K.G., Wolf, G.V., Briscoe, C.B., 1991. Standard Research Methods for Multipurpose Trees and Shrubs. Winrock International, USA.

Maracahipes-Santos, L., Santos, J.O. dos, Reis, S.M., Lenza, E., 2018. Temporal changes in species composition, diversity, and woody vegetation structure of savannas in the Cerrado-

Amazon transition zone. Acta Bot. Bras., 32, 254-263. http://dx.doi.org/10.1590/0102-33062017abb031.

McCalip, B., Oswald, B.P., Kidd, K.R., Weng, Y., Farrish, K.W, 2019. Site factors influence on herbaceous understory diversity in East Texas Pinus palustris savannas. Int. J. Biol., 11, 1-9. http://dx.doi.org/10.5539/ijb.v11n1p1.

Mello, C.R. de, Viola, M.R., 2013. Mapeamento de chuvas intensas no estado de Minas Gerais. R. Bras. Ci. Solo, 37, 37-44. http://dx.doi.org/10.1590/S0100-06832013000100004.

Mendonça, A.H., Russo, C., Melo, A.C.G., Durigan, G., 2015. Edge effects in savanna fragments: a case study in the cerrado. Plant Ecolog. Divers., 8, 493–503. http://dx.doi.org/10.1080/17550874.2015.1014068.

Mews, H.A., Marimon, B.S., Maracahipes, L., Franczak, D.D., Marimon-Junior, B.H., 2011. Dinâmica da comunidade lenhosa de um Cerrado Típico na região Nordeste do Estado de Mato Grosso, Brasil. Biota Neotrop., 11, 73-82. https://doi.org/10.1590/S1676-06032011000100007.

Morais, V.A., Silva, C.A., Scolforo, J.R.S., Mello, J.M. de, Araújo, E.J.G. de, Assis, E.A. de, 2013. Modelagem do teor de carbono orgânico em solos de fragmentos de Cerrado de Januária e Bonito de Minas, Minas Gerais. Pesq. flor. bras., 33, 343–354. https://doi.org/10.4336/2013.pfb.33.76.507.

Moreira, A.G., 2000. Effects of fire protection on savanna structure in Central Brazil. J. Biogeogr., 27, 1021-1029. https://doi.org/10.1046/j.1365-2699.2000.00422.x.

Mota, G. da S., Luz, G.R. da, Mota, N.M., Coutinho, E.S., Veloso, M. das D.M., Fernandes, G.W., Nunes, Y.R.F., 2018. Changes in species composition, vegetation structure, and life

forms along an altitudinal gradient of rupestrian grasslands in south-eastern Brazil. Flora, 238, 32-42. http://dx.doi.org/doi:10.1016/j.flora.2017.03.010.

Murphy, B.P., Bowman, D.M.J.S., 2012. What controls the distribution of tropical forest and savanna?. Ecol. Lett., 15, 748-758. https://doi.org/10.1111/j.1461-0248.2012.01771.x.

Müller, H., Rufin, P., Griffiths, P., Siqueira, A.J.B., Hostert, P., 2015. Mining dense Landsat time series for separating cropland and pasture in a heterogeneous Brazilian savanna landscape. Remote Sens. Environ., 156, 490–499. https://doi.org/10.1016/j.rse.2014.10.014.

Myers, N., Mittermeier, R.A., Mittermeier, C.G., Fonseca, G.A.B. da, Kent, J., 2000. Biodiversity hotspots for conservation priorities. Nature, 403, 853–858. https://doi.org/10.1038/35002501.

Oliveira, A.P. de, Schiavini, I., Vale, V.S. do, Lopes, S. de F., Arantes, C. de S., Gusson, A.E., Prado Júnior, J.A., Dias-Neto, O.C., 2014. Mortality, recruitment and growth of the tree communities in three forest formations at the Panga Ecological Station over ten years (1997-2007). Acta Bot. Bras., 28 234-248. https://doi.org/10.1590/S0102-33062014000200010.

Oliveira, P.E. de, Raczka, M., McMichael, C.N.H., Pinaya, J.L.D., Bush, M.B., 2020. Climate change and biogeographic connectivity across the Brazilian cerrado. J. Biogeogr., 47, 396–407. https://doi.org/10.1111/jbi.13732.

Oshiro, T.M., Perez, P.S., Baranauskas, J.A., 2012. How many trees in a random forest?, in: Perner, P. (Ed.), Machine Learning and Data Mining in Pattern Recognition. MLDM 2012. Lecture Notes in Computer Science. Springer, Berlin, Heidelberg. https://doi.org/10.1007/978-3-642-31537-4_13.

Passos, F.B., Marimon, B.S., Phillips, O.L., Morandi, P.S., Neves, E.C. das, Elias, F., Reis, S.N., Oliveira, B. de, Feldpausch, T.R., Marimon Junior, B.H., 2018. Savanna turning into forest: concerted vegetation change at the ecotone between the Amazon and "Cerrado" biomes. Rev. Bras. Bot., 41, 611–619. https://doi.org/10.1007/s40415-018-0470-z.

Pausas, J.G., Dantas, V. de L., 2017. Scale matters: fire–vegetation feedbacks are needed to explain tropical tree cover at the local scale. Global Ecol. Biogeogr., 26, 395–399. https://doi.org/10.1111/geb.12562.

Pelegrino, M.H.P., Silva, S.H.G., Menezes, M.D. de, Silva, E. da, Owens, P.R., Curi, N., 2016. Mapping soils in two watersheds using legacy data and extrapolation for similar surrounding areas. Ciênc. agrotec., 40, 534–546. http://dx.doi.org/10.1590/1413-70542016405011416.

Pennington, R.T., Lehmann, C.E.R., Rowland, L.M., 2018. Tropical savannas and dry forests. Curr. Biol., 28, R541–R545. https://doi.org/10.1016/j.cub.2018.03.014.

Pereira, K.M.G., Cordeiro, N.G., Terra, M. de C.N.S., Pyles, M.V., Cabacinha, C.D., Mello, J.M. de, van der Berg, E., 2020. Protection status as determinant of carbon stock drivers in Cerrado *sensu stricto*. J. Plant Ecol., 13, 361–368. https://doi.org/10.1093/jpe/rtaa024.

Pinheiro, E. da S., Durigan, G., 2009. Dinâmica espaço-temporal (1962-2006) das fitofisionomias em unidade de conservação do Cerrado no sudeste do Brasil. Revista Brasil. Bot., 32, 441-454. https://doi.org/10.1590/S0100-84042009000300005.

Pyles, M.V., Prado-Junior, J.A., Magnago, L.F.S., Paula, A. de, Meira Neto, J.A.A., 2018. Loss of biodiversity and shifts in aboveground biomass drivers in tropical rainforests with different disturbance histories. Biodivers Conserv., 27, 3215–3231. https://doi.org/10.1007/s10531-018-1598-7.

Qin, Y., Xiao, X., Dong, J., Zhou, Y., Wang, J., Doughty, R.B., Chen, Y., Zou, Z., Moore III, B., 2017. Annual dynamics of forest areas in South America during 2007–2010 at 50-m spatial resolution. Remote Sens. Environ., 201, 73–87. https://doi.org/10.1016/j.rse.2017.09.005.

R Core Team., 2020. R: A language and environment for statistical computing. R Foundation for Statistical Computing, Vienna, Austria. https://www.r-project.org/. (accessed 15 June 2020).

Reis, S.M., Lenza, E., Marimon, B.S., Gomes, L., Forsthofer, M., Morandi, B.S., Marimon Junior, B.H., Feldpausch, T.R., Elias, F., 2015. Post-fire dynamics of the woody vegetation of a savanna forest (Cerradão) in the Cerrado-Amazon transition zone. Acta Bot. Bras., 29, 408–416. https://doi.org/10.1590/0102-33062015abb0009.

Resende, F.M., Cimon-Morin, J., Poulin, M., Meyer, L., Loyola, R., 2019. Consequences of delaying actions for safeguarding ecosystem services in the Brazilian Cerrado. Biol. Conserv., 234, 90-99. https://doi.org/10.1016/j.biocon.2019.03.009.

Ribeiro, J.F., Walter, B.M.T., 2008. As principais fitofisionomias do bioma Cerrado, in: Sano, S.M., Almeida, S.P. de, Ribeiro, J.F. (Eds.), Cerrado: Ecologia e flora. Embrapa Cerrado, Planaltina, pp. 152–212.

Rodrigues, C.A., Zirondi, H.L., Fidelis, A., 2021. Fire frequency affects behavior in open savannas of the Cerrado. For. Ecol. Manage., 482, 118850. https://doi.org/10.1016/j.foreco.2020.118850.

Roitman, I., Vanclay, J.K., Hay, J.D., Felfili, J.M., 2016. Dynamic equilibrium and decelerating growth of a seasonal Neotropical gallery forest in the Brazilian savanna. J. Trop. Ecology, 32, 193–200. https://doi.org/10.1017/S026646741600016X.

Santos, G.L. dos, Pereira, M.G., Carvalho, D.C. de, Santos, R.N. dos, Delgado, R.C., Torres, J.L.R., Cravo, M.D. da S., 2019. Relationship between the environmental conditions and floristic patterns in two phytophysiognomies of the Brazilian Cerrado. Environ Dev Sustain., 21, 95–113. https://doi.org/10.1007/s10668-017-0025-7.

Scholes, R.J., Archer, S.R., 1997. Tree-grass interactions in Savannas. Annu. Rev. Ecol. Evol. Syst., 28, 517–544. https://doi.org/10.1146/annurev.ecolsys.28.1.517.

Scolforo, J.R.S., 2006. Procedimentos de mapeamento, in: Scolforo, J.R.S., Carvalho, L. M.T. de (Eds.), Mapeamento e inventário da flora e dos reflorestamentos de Minas Gerais. Editora UFLA, Lavras, pp. 37–57.

Scolforo, J.R.S., Mello, J.M. de, Oliveira, A.D., 2008. Inventário Florestal de Minas Gerais: Cerrado - Florística, estrutura, diversidade, similaridade, distribuição diamétrica e de altura, volumetria, tendências de crescimento e áreas aptas para o manejo florestal. Editora UFLA, Lavras.

Scolforo, H.R., Scolforo, J.R.S., Mello, J.M. de, Mello, C.R. de, Morais, V.A., 2016. Spatial interpolators for improving the mapping of carbon stock of the arboreal vegetation in Brazilian biomes of Atlantic Forest and Savanna. For. Ecol. Manage., 376, 24-35. http://dx.doi.org/10.1016/j.foreco.2016.05.047.

Sheil, D., Jenningst, S., Savill, P., 2000. Long-term permanent plot observations of vegetation dynamics in Budongo, a Ugandan Rain Forest. J. Trop. Ecology, 16, 865–882. https://doi.org/10.1017/S0266467400001723.

Sheil, D., May, R.M., 1996. Mortality and recruitment rate evaluations in heterogeneous Tropical Forests. J. Ecol., 84, 91–100.

Silva, J.M.C. da, Bates, J.M., 2002. Biogeographic patterns and conservation in the South American Cerrado: A Tropical Savanna Hotspot. BioScience, 52, 225–233. https://doi.org/10.1641/0006-3568(2002)052[0225:BPACIT]2.0.CO;2.

Silva, S. de S., Azevedo, G.G., Silveira, O.T., 2011. Social wasps of two Cerrado localities in the northeast of Maranhão state, Brazil (Hymenoptera, Vespidae, Polistinae). Rev. Bras. entomol., 55, 597–602. http://dx.doi.org/10.1590/S0085-56262011000400017.

Silveira, E.M. de O., Silva, S.H.G., Acerbi-Junior, F.W., Carvalho, M.C., Carvalho, L.M.T., Scolforo, J.R.S., Wulder, M.A., 2019a. Object-based random forest modelling of aboveground forest biomass outperforms a pixel-based approach in a heterogeneous and mountain tropical environment. Int. J. Appl. Earth Obs. Geoinf., 78, 175–188. https://doi.org/10.1016/j.jag.2019.02.004.

Silveira, E.M. de O., Terra, M.C.N.S., Acerbi-Junior, F.W., Scolforo, J.R.S., 2019b. Estimating aboveground biomass loss from deforestation in the Savanna and Semi-arid biomes of Brazil between 2007 and 2017, in: Suratman, M.N., Latif, Z.A., Oliveira, G. de, Brunsell, N., Shimabukuro, Y., Santos, C.A.C. dos. (Eds.), Forest degradation around the world. IntechOpen, London, pp. 1–17. https://doi.org/10.5772/intechopen.85660.

Silveira, E.M. de O., Terra, M. de C.N.S., ter Steege, H., Maeda, E.E., Acerbi Júnior, F.W., Scolforo J.R.S., 2019c. Carbon-diversity hotspots and their owners in Brazilian southeastern Savanna, Atlantic Forest and Semi-Arid Woodland domains. For. Ecol. Manage., 45, 117575. https://doi.org/10.1016/j.foreco.2019.117575.

Silveira, E.M.O., Reis, A.A. dos, Terra, M.C.N.S., Withey, K.D., Mello, J.M. de, Acerbi-Júnior, F.W., Ferraz Filho, A.C., Mello, C.R., 2019d. Spatial distribution of wood volume in Brazilian

savannas. An. Acad. Bras. Ciênc., 91, e20180666. https://doi.org/10.1590/0001-3765201920180666.

Souza, A.A., Galvão, L.S., Santos, J.R., 2010. Relationships between Hyperion-derived vegetation indices, biophysical parameters, and elevation data in a Brazilian savannah environment. Remote Sens. Lett., 1, 55-64. https://doi.org/10.1080/01431160903329364.

Staver, A.C., Archibald, S., Levin, S.A., 2011. The global extent and determinants of savanna and forest as alternative biome states. Science, 334, 230-232. https://doi.org/10.1126/science.1210465.

Strassburg, B.B.N., Brooks, T., Feltran-Barbiere, R., Iribarrem, A., Crouzelles, R., Loyola, R., Latawiec, A.E., Oliveira Filho, F.J.B., Scaramuzza, C.A. de M., Scarano, F.R., Soares Filho, B., Balmfort, A., 2017. Moment of truth for the Cerrado hotspot. Nat. Ecol. Evol., 1, 0099. https://doi.org/10.1038/s41559-017-0099.

Stevens, N., Lehmann, C.E.R., Murphy, B.P., Durigan, G., 2017. Savanna woody encroachment is widespread across three continents. Global Change Biol., 23, 235-244. https://doi.org/10.1111/gcb.13409.

Sullivan, M.J.P., Lewis, S.L., Affun-Baffoe, K., Castilho, C., Costa, F., Sanchez, A.C., Ewango, C.E.N., Hubau, W., Marimon, B., Monteagudo-Mendonza, A., Qie, L., Sonké, B., Martinez, R.V., Baker, T.R., Brienen, R.J.W., Feldpausch, T.R., Galbraith, D., Gloor, M., Malhi, Y., Aiba, S-I., Alexiades, M.N., Almeida, E.C., Oliveira, E.A. de, Dávila, E.A., Loayza, P.A., Andrade, A., Vieira, S.A., Aragão, L.E.O.C., Araujo-Murakami, A., Arets, E.J.M.M., Arroyo, L., Ashton, P., Aymard C., G., Baccaro, F.B., Banin, L.F., Baraloto, C., Camargo, P.B., Barlow, J., Barroso, J., Bastin, J-F., Batterman, S.A., Beeckman, H., Begne, S.K., Bennett, A.C., Berenguer, E., Berry, N., Blanc, L., Boeckx, P., Bogaert, J., Bonal, D., Bongers, F., Brandfort, M., Brearley,

F.Q., Brncic, T., Brown, F., Burban, B., Camargo, J.L., Castro, W., Céron, C., Ribeiro, S.C., Moscoso, V.C., Chave, J., Chezeaux, E., Clark, C.J., Souza, F.C. de, Collins, M., Comiskey, J.A., Valverde, F.C., Medina, M.C., Costa, L. da, Dančák, M., Dargie, G.C., Davies, S., Cardozo, N.D., Haulleville, T. de, Medeiros, M.B. de, Pasquel, J. del A., Derroire, G., Di Fiore, A., Doucet, J-L., Dourdain, A., Droissart, V., Duque, L.F., Ekoungoulou, R., Elias, F., Erwin, T., Esquievel-Muelbert, A., Fauset, S., Ferreira, J., Llampazo, G.F., Foli, E., Ford, A., Gilpin, M., Hall, J.S., Hamer, K.C., Hamilton, A.C., Harris, D.J., Hart, T.D., Hédl, R., Herault, B., Herrera, R., Higuchi, N., Hladik, A., Coronado, E.H., Huamantupa-Chuquimaco, I., Huasco, W.H., Jeffery, K.J., Jimenez-Rojas, E., Kalamandeen, M., Djuikouo, M.N.K., Kearsley, E., Umetsu, R.K., Kho, L.K., Killeen, T., Kitayama, K., Klitgaard, B., Koch, A., Labrière, N., Laurence, W., Laurence, S., Leal, M.E., Levesley, A., Lima, A.J.N., Lisingo, J., Lopes, A.P., Lopez-Gonzalez, G., Lovejoy, T., Lovett, J.C., Lowe, R., Magnusson, W.E., Malumbres-Olarte, J., Manzatto, A.G., Marimon Junior, B.H., Marshall, A.R., Marthews, T., Reis, S.M. de A., Maycock, C., Melgaço, K., Mendonza, C., Metali, F., Mihindou, V., Milliken, W., Mitchard, E.T.A., Morandi, P.S., Mossman, H.L., Nagy, L., Nascimento, H., Neill, D., Nilus, R., Vargas, P.N., Palacios, W., Camacho, N.P., Peacock, J., Pendry, C., Mora, M.C.P., Pickavance, G.C., Pipoly, J., Pitman, N., Playfair, M., Pooter, L., Poulsen, J.R., Poulsen, A.D., Preziosi, R., Prieto, A., Primack, R.B., Ramírez-Angulo, H., Reitsma, J., Réjou-Méchain, M., Correa, Z.R., Sousa, T.R. de, Bayona, L.R., Roopsind, A., Rudas, A., Rutishauser, E., Salim, K.A., Salomão, R.P., Schietti, J., Sheil, D., Silva, R.C., Espejo, J. S., Valeria, C.S., Silveira, M., Simo-Droissart, M., Simon, M.F., Singh, J., Shareva, Y.C.S., Stahl, C., Stropp, J., Sukri, L., Sumderland, T., Svátek, M., Swaine, M.D., Swamy, V., Taedoumg, H., Talbot, J., Taplin, J., Taylor, D., ter Steege, H., Terborgh, J., Thomas, R., Thomas, S.T., Torres-Lezama, A., Umunay, P., Gamarra, L.V., van der Heijden, G., van der Hout, P., van der Meer, P., van Nieuwstadt, M., Verbeeck, H., Vernimmen, R., Vicentini, A., Vieira, I.C.G., Torre, E.V., Vleminckx, J., Vos, V., Wang, O.,

White, L.J.P., Willcock, E., Woods, J.T., Wortel, V., Young, K., Zagt, R., Zemagho, L., Zuidema, P.A., Zwerts, J.A., Phillips, O.L., 2020. Long-term thermal sensitivity of Earth's tropical forests. Science, 368, 869–874. https://doi.org/10.1126/science.aaw7578.

Sun, W., Shao, Q., Liu, J., 2013. Soil erosion and its response to the changes of precipitation and vegetation cover on the Loess Plateau. J. Geogr. Sci., 23, 1091–1106. https://doi.org/10.1007/s11442-013-1065-z.

Terra, M. de C.N.S., Santos, R.M. dos, Prado Júnior, J.A. do, Mello, J.M. de, Scolforo, J.R.S., Fontes, M.A.L., Schiavini, I., Reis, A.A. dos, Bueno, I.T., Magnago, L.F.S., ter Steege, I., 2018. Water availability drives gradients of tree diversity, structure and functional traits in the Atlantic-Cerrado-Caatinga transition, Brazil. J. Plant Ecol., 11, 803–814. https://doi.org/10.1093/jpe/rty017.

Terra, M. de C.N.S., Prado-Júnior, J.A. do, Souza, C.R. de, Pinto, L.O.R., Silveira, E.M. de O., Cordeiro, N.G., Cirne-Silva, T.M., Mantovani, V.A., Scolforo, J.R.S., Mello, J.M. de., 2021. Tree species dominance in neotropical savanna aboveground biomass and productivity. For. Ecol. Manage., 496, 119430. https://doi.org/10.1016/j.foreco.2021.119430.

Valadão, H., Hay, J.D.V., Tidon, R., 2010. Temporal dynamics and resource availability for drosophilid fruit flies (Insecta, Diptera) in a Gallery Forest in the Brazilian Savanna. Int. J. Ecol., 2010, 1–7. https://doi.org/10.1155/2010/152437.

Wakeling, J.L., Cramer, M.D., Bond, W.J., 2012. The savanna-grassland "treeline": why don't savanna trees occur in upland grasslands?. J. Ecol., 100, 381-391. https://doi.org/10.1111/j.1365-2745.2011.01921.x.

Wei, W., Feng, X., Yang, L., Chen, L., Feng, L., Chen, D., 2019. The effects of terracing and vegetation on soil moisture retention in a dry hilly catchment in China. Sci Total Environ., 647, 1323-1332. https://doi.org/10.1016/j.scitotenv.2018.08.037.

Wiegand, K., Saltz, D., Ward, D., 2006. A patch-dynamics approach to savanna dynamics and woody plant encroachment – Insights from an arid savanna. Perspect. Plant Ecol. Evol. Syst., 7, 229–242. https://doi.org/10.1016/j.ppees.2005.10.001.

Wu, H., Franklin, S.B., Liu, J., Lu, Z., 2017. Relative importance of density dependence and topography on tree mortality in a subtropical mountain forest. For. Ecol. Manage., 384, 169-179. http://dx.doi.org/10.1016/j.foreco.2016.10.049.

Zawawi, A.A., Shiba, M., Jemali, N.J.N., 2014. Landform classification for site evaluation and forest planning: Integration between scientific approach and traditional concept. Sains Malays., 43, 349-358.

Supplementary Information

Figure S1 - Distribution in classes of the Brazilian savanna demographic rates in Minas Gerais state, by using a histogram of frequency, to the data training and validation process.

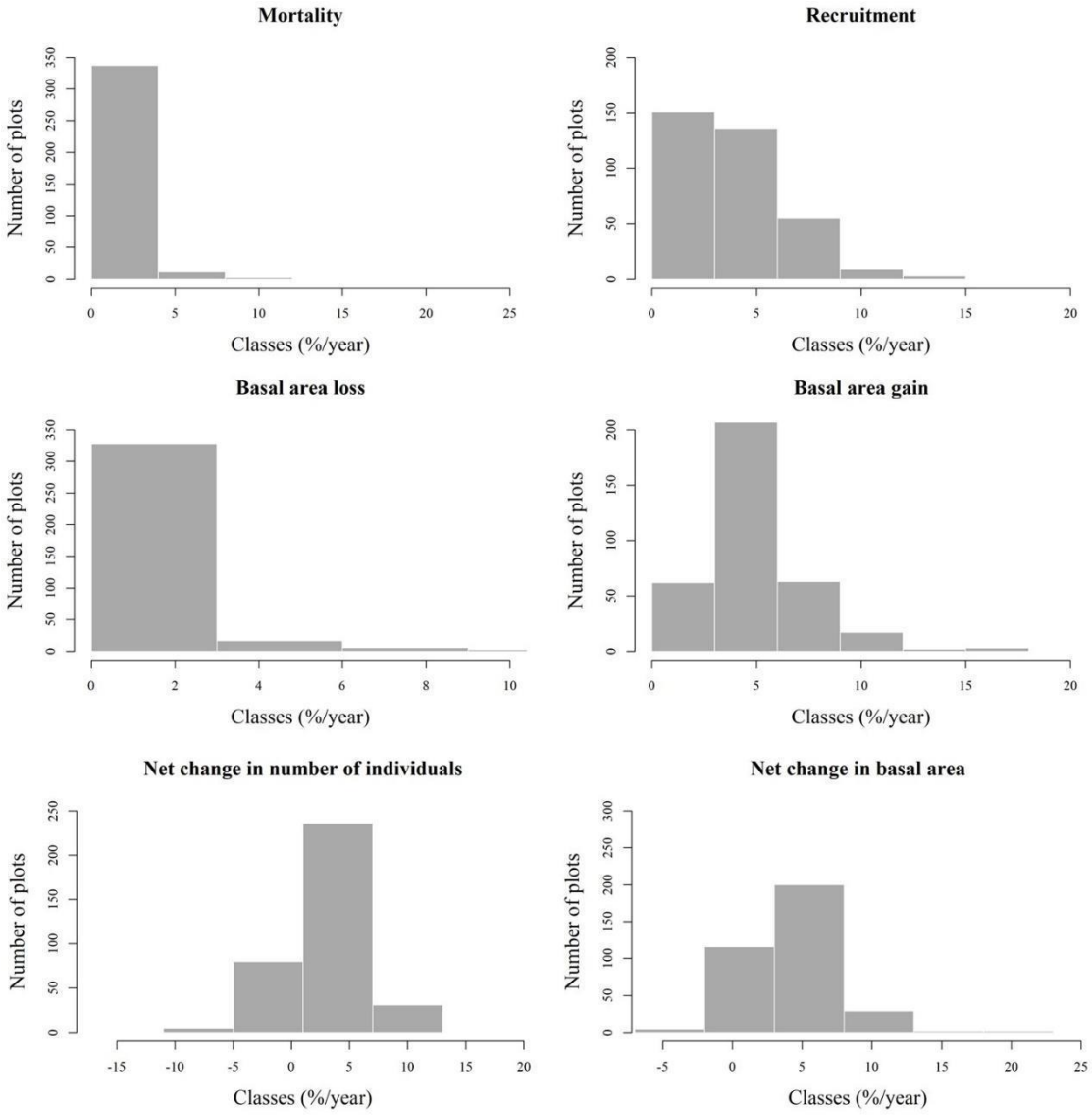

Figure S2 - Best *mtry* for the selection of predictor variables for demographic rates in Brazilian Savanna, Minas Gerais State, southeast of Brazil. In which: Mtry is the number of variables randomly sampled as candidates at each split; OOB is Out of Bag error, a minimization criterion.

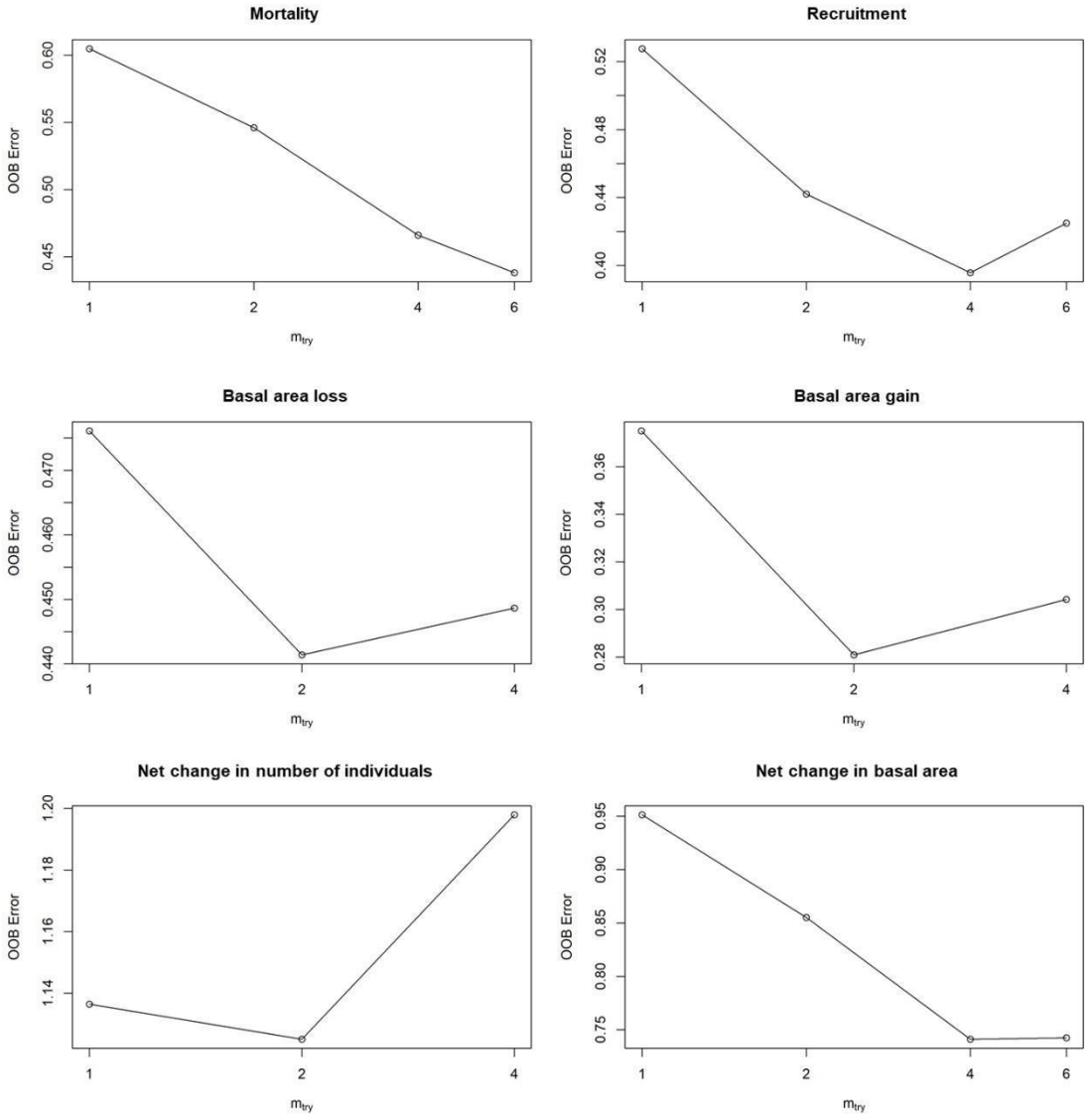

Figure S3 - Scatterplot of the observed and estimated values by the random forest model to the demographic rates in a Brazilian Savanna, Minas Gerais State, southeast of Brazil.

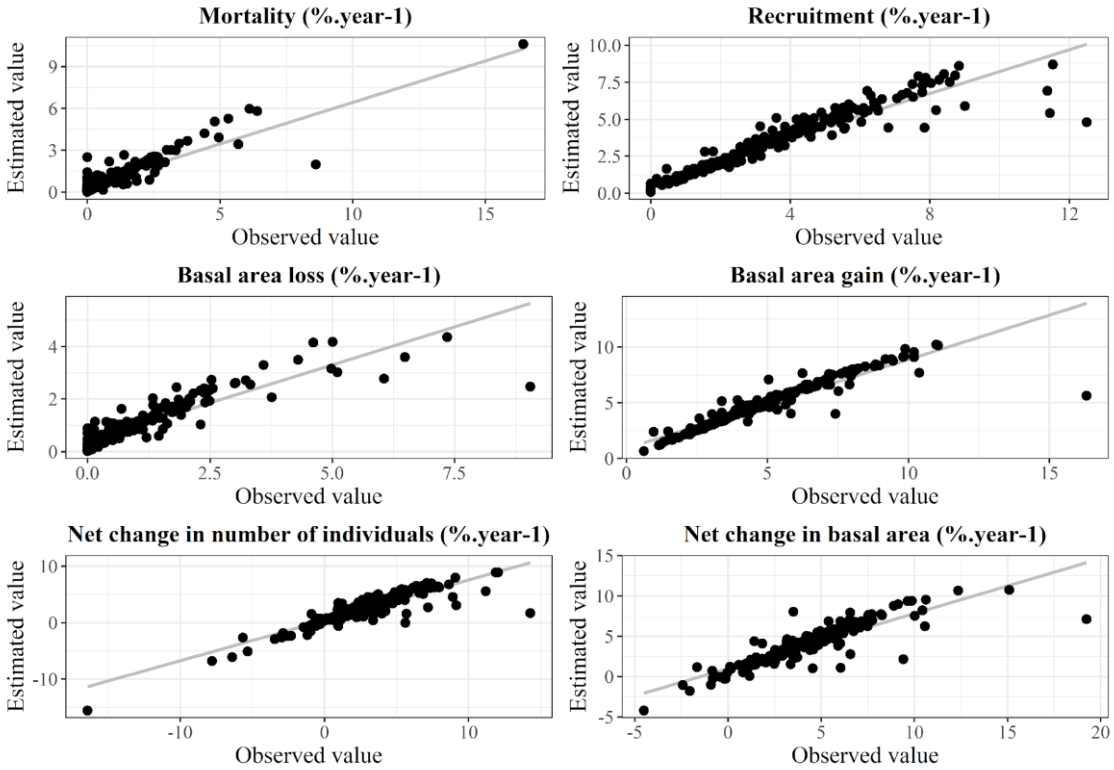

Figure S4 – Brazilian savanna vegetation type distribution in Minas Gerais State, southeast of Brazil. In which the number indicates the state region: 1 is Campo das Vertentes; 2 is Center Region; 3 is Jequitinhonha; 4 is Belo Horizonte metropolitan region; 5 is Northwest; 6 is North; 7 is West; 8 is South; 9 is Southwest; 10 is Mucuri Valley; 11 is Rio Doce Valley; 12 is Zona da Mata.

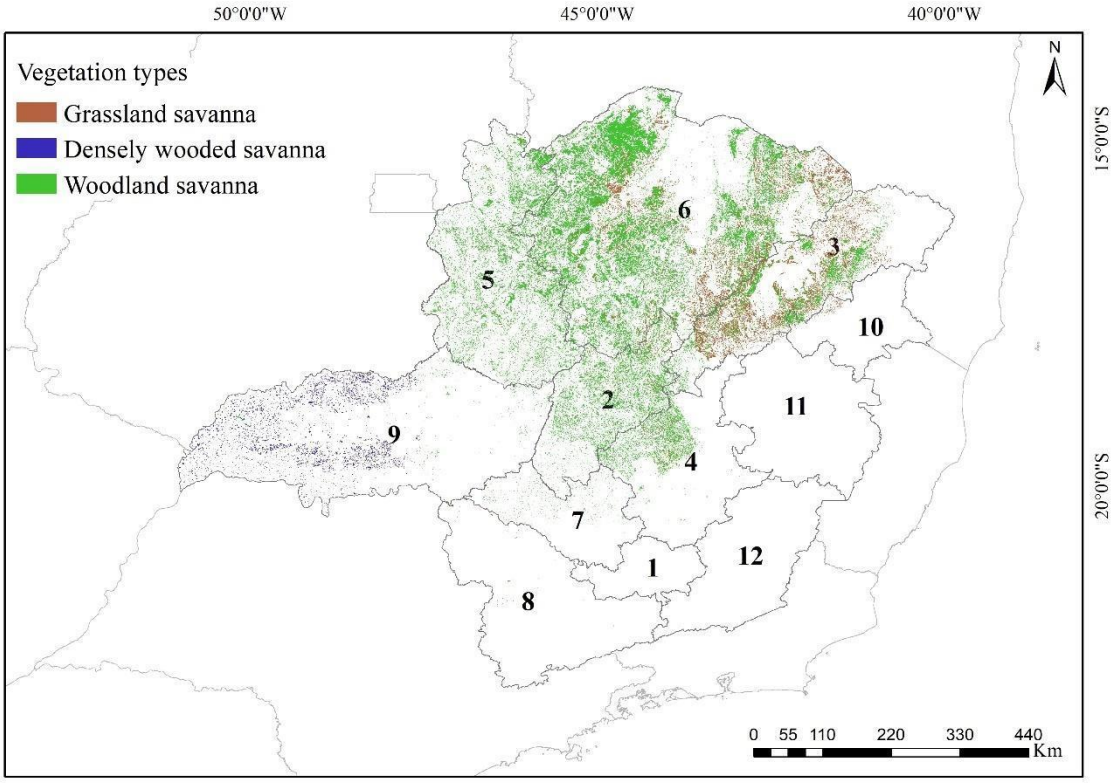

Figure S4: Map of the selected predictor variables of the vegetation dynamics rates in a Brazilian Savanna, Minas Gerais State, southeast of Brazil. In which: ASP is aspect; BIO15 is precipitation seasonality; CNBL is channel network base level; DEM is digital elevation model; HILS is analytical hillshade; LSF is LS factor; MRRTF is multiresolution index of ridge top flatness; Slope is the relative slope position; TWI is topographic wetness index; VD is valley depth; VDCN is vertical distance to channel network.

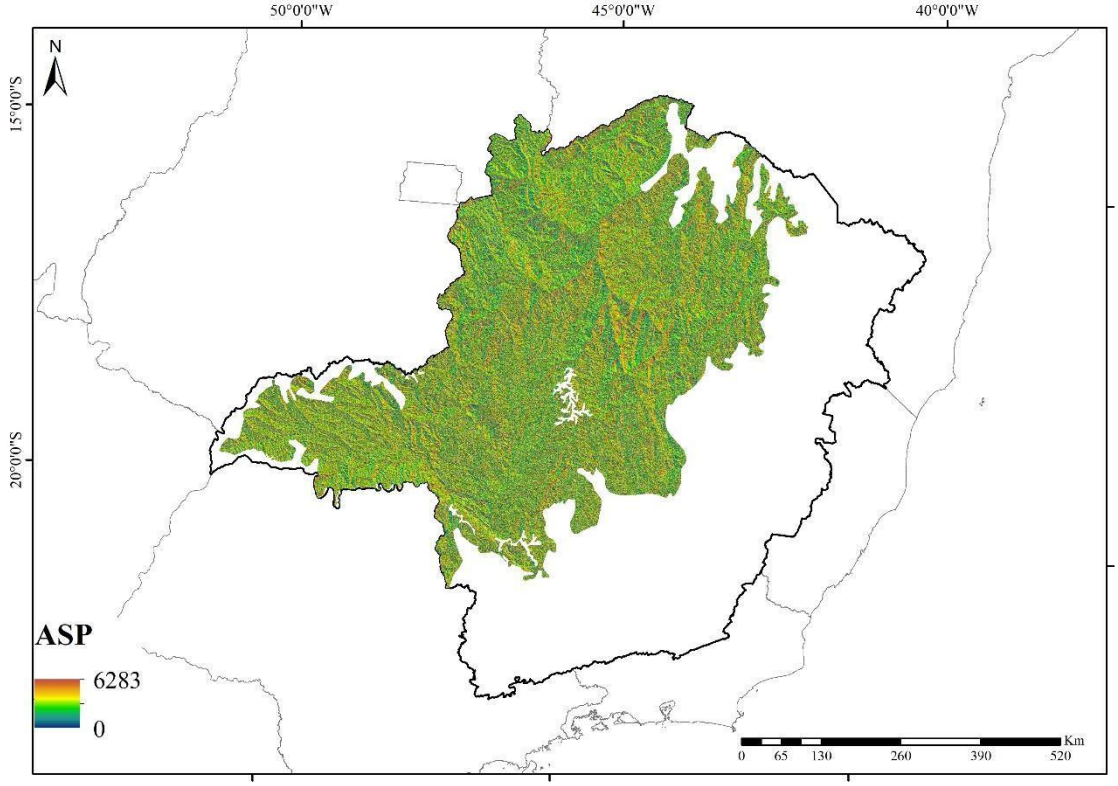

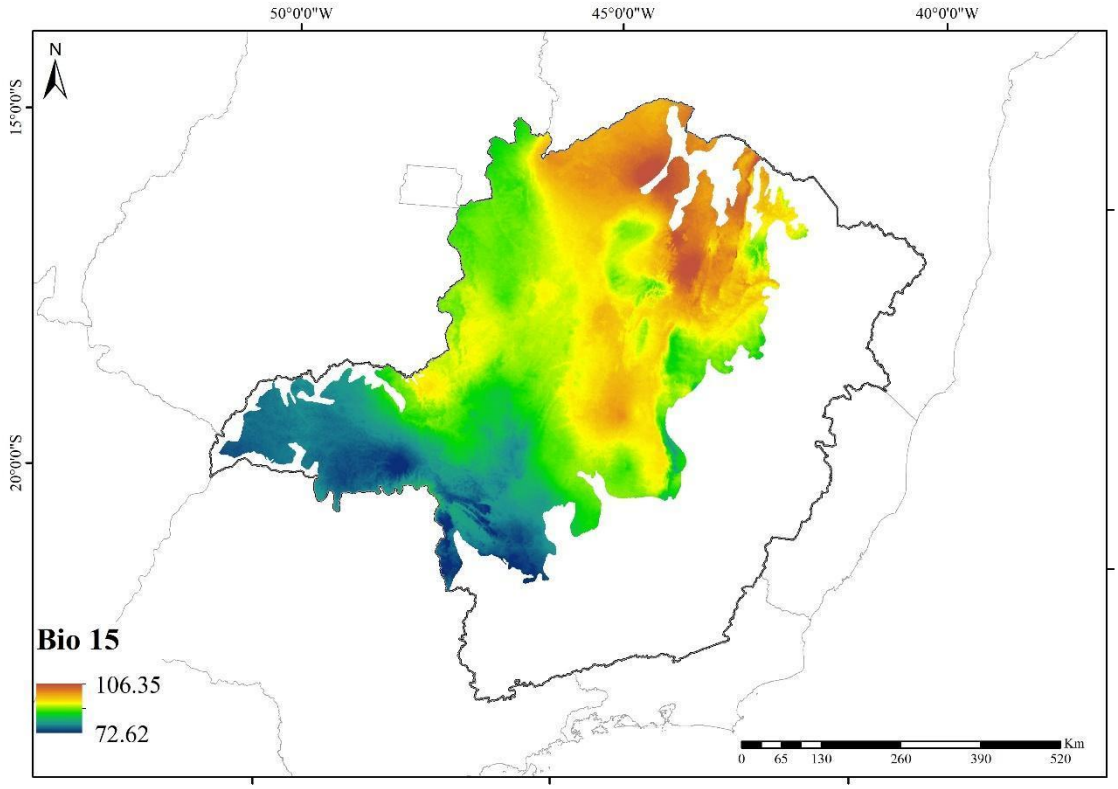
50°0'0"W
45°0'0"W
40°0'0"W
15°0'0"S
20°0'0"S
N
Bio 15
106.35
72.62
0 65 130 260 390 520
Km

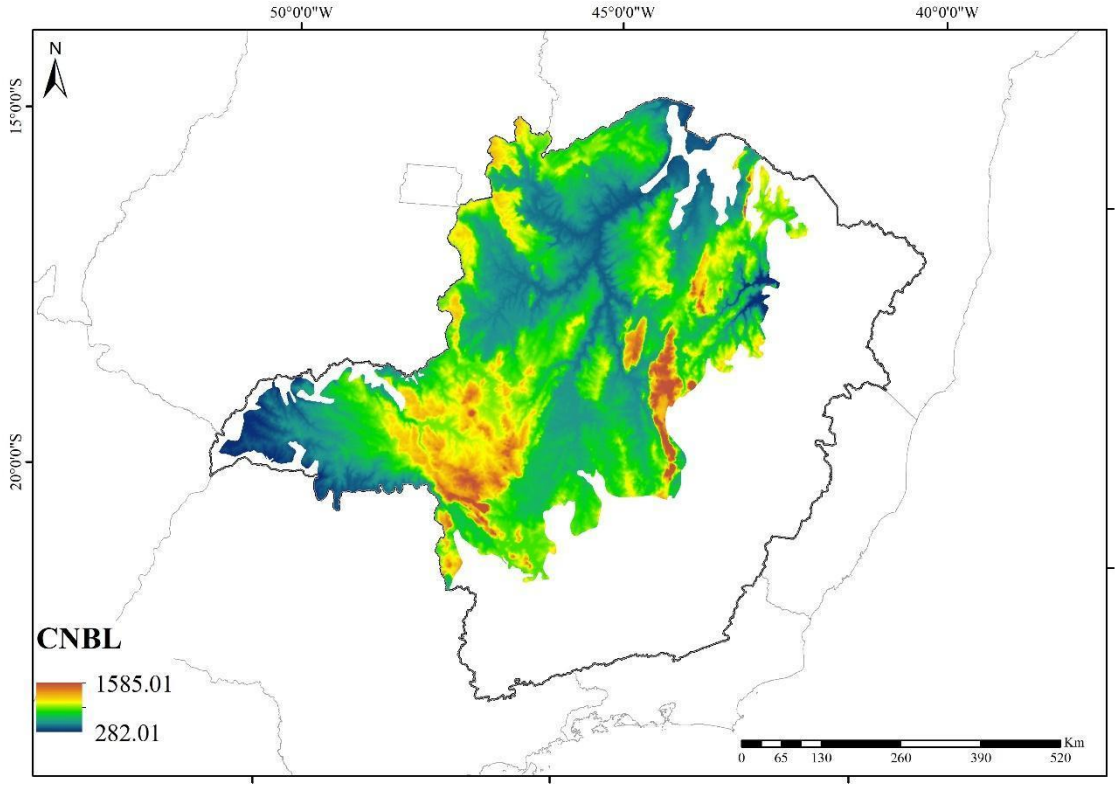
50°0'0"W
45°0'0"W
40°0'0"W
15°0'0"S
20°0'0"S
N
CNBL
1585.01
282.01
0 65 130 260 390 520
Km

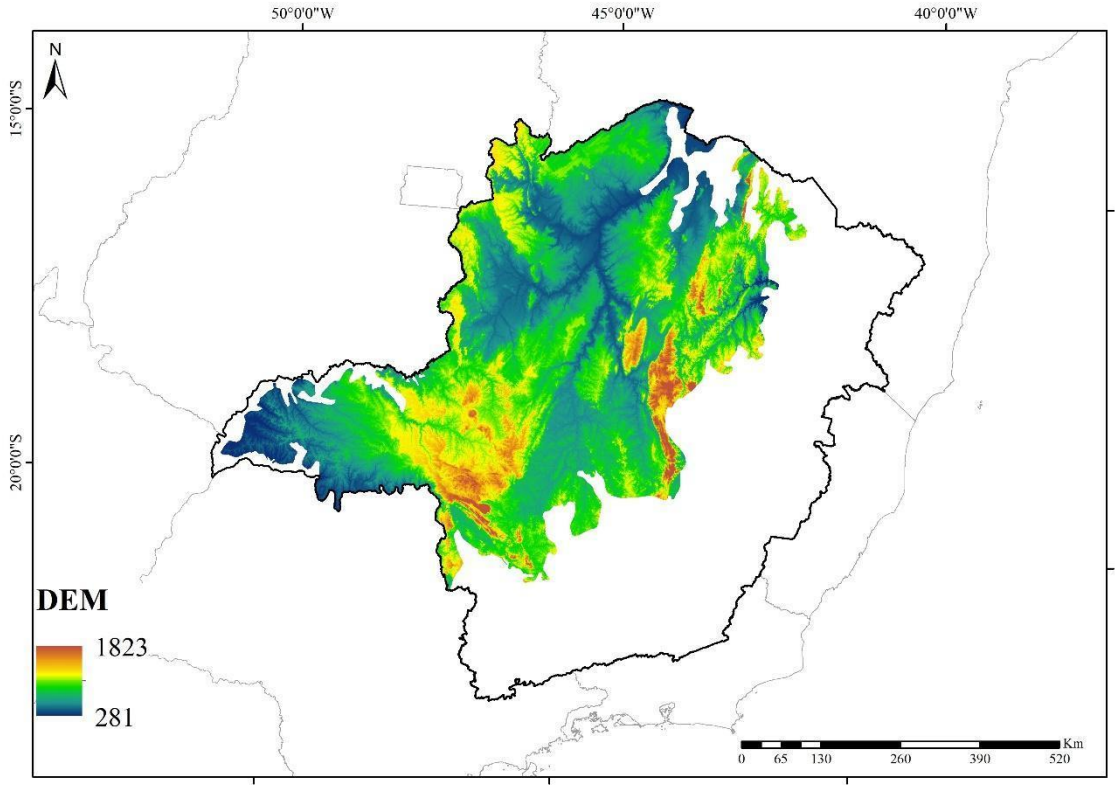
50°0'0"W
45°0'0"W
40°0'0"W
15°0'0"S
20°0'0"S
N
DEM
1823
281
0 65 130 260 390 520
Km

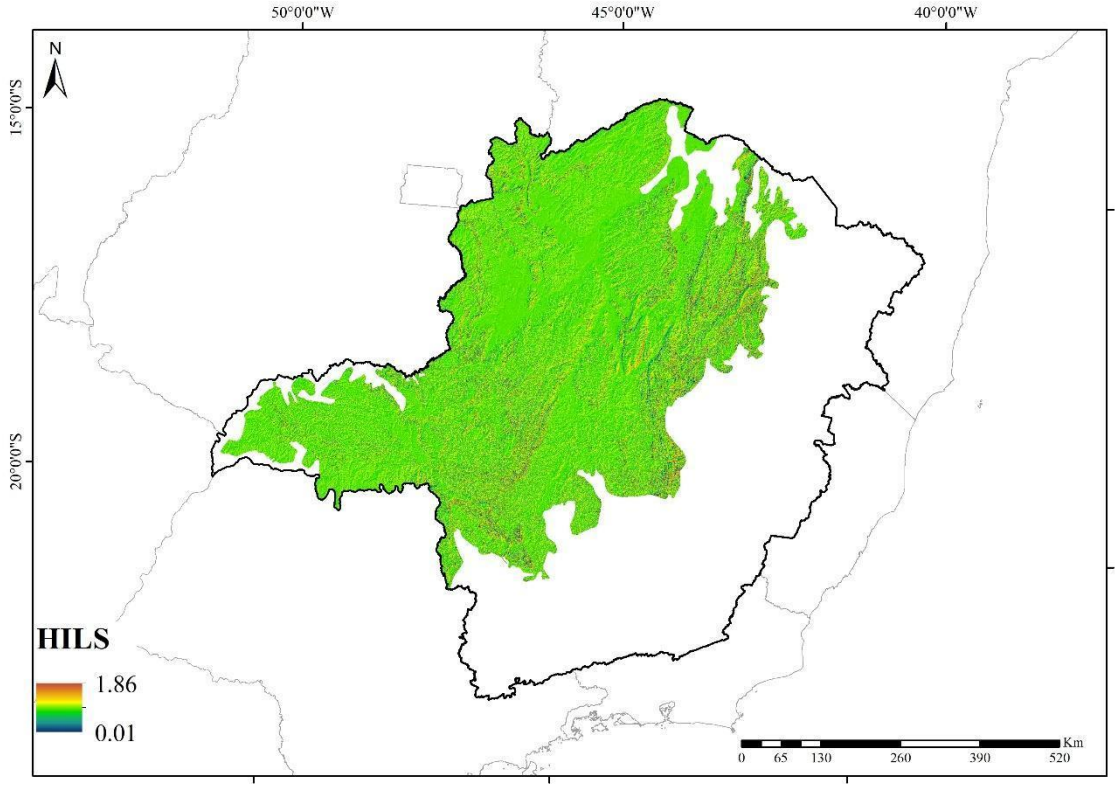
50°0'0"W
45°0'0"W
40°0'0"W
15°0'0"S
20°0'0"S
N
HILS
1.86
0.01
0 65 130 260 390 520
Km

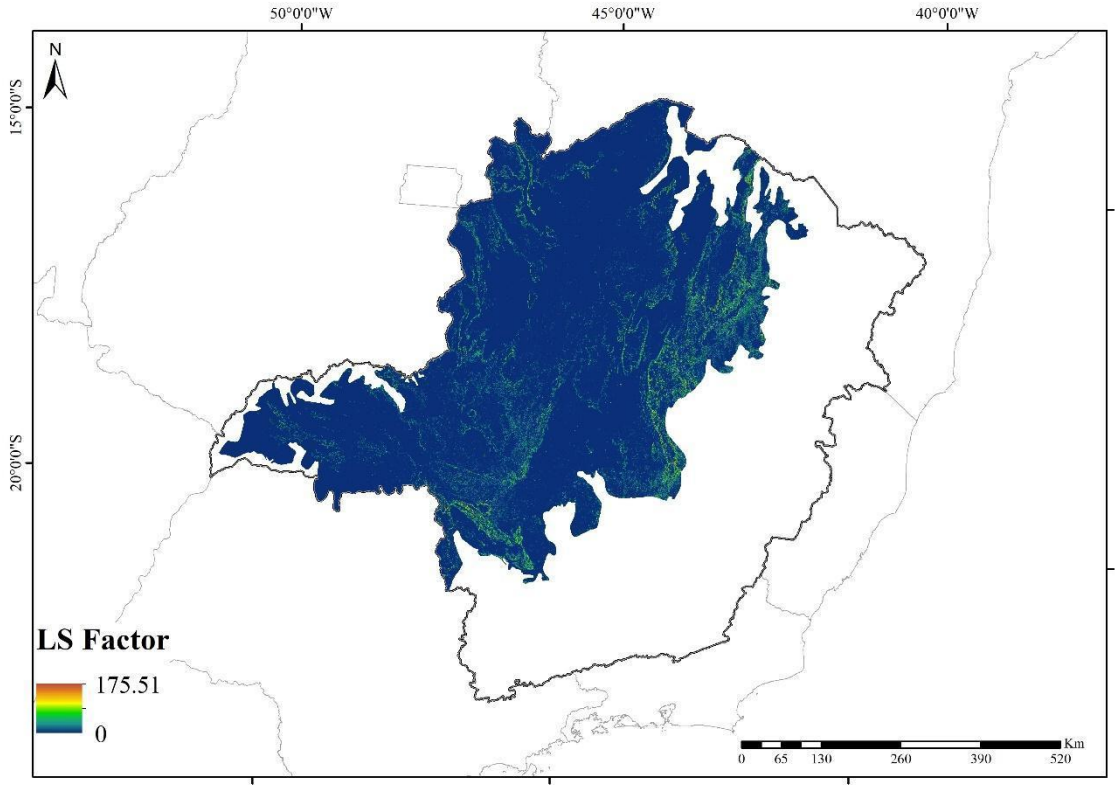
50°0'0"W
45°0'0"W
40°0'0"W
15°0'0"S
20°0'0"S
N
LS Factor
175.51
0
0 65 130 260 390 520
Km

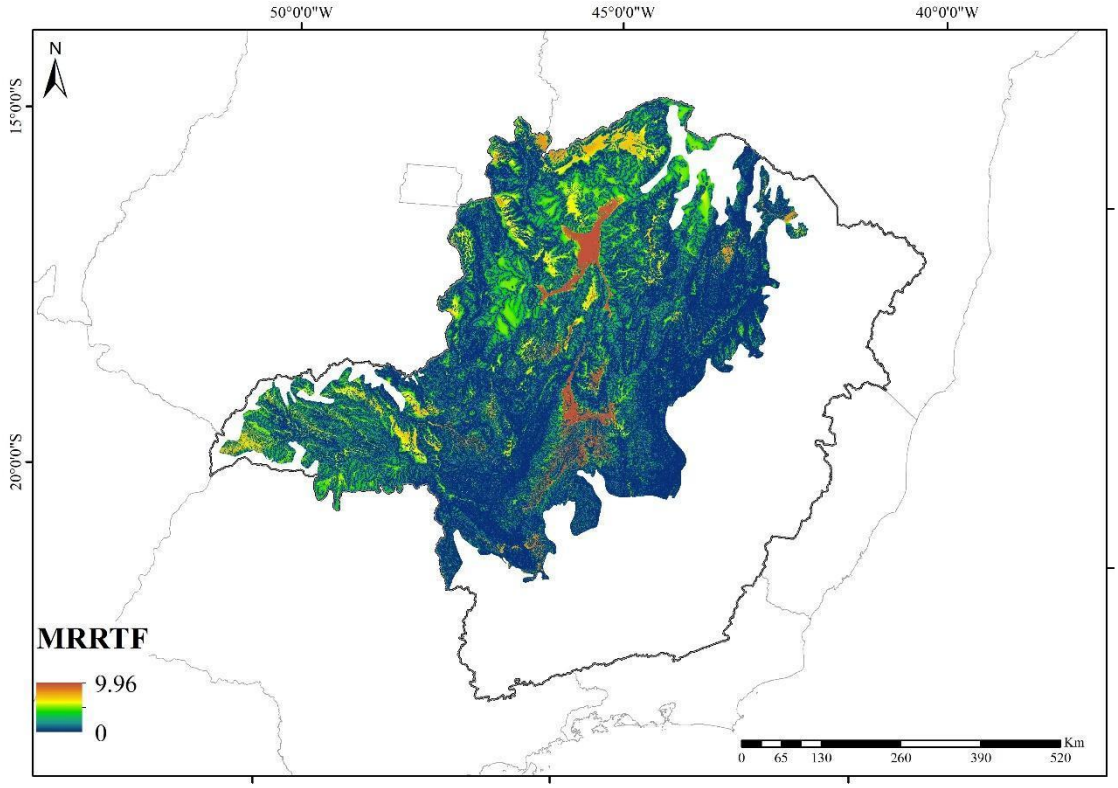
50°0'0"W
45°0'0"W
40°0'0"W
15°0'0"S
20°0'0"S
N
MRRTF
9.96
0
0 65 130 260 390 520
Km

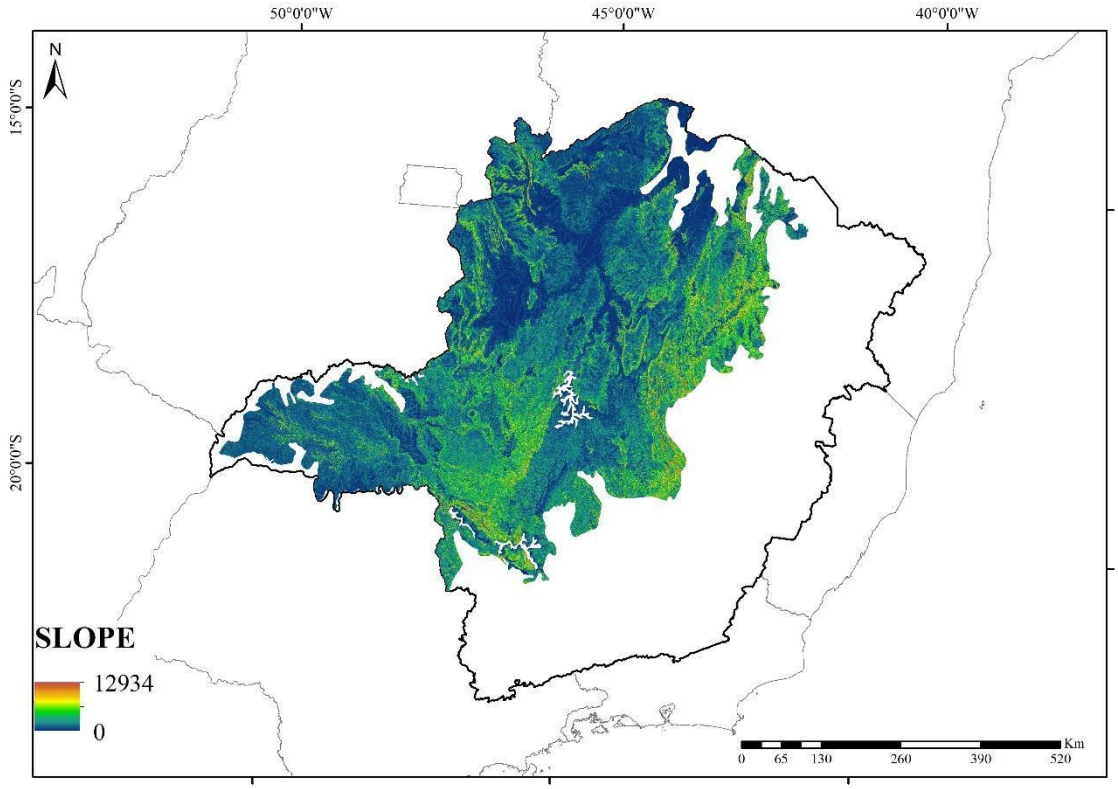
50°0'0"W
45°0'0"W
40°0'0"W
15°0'0"S
20°0'0"S
N
SLOPE
12934
0
0 65 130 260 390 520
Km

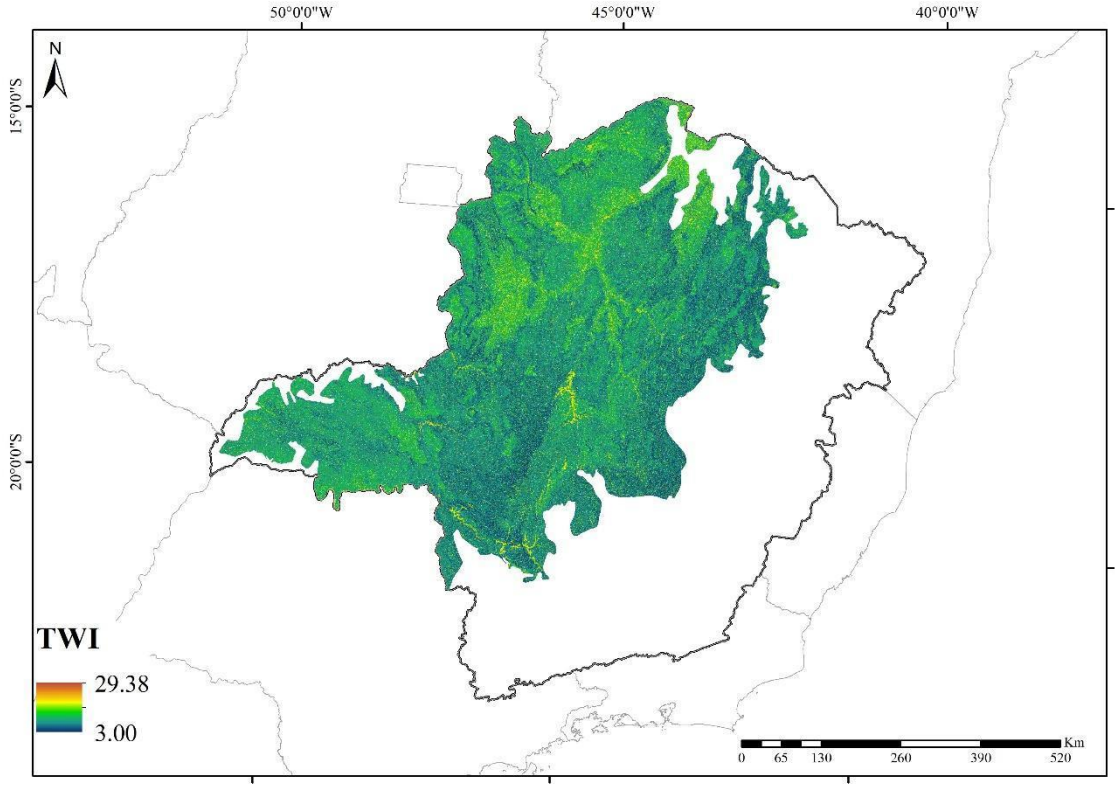
50°0'0"W
45°0'0"W
40°0'0"W
15°0'0"S
20°0'0"S
N
TWI
29.38
3.00
0 65 130 260 390 520
Km

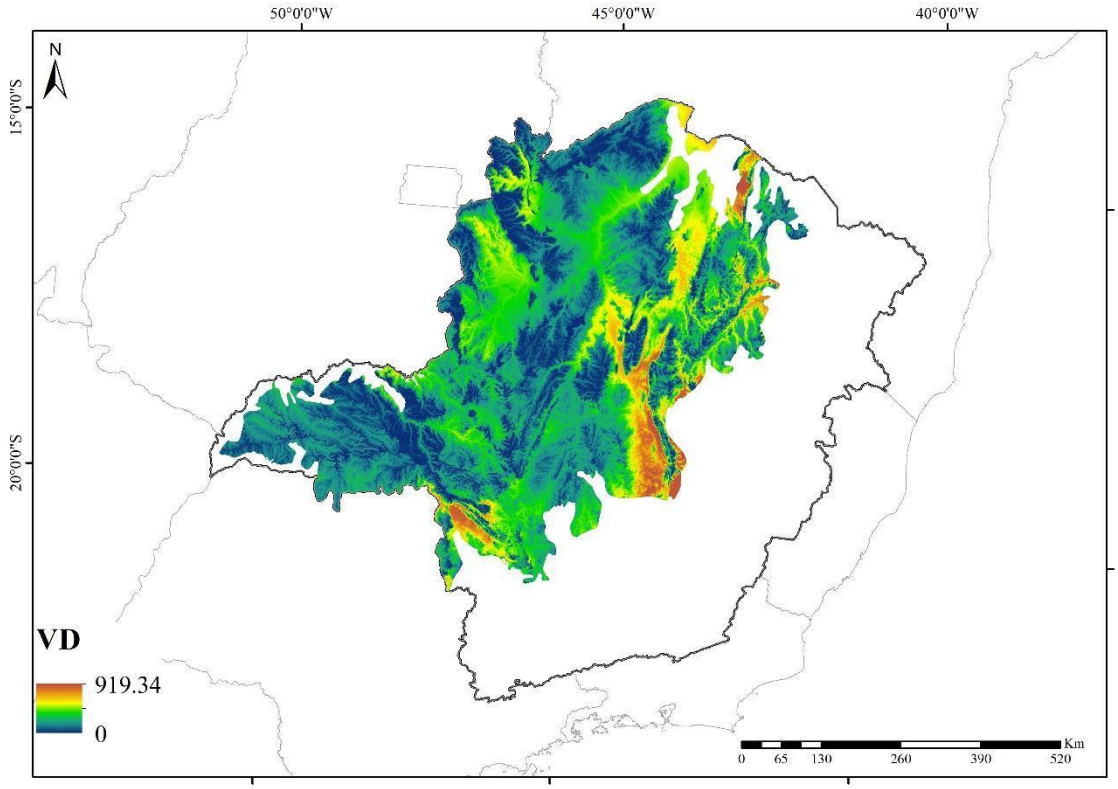
50°0'0"W
45°0'0"W
40°0'0"W
15°0'0"S
20°0'0"S
N
VD
919.34
0
0 65 130 260 390 520
Km

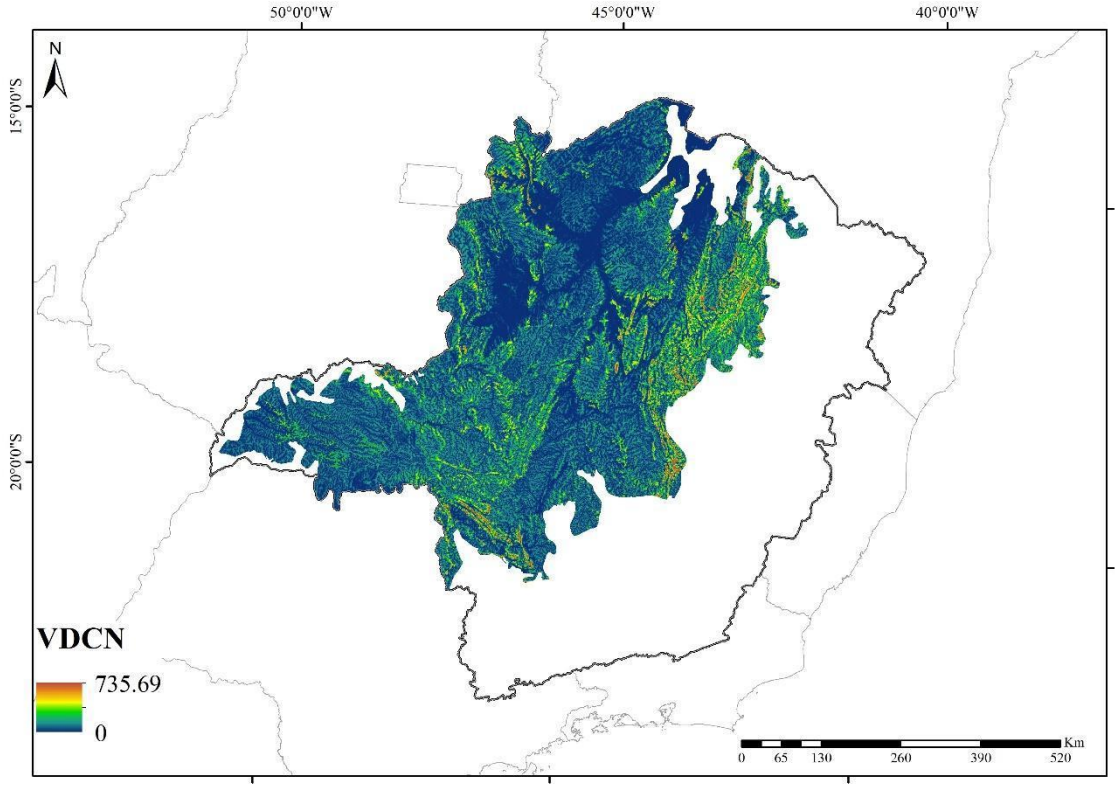
50°0'0"W
45°0'0"W
40°0'0"W
15°0'0"S
20°0'0"S
N
VDCN
735.69
0
0 65 130 260 390 520
Km

Table S1 - Distribution of the Brazilian savanna study area in Minas Gerais State, southeast of Brazil, considering the number of plots for fragment and physiognomy.

Fragment	Number of plots	Physiognomy
13	35	Woodland Savanna
21	7	Woodland Savanna
34	8	Woodland Savanna
38	34	Grassland Savanna
47	16	Woodland Savanna
56	38	Grassland Savanna
72	36	Woodland Savanna
73	12	Woodland Savanna
75	24	Woodland Savanna
86	30	Grassland Savanna
89	17	Woodland Savanna
94	12	Woodland Savanna
96	20	Woodland Savanna
103	20	Densely Wooded Savanna
104	14	Woodland Savanna
106	16	Densely Wooded Savanna
107	15	Densely Wooded Savanna

Table S2 – Date of first and second measurement of the Brazilian savanna study area in Minas Gerais State, southeast of Brazil. In which: t is the interval between the measurements.

Fragment	First measurement	Second measurement	t
13	18/01/2006	19/09/2010	4.74
21	11/08/2006	26/05/2010	3.84
34	24/10/2005	18/03/2010	4.46
38	31/08/2005	07/07/2010	4.92
47	23/05/2006	07/10/2010	4.44
56	24/08/2005	28/08/2010	5.08
72	27/06/2005	26/03/2010	4.81
73	17/06/2005	06/04/2010	4.87
75	16/06/2005	15/04/2010	4.90
86	04/05/2006	25/06/2010	4.20
89	08/06/2005	05/05/2010	4.98
94	03/08/2006	20/07/2010	4.02
96	13/07/2006	21/07/2010	4.08
103	31/05/2006	30/03/2011	4.90
104	20/07/2006	18/02/2011	4.65
106	09/09/2006	25/03/2011	4.61
107	12/09/2006	03/02/2011	4.46

Table S3 - Average demographic rates considering each sampled area of the Brazilian savanna in southeast of Brazil. In which: M is mortality; R is recruitment; L is basal area loss; G is basal area gain; ChN is net change in number of individuals; ChBA is net change in basal area.

Fragment	M	R	L	G	ChN	ChBA
13	0.9554	2.0686	1.0280	3.9093	1.1574	3.0073
21	1.6986	5.0700	2.3134	5.2732	3.5786	3.1382
34	0.2263	3.1363	0.1297	4.0944	3.0400	4.1557
38	2.3068	5.8738	2.2652	7.7097	3.8482	6.0344
47	1.2013	4.3494	1.4936	5.2394	3.3075	3.9633
56	1.2858	7.4487	0.9540	8.0516	6.7221	7.8008
72	0.7556	3.2436	0.8310	3.2823	2.6031	2.5477
73	0.7900	4.6908	1.0523	6.0951	4.1292	5.3974
75	0.7625	3.1488	0.7628	4.1332	2.5113	3.5384
86	0.3610	3.9580	0.3713	4.2311	3.7853	4.0531
89	1.3382	1.8594	1.0677	2.4184	0.5476	1.3942
94	2.0708	4.1333	1.0284	4.7997	2.2508	3.9939
96	2.5265	2.3280	1.9893	3.4335	-0.1510	1.5227
103	0.1540	2.3165	0.0930	5.7273	2.2220	6.0042
104	4.3900	4.6407	1.8549	5.5604	0.2543	3.9368
106	0.1925	2.7663	0.1310	3.9652	2.6588	4.0020
107	1.5753	2.1920	0.9236	4.3550	0.6433	3.5996

Table S4 - Vegetation dynamics rates and terrain, soil and climate variables to the Brazilian Savanna in Minas Gerais state, southeast of Brazil. In which: M is mortality (%.year^{-1}); R is recruitment (%.year^{-1}); ChN is net change in number of individuals (%.year^{-1}); L is Basal area loss (%.year^{-1}); G is basal area gain (%.year^{-1}); ChBA is net change in basal area (%.year^{-1}); BIO1 is annual mean temperature; BIO4 is temperature seasonality; BIO12 is annual precipitation; BIO15 is precipitation seasonality; LSF is LS factor; MRRTF is multiresolution index of ridge top flatness; MRVBF is multiresolution index of valley bottom flatness; TPI is topographic position index; TWI is topographic wetness index; VD is valley depth; VDCN is vertical distance to channel network; CNBL is channel network base level; HILS is analytical hillshade; ASP is aspect; DEM is digital elevation model; SAND is topsoil sand fraction; SILT is topsoil silt fraction; CLAY is topsoil clay fraction; PH_H2O is topsoil PH (H_20) - the measurement of the acidity and alkalinity of the soil; CEC_SOIL is cation exchange capacity in the topsoil; BS is topsoil base saturation; TEB is total exchangeable bases in the topsoil.

Fragment	M	R	ChN	L	G	ChBA	bio1	bio4	bio12	bio15	LSF	MRRTF	MRVBF	TPI
F13P1	0.57	1.12	0.56	0.1586	3.8365	3.8247	207	192.97	1087	88.18	0.125644	0.119074	1.85895	-0.4
F13P2	0.64	1.25	0.62	0.735	3.6438	3.0188	207	192.97	1087	88.18	0.902203	0.180588	1.80462	-1.2
F13P3	1.04	0.78	-0.26	0.3703	3.799	3.5641	207	192.97	1087	88.18	1.0022	0.09284	1.75829	-5.4
F13P4	1.27	0.19	-1.09	1.1691	3.9096	2.8519	207	192.85	1079	88.39	0.722024	0.359661	1.34062	0.2
F13P5	1.26	1.46	0.2	0.808	3.319	2.5973	207	192.25	1079	87.98	0.389421	1.04716	0.907805	2
F13P6	1.55	1.39	-0.17	1.0926	4.8815	3.9834	210	192.25	1071	87.98	1.02701	0.20764	0.728131	-2.2
F13P7	0.43	3.84	3.55	1.1336	4.3554	3.3686	206	192.46	1095	87.5	0.258143	4.34794	1.7869	-0.8

F13P8	0.98	3.2	2.3	1.3899	4.361	3.1066	206	193.16	1095	87.79	0.116036	2.60251	1.71877	0
F13P9	1.23	3.98	2.86	1.3753	3.7339	2.4502	207	192.97	1087	88.18	0.135691	2.2881	0.673137	1
F13P10	0	6.18	6.58	0	5.0634	5.3334	207	192.97	1087	88.18	0.331975	2.40174	1.17853	-1.2
F13P11	0.88	2.52	1.68	0.9198	5.2275	4.5453	207	192.97	1087	88.18	0.277578	1.97504	1.22052	0.2
F13P12	1.12	0.85	-0.28	1.4553	4.5781	3.2726	207	191.76	1087	88.16	0.08587	2.48357	1.22516	2
F13P13	0	2.25	2.3	0.503	3.9959	3.6382	210	192.25	1071	87.98	0.551396	1.2934	0.908299	-0.6
F13P14	0.66	1.45	0.8	0.7948	4.6444	4.0371	210	192.25	1071	87.98	0.313105	1.64172	0.532276	-0.4
F13P15	0.52	0.17	-0.35	0.445	4.3056	4.0342	210	191.8	1071	88.13	0.400667	1.79312	0.164672	2.2
F13P16	2.45	3.56	1.15	2.9771	4.0624	1.1313	206	192.46	1095	87.5	0.594849	0.21899	1.67224	0
F13P17	0	1.24	1.26	0.4654	3.0089	2.6224	206	194.11	1093	88.07	0.341463	1.27524	1.07448	0.6
F13P18	0.33	0.33	0	0.4161	2.2871	1.9148	206	194.11	1093	88.07	0.211127	1.83321	0.332832	1
F13P19	1.35	0.46	-0.89	1.2054	2.5878	1.4191	207	192.97	1087	88.18	0.28502	2.62638	0.312321	0.6
F13P20	0.29	2.92	2.71	0.5143	4.7176	4.4113	207	191.76	1087	88.16	0.246648	2.72864	0.240407	-0.8
F13P21	1.19	0.52	-0.67	0.6699	3.4834	2.915	208	191.76	1081	88.16	0.132076	2.83256	0.141474	0.6
F13P22	0.48	0.71	0.24	0.0754	3.0964	3.1176	208	191.76	1081	88.16	0.598121	1.6131	0.502743	-1.2
F13P23	0.5	2.81	2.37	0.4906	5.0757	4.8302	210	192.68	1071	88.22	0.790116	0.98912	0.360003	0.4
F13P24	1.5	1.06	-0.44	2.3135	4.0814	1.8431	210	191.8	1071	88.13	1.48045	0.179009	0.632213	0.4
F13P26	0.64	2.13	1.53	0.646	5.6629	5.3181	206	194.11	1093	88.07	2.57395	0.054498	0.606523	1.6
F13P27	0	0.53	0.53	0	2.9389	3.0279	206	194.11	1093	88.07	1.63024	0.075806	0.635988	2.2

F13P28	0.32	2.38	2.12	4.2098	2.7142	-1.5373	206	194.11	1093	88.07	0.93037	0.368085	0.510029	0
F13P29	1.08	4.53	3.62	0.7174	3.63	3.0223	208	193.37	1081	88.26	0.593214	1.64837	0.376864	1.2
F13P30	0.47	1.6	1.15	0.3082	3.0423	2.82	208	191.76	1081	88.16	0.311999	1.76717	0.601098	-0.8
F13P31	2.92	5.41	2.63	2.3776	4.7868	2.5303	208	191.76	1081	88.16	0.503958	1.22442	0.551553	1
F13P32	0.63	0.51	-0.13	0.8222	3.0679	2.3168	208	192.68	1081	88.22	2.04975	0.084336	0.544216	0.8
F13P33	1.69	2.37	0.69	0.9148	2.2111	1.3257	208	193.37	1083	88.26	1.99181	0.002899	2.44207	-4.6
F13P34	1.13	2.45	1.35	0.5391	2.3982	1.9048	208	193.37	1083	88.26	1.58579	0.108043	0.777043	-0.6
F13P35	1.97	3.09	1.16	2.4125	5.2273	2.97	208	193.37	1081	88.26	0.73677	1.43738	0.435607	-1.4
F13P36	2.35	3.16	0.83	1.5542	5.0889	3.7242	208	192.68	1081	88.22	1.44561	0.051233	0.804475	-1.6
F21P1	2.61	7.85	5.69	1.8203	7.418	6.0461	208	177.01	901	90.12	0.0548	3.9769	0.0432	1.2000
F21P3	1.57	4.59	3.17	1.5429	5.8481	4.5725	208	176.2	900	89.76	0.0000	2.9801	1.5114	0.0000
F21P6	1.81	5.57	3.99	1.3419	4.5973	3.4123	208	175.15	901	90.19	0.0000	3.9855	1.8799	-0.6000
F21P7	1.55	2.99	1.48	0.8947	4.3408	3.6024	208	176.2	901	89.76	0.0222	3.0570	0.3394	-0.4000
F21P10	0.54	6.45	6.32	5.5677	5.3249	-0.2564	208	175.3	901	89.72	0.2825	3.9837	1.6072	1.4000
F21P11	2.52	3.83	1.36	4.2525	4.2869	0.036	208	178.01	901	90.13	0.1009	2.9866	0.6955	-1.6000
F21P15	1.29	4.21	3.04	0.7738	5.0965	4.5548	208	178.01	900	90.13	0.3156	2.9874	1.3112	-1.6000
F34P1	0	6.47	6.92	0	5.0836	5.3559	219	204.03	1310	89.12	0.488715	2.35538	1.42665	-1
F34P2	0.21	3.49	3.39	0.0645	4.9691	5.1611	218	204.03	1319	89.12	0.947461	0.669689	0.28408	1.6
F34P3	0	3.84	4	0	4.3997	4.6022	219	205.92	1310	88.66	0.042597	3.87599	3.4524	-1.4

F34P4	0	2.65	2.72	0	4.6091	4.8318	218	205.92	1319	88.66	0.465679	2.76992	1.47704	-0.8
F34P5	0.6	1.55	0.97	0.4932	3.9432	3.5916	219	205.92	1310	88.66	0.312668	3.55694	0.299096	1.6
F34P6	0.82	3.23	2.49	0.4118	3.1333	2.8095	219	205.92	1310	88.66	0.317183	2.49404	1.74476	0.6
F34P7	0.18	3.86	3.83	0.068	5.6508	5.9172	219	205.99	1310	89.16	0.312513	2.75378	0.389612	0.8
F34P8	0	0	0	0	0.9667	0.9762	219	205.92	1310	88.66	0.730376	0.039764	1.88714	-1
F38P1	2.54	5.94	3.61	9.0489	7.523	-1.65	231	196.67	1276	89.05	0.4134	9.1775	6.9498	0.4000
F38P3	0.64	7.29	7.18	2.1635	3.9266	1.8351	233	196.67	1269	89.05	0.6260	0.0812	1.9501	-0.6000
F38P4	0.88	5.47	4.86	1.3912	5.6184	4.4788	231	196.67	1276	89.05	0.6205	8.6261	6.9272	0.0000
F38P6	3.51	3.67	0.17	2.0152	6.8163	5.1523	231	196.61	1276	88.96	1.0039	3.6863	6.7526	-2.0000
F38P9	2.12	7.68	6.02	1.0764	7.5355	6.9855	233	198.23	1273	89.41	1.6581	0.0043	1.4836	-2.6000
F38P10	1.42	6.49	5.42	3.937	8.7427	5.2661	231	196.61	1281	88.96	0.1406	3.3329	6.6670	0.8000
F38P11	1.83	4.25	2.52	1.4533	12.3894	12.4826	231	196.61	1281	88.96	0.7689	1.7141	0.0695	1.2000
F38P12	0.59	4.66	4.27	0.5721	11.0093	11.7284	233	196.61	1273	88.96	0.2162	1.9524	1.5116	2.8000
F38P13	1.49	2.87	1.41	1.4617	5.6205	4.4064	233	198.23	1273	89.41	0.2157	1.9807	6.5120	3.4000
F38P14	1.96	6.04	4.34	6.5594	6.1786	-0.4058	231	196.61	1281	88.96	0.8203	2.5686	3.6508	-0.4000
F38P15	1.98	1.77	-0.21	2.1303	3.0207	0.9182	231	196.61	1281	88.96	1.2151	0.2295	0.5762	-2.4000
F38P18	0.83	5.68	5.15	0.217	8.7959	9.4062	231	196.96	1281	88.99	1.0006	3.4107	6.3627	-0.8000
F38P19	0.9	9.01	8.91	0.9191	10.3902	10.5693	231	196.96	1281	88.99	0.6596	0.0071	1.9441	-2.4000
F38P20	0.4	3.31	3.01	0.0538	7.8241	8.4299	231	196.96	1281	88.99	0.6790	1.5091	3.4215	1.6000

F38P22	1.39	5.33	4.16	0.621	5.7137	5.4013	231	196.96	1283	88.99	1.1587	0.0243	1.8290	0.0000
F38P23	2.68	4.98	2.42	1.2782	15.0217	16.1729	233	196.96	1279	88.99	1.0186	0.4182	0.4300	1.4000
F38P25	0	8.59	9.4	0	16.9837	20.4583	231	196.96	1283	88.99	0.9629	0.0322	1.4370	-4.0000
F38P26	9.86	7.2	-2.87	3.6155	5.3163	1.7963	233	196.96	1279	88.99	0.2749	1.7673	1.8570	2.8000
F38P27	1.55	4.28	2.85	2.0816	8.049	6.4898	233	198.38	1279	89.4	0.5143	1.9451	5.5733	1.2000
F38P28	2.53	6.45	4.19	1.7342	7.7804	6.5564	231	196.96	1283	88.99	0.7294	1.0738	0.1629	-0.6000
F38P30	4.2	5.11	0.95	1.2092	5.9928	5.0885	231	197.4	1283	89.14	1.2083	0.0150	1.4537	-2.4000
F38P31	2.37	5.56	3.38	4.0556	8.0132	4.3024	231	196.79	1283	88.83	1.7919	0.0321	0.9126	-1.8000
F38P33	1.83	4.98	3.31	5.0116	7.9804	3.2263	231	197.4	1283	89.14	0.5111	0.0880	2.0974	-1.2000
F38P34	1.2	8.04	7.43	1.3385	8.2257	7.5045	231	196.79	1283	88.83	0.7549	3.7125	6.3928	0.8000
F38P36	1.09	5.68	4.86	2.5349	5.2851	2.9036	230	197.4	1295	89.14	0.5472	0.0171	2.6016	-0.8000
F38P37	3.38	6.89	3.78	1.8632	10.2032	9.2876	230	196.79	1295	88.83	0.9416	0.2040	0.7021	-1.4000
F38P38	1.71	3.26	1.6	2.4317	5.2996	3.0284	230	197.4	1295	89.14	0.6240	0.4457	2.1243	-0.6000
F38P39	2.48	4.47	2.09	2.4913	6.405	4.1815	230	197.4	1295	89.14	0.4954	0.1369	1.9323	2.8000
F38P40	1.01	3.01	2.06	0.3835	4.4203	4.2235	230	197.36	1295	88.9	1.2945	0.4255	0.4525	0.0000
F38P42	3.34	11.44	9.15	0.5759	6.2471	6.0492	232	197.36	1287	89.14	1.7916	0.1064	1.5611	-1.6000
F38P43	6.11	6.11	0	1.7272	7.3289	6.0447	230	195.84	1295	89.01	1.7605	0.1699	0.6511	-0.2000
F38P44	3.5	4.59	1.14	4.6134	6.9744	2.538	230	197.36	1295	88.9	1.1704	1.0151	2.4800	-3.2000
F38P45	7.11	7.11	0	6.453	4.5066	-2.0383	230	197.36	1295	88.9	0.7556	0.3324	0.6003	-2.8000

F38P46	0	12.5	14.28	0	10.9925	12.3501	230	197.36	1295	88.9	1.0234	1.4667	0.2478	-1.6000
F47P1	0.63	4.28	3.81	0.8347	4.7857	4.1497	237	196.12	1144	93.84	0.0509	2.0392	4.9389	0.4000
F47P2	1.96	3.3	1.39	1.1294	4.3694	3.388	236	195.59	1151	93.86	0.0982	2.2988	4.4559	-0.6000
F47P3	7.3	8.73	1.57	10.7176	10.2068	-0.5688	236	195.59	1151	93.86	0.3229	1.9159	4.6153	-0.2000
F47P4	0.7	7.25	7.06	0.4305	8.0988	8.344	237	195.59	1144	93.86	0.3550	1.8201	4.7971	-1.4000
F47P5	1.09	4.02	3.05	1.6669	3.8097	2.2277	237	195.91	1144	93.91	0.0839	0.0233	4.8967	0.4000
F47P6	0	3.63	3.77	0	5.6427	5.9802	236	195.91	1151	93.91	0.2604	1.2437	4.9045	1.6000
F47P7	2	3.22	1.26	2.0872	4.9856	3.0505	236	195.59	1151	93.86	0.3284	2.7269	3.9696	-1.4000
F47P9	1.13	3.84	2.81	0.6046	5.8053	5.5213	236	195.59	1151	93.86	0.4753	0.1655	4.6866	0.0000
F47P10	1.08	3.06	2.05	1.3962	3.5041	2.1845	236	195.91	1151	93.91	0.0564	0.1851	4.8542	2.2000
F47P13	0	2.75	2.82	0.2224	3.6591	3.5672	236	195.41	1151	93.25	0.3112	0.0018	4.4650	-2.2000
F47P14	0.27	3.85	3.73	0.5917	4.1354	3.6965	236	195.75	1151	93.35	0.1577	0.4219	4.6411	0.6000
F47P16	0.5	4.9	4.62	0.8863	6.0116	5.4531	236	195.41	1155	93.25	0.3643	0.0987	3.5543	-1.2000
F47P17	0	5.5	5.82	0	5.2095	5.4958	236	195.41	1155	93.25	0.2689	0.6381	3.4701	-2.0000
F47P18	0	3.98	4.15	0	4.7106	4.9434	235	195.41	1153	93.25	0.1340	2.5430	3.7310	2.4000
F47P19	2.56	2.07	-0.49	3.3306	2.5165	-0.8352	235	195.41	1157	93.25	0.3397	0.5599	3.2244	-0.6000
F47P20	0	5.21	5.5	0	6.3796	6.8143	235	194.47	1157	93.17	0.6057	1.6900	2.9029	-0.8000
F56P1	4.96	6.21	1.33	5.1078	7.9707	3.1108	232	170.47	1165	90.14	0.1783	3.9785	4.8273	0.0000
F56P2	0.75	7.79	7.63	0.2563	6.9326	7.1736	232	170.47	1165	90.14	0.6772	3.7875	0.5121	1.6000

F56P3	2.36	8.25	6.41	1.4761	4.4807	3.1455	232	170.35	1165	90.1	0.5103	3.9507	4.6566	0.2000
F56P4	2.29	4.61	2.43	1.6689	7.1189	5.8677	232	170.35	1165	90.1	1.3527	0.0763	1.5392	-0.2000
F56P5	2.68	3.87	1.24	0.6869	3.9964	3.4472	232	170.35	1165	90.1	0.8077	3.5800	1.9283	0.8000
F56P6	0.96	8.27	7.97	0.1849	13.2821	15.1032	232	170.35	1165	90.1	0.3296	3.9671	4.7814	0.4000
F56P7	2.46	8.47	6.56	1.8284	6.792	5.3253	233	170.35	1157	90.1	0.7770	1.5047	1.8969	-1.0000
F56P8	0.62	4.18	3.71	0.7072	4.7208	4.2125	232	170.35	1165	90.1	0.8180	2.3984	1.9651	-2.8000
F56P9	0.55	6.41	6.26	0.2978	11.0598	12.1002	232	170.35	1165	90.1	0.7201	2.7794	0.5461	0.8000
F56P10	2.59	7.67	5.5	0.6196	8.7639	8.9267	232	170.35	1165	90.1	0.3559	3.9001	4.4794	0.0000
F56P11	0.48	6.41	6.33	0.1017	7.6181	8.1362	233	172.3	1157	90.09	0.5363	0.0670	1.9292	0.0000
F56P12	1.63	10.97	10.49	0.6627	3.6701	3.122	233	170.35	1157	90.1	0.2005	0.4021	2.0111	-1.6000
F56P13	1.59	7.54	6.43	1.1686	6.3215	5.5006	232	170.35	1165	90.1	0.9833	0.8163	0.4605	0.6000
F56P15	1.98	9.31	8.08	2.8046	10.7629	8.9182	233	172.3	1157	90.09	1.0006	0.1774	1.5835	-0.6000
F56P17	0.87	11.53	12.05	0.2178	16.3213	19.2445	233	170.35	1157	90.1	0.6352	1.4287	0.6077	-0.4000
F56P18	1.22	4.89	3.86	1.1001	9.6758	9.4943	233	170.35	1157	90.1	0.4340	1.9681	0.1634	0.4000
F56P19	0.41	8.55	8.89	0.092	8.4505	9.13	233	172.3	1157	90.09	0.7247	0.2080	1.5465	2.6000
F56P20	0.43	5.51	5.37	0.365	5.7668	5.7324	234	172.3	1151	90.09	0.5802	0.1160	1.9806	0.2000
F56P21	2.74	5.08	2.46	1.5379	6.5558	5.3699	234	170.35	1151	90.1	0.5402	1.7906	0.3373	1.6000
F56P22	0	11.37	12.83	0	6.5704	7.0325	233	171.27	1157	90.13	0.3349	1.7411	0.6548	-2.4000
F56P23	1.84	4.8	3.11	1.0233	5.4185	4.647	234	172.3	1151	90.09	0.9209	0.2701	0.9300	0.4000

F56P24	0.6	8.41	8.52	0.2463	10.42	11.3571	234	172.3	1151	90.09	1.0063	0.0112	1.9580	-2.6000
F56P25	0.55	9.77	10.21	0.5799	9.863	10.2989	234	171.97	1151	90.29	1.0896	1.2941	0.5130	-1.2000
F56P26	1.4	9.96	9.51	0.4798	6.4703	6.4049	233	171.27	1157	90.13	0.5185	1.8765	0.1974	0.6000
F56P27	0.76	4.1	3.48	0.4401	5.8477	5.7434	234	171.97	1151	90.29	0.2858	0.1470	2.3922	0.6000
F56P28	0.98	7.83	7.43	0.321	9.8939	10.624	234	171.97	1151	90.29	0.4827	0.0616	2.1175	2.0000
F56P29	1.61	7.5	6.37	2.2076	10.3872	9.1278	234	171.97	1151	90.29	0.4525	1.7573	0.3430	0.8000
F56P30	0	6.63	7.1	0	6.1677	6.5731	234	171.27	1151	90.13	0.8116	1.6187	0.5091	-0.6000
F56P31	2.1	5.29	3.38	0.9362	7.9663	7.6386	234	171.97	1151	90.29	0.6422	0.5188	0.6206	2.4000
F56P32	1.3	7.88	7.14	0.9433	8.4708	8.2242	234	171.97	1151	90.29	0.6628	0.2788	2.5799	-1.0000
F56P33	1.45	11.37	11.19	4.9817	9.462	4.9486	235	171.97	1146	90.29	0.2165	1.8153	2.5666	-0.4000
F56P34	1.56	12.02	11.89	1.3404	9.4039	8.9006	235	172.03	1149	90.19	3.3282	0.0246	2.7483	-2.6000
F56P35	0	5.74	6.09	0	8.9714	9.8556	235	171.68	1149	90.12	1.4073	0.0491	0.8376	0.4000
F56P36	1.38	6.6	5.59	1.167	9.8615	9.6457	235	171.68	1149	90.12	0.6806	0.5110	0.6821	2.0000
F56P37	0.55	8.84	9.09	0.1513	7.7741	8.2653	234	171.97	1151	90.29	1.5489	0.0152	3.1333	-1.8000
F56P38	0	6.31	6.74	0.2674	6.3689	6.5165	235	171.97	1146	90.29	0.5673	1.5387	3.4230	-0.6000
F56P39	0.39	7.67	7.89	0.0821	9.1913	10.0313	235	171.68	1146	90.12	0.0856	0.0108	4.4222	-1.0000
F56P40	0.82	5.44	4.88	0.2013	7.1925	7.5331	235	171.97	1146	90.29	0.4918	0.0952	4.2246	0.8000
F72P1	0.77	0.39	-0.38	0.3309	5.0728	4.9953	231	136.82	1052	97.32	0.1727	6.9794	4.9904	1.2000
F72P2	0.75	1.82	1.09	0.5401	2.0679	1.5601	231	136.82	1052	97.32	0.0000	6.9800	4.9907	0.0000

F72P4	1.23	5.65	4.69	1.1349	4.1453	3.1407	231	136.82	1051	97.32	0.2019	6.9801	4.9908	-1.0000
F72P6	0.33	6.04	6.08	0.7107	4.8967	4.4016	231	136.27	1051	97.14	0.1089	6.9798	4.9907	-1.0000
F72P8	0.34	5.68	5.66	0.9636	7.2204	6.7437	231	137.07	1051	97.34	0.0000	6.9795	4.9905	-0.2000
F72P11	0.33	6.49	6.59	0.2632	4.4792	4.4137	230	136.82	1055	97.32	0.0719	6.9804	4.9909	0.4000
F72P12	0	4.68	4.91	0.8425	4.1487	3.4492	231	136.82	1051	97.32	0.0985	6.9804	4.9909	0.6000
F72P13	1.06	5.55	4.75	6.0611	5.2964	-0.8075	231	137.02	1051	97.39	0.0993	6.9802	4.9908	2.2000
F72P14	1.79	4.41	2.74	1.509	2.2039	0.7105	231	137.02	1051	97.39	0.0319	6.9803	4.9908	-0.4000
F72P15	0.69	1.79	1.12	0.207	1.7009	1.5197	231	137.07	1051	97.34	0.0596	6.9796	4.9905	0.6000
F72P16	0	4.53	4.75	0.2571	5.2558	5.2761	230	136.55	1055	97.09	0.1753	6.9802	4.9908	-1.2000
F72P17	1.59	5.61	4.26	0.3834	3.1526	2.8594	230	136.82	1055	97.32	0.0952	6.9804	4.9909	1.0000
F72P18	1.65	6.52	5.21	2.0179	5.3536	3.5243	230	137.02	1055	97.39	0.0246	6.9804	4.9909	-0.4000
F72P19	0.25	2.83	2.65	0.1263	2.3033	2.2284	230	137.02	1055	97.39	0.1175	6.9804	4.9908	-0.6000
F72P20	0.68	3.72	3.16	0.6974	2.3348	1.6766	231	137.02	1051	97.39	0.0000	6.9802	4.9907	0.8000
F72P21	0.55	2.36	1.85	0.6666	3.1404	2.5539	231	137.02	1051	97.39	0.1048	6.9795	4.9904	1.8000
F72P22	0.27	2.09	1.85	0.2896	2.3371	2.0965	230	136.53	1055	97.23	0.1599	6.9801	4.9906	-1.2000
F72P23	0.47	2.21	1.79	0.4234	3.7678	3.4754	230	136.53	1055	97.23	0.0972	6.9803	4.9907	-1.2000
F72P24	2.07	2.24	0.18	1.072	3.025	2.0139	230	137.02	1055	97.39	0.0821	6.9802	4.9906	-2.2000
F72P25	1.51	0.77	-0.74	1.8928	3.0843	1.2294	230	137.02	1055	97.39	0.1169	6.9797	4.9904	-0.6000
F72P26	0.28	2.88	2.67	0.0289	1.8754	1.8817	230	137.02	1056	97.39	0.0804	6.9795	4.9902	-0.4000

F72P27	1.14	1.79	0.66	0.7275	2.1769	1.4816	230	137.02	1053	97.39	0.2022	6.9778	4.9894	0.4000
F72P28	1.01	2.51	1.54	0.4133	2.211	1.8383	230	136.53	1055	97.23	0.0785	6.9798	4.9904	1.0000
F72P29	0.15	2.83	2.76	0.0258	2.5623	2.6032	230	136.53	1055	97.23	0.0000	6.9791	4.9899	1.6000
F72P30	0.31	2.21	1.94	1.6282	2.9866	1.4002	230	136.53	1056	97.23	0.0001	6.9785	4.9896	1.4000
F72P31	0.92	2.46	1.58	1.28	2.3361	1.0813	230	137.02	1056	97.39	0.2185	6.9777	4.9892	0.4000
F72P32	0.38	0.75	0.37	0.3788	2.4978	2.1732	230	137.02	1056	97.39	0.1085	6.9757	4.9880	-0.6000
F72P33	2.53	2.95	0.43	2.0211	3.2877	1.3097	230	137.02	1056	97.39	0.4550	6.9618	4.9810	2.4000
F72P34	0	1.41	1.43	0	2.7079	2.7832	230	136.53	1058	97.23	0.0992	6.9769	4.9887	-1.2000
F72P35	0.66	3.43	2.87	0.2974	3.177	2.9741	230	136.53	1056	97.23	0.0481	6.9758	4.9881	0.8000
F72P36	0.7	5.2	4.75	0.215	4.8383	4.8584	230	136.53	1056	97.23	0.0000	6.9730	4.9864	0.0000
F72P37	0.31	1.2	0.9	0.1366	1.787	1.6803	230	136.25	1056	97.32	0.0000	6.9711	4.9853	-0.2000
F72P38	0.56	4.26	3.86	0.4832	3.0222	2.6181	230	137.68	1056	97.38	0.1541	6.9699	4.9846	-1.0000
F72P39	1.3	2.9	1.64	1.0881	2.7408	1.6993	230	136.53	1058	97.23	0.0892	6.9664	4.9827	1.2000
F72P40	0.44	1.7	1.28	0.4511	2.3681	1.9635	230	136.25	1058	97.32	0.1376	6.9632	4.9808	0.4000
F72P41	0.18	2.91	2.82	0.352	2.602	2.3101	230	136.25	1056	97.32	0.0482	6.9619	4.9800	-0.8000
F73P1	0	5.8	6.15	1.8691	6.357	4.7925	238	154.28	983	96.36	0.1173	4.1828	5.8928	-0.4000
F73P2	1.87	4.13	2.35	3.0071	5.9873	3.17	238	154.28	983	96.36	0.1069	4.2481	5.8767	0.4000
F73P3	0.27	5.28	5.3	1.7916	6.462	4.993	238	154.28	983	96.36	0.0683	4.1877	6.0386	-0.8000
F73P4	0.63	8.18	8.23	0.4011	9.8166	10.4403	238	154.28	983	96.36	0.0681	4.2596	6.0316	-0.8000

F73P5	0.97	7.52	7.08	0.8369	7.9685	7.7491	238	154.28	983	96.36	0.2466	4.1548	6.2073	1.0000
F73P6	0.7	2.79	2.15	0.6348	4.642	4.2022	238	154.28	983	96.36	0.2172	4.2343	6.2071	1.2000
F73P7	1.51	5.17	3.86	0.5384	5.2589	4.9826	238	154.28	983	96.36	0.3517	4.1681	6.3596	-0.4000
F73P9	1	2.65	1.7	0.5358	5.975	5.7848	238	154.28	976	96.36	0.1259	4.3192	6.5429	1.0000
F73P10	0.31	3.14	2.92	0.5312	4.1295	3.7533	238	155.62	976	96.26	0.2522	4.3111	6.5677	3.4000
F73P12	0.85	4.89	4.25	0.2896	4.4293	4.3315	238	155.62	976	96.26	0.1786	4.3581	6.6636	-0.4000
F73P14	0.7	4.2	3.65	0.7794	6.5	6.1183	238	155.62	968	96.26	0.0815	4.3562	6.7342	-0.2000
F73P15	0.67	2.54	1.91	1.4129	5.6146	4.4516	238	156.21	968	96.36	0.0001	4.3177	6.7002	0.6000
F75P1	0.66	2.48	1.87	1.9106	2.9969	1.1198	235	147.27	1113	96.33	1.0466	0.5043	0.4740	-1.6000
F75P2	2.93	0	-2.93	1.6298	2.7171	1.1176	235	148	1113	96.3	1.3140	0.0470	0.8821	-1.0000
F75P3	2	1.23	-0.78	0.8383	3.4823	2.7394	235	148	1113	96.3	0.4130	0.3800	1.9056	-0.2000
F75P4	0.39	2.57	2.23	0.6115	5.2159	4.8578	235	148	1112	96.3	0.3655	0.9441	4.2289	2.6000
F75P5	1.57	0.61	-0.97	0.5553	2.6697	2.1724	235	148	1111	96.3	0.8149	0.0721	4.7201	-1.2000
F75P6	0.55	2.59	2.09	0.4887	5.2555	5.0313	234	148	1118	96.3	0.1533	0.0033	4.6901	-0.2000
F75P7	1.23	2.13	0.92	1.367	3.7993	2.5283	235	148.75	1111	96.35	0.3740	0.1820	4.7486	1.2000
F75P11	0.22	3.8	3.71	0.1051	4.7551	4.8822	234	148	1118	96.3	0.3454	0.0395	4.7464	-0.2000
F75P12	0	6	6.38	0	5.0646	5.3348	234	148.75	1118	96.35	0.2444	0.4983	4.6775	1.2000
F75P13	0	3.65	3.79	0	4.5421	4.7582	235	148.75	1111	96.35	0.2102	1.9011	4.7444	-0.2000
F75P14	1.53	5.98	4.74	0.9209	6.8257	6.3374	235	148.75	1111	96.35	0.3366	1.4191	4.7910	0.6000

F75P15	0.41	4.05	3.79	0.2649	4.3779	4.3013	233	148.27	1119	96.5	0.7476	0.6848	0.5568	-0.8000
F75P16	0.65	0.97	0.32	0.6471	2.1206	1.5054	233	148.27	1119	96.5	0.5362	2.4262	2.3344	-1.0000
F75P17	0.83	3.45	2.71	0.597	2.7746	2.2397	234	148.06	1118	96.34	0.3593	2.7875	4.8782	-0.4000
F75P20	0.23	7.06	7.35	1.0457	5.7127	4.9498	235	148.75	1112	96.35	0.4127	1.8604	4.7457	2.0000
F75P21	0.52	7.78	7.88	0.1821	3.9885	3.9645	236	148.26	1106	96.19	0.2819	1.5561	4.7731	-0.2000
F75P22	0	1.65	1.68	0.4562	3.31	2.9516	233	148.06	1119	96.34	0.7297	2.9663	4.8424	-0.8000
F75P23	1.37	3.61	2.33	0.5805	6.384	6.1992	233	148.06	1119	96.34	0.4549	2.9766	4.8924	0.2000
F75P24	0.36	1.22	0.87	0.5045	2.825	2.388	234	148.06	1118	96.34	0.6585	2.9069	4.7207	-1.0000
F75P25	0.6	2.28	1.72	2.4806	3.2501	0.7954	235	148.06	1112	96.34	0.8150	2.6568	4.5849	-0.8000
F75P26	0.19	2.85	2.74	0.4213	4.7708	4.5673	235	148.27	1112	96.31	0.8775	1.3063	4.7298	-3.0000
F75P27	0	4.45	4.66	0.1005	5.7832	6.0314	235	148.26	1112	96.19	1.2413	0.0120	4.5988	0.0000
F75P30	0.55	2.76	2.27	0.221	4.2236	4.1791	234	148.06	1119	96.34	0.3214	2.9500	4.7683	0.6000
F75P31	1.51	2.4	0.9	2.3795	2.3507	-0.0295	235	148.27	1112	96.31	0.3649	2.8945	4.7684	-0.4000
F86P1	0.78	2.94	2.22	0.9071	3.0843	2.2465	207	181.33	963	91.18	0.3273	2.6360	0.2481	0.6000
F86P2	0	0.69	0.69	0	3.572	3.7043	207	181.33	963	91.18	0.2103	1.9230	0.1653	0.6000
F86P3	0	6.23	6.65	0	5.8368	6.1986	204	181.33	961	91.18	0.1664	2.8857	0.3671	0.8000
F86P4	1.31	3.7	2.47	0.2652	4.63	4.5767	207	181.87	963	90.77	0.5523	1.1911	0.5853	0.0000
F86P5	0	4.58	4.79	0	7.1106	7.6549	204	181.87	961	90.77	0.4671	0.3824	1.0821	-1.2000
F86P6	0.75	5.32	4.82	0.6676	3.8554	3.3157	204	181.87	961	90.77	0.4682	0.5368	0.9714	0.4000

F86P7	0	3.9	4.06	0	4.9101	5.1637	205	181.87	962	90.77	0.5632	0.3296	1.4037	1.0000
F86P8	0	1.01	1.02	0	2.7054	2.7807	205	181.87	962	90.77	0.6305	0.3852	1.1749	0.0000
F86P9	0.75	1.48	0.74	2.4069	2.5096	0.1053	205	181.89	962	90.59	0.5994	1.5777	0.3114	0.8000
F86P10	0	2.32	2.37	1.5801	4.1167	2.6455	210	181.89	969	90.59	0.8416	1.1327	0.5047	1.0000
F86P11	0.91	3.02	2.17	0.5211	6.6563	6.5727	205	181.89	962	90.59	0.3289	2.7073	0.8421	-1.2000
F86P12	1.69	3.96	2.37	1.2927	5.1005	4.0124	205	181.89	962	90.59	0.6606	1.4822	0.7053	0.2000
F86P13	0	1.48	1.5	0	4.1799	4.3622	205	181.89	961	90.59	0.4442	1.6083	0.4076	0.2000
F86P14	0.46	3.41	3.05	0.0823	4.5275	4.6559	205	181.89	962	90.59	0.1485	2.9056	1.1089	0.6000
F86P15	0	6.27	6.69	0	6.623	7.0928	205	181.89	961	90.59	0.2773	1.6945	0.3444	2.8000
F86P16	0	3.21	3.32	0.3922	4.5339	4.3383	205	181.89	961	90.59	0.6757	0.6530	0.2575	2.0000
F86P17	1.05	3.9	2.96	0.6259	3.9396	3.4496	205	181.89	961	90.59	0.2832	2.9783	0.5848	1.6000
F86P18	0	1.15	1.17	0.8684	3.2999	2.5145	205	181.89	961	90.59	0.8295	0.2470	1.0612	0.6000
F86P19	0	3.72	3.86	0	2.2773	2.3304	205	182.54	961	90.78	0.1775	2.9710	1.5964	-0.2000
F86P20	0	3.67	3.81	0	6.9237	7.4388	205	181.89	961	90.59	1.0711	0.0758	1.3771	-0.2000
F86P21	0	3.96	4.13	0	3.4729	3.5978	205	182.54	961	90.78	0.0846	3.5040	0.4101	0.6000
F86P22	0.67	1.94	1.3	1	4.5442	3.7128	205	181.89	961	90.59	0.5475	0.5654	1.5683	-1.0000
F86P23	0	6.42	6.86	0	1.4955	1.5182	205	183.76	961	90.53	1.3629	0.2934	0.2680	2.6000
F86P24	0	6.4	6.83	0	3.3775	3.4955	205	182.24	961	90.66	0.6630	2.5660	0.9107	0.6000
F86P25	0	5.27	5.56	0	4.2805	4.472	205	182.24	961	90.66	0.6073	0.3940	0.9497	1.2000

F86P26	0.86	4.67	3.99	0.3484	3.3439	3.0991	205	183.76	961	90.53	0.8274	0.4653	0.4638	0.4000
F86P27	0.67	8.57	8.65	0.1194	4.9935	5.1302	205	182.24	961	90.66	0.4422	2.6433	1.5477	-0.2000
F86P28	0	4.25	4.44	0	4.662	4.8899	205	183.76	961	90.53	0.4762	1.5564	0.5384	0.4000
F86P29	0	3.6	3.74	0	3.3364	3.4515	205	182.24	961	90.66	0.3919	1.1348	1.0412	0.4000
F86P30	0.93	7.7	7.33	0.0617	3.0351	3.0664	204	183.28	960	90.98	0.6682	1.0551	0.8786	-1.2000
F89P1	2.23	2.65	0.42	1.5859	2.3381	0.7703	231	133.68	1173	95.06	0.6024	0.1963	1.6087	0.8000
F89P2	0.55	3.05	2.58	0.204	3.0781	2.9654	231	133.68	1174	95.06	0.4400	1.6227	0.2839	2.0000
F89P4	0.6	1.73	1.15	0.2076	2.8919	2.7642	228	134.1	1195	94.95	0.6697	2.7375	0.8837	-1.8000
F89P7	2.65	3.54	0.92	1.8671	2.7048	0.861	231	133.68	1174	95.06	0.2219	0.7120	2.7436	0.2000
F89P8	0.49	1.9	1.43	0.0738	2.9174	2.9291	231	133.68	1174	95.06	0.4357	1.4967	0.6503	-1.0000
F89P12	0.62	1.21	0.6	0.2409	2.6374	2.4614	230	133.93	1181	95	0.9820	0.5497	0.3382	0.6000
F89P13	2.19	1.29	-0.92	0.867	1.6299	0.7756	231	133.68	1174	95.06	0.0780	1.9441	3.7909	2.2000
F89P14	0.73	0.73	0	0.3467	2.7681	2.4903	231	133.68	1174	95.06	0.2918	0.0169	2.8098	-2.4000
F89P15	1.53	4.84	3.47	1.7925	3.0323	1.2785	231	133.68	1174	95.06	0.8538	0.5210	0.7581	-1.0000
F89P16	1.63	0.83	-0.8	2.4314	2.2541	-0.1813	231	134.95	1174	95.12	0.8757	0.7110	0.3767	-0.6000
F89P17	0.87	1.7	0.84	0.6861	2.4808	1.8403	231	133.93	1174	95	0.5149	0.8459	0.2464	3.8000
F89P19	1.02	4.58	3.73	0.4061	3.9774	3.7192	232	134.75	1168	95.19	0.4898	1.7130	3.8900	0.4000
F89P20	1.41	0.95	-0.46	0.8673	1.8202	0.9705	232	135.38	1168	95.17	0.9083	0.0986	3.6725	-2.6000
F89P21	1.29	0.87	-0.42	0.4114	1.2108	0.8092	231	134.95	1174	95.12	0.2599	1.2611	2.9374	1.2000

F89P22	0.6	0	-0.6	4.3036	1.1571	-3.1834	231	134.95	1174	95.12	0.1702	0.0185	2.9214	0.2000
F89P23	3.17	0.85	-2.34	1.3101	1.1884	-0.1231	231	134.95	1174	95.12	0.4935	0.1030	2.6715	0.2000
F89P24	1.17	0.89	-0.29	0.5492	3.0263	2.5544	231	133.93	1174	95	0.2390	0.0042	2.9707	-1.0000
F94P1	1.32	6.1	5.09	0.8761	5.2106	4.5727	206	151.52	831	92.41	0.0443	3.3946	0.5064	0.2000
F94P2	0	7.85	8.51	0	7.192	7.7493	207	151.52	825	92.41	0.3067	0.3745	1.6208	1.0000
F94P3	16.43	0	-16.43	7.3492	2.9723	-4.5109	207	151.52	825	92.41	1.9539	0.0560	0.9331	-1.6000
F94P4	1.12	3.2	2.14	0.597	3.5826	3.0965	207	151.52	828	92.41	0.0948	3.1967	2.7273	0.4000
F94P5	0	5.17	5.46	0	6.3353	6.7638	207	153.51	828	93.16	0.9185	0.1542	1.0196	-2.2000
F94P6	1.21	4.43	3.38	0.2514	3.4695	3.3337	207	153.51	828	93.16	1.0674	0.1714	0.8997	-0.2000
F94P7	1.55	6.06	4.8	0.8188	5.6757	5.1491	207	151.81	828	93.24	0.0501	2.9858	3.2727	-1.2000
F94P8	0.96	3.85	3.01	0.3485	5.3726	5.3094	207	151.81	825	93.24	0.3633	1.6002	0.5661	0.4000
F94P11	1.23	3.48	2.33	1.5451	3.2644	1.7773	208	152.13	820	93.27	0.6444	2.5209	0.6367	-0.8000
F94P12	0	2.14	2.19	0	5.0576	5.3271	209	151.81	816	93.24	0.3133	2.8560	0.4994	-0.2000
F94P13	0.6	4.39	3.95	0.0996	5.2298	5.4132	209	151.81	816	93.24	0.3264	1.8230	0.5378	-1.0000
F94P14	0.43	2.93	2.58	0.4556	4.2343	3.9458	209	152.89	816	93.31	0.6372	0.2047	2.5651	-0.8000
F96P1	2.31	1.76	-0.56	1.0321	3.6242	2.6896	211	167.15	1016	94.62	1.4391	0.3135	0.4204	-1.4000
F96P2	1.35	2.36	1.04	0.7612	2.9467	2.2519	211	167.15	1016	94.62	0.9226	0.3815	0.4461	1.6000
F96P3	3.07	4.76	1.78	6.4855	4.6614	-1.9134	209	167.15	1025	94.62	1.0504	0.2999	0.4627	1.6000
F96P4	1.28	2.77	1.53	0.4663	4.8344	4.59	209	166.96	1025	94.62	2.0645	0.1855	0.4514	0.4000

F96P6	0.71	5.59	5.17	0.6589	3.2135	2.6394	211	167.15	1016	94.62	1.4992	0.2835	0.4047	-1.0000
F96P7	0.31	3.71	3.53	2.4958	3.2674	0.7976	209	167.15	1025	94.62	1.4370	0.2668	0.4804	-1.6000
F96P9	0	2.4	2.46	0	5.8656	6.2311	210	167.15	1022	95.14	1.1131	0.5731	0.2600	0.4000
F96P10	0	1.19	1.2	0	2.8388	2.9218	211	167.15	1016	94.62	0.9485	0.6845	0.2722	-0.6000
F96P11	2.4	4.53	2.23	3.0289	5.052	2.1307	209	166.96	1025	94.62	0.7728	0.7038	0.4569	-1.0000
F96P12	6.4	0	-6.4	2.3067	1.6648	-0.6528	209	166.96	1025	94.62	1.2250	0.2519	0.5295	1.4000
F96P13	0.5	2.38	1.92	0.9248	3.7317	2.9157	210	167.15	1022	95.14	1.3785	0.2432	0.5178	-0.6000
F96P14	5.69	1.59	-4.17	1.7936	3.6122	1.8868	210	167.15	1022	95.14	1.1461	0.3328	0.4908	0.0000
F96P15	4.42	1.89	-2.58	2.3793	4.4566	2.1742	206	167.15	1036	95.14	0.6800	1.2770	0.2345	2.0000
F96P16	3.78	1.51	-2.31	1.1326	2.2678	1.1616	206	165.85	1036	94.53	0.4735	2.8334	0.1620	0.0000
F96P17	0.96	0	-0.96	0.287	1.3144	1.0411	206	165.85	1036	94.53	0.4480	2.2851	0.1635	2.0000
F96P18	3	2.23	-0.79	3.236	3.3966	0.1663	210	167.15	1022	95.14	1.7662	0.1877	0.5616	-2.2000
F96P19	1.57	6.81	5.62	0.8013	5.0744	4.5014	206	167.15	1036	95.14	1.5189	0.2213	0.5065	0.4000
F96P20	3.45	0	-3.45	1.5979	0.6989	-0.9054	206	165.85	1036	94.53	0.9527	1.5780	0.6555	0.8000
F96P21	5.32	0	-5.32	6.801	0.6219	-6.2178	206	165.85	1036	94.53	1.4660	0.3928	0.2942	-3.8000
F96P22	4.01	1.08	-2.96	3.5971	5.5275	2.0433	206	165.85	1036	94.53	1.6130	0.6544	0.0380	4.8000
F103P1	0	2.44	2.5	0	6.3352	6.7637	234	203.99	1402	76.51	0.1981	6.0742	5.5336	-0.2000
F103P2	0.16	4.64	4.69	0.0422	7.0642	7.5558	234	202.28	1402	76.68	0.4017	7.5114	6.4099	-0.6000
F103P3	0.15	3.12	3.06	0.0493	8.8394	9.6425	234	202.28	1401	76.68	0.2103	7.6003	6.5201	1.0000

F103P4	0.12	1.61	1.52	0.0611	7.2211	7.7174	234	203.75	1401	76.67	0.3116	7.6232	6.5494	-0.8000
F103P5	0.11	1.3	1.2	0.032	5.8381	6.1661	234	202.28	1406	76.68	0.3483	7.6762	6.5951	-1.2000
F103P6	0.17	2.88	2.78	0.2983	6.6458	6.7994	234	202.28	1406	76.68	0.0000	7.6658	6.5862	1.2000
F103P7	0.16	1.69	1.56	0.0703	5.0955	5.295	234	202.28	1406	76.68	0.2917	7.3941	6.2830	0.4000
F103P8	0	3.78	3.93	0	7.7013	8.3439	234	203.2	1405	76.88	0.4274	3.9751	3.8647	3.8000
F103P9	0.16	3.28	3.22	0.0288	5.3708	5.6452	234	203.2	1405	76.88	0.2791	3.6455	0.1320	4.8000
F103P10	0.23	1.83	1.64	0.1088	4.0988	4.1605	234	203.2	1405	76.88	0.8613	0.0333	1.8188	1.8000
F103P11	0.13	2.63	2.56	0.1639	6.1519	6.3805	234	202.5	1407	76.6	1.0232	0.0898	0.8591	0.2000
F103P12	0	1.36	1.38	0	8.4966	9.2856	234	202.32	1405	76.73	0.1268	6.2642	5.8204	-0.6000
F103P13	0	2.18	2.23	0	4.5282	4.7429	235	201.55	1402	76.58	0.5784	3.8540	1.8431	0.2000
F103P14	0.28	1.62	1.36	0.3483	3.4962	3.262	235	201.55	1402	76.58	0.7394	0.0194	1.9778	-3.2000
F103P15	0.63	3.45	2.92	0.3106	5.1881	5.1443	235	201.55	1402	76.58	0.9134	0.0388	1.9870	-1.6000
F103P16	0.18	1.93	1.78	0.0439	4.387	4.5423	237	203.18	1400	76.87	1.2811	0.2563	0.6665	0.2000
F103P17	0	2.44	2.5	0	5.1142	5.3899	237	203.18	1400	76.87	0.6033	1.8118	0.2005	1.6000
F103P18	0	0.74	0.74	0	4.5817	4.8017	235	201.62	1406	76.61	0.6805	3.8029	0.7678	-0.6000
F103P19	0.14	1.93	1.83	0.0307	4.4792	4.6571	235	201.62	1406	76.61	0.7714	0.4384	0.5173	0.2000
F103P20	0.46	1.48	1.04	0.2726	3.9123	3.7879	237	201.81	1400	76.81	0.4531	0.8876	0.5236	2.4000
F104P3	2.67	1.24	-1.45	0.6909	5.9625	5.6059	233	190.55	1348	78.51	1.0269	2.9592	3.4113	-2.2000
F104P4	0.69	7.35	7.19	0.2896	5.4081	5.4111	233	190.62	1348	78.34	0.3702	2.9226	2.3975	1.2000

F104P5	1	4.53	3.69	0.5088	3.7423	3.3591	235	190.62	1333	78.34	0.4925	2.6647	1.8615	-2.2000
F104P6	0.16	5.45	5.59	0.1104	5.0471	5.1992	235	190.62	1333	78.34	0.8541	0.1623	0.8082	-2.2000
F104P8	3.47	4.39	0.96	0.9362	4.2994	3.5143	233	188.39	1348	77.99	0.1368	2.9893	4.7799	2.0000
F104P9	22.04	12.98	-10.4	9.4575	7.2148	-2.417	233	188.39	1348	77.99	0.7035	2.9632	4.6844	-1.2000
F104P10	0.21	5.28	5.35	0.0579	5.124	5.3397	233	189.83	1348	77.95	0.9209	0.2663	1.6886	0.0000
F104P13	1.06	5.1	4.25	0.4146	8.5367	8.8801	235	188.39	1330	77.99	0.7469	0.1009	1.7912	-1.4000
F104P14	8.21	0.45	-7.79	2.285	4.2234	2.0239	233	188.39	1345	77.99	0.1705	3.5754	4.9020	1.4000
F104P15	8.61	3.14	-5.65	3.7672	4.33	0.5883	233	188.39	1345	77.99	0.6600	3.0890	4.7013	0.0000
F104P16	2.17	4.88	2.85	2.1033	4.5663	2.5808	233	189.83	1345	77.95	0.5154	0.5594	0.9301	0.0000
F104P18	6.07	3.17	-3	2.6519	5.8884	3.439	235	188.39	1330	77.99	0.7652	0.5786	0.5300	-0.8000
F104P19	4.8	3.66	-1.18	2.5607	7.9136	5.8129	233	188.39	1345	77.99	0.1173	3.8963	4.9285	0.2000
F104P20	0.3	3.35	3.15	0.134	5.5885	5.7773	233	188.39	1345	77.99	0.3674	2.8576	3.6402	-0.6000
F106P1	0.62	2.07	1.49	0.1104	3.1723	3.1622	235	190.88	1389	77.72	1.1956	0.8757	0.0383	4.0000
F106P2	0.12	2.57	2.52	0.0295	4.3278	4.4927	235	190.88	1389	77.72	1.4691	0.1449	0.6084	1.0000
F106P3	0.17	0.34	0.17	0.3409	4.0698	3.8871	235	189.58	1389	77.57	1.9923	0.0584	0.7583	1.8000
F106P4	0.11	1.77	1.69	0.0203	3.8738	4.0088	235	189.58	1389	77.57	1.7783	0.2073	0.3807	3.0000
F106P5	0	4.23	4.42	0	4.1032	4.2788	235	190.88	1389	77.72	0.3272	1.9656	0.0802	1.4000
F106P6	0.13	2	1.91	0.091	3.6385	3.6814	235	189.58	1389	77.57	0.9709	0.4979	0.9074	-0.8000
F106P7	0.16	3.69	3.66	0.0911	5.1737	5.3599	235	189.58	1389	77.57	0.5194	1.6099	0.1950	2.2000

F106P8	0	1.72	1.75	0	4.5137	4.7271	235	189.58	1389	77.57	1.1529	0.0541	1.3343	0.4000
F106P9	0	2.96	3.05	0	4.3183	4.5132	235	189.58	1389	77.57	0.4828	1.9601	0.0487	1.2000
F106P10	0	3.61	3.74	0	4.6278	4.8523	235	189.58	1389	77.57	0.2158	1.9785	0.3485	1.8000
F106P11	0.29	3.41	3.23	0.2767	1.4827	1.2242	235	189.58	1389	77.57	0.0746	1.9830	0.0258	2.0000
F106P12	0	3.57	3.71	0	3.3914	3.5105	232	189.58	1399	77.57	0.7353	0.9732	0.4104	-0.6000
F106P13	0.31	3.98	3.82	0.2024	3.3907	3.3002	236	189.58	1386	77.57	1.4709	0.4515	0.2012	4.4000
F106P14	0.51	3.46	3.05	0.2771	4.1306	4.0195	235	189.58	1389	77.57	0.8287	0.5069	0.2927	4.2000
F106P15	0.66	3.36	2.79	0.6558	5.8399	5.5056	235	189.58	1389	77.57	0.8879	1.7614	0.4199	0.2000
F106P16	0	1.52	1.54	0	3.389	3.5079	232	189.58	1399	77.57	1.7966	0.5995	0.0326	-2.6000
F107P1	0.51	1.5	1	0.1011	2.5853	2.5501	244	168.94	1469	78.57	0.3084	3.0429	0.4792	0.4000
F107P2	0.48	1.17	0.7	0.1382	4.4495	4.512	244	168.94	1467	78.57	0.1951	2.9052	1.5398	1.4000
F107P3	0.92	1.94	1.04	0.5972	4.7916	4.4055	244	168.94	1467	78.57	0.0900	2.8430	1.3768	-0.6000
F107P4	1.56	2.99	1.48	1.0832	3.1352	2.1184	244	170.75	1467	78.74	0.3078	2.7208	0.1475	2.2000
F107P5	2.49	1.54	-0.97	1.3422	4.5082	3.3155	244	168.94	1469	78.57	0.1218	4.4505	5.2982	1.8000
F107P6	0.47	1.38	0.92	0.1226	5.3492	5.5221	244	168.94	1467	78.57	0.2697	3.8478	4.7032	-0.8000
F107P7	1.84	2.09	0.25	0.8446	4.0164	3.3045	244	168.94	1467	78.57	0.1537	3.5169	4.2012	0.6000
F107P8	3.4	2.61	-0.81	1.0485	2.8469	1.8511	244	170.74	1470	78.5	0.0312	5.1325	5.3451	1.0000
F107P9	1.78	0.61	-1.17	0.5908	3.3572	2.8625	244	169.75	1470	78.57	0.1481	4.6557	5.2731	1.6000
F107P10	2.21	2.58	0.38	1.9133	5.7742	4.0975	244	169.75	1471	78.57	0.0351	5.2716	5.4296	-1.0000

F107P11	2.23	2.86	0.65	1.0753	5.115	4.2575	244	169.75	1471	78.57	0.2259	4.2375	5.2477	-0.8000
F107P12	0.23	0.91	0.69	0.1301	2.8086	2.7559	244	169.75	1470	78.57	0.3398	4.0018	4.8902	-0.4000
F107P13	1.66	1.66	0	1.3253	4.2899	3.0975	244	169.75	1471	78.57	0.2287	4.7639	5.2897	1.0000
F107P14	1.41	2.92	1.56	2.0995	5.5386	3.6407	244	169.75	1471	78.57	0.1289	5.4623	5.4250	0.6000
F107P15	2.44	6.12	3.93	1.4421	6.7597	5.7031	244	170.14	1471	78.63	0.3625	4.3716	5.2587	1.8000

Cont.

TWI	VD	VDCN	CNBL	HILS	ASP	DEM	Slope	SAND	SILT	CLAY	PH_H2O	CEC_SOIL	BS	TEB
10.3995	98.1838	47.2394	914.761	0.771257	5.49779	962	0.014141	50.2	10.2	39.6	5.32	10.2	33.4	3.24
9.811	103.89	40.4406	915.559	0.728918	5.62214	956	0.056947	50.2	10.2	39.6	5.32	10.2	33.4	3.24
10.6049	121.997	19.7497	917.253	0.747342	6.28319	936	0.054945	50.2	10.2	39.6	5.32	10.2	33.4	3.24
8.84377	125.396	18.465	914.535	0.754711	0.179853	933	0.055844	50.2	10.2	39.6	5.32	10.2	33.4	3.24
8.2622	129.845	22.2635	905.736	0.757544	6.28319	928	0.039979	50.2	10.2	39.6	5.32	10.2	33.4	3.24
8.75689	148.859	12.0035	895.996	0.718672	5.85078	908	0.071467	50.2	10.2	39.6	5.32	10.2	33.4	3.24
10.5711	85.8738	66.0977	910.902	0.764229	5.17646	977	0.022357	50.2	10.2	39.6	5.32	10.2	33.4	3.24
7.39786	86.2968	62.7224	913.281	0.771362	0.000854	974	0.014141	50.2	10.2	39.6	5.32	10.2	33.4	3.24
7.95825	90.7195	56.1764	914.824	0.767781	6.03821	971	0.020613	50.2	10.2	39.6	5.32	10.2	33.4	3.24
9.83372	99.1304	46.4022	915.598	0.757148	5.25281	962	0.029146	50.2	10.2	39.6	5.32	10.2	33.4	3.24

9.53501	108.233	37.0354	914.965	0.760714	5.90268	952	0.026919	50.2	10.2	39.6	5.32	10.2	33.4	3.24
8.49642	114.689	34.5494	910.451	0.771257	5.49779	945	0.014141	50.2	10.2	39.6	5.32	10.2	33.4	3.24
9.50848	127.7	27.166	903.834	0.746695	5.92441	931	0.042694	50.2	10.2	39.6	5.32	10.2	33.4	3.24
10.5465	138.131	24.6212	895.379	0.771488	0.197396	920	0.02549	50.2	10.2	39.6	5.32	10.2	33.4	3.24
7.91187	147.496	20.2726	889.727	0.746695	5.92441	910	0.042694	50.2	10.2	39.6	5.32	10.2	33.4	3.24
9.10407	91.1461	60.8151	912.185	0.765125	4.39064	973	0.047399	50.2	10.2	39.6	5.32	10.2	33.4	3.24
7.78308	92.5691	55.3903	915.61	0.789692	3.83613	971	0.032005	50.2	10.2	39.6	5.32	10.2	33.4	3.24
8.1668	93.9838	51.7827	917.217	0.775105	4.33188	969	0.026919	50.2	10.2	39.6	5.32	10.2	33.4	3.24
8.36975	100.09	45.8343	916.166	0.753596	5.60844	962	0.032005	50.2	10.2	39.6	5.32	10.2	33.4	3.24
8.57542	104.86	42.4052	914.595	0.757121	5.49779	957	0.028277	50.2	10.2	39.6	5.32	10.2	33.4	3.24
8.82889	111.938	39.8271	909.173	0.767729	5.69518	949	0.018026	50.2	10.2	39.6	5.32	10.2	33.4	3.24
9.86424	122.939	33.7036	903.296	0.743024	5.33264	937	0.042985	50.2	10.2	39.6	5.32	10.2	33.4	3.24
8.66287	135.366	27.9535	896.047	0.736629	4.87754	924	0.060753	50.2	10.2	39.6	5.32	10.2	33.4	3.24
8.46564	153.726	13.7994	891.201	0.717116	4.76497	905	0.094846	50.2	10.2	39.6	5.32	10.2	33.4	3.24
8.73989	117.859	23.8342	923.166	0.769508	4.11381	947	0.136442	50.2	10.2	39.6	5.32	10.2	33.4	3.24
7.42797	117.269	22.0107	924.989	0.795602	3.8967	947	0.1162	50.2	10.2	39.6	5.32	10.2	33.4	3.24
8.03323	113.368	30.5701	919.43	0.808992	3.63553	950	0.07369	50.2	10.2	39.6	5.32	10.2	33.4	3.24
7.71458	110.758	36.9811	915.019	0.794042	3.80264	952	0.056947	50.2	10.2	39.6	5.32	10.2	33.4	3.24
9.30923	117.827	35.9112	908.089	0.764423	4.71239	944	0.029991	50.2	10.2	39.6	5.32	10.2	33.4	3.24

8.48894	124.198	33.9628	903.037	0.746857	4.93106	937	0.046065	50.2	10.2	39.6	5.32	10.2	33.4	3.24
8.06066	150.621	13.2359	896.764	0.705685	4.67241	910	0.124453	50.2	10.2	39.6	5.32	10.2	33.4	3.24
14.1972	145.358	0	919.002	0.736192	5.90276	918	0.055844	50.2	10.2	39.6	5.32	10.2	33.4	3.24
8.21273	142.813	8.6759	912.324	0.841859	3.38657	921	0.102715	50.2	10.2	39.6	5.32	10.2	33.4	3.24
8.60207	134.795	22.0678	905.932	0.762127	4.36362	928	0.058457	50.2	10.2	39.6	5.32	10.2	33.4	3.24
8.98682	161.219	2.60944	898.391	0.704871	5.12494	901	0.110231	50.2	10.2	39.6	5.32	10.2	33.4	3.24
8.0317	99.4417	169.3250	671.6750	0.7748	5.8183	841.0000	0.0158	62.15	15.75	22.1	5.7	7.15	63.35	4.57
13.4086	102.0440	184.3550	655.6480	0.7854	1.5708	839.0000	0.0000	62.15	15.75	22.1	5.7	7.15	63.35	4.57
12.2711	100.4270	164.0270	676.9750	0.7854	5.4978	840.0000	0.0050	62.15	15.75	22.1	5.7	7.15	63.35	4.57
9.5593	100.1670	173.8580	668.1460	0.7819	0.0020	841.0000	0.0100	62.15	15.75	22.1	5.7	7.15	63.35	4.57
7.0369	95.7703	152.9690	693.0340	0.7502	5.1165	845.0000	0.0427	62.15	15.75	22.1	5.7	7.15	63.35	4.57
11.0745	98.6171	157.5050	686.4980	0.7748	5.1765	843.0000	0.0158	62.15	15.75	22.1	5.7	7.15	63.35	4.57
9.5829	96.7360	154.0490	691.9520	0.7572	5.2525	845.0000	0.0353	62.15	15.75	22.1	5.7	7.15	63.35	4.57
9.33974	80.7235	44.3711	694.629	0.775563	0.519146	739	0.040289	85.6	3.8	10.6	6.7	5.4	66.2	3.28
7.03425	66.5912	58.0175	695.982	0.75328	0.358771	754	0.085233	85.6	3.8	10.6	6.7	5.4	66.2	3.28
12.7886	85.614	40.1933	693.807	0.78894	3.14159	734	0.005	85.6	3.8	10.6	6.7	5.4	66.2	3.28
9.52504	82.4836	42.8055	695.194	0.771899	0.404892	738	0.03806	85.6	3.8	10.6	6.7	5.4	66.2	3.28
7.16461	82.9142	43.6098	693.39	0.814052	3.14159	737	0.039979	85.6	3.8	10.6	6.7	5.4	66.2	3.28
8.559	87.7969	38.1161	694.884	0.77532	0.463876	733	0.042694	85.6	3.8	10.6	6.7	5.4	66.2	3.28

7.53079	86.8114	40.4861	692.514	0.820832	1.97569	733	0.03806	85.6	3.8	10.6	6.7	5.4	66.2	3.28
10.914	98.697	28.0804	693.92	0.824414	1.92957	722	0.042694	85.6	3.8	10.6	6.7	5.4	66.2	3.28
7.7260	167.4710	50.2199	568.7800	0.8004	3.6052	619.0000	0.0447	22	34.6	43.4	4.86	7.2	22.2	1.5
10.5775	198.2780	20.2543	568.7460	0.8106	3.2660	589.0000	0.0403	22	34.6	43.4	4.86	7.2	22.2	1.5
7.7705	170.7210	47.1176	568.8820	0.8011	3.6820	616.0000	0.0582	22	34.6	43.4	4.86	7.2	22.2	1.5
8.6982	176.2440	41.9549	569.0450	0.8560	2.4559	611.0000	0.0709	22	34.6	43.4	4.86	7.2	22.2	1.5
10.3100	209.6050	10.2301	568.7700	0.8467	3.0792	579.0000	0.0800	22	34.6	43.4	4.86	7.2	22.2	1.5
7.9218	164.9620	53.8184	569.1820	0.8066	2.3562	623.0000	0.0212	22	34.6	43.4	4.86	7.2	22.2	1.5
6.5691	177.4180	41.9105	569.0900	0.8231	3.4633	611.0000	0.0789	22	34.6	43.4	4.86	7.2	22.2	1.5
7.0804	184.7810	35.0107	568.9890	0.8138	1.8926	604.0000	0.0316	22	34.6	43.4	4.86	7.2	22.2	1.5
6.9771	187.2350	33.2617	568.7380	0.8172	2.2455	602.0000	0.0320	22	34.6	43.4	4.86	7.2	22.2	1.5
7.7255	168.2290	50.6248	569.3750	0.7879	3.9270	620.0000	0.0706	22	34.6	43.4	4.86	7.2	22.2	1.5
8.2783	185.5950	33.6542	569.3460	0.8235	3.5004	603.0000	0.0852	22	34.6	43.4	4.86	7.2	22.2	1.5
7.9768	171.4060	47.3452	569.6550	0.7814	4.0177	617.0000	0.0779	22	34.6	43.4	4.86	7.2	22.2	1.5
11.8213	195.8680	23.4037	569.5960	0.8139	2.9997	593.0000	0.0353	22	34.6	43.4	4.86	7.2	22.2	1.5
7.3871	169.7730	49.0963	569.9040	0.8490	2.5749	619.0000	0.0651	22	34.6	43.4	4.86	7.2	22.2	1.5
9.8457	203.7950	16.1909	569.8090	0.8491	2.6780	586.0000	0.0670	22	34.6	43.4	4.86	7.2	22.2	1.5
6.5653	207.2580	13.8085	569.1910	0.8611	1.6757	583.0000	0.0952	22	34.6	43.4	4.86	7.2	22.2	1.5
11.1935	196.8000	22.7330	570.2670	0.8349	2.3562	593.0000	0.0495	22	34.6	43.4	4.86	7.2	22.2	1.5

6.8893	198.2650	22.1139	569.8860	0.7719	4.3075	592.0000	0.0381	22	34.6	43.4	4.86	7.2	22.2	1.5
6.6183	203.7280	17.7799	569.2200	0.7440	4.7124	587.0000	0.0599	22	34.6	43.4	4.86	7.2	22.2	1.5
7.1946	170.7110	48.2334	570.7670	0.8393	3.0703	619.0000	0.0701	22	34.6	43.4	4.86	7.2	22.2	1.5
9.2058	211.6460	8.8586	570.1410	0.8430	3.0750	579.0000	0.0750	22	34.6	43.4	4.86	7.2	22.2	1.5
9.1528	173.9060	44.6324	571.3680	0.8144	3.6733	616.0000	0.0983	22	34.6	43.4	4.86	7.2	22.2	1.5
11.9917	205.8490	13.8888	571.1110	0.7929	3.6820	585.0000	0.0291	22	34.6	43.4	4.86	7.2	22.2	1.5
7.1634	165.1990	53.0130	571.9870	0.8020	3.7296	625.0000	0.0720	22	34.6	43.4	4.86	7.2	22.2	1.5
12.1153	197.3430	21.7242	572.2770	0.8068	3.1414	589.0000	0.0255	22	34.6	43.4	4.86	7.2	22.2	1.5
7.5795	173.7870	43.9614	573.0390	0.8566	2.8200	617.0000	0.0742	22	34.6	43.4	4.86	7.2	22.2	1.5
8.3608	187.1720	30.7333	573.2670	0.7974	3.7298	604.0000	0.0492	22	34.6	43.4	4.86	7.2	22.2	1.5
7.2449	191.6490	26.7932	573.2070	0.8078	1.1907	600.0000	0.0670	22	34.6	43.4	4.86	7.2	22.2	1.5
7.3864	189.1230	30.0970	572.9030	0.8516	1.4711	603.0000	0.1002	22	34.6	43.4	4.86	7.2	22.2	1.5
11.3097	206.2700	15.0737	571.9260	0.8562	2.6477	587.0000	0.0737	22	34.6	43.4	4.86	7.2	22.2	1.5
7.7504	172.1840	45.1344	573.8660	0.8857	2.9276	619.0000	0.1123	22	34.6	43.4	4.86	7.2	22.2	1.5
10.2896	186.8650	30.6160	574.3840	0.8490	2.3562	605.0000	0.0636	22	34.6	43.4	4.86	7.2	22.2	1.5
8.0557	180.3440	37.8259	574.1740	0.7945	0.8961	612.0000	0.0639	22	34.6	43.4	4.86	7.2	22.2	1.5
7.4711	174.7290	43.9733	574.0270	0.8700	2.3562	618.0000	0.0847	22	34.6	43.4	4.86	7.2	22.2	1.5
11.0925	357.6040	4.1958	503.8040	0.7854	0.7842	508.0000	0.0071	44.8	13.4	41.8	5.34	8.4	46.2	5.18
10.9305	351.1610	6.4398	507.5600	0.7819	0.4636	514.0000	0.0112	44.8	13.4	41.8	5.34	8.4	46.2	5.18

9.3788	352.5720	6.4093	506.5910	0.7680	0.1651	513.0000	0.0304	44.8	13.4	41.8	5.34	8.4	46.2	5.18
11.3207	352.9890	6.3473	506.6530	0.7822	0.6435	513.0000	0.0250	44.8	13.4	41.8	5.34	8.4	46.2	5.18
7.9452	355.4120	3.6487	507.3520	0.7960	1.5697	509.0000	0.0200	44.8	13.4	41.8	5.34	8.4	46.2	5.18
7.9205	351.8430	9.7485	505.2510	0.7536	5.6087	515.0000	0.0353	44.8	13.4	41.8	5.34	8.4	46.2	5.18
10.9313	344.7880	10.9275	510.0730	0.7679	6.2832	521.0000	0.0250	44.8	13.4	41.8	5.34	8.4	46.2	5.18
8.7193	351.5980	4.2459	510.7540	0.8278	2.1914	515.0000	0.0430	44.8	13.4	41.8	5.34	8.4	46.2	5.18
8.1590	351.8950	6.1221	508.8780	0.7748	5.8205	515.0000	0.0180	44.8	13.4	41.8	5.34	8.4	46.2	5.18
11.5008	353.8380	0.0000	513.0030	0.7927	1.1065	512.0000	0.0250	44.8	13.4	41.8	5.34	8.4	46.2	5.18
9.7160	345.2450	10.4438	511.5560	0.7677	5.6952	522.0000	0.0180	44.8	13.4	41.8	5.34	8.4	46.2	5.18
10.0842	341.8120	8.6177	516.3820	0.8068	1.5708	525.0000	0.0300	44.8	13.4	41.8	5.34	8.4	46.2	5.18
15.9822	350.1890	0.0000	517.0050	0.7748	5.8190	515.0000	0.0224	44.8	13.4	41.8	5.34	8.4	46.2	5.18
7.2870	338.4720	15.4865	513.5140	0.7642	5.8195	529.0000	0.0224	44.8	13.4	41.8	5.34	8.4	46.2	5.18
9.2472	342.2170	5.5486	519.4510	0.8172	2.2455	525.0000	0.0320	44.8	13.4	41.8	5.34	8.4	46.2	5.18
10.2436	344.5890	5.1292	517.8710	0.7503	6.0382	523.0000	0.0412	44.8	13.4	41.8	5.34	8.4	46.2	5.18
8.7155	110.2000	63.9739	555.0260	0.7642	5.8195	619.0000	0.0224	78	5.5	16.5	4.95	3.5	38	1.3
7.1607	116.8210	59.1320	553.8680	0.7221	5.8195	613.0000	0.0670	78	5.5	16.5	4.95	3.5	38	1.3
8.5512	116.7060	57.3825	555.6170	0.7395	5.4210	613.0000	0.0461	78	5.5	16.5	4.95	3.5	38	1.3
8.5559	131.4490	46.4203	552.5800	0.6972	5.5378	599.0000	0.0882	78	5.5	16.5	4.95	3.5	38	1.3
9.2575	128.3270	47.6339	554.3660	0.7289	5.3734	602.0000	0.0569	78	5.5	16.5	4.95	3.5	38	1.3

8.3531	114.2760	58.7770	557.2230	0.7646	4.5705	616.0000	0.0353	78	5.5	16.5	4.95	3.5	38	1.3
9.2106	136.8300	43.0176	550.9820	0.7547	0.1799	594.0000	0.0558	78	5.5	16.5	4.95	3.5	38	1.3
10.9136	142.9540	35.0089	552.9910	0.7615	4.4936	588.0000	0.0509	78	5.5	16.5	4.95	3.5	38	1.3
7.8610	124.0790	51.9537	555.0460	0.7874	3.9270	607.0000	0.0636	78	5.5	16.5	4.95	3.5	38	1.3
8.5896	117.0210	56.0158	557.9840	0.7501	5.6952	614.0000	0.0360	78	5.5	16.5	4.95	3.5	38	1.3
10.2333	141.4730	40.5480	549.4520	0.7719	0.4050	590.0000	0.0474	78	5.5	16.5	4.95	3.5	38	1.3
11.9054	145.5870	34.5164	551.4860	0.7926	3.4633	584.0000	0.0291	78	5.5	16.5	4.95	3.5	38	1.3
7.5817	131.7060	46.4551	553.5450	0.7419	4.5270	600.0000	0.0812	78	5.5	16.5	4.95	3.5	38	1.3
8.3462	147.3770	37.1504	547.8500	0.7846	0.7378	585.0000	0.0742	78	5.5	16.5	4.95	3.5	38	1.3
8.0563	137.1470	42.1746	552.8250	0.7799	4.0514	595.0000	0.0569	78	5.5	16.5	4.95	3.5	38	1.3
7.8761	130.2600	47.1054	554.8950	0.7578	0.1107	602.0000	0.0452	78	5.5	16.5	4.95	3.5	38	1.3
7.4784	151.0830	34.9780	547.0220	0.7841	0.7328	582.0000	0.0672	78	5.5	16.5	4.95	3.5	38	1.3
8.5481	158.1810	25.7993	549.2010	0.7471	4.8121	575.0000	0.0502	78	5.5	16.5	4.95	3.5	38	1.3
7.4841	139.8370	40.8304	552.1700	0.7510	4.6217	593.0000	0.0552	78	5.5	16.5	4.95	3.5	38	1.3
8.8297	140.9410	37.7786	554.2240	0.7753	0.4638	591.0000	0.0381	78	5.5	16.5	4.95	3.5	38	1.3
7.5615	158.7880	28.9165	546.0830	0.7954	0.8761	575.0000	0.0779	78	5.5	16.5	4.95	3.5	38	1.3
10.5051	169.8790	15.6540	548.3460	0.7547	4.5325	564.0000	0.0657	78	5.5	16.5	4.95	3.5	38	1.3
7.7333	149.5270	32.5872	551.4130	0.7085	5.0712	584.0000	0.0852	78	5.5	16.5	4.95	3.5	38	1.3
7.2763	146.6260	33.5620	553.4380	0.7510	0.0906	587.0000	0.0502	78	5.5	16.5	4.95	3.5	38	1.3

8.7671	171.7420	17.9711	545.0290	0.7608	6.1179	563.0000	0.0304	78	5.5	16.5	4.95	3.5	38	1.3
8.4081	170.5770	16.6102	547.3900	0.7505	4.8233	564.0000	0.0452	78	5.5	16.5	4.95	3.5	38	1.3
8.1778	160.6610	24.3933	549.6070	0.7431	5.1760	574.0000	0.0447	78	5.5	16.5	4.95	3.5	38	1.3
8.2139	160.5510	21.4517	552.5480	0.7333	6.1305	574.0000	0.0657	78	5.5	16.5	4.95	3.5	38	1.3
6.9369	174.6560	18.7917	542.2080	0.7518	0.2268	561.0000	0.0666	78	5.5	16.5	4.95	3.5	38	1.3
8.5373	177.5180	11.7070	546.2930	0.7473	4.7124	558.0000	0.0549	78	5.5	16.5	4.95	3.5	38	1.3
9.6841	169.3520	17.3981	548.6020	0.7642	5.1760	566.0000	0.0224	78	5.5	16.5	4.95	3.5	38	1.3
17.7141	205.6930	0.0000	531.0000	0.7432	5.0342	531.0000	0.0618	78	5.5	16.5	4.95	3.5	38	1.3
8.0630	197.7410	4.7419	534.2580	0.6904	5.3145	539.0000	0.1146	78	5.5	16.5	4.95	3.5	38	1.3
7.3991	183.3300	14.4544	538.5460	0.7369	6.2064	553.0000	0.0651	78	5.5	16.5	4.95	3.5	38	1.3
12.3172	193.3920	1.0913	541.9090	0.7328	5.0612	543.0000	0.0585	78	5.5	16.5	4.95	3.5	38	1.3
8.9091	180.2480	9.7156	546.2840	0.7395	5.2710	556.0000	0.0471	78	5.5	16.5	4.95	3.5	38	1.3
11.0771	195.0910	0.7865	541.2140	0.7784	4.7114	541.0000	0.0112	78	5.5	16.5	4.95	3.5	38	1.3
7.7602	190.1490	3.4666	543.5330	0.7360	5.6400	547.0000	0.0500	78	5.5	16.5	4.95	3.5	38	1.3
7.1503	77.9987	6.7096	722.2980	0.7607	5.9021	728.0000	0.0200	78	5.5	16.5	4.95	3.5	38	1.3
10.6084	78.0586	6.6270	722.3800	0.7854	3.6052	728.0000	0.0100	78	5.5	16.5	4.95	3.5	38	1.3
12.7777	80.2258	4.5109	722.4920	0.7995	2.3553	726.0000	0.0150	78	5.5	16.5	4.95	3.5	38	1.3
9.6874	78.3618	6.5635	722.4410	0.7855	0.7839	728.0000	0.0112	78	5.5	16.5	4.95	3.5	38	1.3
12.7495	78.4482	6.8097	722.1910	0.7854	6.2832	728.0000	0.0050	78	5.5	16.5	4.95	3.5	38	1.3

10.2229	78.2211	6.0881	722.9160	0.7784	0.0007	729.0000	0.0224	78	5.5	16.5	4.95	3.5	38	1.3
10.9580	76.3256	7.8956	723.1040	0.7819	0.4645	731.0000	0.0112	78	5.5	16.5	4.95	3.5	38	1.3
7.3918	75.3848	9.0382	722.9620	0.7677	5.6952	732.0000	0.0112	78	5.5	16.5	4.95	3.5	38	1.3
11.3544	76.4292	8.0696	722.9340	0.7819	6.2832	730.0000	0.0100	78	5.5	16.5	4.95	3.5	38	1.3
8.4288	74.5210	10.2706	722.7290	0.7890	1.1072	733.0000	0.0112	78	5.5	16.5	4.95	3.5	38	1.3
11.2330	78.1553	5.4804	723.5220	0.7784	0.3211	728.0000	0.0224	78	5.5	16.5	4.95	3.5	38	1.3
8.1846	75.2891	8.3147	723.6850	0.7784	0.3211	732.0000	0.0180	78	5.5	16.5	4.95	3.5	38	1.3
10.0504	76.3474	7.2490	723.7550	0.7889	1.5708	730.0000	0.0100	78	5.5	16.5	4.95	3.5	38	1.3
12.6552	76.4086	7.1861	723.8160	0.7784	0.0007	730.0000	0.0112	78	5.5	16.5	4.95	3.5	38	1.3
13.5843	74.5231	9.0544	723.9460	0.7854	6.2832	733.0000	0.0000	78	5.5	16.5	4.95	3.5	38	1.3
7.6819	71.5756	11.9506	724.0490	0.7678	5.6957	736.0000	0.0250	78	5.5	16.5	4.95	3.5	38	1.3
10.7725	77.3093	5.3882	724.6150	0.7713	5.9605	730.0000	0.0200	78	5.5	16.5	4.95	3.5	38	1.3
10.8802	74.3888	8.4692	724.5320	0.7748	5.8203	732.0000	0.0141	78	5.5	16.5	4.95	3.5	38	1.3
10.0321	74.4540	8.3721	724.6300	0.7819	0.4636	732.0000	0.0112	78	5.5	16.5	4.95	3.5	38	1.3
12.6616	76.5767	6.1657	724.8400	0.7925	1.5698	730.0000	0.0150	78	5.5	16.5	4.95	3.5	38	1.3
10.7709	76.6346	6.0300	724.9770	0.7784	4.7134	730.0000	0.0100	78	5.5	16.5	4.95	3.5	38	1.3
7.5940	73.6992	8.8293	725.1710	0.7572	5.4982	734.0000	0.0353	78	5.5	16.5	4.95	3.5	38	1.3
7.5723	72.4231	9.5972	725.4210	0.7748	4.7124	734.0000	0.0150	78	5.5	16.5	4.95	3.5	38	1.3
10.3943	71.5854	10.1001	725.9000	0.7854	3.5540	736.0000	0.0000	78	5.5	16.5	4.95	3.5	38	1.3

10.5170	71.6565	9.9542	726.0460	0.7855	1.7682	736.0000	0.0050	78	5.5	16.5	4.95	3.5	38	1.3
10.3552	73.7208	8.0436	725.9560	0.7961	1.3253	734.0000	0.0255	78	5.5	16.5	4.95	3.5	38	1.3
11.4288	73.8569	7.5237	726.4760	0.7819	0.4636	734.0000	0.0112	78	5.5	16.5	4.95	3.5	38	1.3
7.0526	73.9077	7.7045	726.2960	0.8316	1.8625	734.0000	0.0569	78	5.5	16.5	4.95	3.5	38	1.3
11.0552	72.6465	8.0938	726.9230	0.7819	0.4604	734.0000	0.0158	78	5.5	16.5	4.95	3.5	38	1.3
8.2471	71.7415	8.8804	727.1200	0.7925	1.5732	736.0000	0.0158	78	5.5	16.5	4.95	3.5	38	1.3
14.0942	72.8818	7.4614	727.5480	0.7854	3.1416	734.0000	0.0000	78	5.5	16.5	4.95	3.5	38	1.3
13.1323	72.9542	7.2188	727.7900	0.7854	4.1037	734.0000	0.0050	78	5.5	16.5	4.95	3.5	38	1.3
10.6043	73.0096	7.2310	727.7800	0.7785	4.3897	735.0000	0.0206	78	5.5	16.5	4.95	3.5	38	1.3
8.2564	69.9275	9.3612	728.6390	0.7749	0.0019	738.0000	0.0200	78	5.5	16.5	4.95	3.5	38	1.3
8.2568	69.0107	10.0838	728.9160	0.7714	6.2832	739.0000	0.0200	78	5.5	16.5	4.95	3.5	38	1.3
10.8116	72.0811	7.0014	728.9990	0.7925	2.3562	736.0000	0.0071	78	5.5	16.5	4.95	3.5	38	1.3
10.0550	230.8700	9.5703	515.4300	0.7995	2.3562	525.0000	0.0141	78	5.5	16.5	4.95	3.5	38	1.3
8.7557	230.7440	8.9741	516.0260	0.7713	5.0341	525.0000	0.0158	78	5.5	16.5	4.95	3.5	38	1.3
9.9518	230.8740	10.0476	514.9520	0.7925	1.5708	525.0000	0.0100	78	5.5	16.5	4.95	3.5	38	1.3
9.9389	230.7480	9.4385	515.5610	0.7784	4.7124	525.0000	0.0100	78	5.5	16.5	4.95	3.5	38	1.3
7.6460	230.8190	10.7041	514.2960	0.8172	2.4669	525.0000	0.0320	78	5.5	16.5	4.95	3.5	38	1.3
7.9400	231.6920	9.0934	514.9070	0.7858	3.9270	524.0000	0.0283	78	5.5	16.5	4.95	3.5	38	1.3
8.5339	236.7640	5.3546	513.6450	0.7931	3.7295	519.0000	0.0360	78	5.5	16.5	4.95	3.5	38	1.3

7.7923	236.7070	6.4633	512.5430	0.7713	4.7127	518.0000	0.0050	78	5.5	16.5	4.95	3.5	38	1.3
7.0063	236.7100	6.9531	512.0550	0.7860	3.9273	519.0000	0.0269	78	5.5	16.5	4.95	3.5	38	1.3
8.7240	241.6730	3.3844	510.6160	0.7785	4.2491	514.0000	0.0224	78	5.5	16.5	4.95	3.5	38	1.3
10.0598	242.6280	2.6585	510.3440	0.7820	4.2450	512.0000	0.0112	78	5.5	16.5	4.95	3.5	38	1.3
16.9318	244.4720	0.1245	510.8980	0.7854	3.2613	511.0000	0.0050	78	5.5	16.5	4.95	3.5	38	1.3
7.9645	101.5180	33.5780	611.4220	0.7080	5.2315	645.0000	0.0804	78	5.5	16.5	4.95	3.5	38	1.3
8.4106	113.1140	23.3057	610.6940	0.6972	5.5378	634.0000	0.0882	78	5.5	16.5	4.95	3.5	38	1.3
10.7114	125.5600	13.9750	609.0250	0.7644	6.2830	623.0000	0.0304	78	5.5	16.5	4.95	3.5	38	1.3
6.8828	130.8700	11.4912	607.5090	0.7829	0.7086	619.0000	0.0461	78	5.5	16.5	4.95	3.5	38	1.3
13.7170	142.2410	3.1024	605.8980	0.7717	0.3214	609.0000	0.0381	78	5.5	16.5	4.95	3.5	38	1.3
13.1490	138.7240	5.4667	606.5360	0.7748	5.8200	611.0000	0.0112	78	5.5	16.5	4.95	3.5	38	1.3
7.5164	141.3630	6.0898	604.9100	0.7792	0.6203	611.0000	0.0430	78	5.5	16.5	4.95	3.5	38	1.3
8.3722	131.8250	11.3681	606.6320	0.8036	1.2924	618.0000	0.0364	78	5.5	16.5	4.95	3.5	38	1.3
8.3019	130.1410	15.8579	605.1420	0.7929	1.0304	621.0000	0.0291	78	5.5	16.5	4.95	3.5	38	1.3
8.7005	134.7720	14.8159	603.1840	0.7607	5.3559	618.0000	0.0250	78	5.5	16.5	4.95	3.5	38	1.3
8.2394	143.2370	10.6294	600.3710	0.7682	4.4341	611.0000	0.0364	78	5.5	16.5	4.95	3.5	38	1.3
8.0952	109.0150	31.3832	607.6170	0.7293	5.9614	639.0000	0.0632	78	5.5	16.5	4.95	3.5	38	1.3
9.3686	116.6040	25.1255	606.8740	0.7467	5.9244	632.0000	0.0427	78	5.5	16.5	4.95	3.5	38	1.3
8.6368	122.0310	22.6676	605.3320	0.8208	2.1588	628.0000	0.0360	78	5.5	16.5	4.95	3.5	38	1.3

7.4928	135.3680	19.4817	599.5180	0.7615	0.2187	619.0000	0.0509	78	5.5	16.5	4.95	3.5	38	1.3
7.4215	144.3910	13.0598	597.9450	0.7501	5.3002	610.0000	0.0320	78	5.5	16.5	4.95	3.5	38	1.3
7.7474	104.8500	41.1398	603.8600	0.7369	6.2064	645.0000	0.0651	78	5.5	16.5	4.95	3.5	38	1.3
7.9765	109.4620	37.8953	603.1050	0.7614	0.2187	641.0000	0.0461	78	5.5	16.5	4.95	3.5	38	1.3
8.8955	122.9520	27.5140	601.4860	0.7398	5.9917	629.0000	0.0522	78	5.5	16.5	4.95	3.5	38	1.3
10.1373	133.2980	20.2577	599.7420	0.7434	6.0858	620.0000	0.0509	78	5.5	16.5	4.95	3.5	38	1.3
11.8318	145.5060	10.4750	598.5250	0.7467	5.0712	609.0000	0.0427	78	5.5	16.5	4.95	3.5	38	1.3
8.9638	150.9900	8.5269	596.4730	0.7527	4.3906	605.0000	0.0789	78	5.5	16.5	4.95	3.5	38	1.3
8.0093	120.8090	32.8958	599.1040	0.7682	4.4341	632.0000	0.0364	78	5.5	16.5	4.95	3.5	38	1.3
8.3060	131.1620	25.5645	597.4360	0.7502	5.1173	623.0000	0.0381	78	5.5	16.5	4.95	3.5	38	1.3
8.1001	101.0370	73.2081	856.7920	0.8174	1.8491	930.0000	0.0364	47.05	14.35	38.6	5.015	11.3	20.8	2
8.1479	104.5540	70.3309	855.6690	0.8102	1.9513	926.0000	0.0269	47.05	14.35	38.6	5.015	11.3	20.8	2
8.3701	98.3409	78.1381	854.8620	0.8066	2.6780	933.0000	0.0224	47.05	14.35	38.6	5.015	11.3	20.8	2
8.7329	110.3750	67.5153	852.4850	0.8280	2.8198	920.0000	0.0474	47.05	14.35	38.6	5.015	11.3	20.8	2
9.5404	107.1480	71.7792	852.2210	0.8208	2.7367	924.0000	0.0381	47.05	14.35	38.6	5.015	11.3	20.8	2
8.3481	107.1740	73.0290	850.9710	0.8279	2.6780	924.0000	0.0447	47.05	14.35	38.6	5.015	11.3	20.8	2
7.7234	111.2630	73.7779	845.2220	0.8250	1.5708	919.0000	0.0549	47.05	14.35	38.6	5.015	11.3	20.8	2
8.7827	114.5550	72.6391	842.3610	0.8007	1.0637	915.0000	0.0514	47.05	14.35	38.6	5.015	11.3	20.8	2
7.7664	118.8420	69.7952	840.2050	0.8148	1.3045	910.0000	0.0569	47.05	14.35	38.6	5.015	11.3	20.8	2

7.9863	129.9030	61.5012	836.4990	0.8526	2.0989	898.0000	0.0694	47.05	14.35	38.6	5.015	11.3	20.8	2
9.1788	110.5600	77.5026	841.4970	0.7999	1.2491	919.0000	0.0316	47.05	14.35	38.6	5.015	11.3	20.8	2
8.6464	117.6180	73.1570	837.8430	0.8384	2.1588	911.0000	0.0540	47.05	14.35	38.6	5.015	11.3	20.8	2
8.8626	123.9180	69.5607	834.4390	0.8175	1.6952	904.0000	0.0403	47.05	14.35	38.6	5.015	11.3	20.8	2
8.4092	108.3230	81.5265	839.4740	0.8031	2.8966	921.0000	0.0206	47.05	14.35	38.6	5.015	11.3	20.8	2
6.9338	108.8530	82.4271	837.5730	0.8208	1.9757	920.0000	0.0381	47.05	14.35	38.6	5.015	11.3	20.8	2
7.5897	121.9190	72.4082	833.5920	0.8423	2.8198	906.0000	0.0632	47.05	14.35	38.6	5.015	11.3	20.8	2
7.5949	103.5450	86.4622	839.5380	0.8207	2.3562	926.0000	0.0353	47.05	14.35	38.6	5.015	11.3	20.8	2
8.4104	113.6090	79.4103	835.5900	0.8457	2.7468	915.0000	0.0649	47.05	14.35	38.6	5.015	11.3	20.8	2
9.3024	106.2860	85.1672	837.8330	0.7962	1.3258	923.0000	0.0206	47.05	14.35	38.6	5.015	11.3	20.8	2
8.9670	114.5950	78.9788	835.0210	0.8527	2.0032	914.0000	0.0715	47.05	14.35	38.6	5.015	11.3	20.8	2
7.9817	102.4850	88.7270	838.2730	0.7961	3.1416	927.0000	0.0150	47.05	14.35	38.6	5.015	11.3	20.8	2
8.7314	110.5550	83.9562	834.0440	0.8314	2.1294	918.0000	0.0471	47.05	14.35	38.6	5.015	11.3	20.8	2
7.4552	122.6300	75.0851	829.9150	0.8747	2.8966	905.0000	0.1027	47.05	14.35	38.6	5.015	11.3	20.8	2
9.3660	106.5270	88.4138	833.5860	0.8315	1.9890	922.0000	0.0492	47.05	14.35	38.6	5.015	11.3	20.8	2
8.6670	111.5390	87.3876	828.6120	0.8282	1.7682	916.0000	0.0509	47.05	14.35	38.6	5.015	11.3	20.8	2
8.8935	122.6280	79.1760	824.8240	0.8219	1.4057	904.0000	0.0608	47.05	14.35	38.6	5.015	11.3	20.8	2
9.0776	111.5000	87.8699	828.1300	0.8243	2.4469	916.0000	0.0390	47.05	14.35	38.6	5.015	11.3	20.8	2
9.0415	117.5900	84.5203	824.4800	0.8209	1.8158	909.0000	0.0412	47.05	14.35	38.6	5.015	11.3	20.8	2

9.0716	115.5020	87.3972	823.6030	0.8208	2.5536	911.0000	0.0360	47.05	14.35	38.6	5.015	11.3	20.8	2
8.7356	116.4500	86.9717	823.0280	0.8351	1.9513	910.0000	0.0538	47.05	14.35	38.6	5.015	11.3	20.8	2
9.3821	92.9542	8.5656	737.4340	0.7829	0.7087	746.0000	0.0500	78	5.5	16.5	4.95	3.5	38	1.3
7.9451	78.8715	19.4912	740.5090	0.7578	0.1107	760.0000	0.0452	78	5.5	16.5	4.95	3.5	38	1.3
8.7150	52.6904	37.2665	748.7330	0.7974	0.9828	786.0000	0.0540	78	5.5	16.5	4.95	3.5	38	1.3
8.4160	97.0573	9.0916	732.9120	0.7963	1.1903	741.0000	0.0269	78	5.5	16.5	4.95	3.5	38	1.3
9.8239	89.9757	13.0508	735.9490	0.7610	6.2832	749.0000	0.0350	78	5.5	16.5	4.95	3.5	38	1.3
7.2004	63.6832	20.7125	754.2880	0.7349	4.5953	775.0000	0.0854	78	5.5	16.5	4.95	3.5	38	1.3
7.5769	96.1705	13.8433	729.1570	0.7748	4.7124	743.0000	0.0150	78	5.5	16.5	4.95	3.5	38	1.3
12.7943	101.0990	6.1674	731.8330	0.7677	5.3005	738.0000	0.0224	78	5.5	16.5	4.95	3.5	38	1.3
8.7607	93.0337	11.0955	734.9050	0.7588	0.3218	746.0000	0.0679	78	5.5	16.5	4.95	3.5	38	1.3
7.4822	82.9753	17.6517	738.3480	0.7115	5.7315	756.0000	0.0762	78	5.5	16.5	4.95	3.5	38	1.3
7.1530	74.8840	20.4167	743.5830	0.7400	4.8922	764.0000	0.0558	78	5.5	16.5	4.95	3.5	38	1.3
7.1833	106.3310	8.7422	724.2580	0.7362	5.0929	733.0000	0.0538	78	5.5	16.5	4.95	3.5	38	1.3
12.4388	108.2310	3.1638	727.8360	0.7539	6.1588	731.0000	0.0403	78	5.5	16.5	4.95	3.5	38	1.3
7.5639	100.1730	8.3911	730.6090	0.7537	5.1763	739.0000	0.0474	78	5.5	16.5	4.95	3.5	38	1.3
10.1050	103.1180	1.0405	734.9630	0.7677	5.6954	736.0000	0.0390	78	5.5	16.5	4.95	3.5	38	1.3
8.1705	97.0183	2.7091	739.2910	0.7432	5.0342	742.0000	0.0522	78	5.5	16.5	4.95	3.5	38	1.3
18.8425	96.9719	0.0000	742.0030	0.7854	3.9270	741.0000	0.0112	78	5.5	16.5	4.95	3.5	38	1.3

10.3768	41.3505	52.5938	950.4060	0.7925	2.3555	1003.0000	0.0050	52.25	11.1	36.65	4.9	8.3	21.55	1.105
8.0693	54.8629	31.7938	959.2060	0.8104	3.1416	991.0000	0.0350	52.25	11.1	36.65	4.9	8.3	21.55	1.105
9.0275	72.7281	9.8677	964.1320	0.8911	2.2896	974.0000	0.1059	52.25	11.1	36.65	4.9	8.3	21.55	1.105
8.1549	39.8894	51.7833	953.2170	0.7926	1.2491	1005.0000	0.0158	52.25	11.1	36.65	4.9	8.3	21.55	1.105
8.6637	55.6970	31.3669	959.6330	0.8525	2.3036	991.0000	0.0672	47.05	14.35	38.6	5.015	11.3	20.8	2
8.6690	67.6404	17.1025	962.8980	0.8595	2.4038	980.0000	0.0742	47.05	14.35	38.6	5.015	11.3	20.8	2
11.0012	38.7046	53.2755	954.7240	0.7925	2.3562	1008.0000	0.0071	47.05	14.35	38.6	5.015	11.3	20.8	2
8.6928	52.1837	37.7248	958.2750	0.8208	2.5536	996.0000	0.0360	47.05	14.35	38.6	5.015	11.3	20.8	2
8.9631	59.1611	38.7269	949.2730	0.7434	4.9098	988.0000	0.0509	47.05	14.35	38.6	5.015	11.3	20.8	2
8.8431	57.6858	38.4481	952.5520	0.7824	4.0377	991.0000	0.0320	47.05	14.35	38.6	5.015	11.3	20.8	2
9.4327	68.7715	25.3820	956.6180	0.8034	3.3067	982.0000	0.0304	47.05	14.35	38.6	5.015	11.3	20.8	2
9.1747	85.3198	6.7438	960.2560	0.8314	2.7230	967.0000	0.0632	47.05	14.35	38.6	5.015	11.3	20.8	2
8.2527	285.3340	40.3092	836.6910	0.8806	2.4669	877.0000	0.0958	68.95	12.15	18.9	4.97	6.55	29.9	3.19
8.3130	278.7170	49.3536	838.6460	0.8560	2.3562	888.0000	0.0706	68.95	12.15	18.9	4.97	6.55	29.9	3.19
8.0403	272.4640	57.5460	841.4540	0.8433	3.1416	899.0000	0.0798	68.95	12.15	18.9	4.97	6.55	29.9	3.19
8.7123	277.6530	55.1450	845.8550	0.8661	3.1850	901.0000	0.1146	68.95	12.15	18.9	4.97	6.55	29.9	3.19
7.9319	259.8570	65.5731	839.4270	0.8876	2.4593	905.0000	0.1027	68.95	12.15	18.9	4.97	6.55	29.9	3.19
8.2354	248.3930	78.5120	842.4880	0.8774	2.6547	921.0000	0.0959	68.95	12.15	18.9	4.97	6.55	29.9	3.19
7.7641	253.6610	68.9758	839.0240	0.8570	1.7455	908.0000	0.0861	68.95	12.15	18.9	4.97	6.55	29.9	3.19

7.8816	232.3240	91.7966	843.2030	0.8596	2.1225	935.0000	0.0762	68.95	12.15	18.9	4.97	6.55	29.9	3.19
8.3313	229.3220	96.8036	846.1960	0.8456	2.6423	943.0000	0.0626	68.95	12.15	18.9	4.97	6.55	29.9	3.19
7.6546	226.6770	100.7790	850.2210	0.8674	2.8707	951.0000	0.0931	68.95	12.15	18.9	4.97	6.55	29.9	3.19
8.4197	265.8880	54.5687	839.4310	0.8408	1.4057	894.0000	0.0910	68.95	12.15	18.9	4.97	6.55	29.9	3.19
7.9861	242.0450	79.9612	842.0390	0.8235	1.2120	922.0000	0.0852	68.95	12.15	18.9	4.97	6.55	29.9	3.19
7.3942	219.4740	103.3900	845.6100	0.8289	1.4940	949.0000	0.0651	68.95	12.15	18.9	4.97	6.55	29.9	3.19
7.5686	207.1390	116.8770	851.1230	0.8349	2.4981	968.0000	0.0500	68.95	12.15	18.9	4.97	6.55	29.9	3.19
7.1459	206.0480	120.0680	854.9320	0.8282	2.9442	975.0000	0.0509	68.95	12.15	18.9	4.97	6.55	29.9	3.19
8.5807	258.1130	61.5506	842.4490	0.8151	1.0223	904.0000	0.1051	68.95	12.15	18.9	4.97	6.55	29.9	3.19
8.0766	233.3190	86.9011	846.0990	0.8451	1.3734	933.0000	0.1016	68.95	12.15	18.9	4.97	6.55	29.9	3.19
7.8877	211.2250	110.3950	849.6050	0.8296	1.3734	960.0000	0.0763	68.95	12.15	18.9	4.97	6.55	29.9	3.19
8.0359	224.8780	93.9286	850.0710	0.8549	1.5208	944.0000	0.0998	68.95	12.15	18.9	4.97	6.55	29.9	3.19
6.2936	208.7980	110.2630	854.7370	0.6520	5.3929	965.0000	0.1343	68.95	12.15	18.9	4.97	6.55	29.9	3.19
10.0853	86.9419	54.3440	371.6560	0.7996	3.1416	426.0000	0.0250	85.6	3.8	10.6	6.7	5.4	66.2	3.28
10.5602	85.0396	57.3003	370.7000	0.8069	1.5708	428.0000	0.0250	85.6	3.8	10.6	6.7	5.4	66.2	3.28
7.5546	81.1008	62.1342	369.8660	0.8137	2.6017	432.0000	0.0320	85.6	3.8	10.6	6.7	5.4	66.2	3.28
10.5224	83.1621	61.1185	368.8810	0.8067	2.9437	430.0000	0.0255	85.6	3.8	10.6	6.7	5.4	66.2	3.28
11.2284	86.4575	60.0038	366.9960	0.7892	3.7853	427.0000	0.0291	85.6	3.8	10.6	6.7	5.4	66.2	3.28
10.3943	81.5208	66.0384	365.9620	0.7854	3.6741	432.0000	0.0071	85.6	3.8	10.6	6.7	5.4	66.2	3.28

7.1854	80.6348	68.5619	364.4380	0.7502	5.1173	433.0000	0.0381	85.6	3.8	10.6	6.7	5.4	66.2	3.28
6.4696	75.6982	74.8137	363.1860	0.7762	4.1244	438.0000	0.0540	85.6	3.8	10.6	6.7	5.4	66.2	3.28
6.5961	81.7617	70.1130	361.8870	0.7575	6.2832	432.0000	0.0400	85.6	3.8	10.6	6.7	5.4	66.2	3.28
7.8770	97.8250	55.4221	360.5780	0.7262	4.9235	416.0000	0.0715	85.6	3.8	10.6	6.7	5.4	66.2	3.28
8.3908	103.9400	51.1648	358.8350	0.7340	4.7124	410.0000	0.0749	85.6	3.8	10.6	6.7	5.4	66.2	3.28
10.0126	92.0049	59.2899	362.7100	0.7749	6.2832	422.0000	0.0250	85.6	3.8	10.6	6.7	5.4	66.2	3.28
10.4195	98.0708	54.6938	361.3060	0.7897	0.8757	416.0000	0.0403	85.6	3.8	10.6	6.7	5.4	66.2	3.28
12.2460	119.1760	35.7957	359.2040	0.7931	0.9828	395.0000	0.0360	85.6	3.8	10.6	6.7	5.4	66.2	3.28
9.0963	123.2420	33.3661	357.6340	0.7293	5.0341	391.0000	0.0632	85.6	3.8	10.6	6.7	5.4	66.2	3.28
8.5810	123.3610	35.2544	355.7460	0.7274	4.7124	391.0000	0.0848	85.6	3.8	10.6	6.7	5.4	66.2	3.28
7.3143	119.4270	40.7747	354.2250	0.7366	4.8775	395.0000	0.0608	85.6	3.8	10.6	6.7	5.4	66.2	3.28
7.3987	101.5600	54.3210	358.6790	0.8289	1.4940	413.0000	0.0800	85.6	3.8	10.6	6.7	5.4	66.2	3.28
7.5510	109.6290	48.2419	356.7580	0.8052	1.0427	405.0000	0.0694	85.6	3.8	10.6	6.7	5.4	66.2	3.28
7.2023	116.7510	43.3989	354.6010	0.7581	0.1974	398.0000	0.0509	85.6	3.8	10.6	6.7	5.4	66.2	3.28
8.9816	106.0730	48.3795	593.6200	0.7185	5.2405	642.0000	0.0694	85.6	3.8	10.6	6.7	5.4	66.2	3.28
7.7827	111.0840	42.3873	593.6130	0.7648	4.4674	636.0000	0.0412	85.6	3.8	10.6	6.7	5.4	66.2	3.28
10.4362	119.4180	33.4145	593.5860	0.7610	6.2832	627.0000	0.0350	85.6	3.8	10.6	6.7	5.4	66.2	3.28
9.0271	124.4100	27.3885	593.6110	0.7254	5.6725	621.0000	0.0610	85.6	3.8	10.6	6.7	5.4	66.2	3.28
7.3907	92.7195	62.3961	594.6040	0.7927	3.6052	657.0000	0.0224	85.6	3.8	10.6	6.7	5.4	66.2	3.28

8.3984	98.8962	54.6424	595.3580	0.8011	3.6820	650.0000	0.0582	85.6	3.8	10.6	6.7	5.4	66.2	3.28
8.9109	112.8790	39.6145	595.3850	0.7443	4.6356	635.0000	0.0651	85.6	3.8	10.6	6.7	5.4	66.2	3.28
9.0128	113.2430	42.2049	595.7950	0.8182	1.3909	638.0000	0.0558	85.6	3.8	10.6	6.7	5.4	66.2	3.28
7.6535	90.4109	63.1970	596.8030	0.8101	2.2143	660.0000	0.0250	85.6	3.8	10.6	6.7	5.4	66.2	3.28
8.4855	96.3744	56.0095	596.9910	0.7510	4.6217	653.0000	0.0552	85.6	3.8	10.6	6.7	5.4	66.2	3.28
8.7361	110.3220	41.0279	596.9720	0.7505	4.8231	638.0000	0.0452	85.6	3.8	10.6	6.7	5.4	66.2	3.28
7.7713	102.9590	51.0557	597.9440	0.8491	2.0344	649.0000	0.0670	85.6	3.8	10.6	6.7	5.4	66.2	3.28
8.2338	88.9048	63.6050	598.3950	0.8031	2.1588	662.0000	0.0180	85.6	3.8	10.6	6.7	5.4	66.2	3.28
8.9712	97.8306	53.4730	598.5270	0.7610	4.7124	652.0000	0.0350	85.6	3.8	10.6	6.7	5.4	66.2	3.28
6.4425	92.1128	33.0274	554.9730	0.8119	0.9828	588.0000	0.1077	85.6	3.8	10.6	6.7	5.4	66.2	3.28
8.0466	97.8776	27.5316	554.4680	0.7214	0.0500	582.0000	0.0998	85.6	3.8	10.6	6.7	5.4	66.2	3.28
8.3499	102.7950	22.9674	554.0330	0.7747	0.6350	577.0000	0.1175	85.6	3.8	10.6	6.7	5.4	66.2	3.28
6.9523	97.5703	28.2094	553.7910	0.7764	0.6511	582.0000	0.1312	85.6	3.8	10.6	6.7	5.4	66.2	3.28
7.3335	84.7461	39.3527	555.6470	0.7756	0.5191	595.0000	0.0403	85.6	3.8	10.6	6.7	5.4	66.2	3.28
8.5308	89.5146	35.0244	554.9760	0.7809	0.6857	590.0000	0.0709	85.6	3.8	10.6	6.7	5.4	66.2	3.28
7.1969	80.2903	44.4647	554.5350	0.7692	0.4636	599.0000	0.0558	85.6	3.8	10.6	6.7	5.4	66.2	3.28
8.0412	88.0753	36.6796	554.3200	0.7311	0.0588	591.0000	0.0849	85.6	3.8	10.6	6.7	5.4	66.2	3.28
7.1110	82.4590	40.1052	556.8950	0.8351	1.9513	597.0000	0.0538	85.6	3.8	10.6	6.7	5.4	66.2	3.28
7.3641	76.2275	47.1738	555.8260	0.8103	1.7359	603.0000	0.0304	85.6	3.8	10.6	6.7	5.4	66.2	3.28

7.7942	70.0027	53.8577	555.1420	0.7995	2.3562	609.0000	0.0141	85.6	3.8	10.6	6.7	5.4	66.2	3.28
7.8073	71.7864	52.2238	554.7760	0.7625	0.3948	607.0000	0.0649	85.6	3.8	10.6	6.7	5.4	66.2	3.28
6.4842	90.1655	31.0369	557.9630	0.8538	3.3866	589.0000	0.1231	85.6	3.8	10.6	6.7	5.4	66.2	3.28
6.8408	82.9335	39.5836	556.4160	0.8467	3.0792	596.0000	0.0800	85.6	3.8	10.6	6.7	5.4	66.2	3.28
7.3642	73.7822	49.7182	555.2820	0.8598	2.6780	605.0000	0.0781	85.6	3.8	10.6	6.7	5.4	66.2	3.28
6.6598	61.5668	62.0996	554.9000	0.8653	1.3521	617.0000	0.1374	85.6	3.8	10.6	6.7	5.4	66.2	3.28
8.0211	138.3300	49.3262	464.6740	0.7860	0.7854	514.0000	0.0353	85.6	3.8	10.6	6.7	5.4	66.2	3.28
8.3291	145.3150	43.1946	463.8050	0.7822	0.6435	507.0000	0.0250	85.6	3.8	10.6	6.7	5.4	66.2	3.28
10.4916	150.3030	39.0964	462.9040	0.7960	2.0344	502.0000	0.0112	85.6	3.8	10.6	6.7	5.4	66.2	3.28
7.0275	151.2920	39.0348	461.9650	0.7466	5.7640	501.0000	0.0403	85.6	3.8	10.6	6.7	5.4	66.2	3.28
7.4173	129.9930	58.2805	463.7200	0.7750	0.2450	522.0000	0.0206	85.6	3.8	10.6	6.7	5.4	66.2	3.28
9.8009	139.9780	48.8330	463.1670	0.7643	6.0858	512.0000	0.0255	85.6	3.8	10.6	6.7	5.4	66.2	3.28
8.3653	145.9640	43.2907	462.7110	0.7856	0.7858	505.0000	0.0180	85.6	3.8	10.6	6.7	5.4	66.2	3.28
8.6147	132.7610	55.4973	463.5030	0.7854	3.9289	519.0000	0.0050	12.6	24.8	62.6	5.32	10	34.6	3.48
7.7872	137.6570	51.2087	462.7910	0.7786	4.2487	514.0000	0.0224	12.6	24.8	62.6	5.32	10	34.6	3.48
11.8257	139.6370	49.5296	462.4700	0.7819	4.7124	512.0000	0.0050	12.6	24.8	62.6	5.32	10	34.6	3.48
10.2934	141.6250	47.5000	462.5000	0.7856	0.7854	510.0000	0.0212	12.6	24.8	62.6	5.32	10	34.6	3.48
10.1779	145.3980	44.1974	461.8030	0.7571	5.4978	506.0000	0.0283	12.6	24.8	62.6	5.32	10	34.6	3.48
8.5666	142.3830	47.2769	461.7230	0.7963	3.5221	509.0000	0.0269	12.6	24.8	62.6	5.32	10	34.6	3.48

7.9276	137.2810	52.3452	461.6570	0.7996	3.1416	513.0000	0.0150	12.6	24.8	62.6	5.32	10	34.6	3.48
7.4150	137.2730	51.5918	462.4080	0.7685	0.3590	514.0000	0.0427	12.6	24.8	62.6	5.32	10	34.6	3.48

Table S5. Selected variables by the random forest model to demographic rates in the Brazilian savanna, Minas Gerais State, southeast of Brazil. In which: %IncMSE is the importance value from the variable.

Demographic Rates	Variables	%IncMSE
Mortality	Valley Depth (VD)	55.42
	Aspect (ASP)	51.88
	Vertical Distance to Channel Network (VDCN)	46.78
	LS Factor (LSF)	42.10
Recruitment	Precipitation seasonality (BIO15)	102.29
	Multiresolution index of Ridge Top Flatness (MRRTF)	101.53
	Channel Network Base Level (CNBL)	97.57
	Aspect (ASP)	95.26
Basal area loss	Relative Slope Position (Slope)	71.90
	Precipitation seasonality (BIO15)	71.39
	Aspect (ASP)	65.74
	Valley Depth (VD)	62.89
Basal area gain	Channel Network Base Level (CNBL)	266.57
	Topographic Wetness Index (TWI)	154.59
Net change in number of individuals	Valley Depth (VD)	66.05
	Analytical Hillshade (HILS)	66.01
	Channel Network Base Level (CNBL)	64.29
	Precipitation seasonality (BIO15)	64.29

	Vertical Distance to Channel Network (VDCN)	64.11
Net change in basal area	Analytical Hillshade (HILS)	132.94
	Channel Network Base Level (CNBL)	123.34
	Precipitation seasonality (BIO15)	117.29